2021

Biomechanics of Head Impacts in an Unhelmeted Sport

Stephen Tiernan
Technological University Dublin

Biomechanics of Head Impacts in an Unhelmeted Sport

A thesis submitted in partial fulfilment of the requirements for the degree of Doctor of Philosophy of Technological University Dublin

By

Stephen Tiernan M.Eng.Sc

School of Mechanical and Design Engineering

Technological University Dublin

Supervisors: Dr. Barry Duignan & Dr. Graham Gavin

Dublin, Ireland

May 2021

Abstract

Concussion in sport is very common and often the injury is undetectable using CT and MRI scans. In addition, approximately 50% of concussions are unreported.

The project initially investigated the suitability of a skin patch sensor and a head-band sensor for the measurement of head impacts in unhelmeted sports. It was found that both were unsuitable due to large angular acceleration errors. The study then collaborated with CAMLab at Stanford University and 25 Mixed Martial Arts (MMA) athletes were fitted CAMLab's validated instrumented mouthguard. 451 video confirmed impacts were recorded at 19 sparring and 11 competitive MMA events. Five concussions were diagnosed during the competitive events. The most severe impacts were simulated using the Global Human Body Model Consortium head model.

The average resultant linear acceleration of the impacts that resulted in a concussion was approximately 20% lower than concussive studies of US football while the resultant average angular acceleration was 34% higher. It is hypothesised that these differences are due to the high energy frontal impacts in US football as opposed to the 'hook' style punches in MMA. Large strains in the mid-brain occurred from frontal impacts whereas lateral impacts resulted in large strains in the corpus callosum. It was found that the average strain in the corpus callosum of the concussed athletes was 0.27 which was 88% higher than that in uninjured fighters. In collaboration with the Genetics department in Trinity College Dublin it was found that the maximum principal strain correlated (R^2=0.84) with the volume fraction of blood brain barrier disruption post-fight. In conjunction with Stanford University, it was found that the spectral density of MMA impacts was higher than that in US football.

This study is the first known study to measure *in vivo* head impacts in unhelmeted athletes that have suffered a concussion.

Declaration

I certify that this thesis which I now submit for examination for the award of Doctor of Philosophy is entirely my own work and has not been taken from the work of others, save and to the extent that such work has been cited and acknowledged within the text of my work.

This thesis was prepared according to the regulations for graduate study by research of the Technological University Dublin and has not been submitted in whole or in part for another award in any other third level institution.

The work reported on in this thesis conforms to the principles and requirements of the TU Dublin's guidelines for ethics in research.

TU Dublin has permission to keep, lend or copy this thesis in whole or in part, on condition that any such use of the material of the thesis be duly acknowledged.

Signature ____________________ Date 31/5/2021

Candidate Stephen Tiernan

Acknowledgements

I would like to thank all who have helped and supported me in my 21 years of working in the Mechanical Engineering Department at the Tallaght Campus. In particular I would like to thank Fiona Cranley (Head of School) and Diarmuid Rush (Head of Department) for their help and support with my research work.

I would like to thank Dr. Graham Gavin and Dr. Barry Duignan for their guidance and patience in preparing this thesis. They have the unenviable task of supervising a project which they had not proposed.

I would like to thank all the women in my life!

My daughters, Aoife, Róisín and Alanna for their help, humour, patience, and simply being.

My mother for bringing me into this life and still being at my side.

Finally, to Maddie for being my life-long supporter, through thick and thin.

"There is a crack in everything, that's how the light gets in." Leonard Cohen 1992

Abbreviations

TBI	Traumatic Brain Injury
mTBI	Mild Traumatic Brain Injury
CT	Computerised Tomography
MRI	Magnetic Resonance Image
BBB	Blood Brain Barrier
MMA	Mixed Martial Arts
SCAT	Sport Concussion Assessment Tool
LOC	Loss of Consciousness
CSF	Cerebrospinal Fluid
DAI	Diffuse Axonal Injury
US	United States
PCS	Post Concussion Syndrome
CTE	Chronic Traumatic Encephalopathy
NFL	National Football League
ImPACT	Immediate Post Concussion Assessment Cognitive Test
RFU	Rugby Football Union
IRFU	Irish Rugby Football Union
HITS	Head Impact Telemetry System
PLA	Peak Linear Acceleration
PRA	Peak Rotational Acceleration
FE	Finite Element
GHBMC	Global Human Body Model Consortium
WSUHIM	Wayne State University Head Injury Model
UCDBTM	University College Dublin Brain Trauma Model
SUFEHM	Strasbourg University Finite Element Human Head
KTH FEHM	Kungliga Tekniska Högskolan Finite Element Head Model
THUMS	Total Human Model for Safety
NHTSA	National Highway Traffic Safety Administration
AIS	Abbreviated Injury Scale
CP	Combined Probability
BrIC	Brain Injury Criteria
RVCI	Rotational Velocity Change Index
HIC	Head Impact Criterion
HIP	Head Impact Power
MPS	Maximum Principal Strain
SD	Standard Deviation
IRB	Institutional Review Board
LHS	Left Hand Side
RHS	Right Hand Side
TKO	Technical Knockout
KO	Knock Out
NHTSA	National Highway Traffic Safety Association

Contents

Abstract i

Declaration ii

Acknowledgements iii

Abbreviations iv

Figures x

Tables xii

Chapter 1: Introduction 1

1.1 Concussion research collaborations 2

1.2 Aim and objectives 5

1.3 Thesis layout 5

Chapter 2: Literature Review 10

2.1 Head anatomy 11

2.1.1 Skull 11

2.1.2 Meninges 12

2.1.3 Fore-brain 12

2.1.4 Brain stem 16

2.2 The brains response to impact 17

2.3 Concussion in sport 19

2.3.1 Severity of injury 19

2.3.2 Repeated mTBI, sub-concussive impacts and long term effects 21

2.3.3 Diagnosis of concussion 23

2.3.4 Prevalence of concussion in sport 24

2.3.5 Factors that affect the rate of concussion 27

2.3.6 Under-reporting of concussion 28

2.3.7 Summary of concussion in sport 28

2.5 The measurement of 6D head kinematics 29

2.5.1 Head Impact Telemetry System (HITS) 29
2.5.2 Instrumented skullcaps and headbands 31
2.5.3 Skin patch sensors 31
2.5.4 Instrumented mouthguards...32
2.5.5 Summary of head impact measurement systems 34
2.5 Simulation of head impacts 35
2.5.1 Wayne State University Head Injury Model (WSUHIM).........................37
2.5.2 University College Dublin Brain Trauma Model (UCDBTM)................38
2.5.3 Strasbourg University FE Head Model (SUFEHM) 39
2.5.4 Kungliga Tekniska Hȍgskolan FE Human Head Model (KTH FEHM)...40
2.5.5 Total Human Model for Safety (THUMS)...40
2.5.6 Summary of head models...40
2.5.7 Limitations of existing brain models..41
2.6 Concussion injury tolerance thresholds...42
2.6.1 Kinematic injury criteria 43
2.6.2 The Influence of impact direction and duration.......................................49
2.6.3 Summary of kinematic injury predictors..52
2.6.4 Injury criteria based on finite element head simulations 52
2.6.5 Summary of brain distortion injury criteria 57
2.7 Mixed martial arts 58
2.7.1 Mixed martial arts background 58
2.7.2 Injuries in mixed martial arts 59
2.7.3 Mixed martial arts in Ireland...59
2.8 References 60

Chapter 3: Evaluation of skin mounted sensor for head impact measurement...............73
3.1 Introduction 74
3.2 Methods 76

3.3 Results 81
3.3.1 Linear aceleration 81
3.3.2 Angular velocity 86
3.3.3 Angular acceleration 87
3.4 Discussion 89
3.5 Conclusions 91
3.6 References 92
Chapter 4: Repeatability and reliability evaluation of a wireless headband sensor 95
4.1 Introduction 95
4.2 Methods 97
4.2.1 Measurement device 97
4.2.2 Data processing 97
4.2.3 Testing procedure 97
4.2.4 Statistical analysis 98
4.3 Results 99
4.4 Discussion 100
4.5 Conclusions 102
4.6 References 102
Chapter 5: Measurement of 6-Dimenaional Kinematics in Mixed Martial Arts
5.1 Introduction 106
5.1.1 Head impact sensors 110
5.1.2 Mixed martial arts 112
5.2 Method 112
5.2.1 Data capture and analysis 114
5.3 Results 117
5.3.1 Results for the concussed fighters 122
5.4 Discussion 130
5. 5 Conclusion 133
5.6 References 133
Chapter 6: Setup and Sensitivity Analysis of the GHBMC Head and Neck Model 138
6.1 Introduction 138
6.1.1 GHBMC head model 138
6.2 Co-ordinate systems 140
6.2.1 Preparation of acceleration data for simulation 142

6.2.2 Application of acceleration to the simulation model 142
6.2.3 Solving and post-processing 143
6.3 Investigation of model sensitivity 143
6.3.1 Method 1: Strain versus angular acceleration 143
6.3.2 Method 2: Strain versus impact duration 144
6.3.3 Method 3: Strain versus brain tissue stiffness 144
6.4 Results 146
6.4.1 Results 1: Acceleration magnitude and direction.................................. 146
6.4.2 Results 2: Duration.. 148
6.4.3 Results 3: Material Properties 149
6.5 Discussion.. 150
6.6 References 152
Chapter 7: The effect of impact location on brain strain 154
7.1 Introduction 155
7.2 Methods 157
7.2.1 Drop tests 157
7.2.2 Simulation 158
7.3 Results 161
7.3.1 Constant impact energy... 161
7.3.2 Same acceleration profiles applied to different locations 163
7.4 Discussion.. 164
7.5 Conclusion.. 168
7.6 References 168
Chapter 8: Finite element simulation of head impacts in mixed martial arts............... 171
8.1 Introduction 172
8.2 Methods 172
8.2.1 Statistical analysis………………………………………………................. 173
8.3 Results 174
8.3.1 Simulation of the concussion cases ……………………………………... 178
8.4 Discussion.. 184
8.5 Conclusion.. 186
8.6 References 187
Chapter 9: Conclusion.. 189
9.1 Summary of the original contributions of this research 189

9.2 Recommendations and future work ... 192
9.2.1 Potential collaborations for future work ... 193
9.3 References ... 195
Appendix 1: Author contribution statements ... 197
Appendix 2: Matlab programs ... 200
Appendix 3: Material properties of head model ... 211
Full list of publications ... 213

Figures

Figure 1-1: Concussion Research Interest Group 3
Figure 1-2: Overall Concussion Study 4
Figure 2-1: MRI showing the layers of the human head 11
Figure 2-2: Layers of the meninges covering the brain 12
Figure 2-3: Human brain – sagittal section 13
Figure 2-4: Major brain lobes and functions 14
Figure 2-5: Falx running longitudinally through the skull 16
Figure 2-6: Mechanism of concussion 17
Figure 2-7: Lateral distortion of the falx 19
Figure 2-8: HITS system for measuring accelerations 29
Figure 2-9: HITS sample data in collegiate American football players 30
Figure 2-10: Reebok Checklight (left) SIM-G (right) 31
Figure 2-11: xPatch placed on the mastoid bone behind the ear 31
Figure 2-12: Stanford CAMLab instrumented mouthguard MiG1.0 33
Figure 2-13: Instrumented Mouthguards (a) MiG2.0 Stanford, (b) Prevent BioMetrics and (c) PROTECHT 35
Figure 2-14: Wayne State University Head Injury Model 38
Figure 2-15: UCD FE model 39
Figure 2-16: Wayne State Tolerance Curve 43
Figure 2-17: Combined probabilit 47
Figure 2-18: Impact duration versus acceleration 51
Figure 3-1: (a) Drop test rig (view 1) (b) Drop test rig (view 2). 78
Figure 3-2: Impact locations (a) Front (b)Left, (c) Right, (d) Rear 79
Figure 3-3: Linear and angular acceleration from reference accelerometers following a frontal impact at a drop height of 360mm (Test number 10) 80
Figure 3-4: Linear acceleration and angular velocity regression analysis for frontal impacts 83
Figure 3-5: Box plot showing median and interquartile range for the linear acceleration recorded by the Kistler accelerometer for each drop height 84
Figure 3-6: Box plot showing median and interquartile range for the linear acceleration recorded by the xPatch on the left side accelerometer for each drop height..................... 84

Figure 3-7: Box plot showing median and interquartile range for the linear acceleration recorded by the right hand xPatch on the accelerometer for each drop height 85
Figure 3-8: Linear and angular acceleration following a frontal impact, LHS and RHS xPatch and reference data shown. 86
Figure 4-1: Hybrid 3 headform with SIM-G sensor.. 98
Figure 4-2: Comparison of SIM-G linear and angular acceleration with reference sensors 100
Figure 5-1: Wayne State Tolerance Curve [26] 109
Figure 5-2: CAMLab Instrumented mouthguard 112
Figure 5-3: Impact direction sectors 114
Figure 5-4: Sample data from sparring session (Note: 3ms pre trigger and 27ms post trigger is displayed) 116
Figure 5-5: Number and severity of linear and angular accelerations during competitive events 119
Figure 5-6: Duration of linear and angular resultant accelerations of the most severe impact (highest angular acceleration) recorded at each competitive event and sparring session 120
Figure 5-7: Angular acceleration versus linear acceleration of the most severe impact (highest angular acceleration) recorded at each competitive event and sparring session 121
Figure 5-8: Percentages of impacts in different directions ………………………….. 121
Figure 5-9: Concussion Case 1 125
Figure 5-10: Concussion Case 2 126
Figure 5-11: Concussion Case 3 127
Figure 5-12: Concussion Case 4 128
Figure 5-13: Concussion Case 5 129
Figure 6-1: The GHBMC head and neck model 129
Figure 6-2: Brain parts in the GHBMC model 129
Figure 6-3: Anatomical Planes 130
Figure 6-4: Co-ordinate system of the Stanford mouthguard and GHBMC head model 131
Figure 6-5: Sample angular acceleration curve magnitude: 5krad/s/s and 6ms duration 134
Figure 6-6: Shear modulus of the GHBMC viscoelastic brain material 136

Figure 6-7: (a) Strain in the corpus callosum for angular accelerations about a single axis (b) Green Lagrange Strain Scale 137
Figure 6-8: Strain plots for angular acceleration only about X, Y and Z axes 137
Figure 6-9: Strain versus duration for angular acceleration about X and Z axes 138
Figure 6-10: Strain plots – 5krad/s^2 angular acceleration about X axis 138
Figure 6-11: Strain for different material models 139
Figure 7-1: Head portion of the GHBMC model..158
Figure 7-2: Strain and pressure in the corpus callosum..162
Figure 7-3: Pressure response following a severe impact...162
Figure 7-4: Maximum principal strain in different brain regions 164
Figure 7-5: Maximum principal strain following a severe lateral impact.....................165
Figure 7-6: Maximum principal strain following a severe frontal impact....................167
Figure 8-1: Typical head acceleration data collected by instrumented mouthguard ...173
Figure 8-2: Average strains with standard deviation in various brain regions 175
Figure 8-3: Stress and strain rate with standard deviation in the corpus callosum.......175
Figure 8-4: Transverse and Sagittal brain cross sections: Strain plots – Fighter 5 Bout 1 Impact 21 – Concussed 177
Figure 8-5: Transverse and Sagittal brain cross sections: Strain – Fighter 10 Bout 1 Impact 50 – Uninjured 177
Figure 8-6: Strain and blood brain barrier disruption Case 1 179
Figure 8-7: Strain and blood brain barrier disruption Case 2 180
Figure 8-8: Strain and blood brain barrier disruption Case 3 181
Figure 8-9: Strain and blood brain barrier disruption Case 4 182
Figure 8-10: Strain and blood brain barrier disruption Case 5 183

Tables

Table 2-1: Concussion injury scale 20
Table 2-2: Symptoms of Concussion 20
Table 2-3: Rates of concussion in various sports...25
Table 2-4: Brain model characteristics 36
Table 2-5: Linear and angular acceleration thresholds for concussion...........................44
Table 2-6: Brain injury thresholds 56

Table 3-1: Sample results from 360mm frontal drop.....81
Table 3-2: Summary of linear acceleration results for frontal impacts.....82
Table 3-3: Summary of angular velocity for frontal impacts.....87
Table 3-4: Summary of rotational acceleration for frontal impacts.....88
Table 3-5: Summary of errors (xPatch relative to reference device).....88
Table 4-1 Pearson's Correlation coefficients for data from the SIM-G and the reference sensors.....99
Table 4-2: Cronbach's Alpha coefficient (α) for the repeatability of the SIM-G sensor 99
Table 5-1: Published linear and angular accelerations thresholds for concussion.....108
Table 5-2: Study Participants.....113
Table 5-3: Head Impacts from each competitive event with the highest resultant angular acceleration.....118
Table 5-4: Averages and standard deviations of the impacts with the highest angular acceleration at competitive events and sparring sessions criteria.....119
Table 5-5: Correlation between linear and angular acceleration for each impact direction.....122
Table 5-6: Detials of the impact with the highest angular acceleration for each event that ended with a concussion.....124
Table 6-1: Material properties of principal brain parts of version 4.5 GHBMC.....130
Table 6-2: Development of the material properties of the GHBMC.....135
Table 7-1: Finite element strain injury criteria.....157
Table 7-2: Average resultant peak acceleration for frontal impacts.....158
Table 7-3: Acceleration and strain data from tests in which the impact energy was constant.....160
Table 7-4: Acceleration data for simulations where the same accelerations were applied in different directions.....161
Table 8-1: Results of stastical t-tests between concussed and uninjured athletes.....176
Table 8-2: Simulation results for the concussed fighters.....178

Chapter 1

Introduction

The word concussion is derived from the Latin word ‘concutere’ meaning to shake violently. Although there is no universal definition for concussion the most widely recognised definition is from the International Conference on Concussion held in Vienna in 2017 which defined concussion as:

“A complex pathophysiological process affecting the brain, induced by biomechanical forces[1]*.”*

Concussion, or mild traumatic brain injury (mTBI), is highly prevalent in sport with between 1.6 and 3.8 million sports related concussions in the United States each year [2]. Concussion is very difficult to diagnose partly due to the lack of definitive, measurable criteria to identify mTBI and quantify its severity. Many studies have reported that approximately 50% of concussions go unreported. This is thought to be due to the difficulty in diagnosis and also different interpretations of what constitutes a concussion [3].

Despite concussion being very prevalent there is a lack of scientific knowledge relating to the injury, in particular:

- There is no objective method to identify the injury (generally mTBI injuries do not show on standard MRI, CT scans, or blood tests). Subjective cognitive tests such as SCAT 5 and HIA are used.
- It is not understood where and what actual injury has occurred; it is probable that the injury depends on the severity and location of the impact [4]. The injury may also be diffuse or localised [5].

- As the injury cannot be measured neither can the recovery be scientifically determined. It is normally determined by the respite of symptoms associated with concussion.
- The long term consequences of concussive or sub-concussive impacts is unknown although concussion has been linked to Chronic Traumatic Encephalopathy (CTE) and the early onset of dementia [6].

1.1 Concussion research collaborations

Research on head impacts at Technological University Dublin (TUD) – Tallaght Campus (formally Institute of Technology Tallaght) began in 2003 and investigated the design of bicycle and hurling helmets. In 2012 the focus was shifted to concentrate on concussion in unhelmeted sports. The primary aim of the work was to measure the severity of head impacts and simulate the injury using a finite element model. As impact severity and brain strain are only a part of a complex problem they are best investigated alongside medical and brain pathology research. To enable this multi-disciplined broad approach to concussion research, collaborations were setup with various research groups as shown in Figure 1-1.

The roles of the various partners in this collaboration were:

- The instrumented mouthguards used in this project were developed by CAMLab at Stanford University and Intel Corporation, California. A collaborative agreement was entered into with Dr David Camarillo.
- LS-Dyna was used to run simulations on Amazon Web Services (cloud computing), these resources were provided by CADFEM a UK and Ireland software provider and consultancy.

- The medical investigations including Magnetic Resonance Images (MRI), cognitive tests and blood tests were carried out by medical personal in St James's and Beaumont hospitals.

An investigation of the disruption to the blood brain barrier was undertaken by Dr Mathew Campbell's group in the Genetics Department in Trinity College Dublin. The group have adapted a novel method of comparing pre and post event MRI scans to detect micro changes to the blood brain barrier.

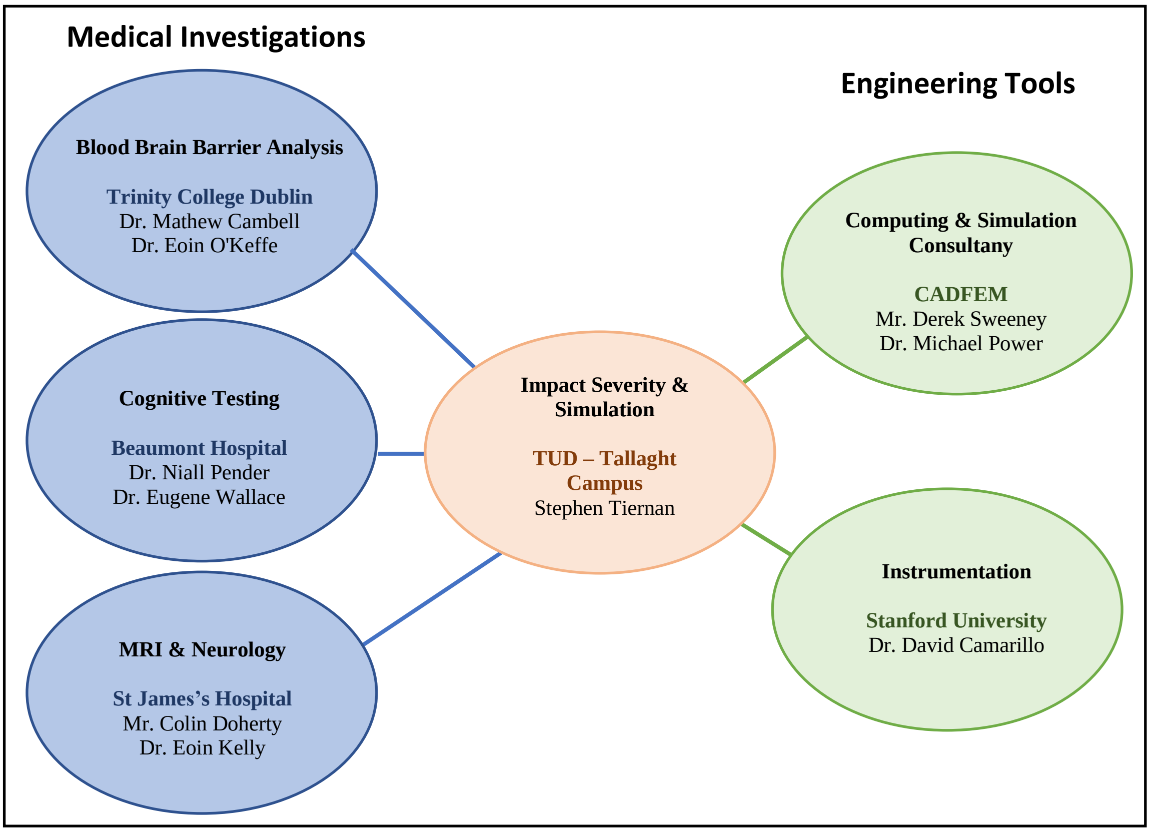

Figure 1-1: Concussion Research Interest Group

TUD Tallaght fitted the MMA fighters with the mouthguards, collected sparring and competition data, performed head simulations and co-ordinated the recording of medical data, head impact data and simulation results. The strength of this concussion group is the diversity of expertise in each research centre. The group aims to improve the treatment, rehabilitation and reduce the incidence of concussion by developing an improved understanding of the biomechanics of the injury. The primary goals of the studies reported in this thesis are the measurement of the severity of a head impact in an unhelmeted sport, the simulation of that impact and the correlation of that data with a medical diagnosis and a blood brain barrier investigation, as shown in Figure 1-2.

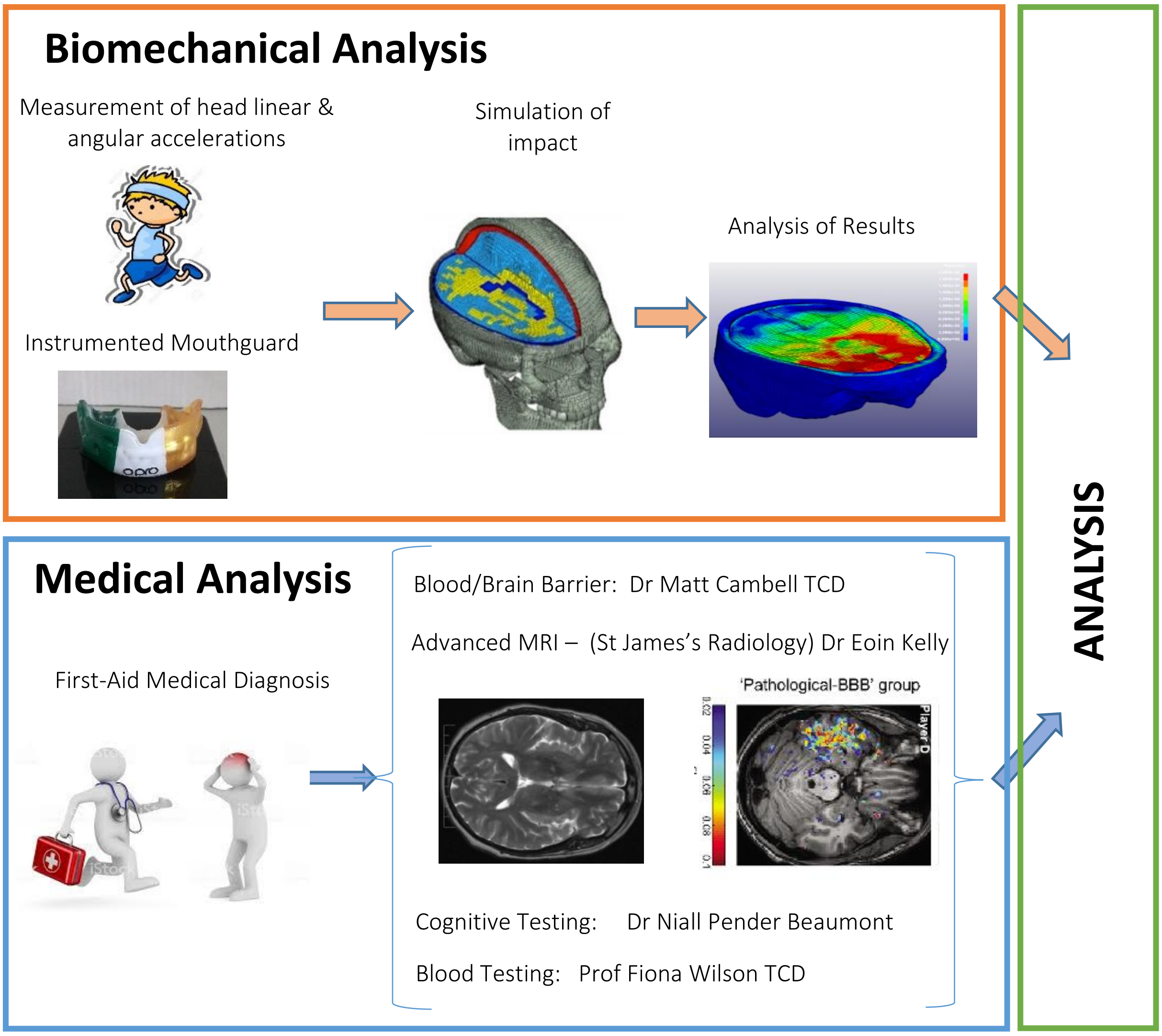

Figure 1-2: Overall Concussion Study

1.2 Aim and objectives

Aim: The aim of this study was to determine the frequency and severity of head impacts in an unhelmeted sport and to correlate this data with brain strain and injury diagnosis.

Objectives:

1. Evaluate head impact sensors used to measure head accelerations in unhelmeted sports.
2. Determine the frequency and severity of sub-concussive impacts experienced by athletes in an unhelmeted contact sport.
3. Measure head accelerations *in vivo* that are experienced by an athlete when a concussive impact is sustained.
4. Simulate the brain's deformation to determine the magnitude and location of brain tissue deformation following a head impact.
5. Determine the influence that impact magnitude and direction have on brain strain.
6. Relate brain strain to medical diagnosis and blood brain barrier disruption.

1.3 Thesis layout

This thesis is based on a series of papers published as part of the concussion research project. The literature review in Chapter 2 discusses relevant research topics and their importance to this project. Chapters 3, 4, 7 and 8 contain the relevant publications as part of this work on sensors and concussion in an unhelmeted sport. Chapter 6 introduces the head finite element model and investigates the sensitivity of the mode to angular accelerations about a particular plane and changes in the material properties of the brain tissue. The concluding chapter discusses the relevance of the work carried out and the original contribution of this work to the understanding of head impact and concussion in sports.

The following is a brief description of the chapters in this thesis. Please note that the introduction and method sections of some of the papers have been edited from their original texts to avoid duplication.

Chapter 3

Paper 1: Evaluation of skin mounted sensor for head impact measurement

This paper investigates the accuracy and repeatability of the xPatch developed by X2 Biosystems (Seattle, WA). The xPatch sensor is attached by double sided adhesive tape to the mastoid bone (just behind the ear). It measures linear acceleration and angular velocity.

S. Tiernan, G. Byrne, and D. M. O'Sullivan, "Evaluation of skin-mounted sensor for head impact measurement," *Proc. Inst. Mech. Eng. Part H J. Eng. Med.*, vol. 233, no. 7, pp. 735–744, 2019. DOI: 10.1177/0954411919850961

Author contributions:

S. Tiernan – Conceived, designed and performed experiments, analysed data and authored the paper.

Mr. G. Byrne (TUD Tallaght Campus): Data collection and analysis.

Dr. D. O'Sullivan (Pusan University, South Korea): Data collection and analysis.

Chapter 4.

Paper 2: Repeatability and reliability evaluation of a wireless head-band sensor.

SIM G developed by Triax, Denmark, is a sensor fitted into a headband, it consists of two triaxial accelerometers and a triaxial accelerometer. This study investigated the correlation of the linear and angular accelerations of the SIM-G sensor with reference sensors.

S. Tiernan, D. O'Sullivan, and G. Byrne, "Repeatability and reliability evaluation of a wireless head-band sensor," *Asian J. Kinesiol.*, *20(4)*, pp. 70–75, 2018.

DOI: 10.15758/ajk.2018.20.4.70

Author contributions:

S. Tiernan – Conceived, designed and performed experiments, analysed data and authored the paper.

Mr. G. Byrne (TUD Tallaght Campus): Data collection and analysis.

Dr. D. O'Sullivan (Pusan University, South Korea): Data collection and analysis.

Chapter 5

Paper 3: Concussion and the Severity of Head Impacts in Mixed Martial Arts.

Head accelerations were measured in Mixed Martial Arts using the Stanford instrumented mouthguard. Head impact severity and direction were analysed from data captured during sparring sessions and competitive events.

Published: S. Tiernan, A. Meagher, D. O'Sullivan, E.O'Keefe, E. Kelly, E. Wallace, C. Doherty, M. Cambell, Y. Liu, A. Domel. "Concussion and the Severity of Head Impacts in Mixed Martial Arts". *Part H: Journal of Engineering in Medicine*. Aug 2020 DOI: 10.1177/0954411920947850.

Author contributions:

S. Tiernan: Conceived, designed and performed experiments, analysed data and authored the paper.

Mr. A. Meagher (TUD Tallaght Campus) & Dr. D. O'Sullivan (Pusan University, South Korea): Acceleration data collection and analysis.

Dr. E. Kelly, Dr. E. Wallace, & C. Doherty (St James's Hospital): Medical examination and reporting.

Dr. M. Cambell & Dr. E.O'Keefe (Trinity College Dublin), &: Medical data collection and analysis.

Dr. L. Yuzhe & Dr. A. Domel (Stanford University): Mouthguard validation and firmware.

Chapter 6.

This chapter introduces the head finite element model and the co-ordinate systems. The chapter also investigates the sensitivity of the model to changes in the magnitude, direction and duration of applied angular accelerations. Additionally, the sensitivity of strain in the corpus callosum to changes in the stiffness of the viscoelastic brain tissue is investigated. This work has not been published.

Chapter 7.

Paper 4: The effect of impact location on brain strain

A finite element study was conducted to investigate the relationship between brain strain and impact direction. The study simulated brain strain using head acceleration data from laboratory Hybrid III headform drop tests.

S. Tiernan and G. Byrne, "The effect of impact location on brain strain," *Brain Inj.*, vol. 33, no. 01, pp. 1–8, 2019. DOI: 10.1080/02699052.2019.1566834.

Author contributions:

S. Tiernan: Conceived, designed and performed experiments, analysed data and authored the paper.

Mr. G. Byrne (TUD Tallaght Campus): Data collection & analysis.

Chapter 8.

Paper 5: Finite Element Simulation of Head Impacts in Mixed Martial Arts

The impact with the highest angular acceleration from each Mixed Martial Arts sparring session and competitive event was simulated. Shear stresses and strains in the core brain regions were investigated and correlated with concussion injuries.

Published: S. Tiernan, A. Meagher, D. O'Sullivan and E. Kelly, "Finite Element Simulation of Head Impacts in Mixed Martial Arts,"*Comput Methods Biomech Biomed Engin. Methods.* Oct 2020. DOI: 10.1080/10255842.2020.1826457.

Author contributions:

S. Tiernan: Conceived, designed and performed all simulations, analysed data and authored the paper.

Mr. A. Meagher (TUD Tallaght Campus): Data collection.

Dr. D.O'Sullivan (Pusan University, South Korea): Data collection.

Dr. E. Kelly (St James's Hospital): Medical Examination and reporting.

Chapter 9.

Conclusion and future work.

Chapter 2

Literature Review

Concussion or mild traumatic brain injury (mTBI) in sport is a minor or moderate injury on the abbreviated injury scale (AIS) of 1 or 2 involving either no loss of consciousness (LOC) or short LOC [7]. In contrast to mTBI a severe traumatic brain injury can involve periods of unconscious of greater than 30 minutes and prolonged amnesia or skull penetration. In this thesis, concussion and mTBI will be regarded as the same condition and the terms may be used interchangeably.

Concussion is very difficult to diagnose, partly due to the lack of definitive, measurable criteria to identify mTBI and quantify its severity. mTBI is normally, but not necessarily, as a result of a blow to the head. The symptoms may include some of the following: headaches (the most common symptom), dizziness, postural instability/balance, nausea, fatigue, blurred vision, loss of consciousness (although this may be so brief that it is difficult to detect), and problems with memory (amnesia tends to be antegrade i.e. an inability to retain information) [8]. Behavioural changes may also occur including: irritability, emotional control, concentration, and sleep disturbance [8]. There are multiple factors that contribute to cause a concussion, these include: linear acceleration/deceleration, angular acceleration, location and direction of impact, and impact duration. This chapter will focus the following topics:

2.1 Head anatomy
2.2 The brain's response to head impact
2.3 Concussion in sport
2.4 Mixed Martial Arts
2.5 The measurement of head impact severity
2.6 The simulation of head impacts
2.7 Injury tolerance thresholds

2.1 Head anatomy

The brain is the most complex of the human organs. It weighs approximately 1.4kg and contains 100 billion nerve cells or neurons [9]. The functions of the individual parts of the brain are only partly understood. The reason for, and extent of, the variation of the brain tissue in different individuals is unclear [10]. This section gives a brief overview of the anatomy of the brain, in particular the regions that are associated with concussion. The human head can be divided into four principal sections (Figure 2-1): skull, meninges, fore-brain and brain stem [11].

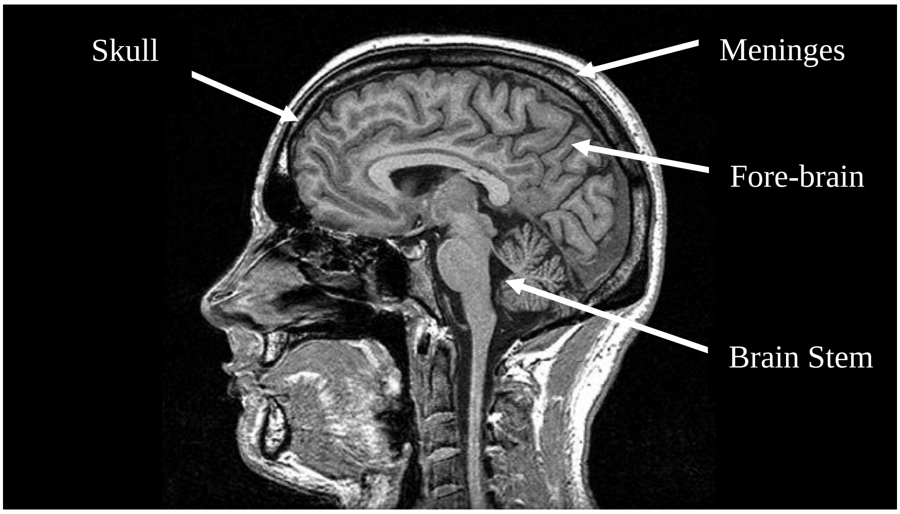

Figure 2-1: MRI showing the layers of the human head [12]

2.1.1 Skull

The skeletal structure of the human head, known as the skull, consists of 22 individual bones, 21 of which are stationary and 1 mobile. The mobile bone, the mandible, allows for the movement of the human jaw [13]. The cranium is made up of eight bones connected along suture lines to create a protective chamber for the brain [13]. The remaining bones form the face. The skull provides skeletal and structural protection for the brain. The meninges beneath provide a supporting framework for the brain, and along with the spinal fluid protect the brain. Typically concussion does not involve fracture of the skull [14]. In this study the skull will be regarded as a rigid body to which head accelerations are applied.

2.1.2 Meninges

The cranial meninges consist of a layered structure which, along with the cerebrospinal fluid (CSF), protect the brain by damping the brains motion [10]. There are 3 principal layers in the meninges; the dura, arachnoid and the pia mater (Figure 2-2).

The dura mater is the outer most layer of the meninges and is a two layered structure consisting of an inner and outer fibrous layer of protection [15]. Beneath the dura is the arachnoid membrane which is not as thick or durable as the dura. Below this is the sub-arachnoid space which is filled with CSF. The final tissue layer is the pia which is very thin and is the only layer to follow the contours of the brain.

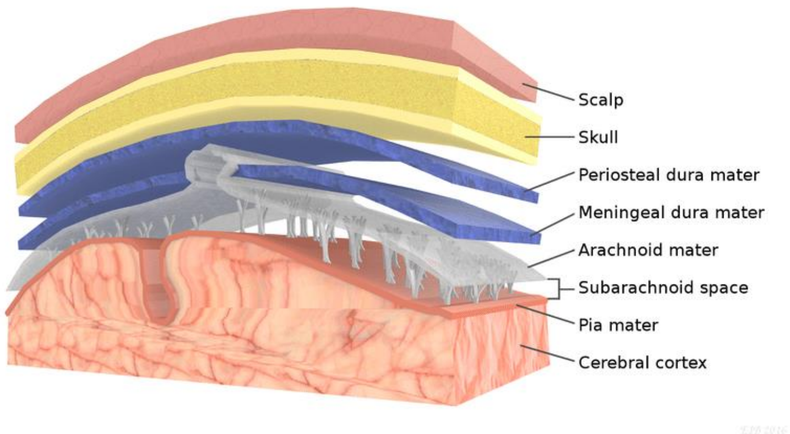

Figure 2-2: Layers of the meninges covering the brain [16]

2.1.3 Fore-brain

The fore-brain is the superior part of the brain and is made up of the cerebrum, cerebellum and corpus callosum (Figure 2-3)[17]. The cerebrum is the largest brain region, it consists of two cerebral hemispheres separated by the longitudinal falx. Below this is the cerebellum which is separated from the cerebrum by the tentorium.

The falx and tentorium are layers of the dura matter which provide stability to the main regions of the brain.

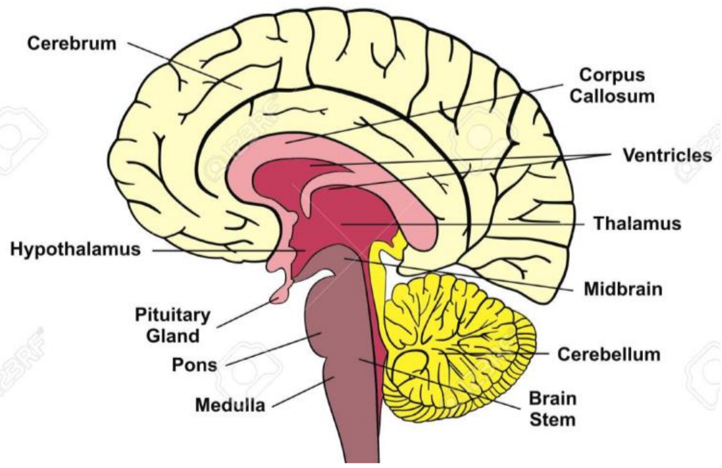

Figure 2-3: Human brain – sagittal section [18]

Cerebrum

The cerebrum consists of grey and white matter and is divided up into a left and right hemisphere. The grey matter is primarily made up of dendrites and synapses which are neuronal cells. The grey matter is associated with learning, attention, thought and memory. To achieve a large surface area, the grey matter has ridges and grooves (gyrus and sulcus). The white matter facilitates communication within the brain, is deep within the cerebrum and consists mainly of myelinated axons. Association fibres are one type of axon and connect the gyruses within the grey matter. Another type of axon, commissural fibres, connect the two hemispheres together. The largest commisural tract between the two hemispheres is the corpus callosum.

The hemispheres of the cerebrum also known as the cerebral cortex are subdivided into lobes as shown in Figure 2-4. The linking of concussive symptoms to brain regions aids in the understanding of the injury mechanism. For example, if an impact is received to the front of the head there may be bruising to the frontal lobe (coup) and to the occipital lobe as the brain returns and overshoots its equilibrium position (contra-coup).

Concussive injuries of this type can lead to blurred vision due to injury within the occipital lobe [19].

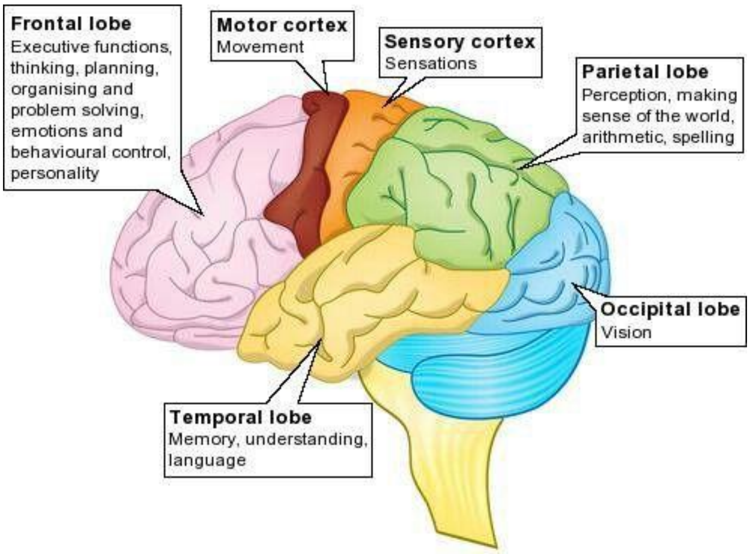

Figure 2-4: Major brain lobes and functions [20]

Cerebellum

The cerebellum is located posterior and inferior to the cerebrum and makes up 10% of the brain mass (Figure 2-3)[13]. It contains a very dense network of neurons [21]. Like the cerebrum it is divided into two hemispheres, left and right, and is covered in a thin layer of grey matter [20]. Commonly known as the automatic processing centre of the brain, the cerebellum plays a key role in sensory communication and motor function. It is involved in the co-ordination of conscious and subconscious movement and balance.

Ventricles

There are 4 cavities located within the brain called ventricles. One is located in each hemisphere of the cerebrum, while the third and fourth run along the brain stem. The ventricles are filled with CSF. CSF is produced in the third and fourth ventricles of the brain and circulates through the ventricles and around the subarachnoid space between the arachnoid matter and the pia matter. There is approximately 125 to 150mL of fluid filling the spaces around the brain. 20% of the CSF fills the ventricles and the rest is in the sub-arachnoid space and the spinal cord [22]. CSF helps to protect the brain by damping any movement of the brain tissue following a head impact. The CSF also provides nutrients to the brain.

Corpus callosum

The corpus callosum connects the left and right hemispheres of the brain with a thick bundle of nerve fibres. The main function of the corpus callosum is to pass motor, sensory and cognitive information between the two sides of the brain [23]. It is made up of white matter axons and is the largest fibre bundle in the brain. It also plays an important role in vision as it combines the separate halves of the visual field and connects with the language centres of the brain [9]. Injury to the corpus callosum has been linked to concussion [24]. It has been identified that direct damage to the corpus callosum can result in a decline in cognitive performance in aging adults [25]. In contrast studies on children with an enlarged corpus callosum have shown a direct correlation between the corpus callosum volume and intelligence, problem solving skills and ability to process information [26].

Tentorium and falx

The tentorium is located above the cerebellum and separates the cerebellum and the brain stem from the brain’s hemispheres. The falx divides the brain’s hemispheres in a longitudinal fashion and acts as a layer of protection between the left and right hemispheres (Figure 2-5).

The superior of the falx is tethered to the superior sagittal sinus, whereas the inferior of the falx is attached to the inferior sagittal sinus which in turn over arches the corpus callosum. The falx helps to protect the brain during rotational movements.

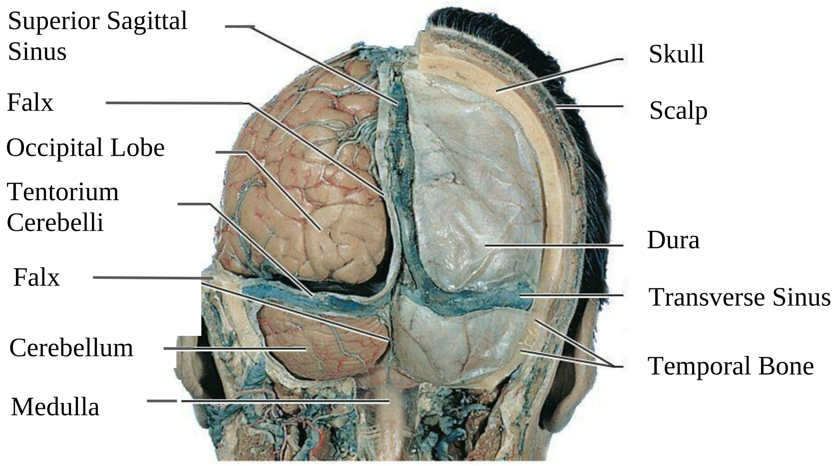

Figure 2-5: Falx running longitudinally through the skull [11]

2.1.4 Brain stem

The brain stem is the relay centre between the cerebrum, cerebellum and the spinal cord. It consists of the thalamus, mid-brain and medulla. The thalamus is an important processing centre for the sensory system relaying communication between areas of the cerebrum.

Thalamus

The thalamus is a located superior to the mid-brain and inferior to the corpus callosum, as shown in Figure 2-3. The thalamus consists primarily of grey matter and regulates awareness and sensory experiences. It relays sensory signals including motor signals. It is connected to the cerebral cortex by nerve fibres that project out in all directions.

Mid brain

The mid-brain is one of the most important components of the central nervous system as all neural transmissions pass through it to the rest of the body. It is involved in eye movement control and auditory and visual processing.

Medulla

The medulla, also called the medulla oblongata, is the most inferior part of the brain stem and links the fore-brain and the spinal cord. The spinal cord and the medulla merge at the opening at the base of the skull. It controls autonomic nervous systems such as breathing, heart and blood vessel function, digestion, sneezing, and swallowing.

2.2 The brains response to impact

In the 1940s and 50s a number of researchers used cadavers and animal models to investigate the mechanics of brain injury [27]. Following this work, it was generally accepted that traumatic brain injury was the result of an abrupt translational deceleration. This deceleration causes the brain to collide with the inside of the skull (coup), and then recoil and impact the back of the skull (contra-coup) (Figure 2-6). This creates a sudden change in intracranial pressure causing contusion (bruising) on the anterior (front) and posterior (back) of the brain.

In research on cats and monkeys in 1940, Denny-Brown and Russell induced concussions in animals and measured the intracranial pressure [28]. They found positive pressures at the impact site and negative pressures on the opposite side and hence confirmed the coup contra-coup response. Their work also pointed to the brain stem as the probable brain structure associated with concussion. Ward et al. found that intracranial pressures above 235kPa would result in a serious brain damage and below 173kPa would not be injurious [29].

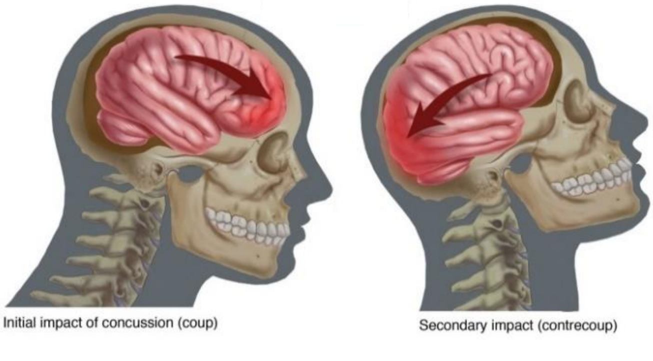

Figure 2-6: Mechanism of concussion [30]

The second mechanism associated with concussion is diffuse axonal injury (DAI). This is the disruption of the axons (nerve fibres) within the brain due to shearing forces. The severity of this type of concussion is determined by the location and extent of axonal damage within the brain [31]. Axonal damage occurs when the brain tissue is subject to non-recoverable strains [32].

High abrupt linear accelerations produce high intracranial pressures and hence contusions and high angular accelerations lead to DAI [33]. In 1943 Holbourn suggested that angular accelerations cause high shear stresses in the brain leading to injury [34]. The most significant animal experiments were performed by Gennarelli et al. in the 1970s and 80s [35][36]. They applied pure linear acceleration pulses ranging from 348g to 1025g to squirrel monkeys, half of whom suffered subdural hematomas in the frontal region of the brain. They also applied pure angular acceleration pulses to another set of monkeys and found extensive hematomas throughout the brain. They concluded that pure linear accelerations did not produce concussion while pure angular accelerations produced a concussion with a loss of consciousness of 2 to 12 minutes [35].

Following autopsies on some of these animals they found that the extent of axonal injury related to the duration of the loss of consciousness (LOC): short durations had axonal injury in the white matter of the cerebral hemispheres whereas injury was evident in the corpus callosum in animals with a longer LOC. The animals with the most severe injuries had axonal injuries in the cerebral hemispheres, the corpus callosum and the brain stem [36].

Animal and simulation studies have confirmed that axonal injury to the corpus callosum is linked to concussive injuries [37][38][39]. Advanced magnetic resonance imaging (MRI) techniques have been used by Yount et al. [40] and Strangman et al. [41] to investigate the corpus callosum in concussed patients. Yount et al. found that the volume of the corpus callosum had decreased and Strangman et al. found that the texture had significantly changed in these patients.

Hernandez et al. hypothesised that one mechanism for concussion is the distortion of the falx following lateral rotations of the brain (Figure 2-7) [42]. This in turn leads to deformation of deep brain tissues, in particular the corpus callosum which results in high strains in the corpus callosum.

Figure 2-7: Lateral distortion of the falx [42].

2.3 Concussion in sport

2.3.1 Severity of injury

Concussion is not well defined and its meaning has changed over the years. It used to be associated with a loss of consciousness but now has a broader meaning. The severity of head injuries has been graded by the Joint Committee on Injury using the abbreviated injury scale (AIS) as shown in Table 2-1. This study will focus on mild and moderate concussions, as this is the most common type of sports related concussion. In general, the injury is a closed head injury not involving skull fracture and is associated with either no LOC or a brief LOC [43]. The injury is typically not visible on either a computer topography (CT) image or magnetic resonance image (MRI) and is diagnosed based on symptoms.

The symptoms may be broken into four categories: somatic, cognitive, emotional and sleep (Table 2-2). The symptoms normally resolve in 7 to 10 days but may be persistent, leading to post-concussion syndrome (PCS) [44]. PCS can last 6 to 12 months [45].

Table 2-1: Concussion injury scale [7]

AIS	Severity	Brain Injury	Concussive Injury
0	No injury		
1	Minor injury		Mild concussion (No LOC)
2	Moderate	Cerebellum and Cerebrum (SAH)	Moderate concussion (LOC < 1 hour)
3	Serious (non-life threatening)	Cerebellum and Cerebrum (contusion, haematoma, laceration, penetration, swelling)	Severe concussion (LOC 1 to 6 hours)
4	Severe (life threatening)	Cerebrum (DAI confined to white matter)	Mild DAI (LOC 6 to 24 hours)
5	Critical (survival uncertain)	Cerebrum (DAI involving corpus callosum) Brainstem (compression, contusion, haemorrhage)	Moderate DAI (LOC > 24 hours)
6	Maximum	Brainstem (laceration, penetrating, transection)	Severe DAI
AIS: Abbreviated injury scale		**SAH: Sub-arachnoid haemorrhage** **LOC: Loss of consciousness**	**DAI: Diffuse axonal injury**

In a study of 79 US football players who suffered a concussion McCrea et al. found LOC occurred in 6.4% of the cases and 13.9% had delayed onset of symptoms such as cognitive function [45]. Their study demonstrated that concussion is transient as 90% of the players recovered their baseline cognitive function and balance within 7 days. All of the athletes fully recovered within the 90 day study time [45].

Table 2-2: Symptoms of Concussion [44]

Somatic	Cognitive	Emotional	Sleep
Headache	Difficulty thinking	Irritability	Sleeping more than usual
Fuzzy or blurry vision	Feeling slow	Sadness	Sleeping less than usual
Dizziness	Difficulty concentrating	Feeling more emotional	Trouble falling asleep
Fatigue	Difficulty remembering new information	Nervousness or anxiety	
Sensitivity to light			
Balance problems			
Nausea or vomiting			

Unfortunately, there is no treatment for concussion except for rest, hydration, and avoidance of light [43]. It is also impossible to accurately predict recovery times or long- term consequences [44].

2.3.2 Repeated mTBI, sub-concussive impacts and long term effects

There is a lot of debate over the long-term effects of repeated concussions: this is partly due to a lack of understanding of concussion in the past and also due to the lack of historical head impact data for athletes. US football has had professional players since 1882 and hence is the greatest source of data on the consequences of repeated head impacts in sport. Since 1945 a total of 497 US football players have died, of these 69% died from brain injuries [46].

Repeated Concussions

It has been shown that athletes who suffer a concussion are more likely to suffer a subsequent concussion. One study by Guskiewicz et al. found that US football players with a history of previous concussions were three times more likely to suffer a concussion when compared with players who had no history of concussion [47]. They found that 30% of players with a history of multiple concussions (greater than three) took more than a week to recover as opposed to 14.6% of players with only one previous concussion. They also found that most (91.7%) of repeat concussions occurred within 10 days of the first concussion. This is similar to the findings of other studies [43][48].

Sub-Concussive Impacts

A US football player who plays for 4 years in high school and 4 years in college could sustain 8000 head impacts [49]. Despite the large numbers of impacts there are relatively few concussions, this led McAlister et al. to investigate the effects of sub-concussive impacts in collegiate sports [50]. They found that learning and memory was affected on a temporary basis in athletes with a large number of sub-concussive impacts. It was also found that there were an abnormal number of white matter voxels in athletes that participated in contact sports. They concluded "*that a single season of football can produce brain MRI changes in the absence of clinical concussion* [51]*"*.

Long Term Effects of Repeated mTBI

In 1928, Martland published a paper describing a condition he associated with boxers who had suffered repeated head trauma, he termed this condition '*Punched Drunk'.* The modern name for this condition is chronic traumatic encephalopathy (CTE)[52]. CTE is characterized by atrophy (dying away) of the cerebral hemispheres, medial temporal lobe, thalamus, mammillary bodies, and brain stem, and is associated with the build-up of an abnormal amount of the tau protein. These changes in the brain can occur years after an athlete retires.

The clinical symptoms associated with CTE are memory loss, attention problems, paranoia, gait problems, depression, suicide, dysarthria, Parkinson's disease, and eventually, progressive dementia. It is difficult to distinguish it from conditions such as Alzheimers or old age dementia [6], and it may only be fully diagnosed in an autopsy. The prevalence of CTE in the general population is unknown.

In the USA CTE is associated with retired National Football League (NFL) players who have suffered repeated concussions over their careers. A post-mortem study, in 2012, of 85 brains of people with histories of repetitive concussion found that 80% had pathological evidence of CTE. These people had an average age of 59.5 years old [53]. The study included 35 former American football players, of these 34 showed signs of CTE and 94% of these players were symptomatic before death. The Boston University Alzheimer's Disease Centre (BU ADC) is the world leading research group investigating CTE. They have an extensive brain bank and aim to establish a diagnostic test for living persons for CTE and to track retired athletes to determine the long-term consequences of repetitive brain trauma.

In 2009 the NFL conceded publicly for the first time that concussions can have lasting consequences and these can include the early onset of progressive dementia and Alzheimer's disease [54]. In 2013 the NFL agreed to a settlement of $765 million to 4,500 retired players and their families. The former athletes and their families accused the NFL of concealing the dangers of concussion and rushing players back onto the field [55].

2.3.3 Diagnosis of concussion

Concussion can be very difficult to diagnose as most symptoms are subjective. It is also very difficult to determine when the injury has healed and the athlete can return to play. The evaluation of concussion should include a clinical examination, self-reporting checklist, postural assessment and neurocognitive testing. There are several tools available to assist in the diagnosis, some of these are suitable for pitch side-line testing whereas others require a medical clinic. The side-line tests generally rely on comparing a score, in a neurocognitive test, to a pre-match or pre-season score. The reliability of these tools is uncertain, they may give an indication of whether a concussion has been sustained but the final diagnosis still requires a trained person with experience in the field. It must also be remembered that the player may not be aware that he or she is concussed and that there is a tendency for under-reporting of symptoms by the player [56].

The most common side-line assessment tool is the Sports Concussion Assessment Tool 5 (SCAT5). The SCAT method of assessing an athlete has eight parts to the test, some are designed for on and some for off the pitch. Each section is scored, and the final score is compared to a baseline test. Both parts measure the physical, verbal and cognitive responses of a player. The test takes approximately 20 minutes to complete and there is both a paper and software version of the test. There are other similar concussion tests such as the King Devick (KD) test and the Immediate Post Concussion Assessment and Cognitive Testing (ImPACT). ImPACT is similar to the SCAT test but is carried out online and has the advantage of storing the player's responses on a cloud server for future analysis.

Part of the problem associated with psychometric tests is that they all rely to some extent on self-reporting e.g. the participant is required to rate their dizziness and headache on a scale of 1 to 10. Players can feel under pressure to under-report for individual or team reasons. It has also become commonplace for players to intentionally under perform in baseline tests at the beginning of the season, so that a reduction in their performance during the season will not be detected [57].

2.3.4 *Prevalence of concussion in sport*

Participation in sporting activities has increased since 1980 and has been linked to positive physical and mental health [58]. Unfortunately, this increase in sport has been associated with an increase in all sporting injuries [59]. It is difficult to compare the incidence of concussion in different sports due to the different methods of reporting and calculation of rates. For example some studies quote concussion rates per player per season whereas others calculate rates per 1000 hours of play. Care must also be taken in interpreting data as quoted rates may include match play, training or both. This study will only consider concussions in contact sports, other sports such as cycling will not be included. Table 2-3 shows the rates of concussion across a range of contact sports. These are calculated based on 1000 hours of activity but do not include training time. The contact sports with the highest rates of concussion are US football, ice hockey, rugby, boxing and martial arts [60].

Table 2-3: Rates of concussion in various sports

Author	Sport	Injury Per 1000 hrs played	Level	Study Size	Year	Country
Kemp [61]	Rugby Union	17.9	Pro	1 season, 588 matches	2018	UK
Marshall [62]	Rugby Union	11.1	College	2 teams, 3 seasons	2001	USA
King [43]	Rugby Union	10.9	Amateur	37 players, 24 matches	2013	New Zealand
Flik [63]	Ice Hockey	2.57	High School	8 teams, 1 season	2005	Canada
Lincoln [64]	Soccer	0.17	High School	25 schools over 11 years	2011	USA
Koh [60]	Boxing	7.9	Amateur		2003	USA
Blake [65]	GAA, Football & Hurling	0.48	Amateur	55 teams	2007 to 2011	Ireland
Booher [66]	US Football	5.56	NFL Pro	81 Divisions, 1 season	2003	USA
Guskiewicz [67]	US Football	3.7 Div 1 5.26 Div 3	College	2905 players, 3 seasons	2003	USA
Myer [68]	US Football	6.84	NFL (Pro)	All NFL matches, 2 seasons	2013	USA
Kontos [69]	US Football	6.16	8 to 12 year old	468 players, 1 season	2013	USA

US football

Concussion is the third most common injury in US football, on average 5% of players are diagnosed with concussion per season [70]. There are 300,000 sports concussions that involve a loss of consciousness in the US each year and the majority of these are in US football [2]. The rate of concussion in US football was investigated by Myer et al. who studied all NFL concussions during 2012 and 2013. They concluded that an average rate of 6.43 concussions occurred per 1000 hours of play. This increased to 6.84 when players who suffered multiple concussion are included [68]. This is higher than the 5.56/1000 hours of play predicted in a survey of head trainers (coaches) [67]. The rate of concussion has been reported to be similar for high school players (5.6%) and college players (5.5%)[66].

Rugby

The United Kingdom Rugby Football Union (RFU) investigated the injury rates of professional rugby players from 2002 to 2018 and found that there was a rise from 3.2 concussions per 1000 match hours in the 2001/2002 season to 17.9 in the 2017/2018 season [61]. They concluded that this increase was partly due to a change in the reporting behaviour of players during this time. It also found that 16% of players suffered at least one concussion in the 2017/2018 season. In a survey of 172 professional rugby players in Ireland 45% reported suffering a concussion in one season (2010/2011) although only 46.6% of these were reported to medical staff [71]. This rate of concussion and reporting is similar in Irish amateur rugby [72].

Contact sports

A study which included many sports including soccer, basketball, volleyball, and water polo found that wrestling and martial arts had the highest risk of concussion at 23.5% for females and 19.3% for males. The study included 980 martial arts athletes [73]. This was approximately double that of any other sport in the study, but the study did not include US football, ice hockey or rugby. The most common injury in mixed martial arts is to the head [74].

Other sports

Koh et al. compared concussion rates in a number of sports between 1985 to 2000 [60]. They reported concussion rates of 9.05 for professional rugby, 3.6 for high school ice hockey, 0.18 for soccer, and 7.9 for amateur boxing (rates are quoted per 1000 hours played). In North America US football generally has been reported to have the highest rate of concussion in contact sports [75][76], although rugby and martial arts were not included in the analysis. The rate for ice hockey has been reported to be between 1.8

and 6.5 per 1000 game hours [77]. The rate of concussion in Gaelic football and hurling is relatively low (0.49 per 1000 hours) when compared to other sports [65].

2.3.5 Factors that affect the rate of concussion

Many factors have been reported to affect the risk of concussion, including the athlete's age, sex, position in a team sport, phase of play, and medical history. It also may depend on the definition or understanding of concussion within a particular sport, the ease of reporting, the attitude to self-reporting and whether a medical practitioner was available (i.e. on the side-line).

Concussion Males versus Females

In a study of a wide variety of US high school sports, Lincoln et al. found that males had twice the number of concussions when compared to females [64]. Although when they investigated sports which had a similar balance of male and female players (softball, basketball and soccer) females had a higher rate of concussion, 0.55 concussions per 1000 hours of play as opposed to 0.2 [64]. A higher rate of concussion in females has been reported in a number of studies and it is not known if this indicates a higher risk of concussion in females as compared to males or a difference in reporting behaviour [78][79].

Athlete Age and concussion

McIntosh et al. carried out a study of head, face and neck injuries in junior rugby in South West Australia during the 2002/2003 season [80]. The study included 1841 injuries and 1159 male junior athletes. 51% of the injuries were to older athletes in the U20s cohort, this decreased with age to 10% in the under 13s. It is likely that older players suffer more injuries due to the more competitive nature of the game and the greater energy involved in a head impact. The recovery time following a concussion does not appear to vary significantly with age [81].

2.3.6 Under-reporting of concussion

McCrea et al. in 2004 surveyed 1532 high school football players and found that 29.9% had a sustained a concussion but only 47.3% had reported their injury, usually to their trainer. The most common reason (66.4%) given for not reporting an injury was that they didn't think it was serious enough to warrant medical attention [82]. 41% said they did not want to leave the game and 22% said they did not want to let down their team-mates. In a study by Fraas et al. of 172 Irish rugby players in the 2010/2011 rugby season there were 92 concussions [71]. Only 46.6% of these concussions were reported to medical staff [71]. There is remarkable consistency in the rate of under-reporting rates of concussions, across different sports, with approximately 50% of concussions not being reported [71][72][82].

2.3.7 Summary of concussion in sport

Rugby, US football and boxing have substantially higher rates of concussion than other contact sports. It is difficult to directly compare the rates of concussion for rugby and US football as the definition of concussion in both sports has changed over time and even today may be different. The rate of concussion for mixed martial arts is not available. This will be covered in more detail in Section 2.4.1.

Concussion in sport has been identified in many countries as a significant health issue yet most countries do not maintain a database of the incidence of concussion [83]. Such a record would allow the rate and risk of concussion in various sports to be determined and compared. The benefit of sport is enormous both in youth and adult sports, but a better understanding of the risks would allow scientifically informed decisions to be made to reduce the risk.

2.5 The measurement of 6D head kinematics

To understand the injuries that athletes sustain following a head impact it is important to be able to measure the magnitude and direction of the head velocity and acceleration. Helmeted sports afford the simplest means of *in vivo* head kinematic measurements due to the space available within the helmet. Whereas unhelmeted sports require a sensor that is both unobtrusive and accurate.

2.5.1 Head Impact Telemetry System (HITS)

The Head Impact Telemetry System (HITS) was developed in 2002 by Simbex, Lebanon, US, to capture head impact data in US football (Figure 2-8). This system measures linear acceleration, and then calculates angular acceleration, impact location and impact duration. The data is transmitted to a side-line computer for real time analysis. The system uses six or nine accelerometers which are mounted elastically to couple them with the head and isolate them from the helmet shell. The computer processes the data and transforms the data to the centre of gravity of the head.

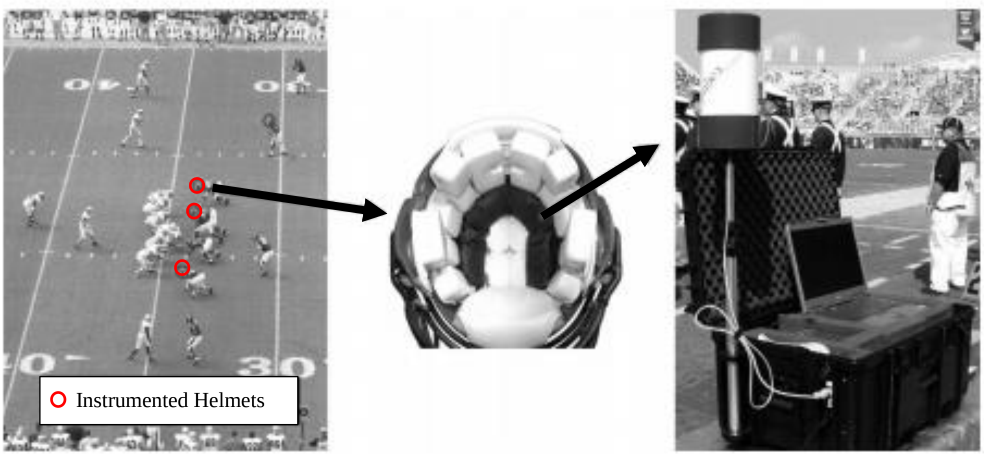

Figure 2-8: HITS system for measuring accelerations [84]

In 2008 the NFL published a database of 289,916 impacts recorded at 13 institutions, including seven high schools, using HITS. This data continues to grow and it is estimated that more than 2 million impacts have now been recorded [85]. This provides the largest data set in the world to analyse the mechanism of concussion and to identify parameters and injury criteria relevant to concussion. Much of the literature relating to concussion is derived from this database [86][87].

The most extensive study to date of the HITS database was that carried out in 2011 by Crisco et al. [88]. They analysed 314 players who wore the HITS system and suffered 286,636 impacts (above 10g) during the 2007, 2008 and 2009 US college football seasons. There was an average of 420 impacts per player with a maximum of 2492 impacts for one player. The distribution of the linear and angular acceleration magnitudes are shown in Figure 2-9. Frontal impacts were the most common, but impact location depended on the player position.

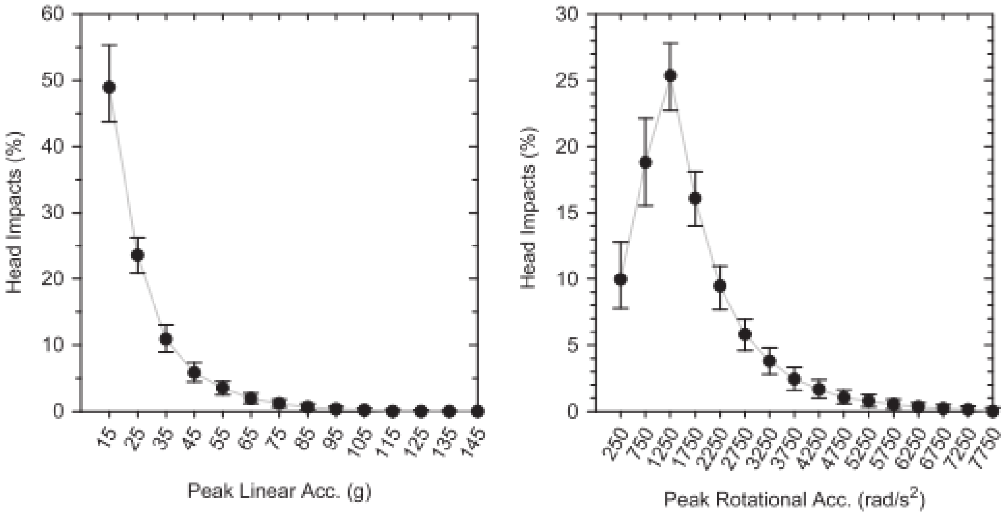

Figure 2-9: HITS sample data in collegiate American football players [88]

Accuracy

A validation study of the HITS system found that HITS overestimated peak linear acceleration (PLA) by 0.9% and underestimated peak angular acceleration (PAA) by 6.1% [85]. The study used a medium-sized US football helmet on a Hybrid III anthropomorphic dummy head. However Jadischke et al. determined that a large helmet should be used with a Hybrid III headform and this larger helmet increased the angular acceleration error to greater than 15% [89].

2.5.2 Instrumented skullcaps and headbands

Reebok, US have developed a sensor, Checklight, that is fitted into a skull cap. This sensor has an LED that changes state from green to yellow or red depending on the severity of an impact. This device has limited usefulness as it does not provide the raw acceleration data. The SIM-G sensor developed by Triax Technologies, Connecticut, US, is a sensor fitted into a headband. It consists of two tri-axial accelerometers, one for impacts up to 100g and the other for impacts over 100g. It also has a tri-axial gyroscope. Both the Checklight and SIM-G are shown in Figure 2-10.

.

Figure 2-10: Reebok Checklight (left) SIM-G (right)

2.5.3 Skin patch sensors

X2 Biosystems developed a commercial sensor (xPatch) that attaches to the mastoid bone behind the ear with double sided adhesive tape Figure 2-11. The xPatch consists of three single-axis accelerometers and three gyroscopes. Data from the device is transformed to the centre of gravity of the head using a rigid body transformation. Angular velocity from the gyroscopes is used to calculate angular acceleration with a five-point differentiation method [90].

Figure 2-11: xPatch placed on the mastoid bone behind the ear [91]

Nevins et al. investigated the accuracy of the xPatch by impacting a Hybrid III headform with projected soft-balls, lacrosse balls and soccer balls [92]. The chin and forehead were impacted with velocities ranging from 10 to 31m/s. They found that the linear acceleration reasonably agreed with a reference sensor (degree of correlation not stated), but that the angular acceleration was under-estimated by up to 25%. They attribute this under-estimation to the low sample frequency of the angular acceleration (400Hz) and the poor degree of coupling of the sensor to the skull. Due to the ease of application, the cost and the unobtrusive nature of the device it has been used in studies in women's soccer [93], rugby [94] and US football unhelmeted practice [95].

2.5.4 Instrumented mouthguards

Instrumented mouthguards have been in development for approximately 50 years. Most of the early devices were large and protruded from the mouth and were often hard-wired back to a fixed station. X2 Biosystems (Seattle, WA) developed a compact device with a tri-axial accelerometer and gyroscope which sampled linear acceleration at 1kHz and angular velocity at 800Hz. This mouthguard was used by King et al. in New Zealand to measure head impacts in amateur rugby during the 2013 season, however no concussions were recorded [96]. This is the only study which recorded *in vivo* head impacts in rugby.

Prevent Biometrics (a spin-off company from Cleveland Clinic, Ohio, US) have also developed an instrumented mouthguard. This mouthguard was tested in 2014 by Bartsch et al. to determine its accuracy. It was reported to have a linear acceleration error of 3% and an angular acceleration error of up to 17%. Correlation with reference sensors was high (R^2>0.99 for linear acceleration and R^2=0.98 for angular acceleration) [97].

Stanford University in collaboration with Intel Co. (California, US) have developed an instrumented mouthguard similar to the X2 mouthguard. The first version, shown in Figure 2-12 of this mouthguard collected linear acceleration data at 1kHz (bandwidth 500Hz) and angular velocity data at 800Hz (bandwidth 184Hz).

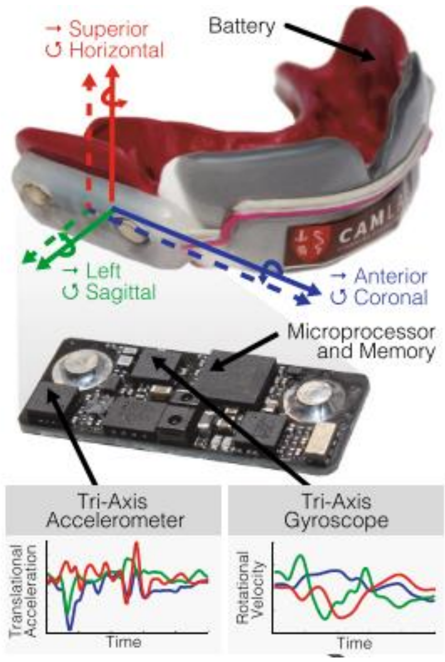

Figure 2-12: Stanford CAMLab instrumented mouthguard MiG1.0 [37]

A new version is now available, MiG2.0, which has upgraded the sample rate of the angular acceleration to 8kHz. An infrared sensor is used to detect the presence of the mouthguard in the mouth [98]. The errors for this mouthguard have been reported to be up to 9.9% for linear acceleration and 9.7% for angular acceleration [99]. A study using high-speed video to track the movement of the head compared the xPatch sensor, the Reebok Checklight, and the Stanford mouthguard during heading of a soccer ball [100]. They found that linear and angular accelerations were over-predicted by both the xPatch and the skull cap and that the mouthguard recorded the most accurate information. This study was limited in that the impact severity was low (<10g). The only published study in which the mouthguard (Stanford MiG2.0) was used *in vivo* to record a concussive impact was by Hernandez et al. in 2016 [37]. In Hernandez's study 513 video confirmed impacts were recorded in three sports: 73 in boxing, 19 in mixed martial arts and 421 in US football. Two cases of concussion in US football were recorded, one with a loss of consciousness and the other self-reported following the event. The loss of consciousness case had a peak linear acceleration of 106g and an angular acceleration of 12,900rad/s^2. The self-reported case had a peak linear acceleration of 85g and an angular acceleration of 7,040rad/s^2.

2.5.5 Summary of head impact measurement systems

The sensor systems with the greatest potential for unhelmeted sports are the SIM-G headband, the xPatch and instrumented mouthguards. This is primarily due to their unobtrusiveness and advanced state of development. This project investigated the repeatability and accuracy of the xPatch and SIM-G sensors as previous studies did not quantify their accuracy for typical concussive head impacts i.e. impacts with linear accelerations above 60g.

Instrumented mouthguards are the most accurate method of measuring head kinematics due to the high degree of coupling with the skull. They can now be manufactured in such a way as to be barely discernible from a regular mouthguard due to the miniaturisation of the electronics. Several research organisations and commercial companies are developing instrumented mouthguards including: Fitguard, California, US, Sports & Wellbeing, PROTECHT, Swansea, UK, Prevent BioMetrics, Ohio, US and CAMLab, Stanford University (Figure 2-13). To ensure optimum coupling with the skull the mouthguards are generally manufactured from a dental mould of an individual's teeth. Both Stanford and Prevent Biometrics are also investigating boil and bit versions. CAMlab at Stanford University tested both their own mouthguard, the Prevent mouthguard and the PROTECHT mouthguard. They found that all gave accurate measurements with average angular acceleration errors less than 13% [88]. It is expected that some or all of these companies will have these products commercially available in 2021.

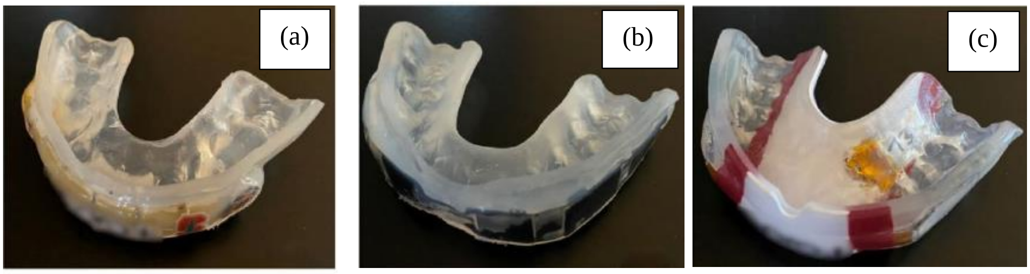

Figure 2-13: Instrumented Mouthguards (a) MiG2.0 Stanford, (b) Prevent BioMetrics and (c) PROTECHT

A collaborative agreement was setup with CAMLab at Stanford University to use their instrumented mouthguard MiG2.0 in this project. This is the first study to use the mouthguard in an unhelmeted sport and the first study outside the US. This mouthguard is currently not commercially available.

2.5 Simulation of head impacts

In vivo measurement of pressure and strain within the brain, during and following a head impact is currently not possible. Therefore, to help understand the brain's bio-mechanical response to an impact several research organisations have created finite element (FE) models of the head and brain. Kinematic data from either actual impacts or impact reconstructions is input to the model and the response of the brain is calculated in terms of pressure, stress and strain. Some of the more developed finite element head models are:

1. Global Human Body Model Consortium (GHBMC) incorporating the Wayne State University Head Injury Model (WSUHIM)
2. University College Dublin Brain Trauma Model (UCDBTM)
3. Strasbourg University FE Head Model (SUFEHM)
4. Kungliga Tekniska Högskolan FE Human Head Model (KTH FEHM)

5. Total Human Model for Safety (THUMS)

Material properties

All of the models use a combination of linear and non-linear material properties. The brain tissue is modelled as a Maxwell viscoelastic material (Equation 2-1) in all of the models with the exception of the KTH model which uses a second order hyper-viscoelastic Ogden model [101]. The UCDBTM model uses a Maxwell viscoelastic model as well as a Mooney-Rivlin material model [24] (Table 2-4).

$$G(t) = G_\infty + (G_o - G_\infty)e^{-\beta t}$$

$G(t)$ is the shear modulus, G_∞ is the long term shear modulus

G_o is the short term shear modulus, β is the viscoelastic decay constant

Equation 2-1: Maxwell shear relaxation equation [102]

The short term shear modulus G_0 determines the distortion of the brain during rapid load situations such as head impacts. A high shear modulus increases shear stress and reduces shear strain [103]. Care must be taken when comparing model results as the shear modulus across models can vary by a factor of up to 16.

Table 2-4: Brain model characteristics

Model	No of elements	Brain tissue material properties	Short term shear modulus	Long term shear modulus	Decay constant
KTH FEM [38]	18,416	Hyper elastic	N/A		
THUMS [104][105]	49,700	Linear viscoelastic	6kPa	2.32kPa	80ms
GHBMC [106]	314,500	Linear viscoelastic	6 to 12kPa	1.2 to 2.4kPa	125ms
ULP FEM [107]	16,824	Hyper elastic & viscoelastic	49kPa	16.7kPa	145s
UCDBTM [108]	26,000	Linear viscoelastic	10 to 22.5kPa	2 to 4.5kPa	80ms

Validation

All of the models in Table 2-4 have been validated against the same cadaver experiments [29][109][110][111][112]. The primary parameters used for validation tests were, pressure, brain motion and skull fracture. Details of the cadaver studies used in the validations are:

- Intracranial pressure has been compared with measurements from eight cadaver head impact tests carried out by Nahum et al. in 1977 [29], and six cadaver experiments by Trosseillie et al. in 1992 [109].
- Brain motion has been validated by comparison with Hardy et al.'s 35 tests on eight cadaver heads. The cadaver head was fitted with a US football helmet for half of these tests. They used a high speed bi-planar X-Ray system to track radio opaque markers inserted in the brain [110][111].
- Skull fracture was validated by comparison with static and dynamic cadaver tests carried out by Yoganandan et al. [112].

2.5.1 Wayne State University Head Injury Model (WSUHIM)

The WSUHIM finite element model has the largest number of parts and the greatest mesh density of all the models. The first version of the WSUHIM was developed in 1993 and was based on a 50^{th} percentile male (Figure 2-14). They obtained the geometry from MRI and CT scans and used Hypermesh and ANSYS ICEM to mesh the model. The model is compatible with both PamCrash and LS-Dyna explicit FE solvers. Since 1993 it has had many revisions, in particular it was modified in 1999 to allow relative motion between the brain and the cranium [110]. The model uses mostly brick elements with the exception of the pia, tentorium, arachnoid, falx, sinus dura and skin, which are modelled with shell elements. The cerebral spinal fluid (CSF) is modelled with solid elements with the bulk modulus of water and a very low shear modulus (0.1 to 0.5kPa). The latest version was validated by Mao et al. in 2013 [106]. This version has been incorporated into a total body model by the Global Human Body Model Consortium (GHBMC). The WSUHIM has been used in numerous studies, primarily in

US football [113][114]. In particular it has been used to develop strain thresholds for concussion [115][116], this is discussed in detail in Section 2.7.4.

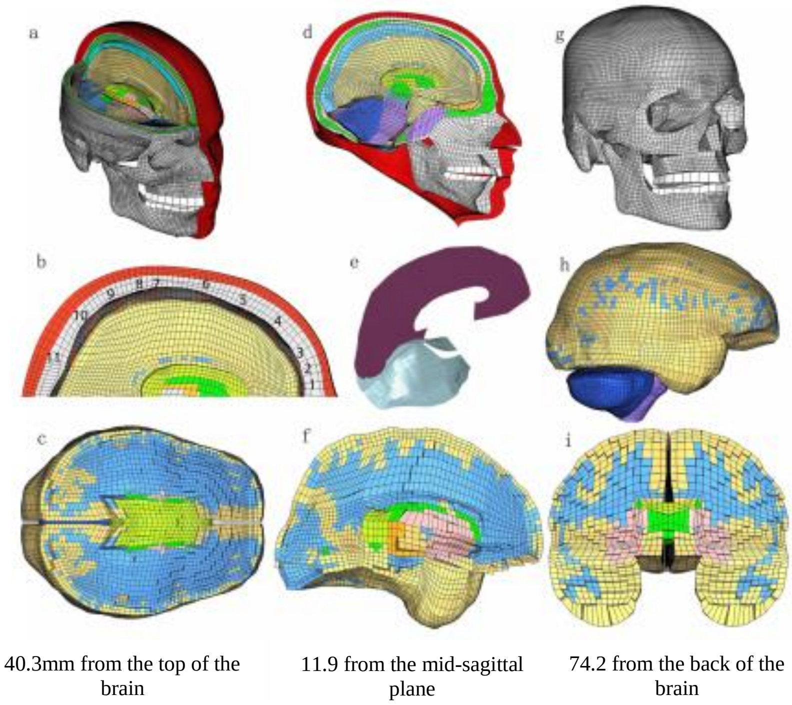

Figure 2-14: Wayne State University Head Injury Model [106]

From left to right: (a) isometric view of the head model with brain exposed; (d) medium sagittal view of the head model; (g) skull and facial bones; (b) 11 bridging veins; (e) falx and tentorium; (h) brain; and (c),(f),(i) brain sectional views in three directions (horizontal, sagittal, and coronal)

2.5.2 University College Dublin Brain Trauma Model (UCDBTM)

University College Dublin have developed their own head model and have validated it by comparing intracranial pressures and displacements with published cadaver tests [117][118]. The model geometry was based on MRI scans. It has approximately 26,000 elements and the material properties are similar to those used in the Wayne State model (Figure 2-15). This model has been used to study impacts in ice hockey [119][120], lacrosse [121] and the performance of equestrian and football helmets[122]. The model has also been used to investigate parameters that affect brain strain such as impact severity, location and duration [24][108][123][124][125].

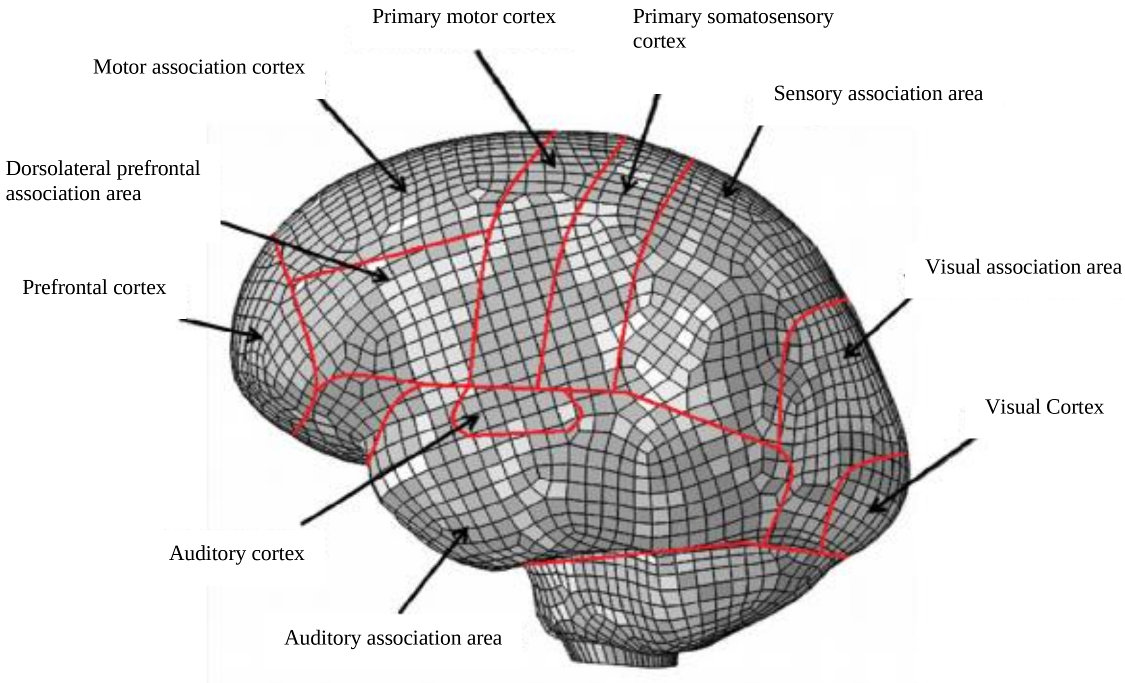

Figure 2-15: UCD FE model [123]

2.5.3 Strasbourg University FE Head Model (SUFEHM)

This model was developed in 1997 by Willinger et al. at the University of Strasbourg [126]. The geometry was created by digitising a skull and using Hypermesh to generate the mesh. It uses a combination of brick and shell elements. The CSF in the subarachnoid space is meshed with brick elements which have an elastic material model with a Young's modulus derived from modal analysis. It has been used to analyse motorcycle accidents, US football impacts and pedestrian impacts [107][127]. It has also been used to evaluate the safety of bicycle and motorcycle helmets [128][129]. Sahoo et al. used the model to develop a new criteria for brain injury based on axonal strain. They proposed that axonal strain was the best predictor of DAI injury with a 50% probability threshold of 14.65% strain [130].

2.5.4 Kungliga Tekniska Högskolan FE Human Head Model (KTH FEHM)

In 2002 Kleiven and Hardy from the Royal Institute of Technology (KTH), Stockholm, Sweden developed a head model consisting of 18,416 elements [101]. Unlike the other models which use a Maxwell viscoelastic brain tissue material the KTH model uses a Mooney- Rivlin hyperelastic law. The brain stem is assumed to be 80% stiffer than the grey matter. Similar to the Wayne State model, sliding is facilitated between the dura and the skull [131]. This model has been used in many studies including the simulation of the US football impacts that Pellman et al. recreated in a laboratory [132][133]. Giordano and Kleiven used the model to determine that axonal orientations are relevant and indicate the anisotropic nature of the axonal tissue [134]. Using the KTH model they have predicted that the maximum axonal strain for reversible injury is 0.07 in the corpus callosum and 0.15 in the brain stem [134]. They have also used the model to investigate the role of bridging veins in concussion but found that further work is required in this area to accurately model the rupture of the veins [135].

2.5.5 Total Human Model for Safety (THUMS)

The THUMS model is a total body model developed by Toyota Central R&D labs, Japan [136]. It is similar to the GHBMC in that it represents a 50^{th} percentile American male and is primarily used to investigate automobile accidents. The brain tissue is modelled with solid elements using viscoelastic material properties and includes sliding between the arachnoid layer and the skull. The model is designed as a base model with detailed sub models. The head model which consists of 49,700 elements has been used to simulated skull and facial bone fracture in vehicle and pedestrian impacts [104][137].

2.5.6 Summary of head models

This study selected the GHBMC as it is a validated and detailed model. The model is available to researchers under license from Elemance Ltd. North Caroline US. The

GHBMC model is a full body model of which the head and neck section were developed by Wayne State University. The head and neck model has been validated against cadaver experiments [134][106]. The head portion of the GHBMC and the Wayne State head model have been used to investigate concussion particularly in US football; these studies will be discussed in detail in Section 2.7.3. This study used the explicit solver LS-Dyna to run simulations on Amazon Web cloud computing Services (AWS).

2.5.7 Limitations of existing brain models

Some of the limitations of existing brain models include:

- Most models are validated using a limited number of cadaver impact tests; it is not known how the response of a cadaver is different to that of a living person.
- The measurements of pressure and displacement in the cadaver tests took place more than 20 years ago and were not as accurate as would be possible today.
- The devices used to measure the brain's response may have influenced the results.
- Generally, the models have been based on a 50th percentile male; work is ongoing to develop female and subject-specific models.
- More recent experiments have been performed on live humans using MRI scans but these, by their nature are limited to very low impacts well below injury level [138].
- The skull bone varies significantly in its thickness from location to location. It also consists of three layers; a layer of cancellous bone sandwiched between two layers of cortical bone, this level of detail is not usually included in the models.

- Biological tissues are often inhomogeneous, anisotropic and nonlinear, detailed mechanical properties for brain tissue are unavailable and many models use simplified isotropic linear and non-linear viscoelastic material models.
- The folded structure of the cerebral cortex is generally not considered in existing models. Consequently, the cerebrospinal fluid in the subarachnoid space between the skull and the brain is modelled as a uniform layer.
- Finally, the tolerance of the brain to pressure gradients, shear strains and stresses is not fully understood. Also, how or why this tolerance varies across individuals is unknown. Threshold values for injury are derived either from animal models, including rats, guinea pigs, and sheep, which are then scaled to represent human brain tissue or from cadavers. It is not known how accurately these relate to living human brain tissue.

Despite all these limitations finite element models contribute significantly to the understanding of the response of the brain to impact.

2.6 Concussion injury tolerance thresholds

John Stapp's pioneering work in the 1940s investigated the effect of deceleration on volunteers, including himself. He demonstrated the effectiveness of safety harnesses which lead to the modern car seat belt. Following Stapp's work researchers in Wayne State University in Detroit subjected cadavers and animals to blunt impacts, and measured the linear deceleration, the duration of the impact and the brain damage experienced by the models. From this work, they developed the Wayne State Tolerance curve shown in Figure 2-16. In 1972 the US National Highway Traffic Safety Administration (NHTSA) developed a mathematical equation (Equation 2-2) based on the Wayne State Tolerance Curve.

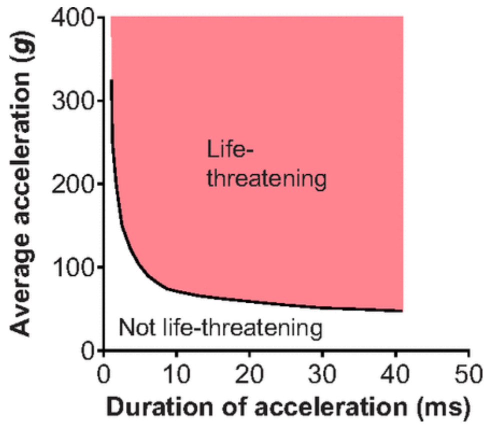

Figure 2-16: Wayne State Tolerance Curve [139]

The Head Injury Criteria (HIC) formula is used today in assessing impacts, in particular car collisions. A HIC_{36} value in excess of 1000 is used to predict an Abbreviated Injury Scale (AIS) of between 2 and 3. An AIS of 2 or 3 in turn relates to a moderate or severe concussion with or without skull fracture (Table 2-1) [139].

$$HIC = max\left[\frac{1}{t_2 - t_1}\int_1^2 adt\right]^{2.5}(t_2 - t_1)$$

$$t_1 = initial\ time\ of\ impact, t_2 = final\ time\ of\ impact, a = acceleration$$

Equation 2-2: HIC Formula

The Wayne State curve and HIC formula are based on time and linear acceleration only and do not include angular acceleration. Following experimental work with animals Gennarelli et al. proposed that concussion is primarily due to angular accelerations [36]. Head impact investigations should therefore include both linear and angular accelerations in their analysis.

2.6.1 Kinematic injury criteria

Many research organisations have tried to establish kinematic measures to predict a concussive injury. Most of this work has focused on US football due to the availability of data from the HITS system and the relatively high rate of concussion. The only other option, up to now, to acquire kinematic data from head impacts was to recreate the impact in a laboratory with anthropomorphic dummies or using kinematic simulation software such as MADYMO, Helmond, Netherlands. A summary of studies which have used both HITS data and recreated head impacts is presented in Table 2-5.

In 2003 Pellman et al. used video analysis of American football games to recreate 31 impacts that resulted in a concussion [140]. They used helmeted Hybrid III dummies in a laboratory and reconstructed the velocity, direction and kinematics of the collisions from the game videos.

Table 2-5: Linear and angular acceleration thresholds for concussion

Author	Linear Acceleration		Angular Acceleration		No. Cases	Impact	Sport	Method	Year
	No Injury	Concussion	No Injury (rad/s^2)	Concussion (rad/s^2)	No Injury	Concussion			
Wilcox [141]		43g (11.5g)		4029.5 (1243)	58	4	Ice Hockey	HITS	2015
McIntosh [142]		103.45g	4300 (3657)	7951 (3562)	40	13	Australian Football	Kinematic simulation	2014
Rowson [4]	26g (19g)	104g (30g)	1072 (850)	4726 (1931)	62974	37	US Football	HITS	2013
Rowson [143]			1230 (915)	5022 (1791)	300977	57	US Football	HITS	2011
Reed [144]	22.1g		1557.4		1821	0	Ice Hockey	HITS	2010
Stojsih [145]	191g max.		17156 max.		60	0	Boxing	Modified HITS	2010
Broglio [49]	25.1g	105g	1626	7229.5	54247	13	US Football	HITS	2010
Guskiewicz [86]		114.6g (54.1g)		5312	88	13	US Football	HITS	2007
Pellman[146] [140]	60g (24g)	98g (28g)	4029 (1438)	6432 (1813)	182	31	US Football	Lab re-construction	2007
Duma [84]	32g (25g)	81g	2022 (2042)	5595	3311	1	US Football	HITS	2005
Newman [147]	54.3g	97.9g	4159	6664	33	25	US Football	Lab re-construction	2000

Note: Standard Deviation shown in brackets.

They found that the average linear acceleration for concussive impacts was 78 (+/-28g) to the facemask and (112g +/- 5g) for other locations. The overall average linear acceleration was 98g (+/-28g) for concussive cases and 60g (+/- 24g) for non-injurious cases. The typical duration of an impact was 15ms. From this work the NFL concluded that there was a 75% probability of a concussion if the resultant linear acceleration was greater than 98g. This was questioned by some researchers, for example:

- Schnebel et al. in a study of 62,480 impacts, reported only 6 concussions out of 620 impacts whose accelerations were above 98g [49].
- Broglio et al. fitted 35 high school players with the HITS instrumented helmets for the 2007 football season. They recorded 19,224 impacts (greater than 10g) [87]. Of those recorded 78 impacts exceed the NFL threshold of 98g but only 5 had diagnosed concussive injuries.

They concluded that the NFL threshold may need to be re-examined or that other variables, such as impact location and angular acceleration need to be considered. Gustiewicz et al. used HITS to record the impacts of 88 collegiate football players from 2004 to 2006, during this time there were 13 concussions with linear accelerations from 60.5g to 168.7g [86]. The authors concluded that they could find no significant relationship between the magnitude of the acceleration (linear or angular) and the incidence of concussion. One of the few studies on unhelmeted impacts in sport, by McIntosh and Patton in 2014, focused on Australian rules football. They used MADYMO software to recreate 13 non-concussive impacts and 27 concussive impacts [142]. They found that the mean peak linear acceleration and mean peak angular acceleration was 103.4g and 7951rad/s^2 for concussive injuries and 59g and 4300rad/s^2 for no injury. The study concluded that acceleration, linear or angular, alone is not a good predictor of concussion.

Criteria that combine linear and angular acceleration

Most head impacts will have both linear and angular accelerations, hence researchers have sought to incorporate both in a formula that can be used to predict the possibility of concussion. Following a large study by Broglio et al. of 54,247 impacts in the HITS database, which included 13 concussive impacts, they developed a flowchart for improving the identification of concussion [49]. They filtered the data based on linear accelerations greater than 96.1g, impact location (front, side and top) and angular acceleration in excess of 8445.6 rad/s^2. Using these criteria, they reduced the number of suspect impacts to 47, 10 of which were concussive injuries. There were three concussions which the flowchart did not detect. Greenwald et al. also used the HITS data, in 2008, to develop the weighted Principal Component Analysis (wPCA) criteria [148]. This used linear acceleration, angular acceleration, and HIC to come up with a single number to predict concussion. This study was based on 449 US football players over three football seasons but only 17 concussions. They found only a 75% positive prediction rate. Interestingly in this paper they noted a large variation in false response rates for individual players: there were individual players who sustained large impacts but did not sustain a concussion while others sustained a concussion with relatively minor impacts. They concluded that every individual has a unique head injury tolerance. Rowson and Duma undertook the largest study of the HITS database to determine a kinematic threshold that related to concussion [4]. They determined that concussive impacts had an average linear acceleration of 104 ± 30g and angular acceleration of 4726 ± 1931rad/s^2. This study was based on a statistical analysis of all the concussion data from the HITS database and NFL data (from the recreation of impacts using Hybrid III crash dummies in the laboratory). The data consisted of 62,974 sub-concussive impacts and 37 diagnosed concussive impacts. Due to under-reporting they calculated that the rate of concussions should have been 244. From this data they developed the Combined Probability relationship (Equation 2-3) to predict the possibility of concussion. This includes both linear and angular accelerations as shown in Figure 2-17.

$$CP = \frac{1}{1 + e^{-(-10.2+0.0433a+8.73x10^{-4}\alpha-9.2x10^{-7}a\alpha)}}$$

CP: Combined Probability, a = linear acceleration, α = angular acceleration

Equation 2-3: Combined prediction model [4]

They concluded that combined probability is a better predictor of concussion than angular acceleration alone but only marginally better than linear acceleration. On examining the HITS database, they achieved 90% true positive rate and a false positive rate of 4% whereas linear acceleration alone achieved a false positive of 4.9% (Figure 2-17).

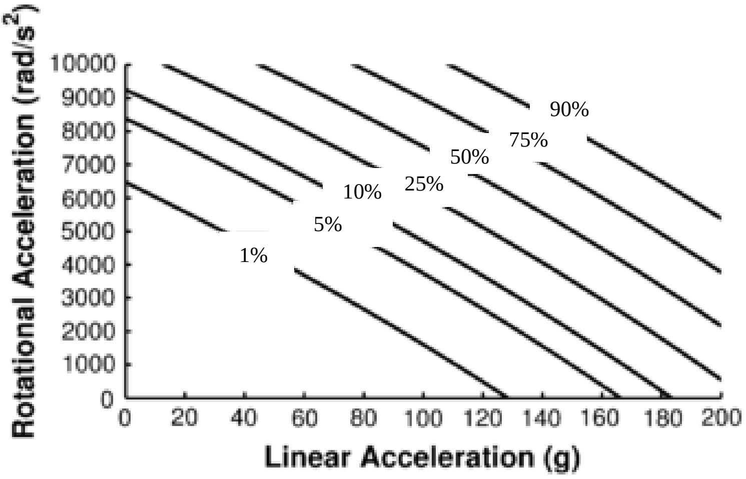

Figure 2-17: Combined probability [4]

The Brain Injury Criteria (BrIC) measure measure was developed by the US National Highway Traffic Safety Administration and is shown in Equation 2-4 [149]. It is based on angular velocity only and is used in the analysis of injuries resulting from vehicle collisions. This criterion was developed by determining the angular velocities that causes particular strain levels within the brain. Although BrIC has been used in concussive studies it was primarily developed to predict AIS+4 injuries (severe life threating injuries). Following human volunteer testing it has been suggested that it is inappropriate for the analysis of concussive injuries as the head was found to tolerate high angular velocities (25rad/s), with low angular accelerations [150].

$$BrIC = \sqrt{\left(\frac{\omega_x}{\omega_{xc}}\right)^2 + \left(\frac{\omega_y}{\omega_{yc}}\right)^2 + \left(\frac{\omega_z}{\omega_{zc}}\right)^2}$$

$\omega_{x,}$ $\omega_{y,}$ and ω_z are maximum angular velocities about x,y and z axes

$\omega_{xc,}$ $\omega_{yc,}$ and ω_{zc} are the critical angular velocities

Equation 2-4: Brain Injury Criteria [149]

In 2000 Newman et al. proposed the Head Impact Power (HIP) criteria, shown in Equation 2-5 [151]. This criterion has the advantage of incorporating linear and angular acceleration, duration and direction (as individual axis components are included). [151]. This criterion has the advantage of incorporating linear and angular acceleration, duration and direction (as individual axis components are included).

$$HIP = \left[ma_x \int a_x dt + ma_y \int a_y dt + ma_z \int a_z dt + I_{xx} \propto_x \int \propto_x dt \right.$$
$$\left. + I_{yy} \propto_y \int \propto_y dt + I_{zz} \propto_z \int \propto_z dt\right]$$

m =mass of the head, I_{xx}, I_{yy} and I_{zz} = moments of inertia of the head around the X,Y and Z axes

a_x, a_y and a_z =linear accelerations of the head in the X,Y and Z directions

α_x, α_y and α_z =angular accelerations of the head around the X,Y and Z axes

Equation 2-5: Head Impact Power (HIP) [151]

Newman et al. recreated 12 US football impacts which included 24 players and 9 concussions. They determined that there was a 5%, 50% and 95% probability of concussion from HIP values of 4.7, 12.79 and 20.88kW, respectively [151].

A comparison of kinematic injury criteria that included linear acceleration only, angular acceleration only and a combination of both linear and angular acceleration was carried out by Hernandez et al. using concussive data from US football [150]. They found that peak angular acceleration was the best predictor of injury followed by HIP. Other criteria such as linear acceleration alone, HIC and BrIC performed poorly.

2.6.2 The Influence of impact direction and duration

Impact direction

A number of studies have shown that lateral translational impacts to the temporal region are more likely to cause mTBI than anterior or posterior impacts [4][152]. This was also found by Delaney et al. when he studied 69 concussions in American football, soccer and ice hockey [153] and also by finite element studies in Wayne State University by Zhang et al. [154]. McIntosh et al.'s study on Australian football found that there was a significant difference between the location of the impact in concussive and non-concussive cases: 60% of concussive cases were impacted in the temporal region, compared to 23% of non-concussive impacts [142]. This was similar to Rowson et al. who found that 57.9% of concussions in US football were to the side of the head (sagittal direction) [4]. It has been found that lateral impacts cause motion of the falx cerebri and that this motion causes high strains in the corpus callosum leading to injury [42].

This project includes a study to investigate the role that impact direction has on brain strain. This included an investigation on whether this change in strain was due to the energy of the impact or the magnitude of the head acceleration. This study is included in Chapter 6 – "The effect of impact location on brain strain" [155].

Impact duration

Longer impact durations increase the strain within the corpus callosum thus increasing the risk of injury [24]. The duration of impacts is dependent on the impact surface and any head protection worn (Figure 2-18). Falls onto hard surfaces have durations of less than 5ms whereas unhelmeted sports impacts have a typical impact duration of 5 to 10ms. It is difficult to compare impact durations across studies as generally the method of calculation has not been specified. In laboratory studies it is assumed that the duration is the time the resultant acceleration is above zero. The same method is not appropriate for data collected *in vivo* as a lower threshold is required to avoid including spurious data. Unhelmeted impacts have a shorter duration than padded helmeted impacts such as those that occur in US football [156]. Impacts in US football have been reported to have a linear acceleration duration from 15ms [157] to 30ms [158], while the linear acceleration in pedestrian head impacts is between 9 to 14.5ms [159].

Hoshizaki et al. concluded that in short duration impacts (<10ms), such as falls onto concrete, the linear acceleration interacted with the angular acceleration to produce high strains in the corpus callosum [24][125]. For longer duration impacts (>10ms), such as those in US football the strains are dependent on angular acceleration alone [24][125]. A simulation study by Yoganandan et al. found that the risk of head injury was a function of both the magnitude of the head acceleration and the duration of an impact. The study determined that an angular acceleration of 5krad/s^2 over 25ms had a similar risk of injury as an angular acceleration of 50krad/s^2 over 5ms [154].

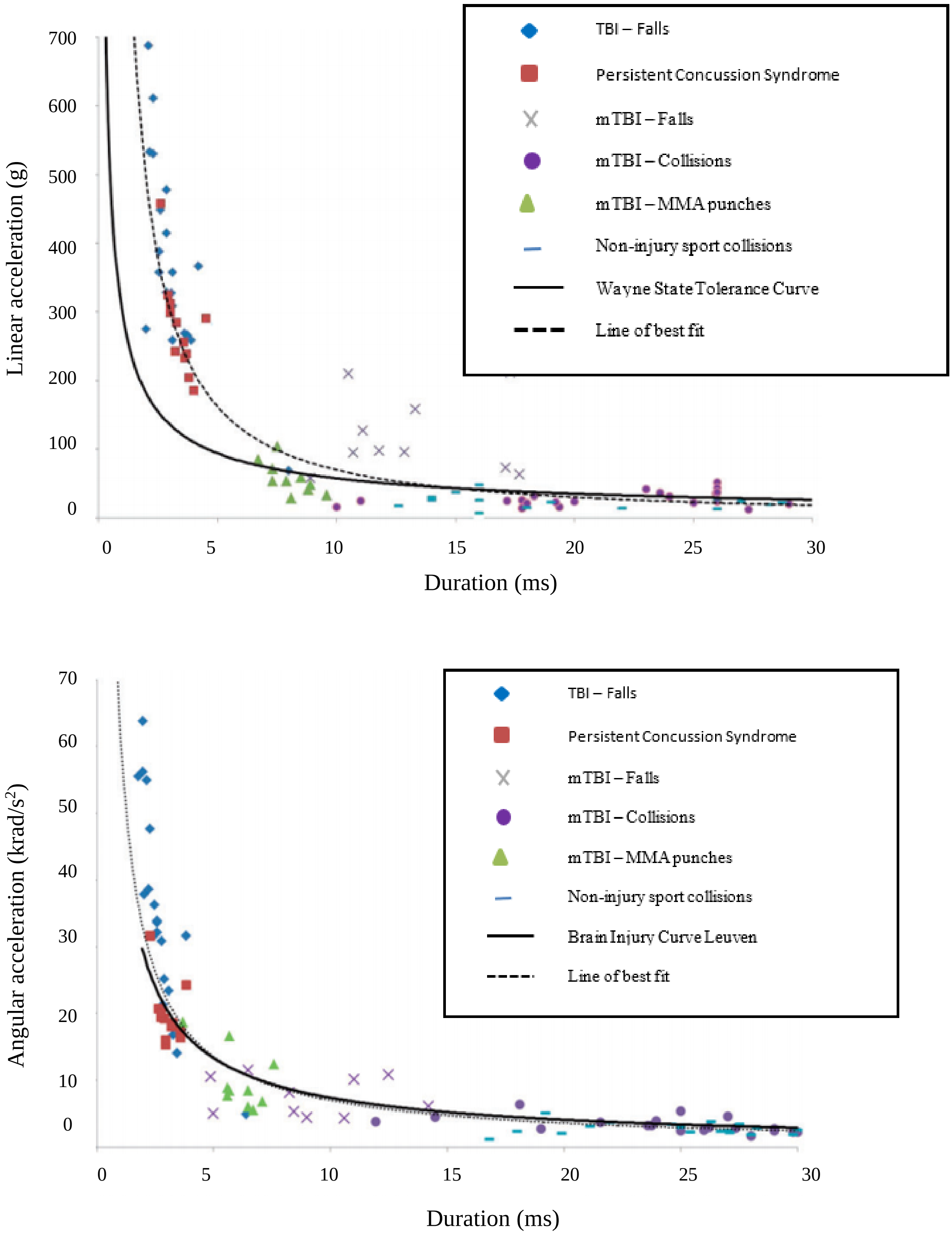

Figure 2-18: Impact duration versus acceleration [125]

2.6.3 Summary of kinematic injury predictors

Linear acceleration has been found to be the best three degree of freedom predictor of concussion [4][158]. Resultant linear accelerations in excess of 98g in US football have been associated with injury [140]. Many testing standards use linear acceleration alone including the European New Car Assessment Program (NCAP) automotive crash tests and bicycle helmet impact tests which are based on impacts of 250g (European Helmet Standard EN1078).

Angular accelerations of between 4030rad/s^2 [141] and 7230rad/s^2 [49] have been associated with concussion in helmeted sports. It is likely that the wide range of angular acceleration is due to the differing degree of injury severity, the lack of concussive data and the accuracy of the measurement system (HITS).

Lateral impacts causing rotations in the coronal and transverse planes have been found to be more likely to result in concussion [4][152]. Also the duration of the impact is correlated with increases in strain within the corpus callosum [24][125].

Criteria such as HIP that combine the magnitude of the linear and angular acceleration, impact direction and impact duration should provide a better kinematic predictor of concussion than linear or angular acceleration alone. HIP values of 12.79 and 20.88kW, have been associated with a 50% and 95% risk of injury, respectively [151]. It has been shown that kinematic measures alone aren’t the best predictors of concussion as they don’t account for brain distortion [158]. Simulation studies are required to investigate criteria that measure brain stress and strain.

2.6.4 Injury criteria based on finite element head simulations

Researchers have sought to determine brain tissue thresholds for concussive injuries as it is thought that these would be more reliable than kinematic measures. Some studies have focused on testing the tolerance of animal brain tissue to strain whilst others have used simulation models to investigate the pressure, strain and stress in the brain following an impact. Generally, kinematic data acquired from in vivo measurements or accident re-constructions is used to define the boundary conditions for simulation models. Some of the criteria from these studies are presented in Table 2-6.

Viano et al. used the WSUHIM to simulate the impacts in US football that Pellman and Newman had recreated in the laboratory [160]. The objective was to correlate the forces and accelerations of the impacts with the clinical characteristics of the player's injuries. Viano modelled impacts to the temporal lobe as these formed the majority of the concussive cases. He found that the early response of the brain was associated with the magnitude of the linear acceleration and occurred approximately 8ms after impact. The mid-term response (after 18ms) was to the temporal lobe on the opposite side (confirming the coup contra-coup response), and the late response (after 22ms) was to the mid brain, including the fornix and corpus callosum [146].

Pressure

Ward et al. stated that intracranial pressures above 235kPa will result in serious brain damage and below 173kPa will not be injurious [29]. In a study Zhang et al. reconstructed 12 head impacts in US football using WSUHIM [114]. They found the expected coup contrecoup pressure response and a transient pressure wave through the brain was evident. Intracranial average coup pressure in concussive cases was 90kPa and had a high correlation with linear acceleration (R^2 = 0.77). Zhang et al. concluded that the higher pressures found by Ward et al. were associated with more serious injuries such as a contusion or cerebral cortex haemorrhage and that pressure was not a good indicator of concussion.

Strain

High strain in the corpus callosum has been shown by a number of studies to be related to concussion injuries [37][38][39]. McAllister et al. simulated impacts in US football and ice hockey and determined that concussed athletes had an average strain in the corpus callosum of 0.28. This correlated with changes in white matter integrity which they determined using fractional anisotropy in MRI scans [39]. Hernandez et al. [37] also found that maximum principal strain in the corpus callosum was the best indicator of concussion in a study which compared kinematic measures to brain distortion measures [42]. They used diffusion tensor imaging to confirm the trauma to the corpus callosum. The average strain in Hernandez's study was 0.3, which was considerably higher than Kleiven's [161] earlier study which found an average strain of 0.21 in concussed athletes. This difference in strain might be explained by the difference in the number of cases in the two studies. Kleiven's study was based on 33 concussed US footballers whilst Hernadez's study had only 2 cases of concussion, one of which was severe and involved a loss of consciousness. In one of the only studies of concussion in unhelmeted sports Patton et al. used kinematic data from reconstructions to simulate impacts in Australian rugby and football [38]. They reported an average strain of 0.31 in the corpus callosum in the cases of concussion. They determined that there was a 50% probability of concussion if strain exceeded 0.15.

Stress

Stress has been investigated by very few studies presumably because it has a direct relationship to strain. In one of the few studies conducted, Von Mises stress was found to correlate with neurological lesions and that Von Mises stress in excess of 18kPa was associated with a 50% risk of moderate neurological lesions [162]. Severe brain injury was associated with Von Mises stresses in excess of 38kPa [162]. These findings are similar to an experimental study on head injuries in sheep which found that a stress of 27kPa was associated with brain injury [163].

Shear Stress

Shear stress in the brain stem has been found to correlate with angular acceleration (R^2 = 0.78) [164]. In a study by Zhang et al. in 2004 they reported that the shear stress in the thalamus differed by 58.5% between concussed and uninjured athletes, but they did not report the shear stress in the corpus callosum [114]. They found that there was an 80% probability of concussion due to DAI if shear stresses in the brain stem exceed 10kPa [164]. Shear stress is dependent on the time-dependent shear modulus of the viscoelastic brain tissue. Hence care must be taken in comparing shear stress and strain magnitudes across studies as the material properties vary with different head models and with different revisions of these models.

Strain Rate

Zhang et al. hypthosised that concussion was related to strain rate in the brain stem and mid-brain. To investigate this they simulated US football impacts using kinematic data from Pellman and Newman's laboratory re-creations [160]. They found that strain rates in the mid-brain of 60 to $80s^{-1}$ were associated with concussion while strain rates in excess of $100s^{-1}$ were related to unconsciousness [165]. A 50% probability of concussion has been predicted for strain rates in the corpus callosum of $48.5s^{-1}$ [161].

Table 2-6: Brain injury thresholds

Strain Criteria

Author	Year	Study	Model	Number of Cases: Uninjured	Number of Cases: Concussed	Strain Threshold	Comment
Shreiber, Bain, Meaney [166]	1997	Rat head impact tests	Rat brain model	N/A	N/A	0.19	50% probability of blood brain barrier damage
Bain, Meaney [167]	2000	Guinea pig optic fibre tests		N/A	N/A	0.21 white matter	Morphological damage
Zhang [114]	2004	NFL re-construction*	WSUHIM	15	9	0.18 white matter	50% probability of mild TBI
Viano [168]	2005	NFL re-construction *	WSUHIM	6	22	0.34 mid-brain 0.38 thalamus	Average values for concussed cases
Kleiven [132]	2007	NFL re-construction*	KTH	25	33	0.21 in corpus callosum.	50% probability of concussion
Deck [159]	2008	Accident re-construction	SUFEHM	N/A	68	0.31	50% probability of diffuse axonal injury
Kimpara [169]	2012	NFL re-construction*	THUMS	25	33	0.32 mid brain	50% probability of concussion
McAllister [39]	2012	Ice hockey & NFL	Dartmouth	N/A	10	0.28 corpus callosum	Mean of concussive cases
Patton, McIntosh, Kleiven [38]	2013	Australian Football & Rugby	KTH	27	13	0.15 corpus callosum 0.31 corpus callosum	50% probability of concussion Average of concussed cases
Mao [106]	2013	Validation & case study	GHBMC (ver. 2013)	5	1	0.265	Contusion
Giordano [134]	2014	NFL re-construction*	KTH	25	33	0.13 corpus callous	50% probability of concussion
Post [170]	2014	11 falls, 8 collisions and 2 projectiles	UCDBTM	N/A	21	0.48 grey matter 0.38 white matter	Maximum strain
Hernandez, Wu [37]	2016	NFL, Boxing, & MMA	KTH	513	2	0.3 corpus callosum	Maximum strain
Sanchez [171]	2019	NFL re-construction*	GHBMC	25	33	0.39	Median strain study using corrected accelerations

Strain Rate Criteria

Author	Year	Study	Model	Number of Cases: Uninjured	Number of Cases: Concussed	Strain Rate Threshold	Comment
Kleiven [161]	2007	NFL re-construction*	KTH	25	33	48.5 s^{-1}	50 % probability of concussion
Zhang [165]	2003	NFL re-construction*	WSUHIM	20	33	60 s^{-1}	50% probability of concussion
McAllister [39]	2012	Ice hockey & NFL	Dartmouth		10	54.3 s^{-1}	Mean in corpus callosum
Sahoo [130]	2008	Accident re-construction	SUFEHM		109	80 s^{-1}	50% probability of diffuse axonal injury

*Same US football data from laboratory re-constructions by Newman et al. [172][147]

Other Parameters

Viano et al. of Wayne State University proposed that the product of strain rate and strain may be the best indication of concussion but this has not been reported in other studies [160]. More recently axonal strain has been investigated by Kleiven et al. [134] and Willinger et al. [130]. Kleiven et al. found that an axonal strain of 7% in the corpus callosum and 15% in the brain stem indicated a 50% probability of injury [134]. While Willinger et al. determined an axonal strain of 14.65% indicated a 50% risk of DAI [130]. Axonal injury typically takes place where there is a change in tissue density such as between the grey and white matter [173]. An example of this change in tissue density occurs in the brain stem and corpus callosum [174]. The investigation of axonal strain requires that the brain tissue is modelled anisotropically. One method of doing this is to use a macroscale model and a microscale model to simulate the detail at a cellular level [175]. The other alternative is to incorporate anisotropy and heterogeneity into existing models [130]. This approach is beyond the scope of the studies reported in this thesis.

2.6.5 Summary of brain distortion injury criteria

Maximum principal strain (MPS) in the corpus callosum and brain stem are the most widely used criteria to investigate concussive injuries. Viano et al. identified strain 'hot spots' in the fornix, midbrain, and corpus callosum of concussed athletes [113]. They determined that these 'hot spots' were significantly correlated with removal from play, cognitive and memory problems, and loss of consciousness. MPS in the corpus callosum was found to be an effective indicator of concussion [133][39] with average strains in concussed athletes between 0.21 [161] and 0.3 [37]. MPS in the core brain regions (corpus callosum, thalamus, mid-brain and brain stem) will be used in this study due to its proven relationship with concussion and the large body of data available, primarily from US football, Caution needs to be used in comparing stress and strain values across studies as they are dependent on the short and long-term shear modulus of the brain tissue. The time-dependent shear modulus dramatically increases the stiffness of the brain tissue for rapidly applied loads [166].

2.7 Mixed martial arts

This project originally planned to investigate head impacts in amateur rugby in Ireland by attaching skin patch sensors to the athletes' head. This was found to contravene World Rugby Regulation 12 (Provisions relating to players' dress). Mixed martial arts (MMA) was then identified as a suitable contact sport for the investigation of head impacts. The primary reasons for this selection were:

- Only two athletes are involved (only one of whom is being monitored)
- Sparring and competitive bouts are of a limited duration (15 minutes)
- Events take place in a confined arena that facilitates video recording
- There is a high rate of head impacts and injuries
- Both the athletes and the trainers were willing to take part in the study.

2.7.1 Mixed martial arts background

Mixed martial arts (MMA) is a competitive, full-contact sport that involves an amalgamation of elements drawn from boxing, wrestling, karate, taekwondo, jujitsu, Muay Thai, judo, and kickboxing [176]. The current version of MMA began in 2001 with the sale of the Ultimate Fighting Championship (UFC) franchise to Zuffa, LLC [177]. They repositioned the sport with the introduction of new rules, weight classes and time limits. These changes helped legitimise the sport and return it to pay-per-view television. In 2016 Zuffa was sold for $4 billion [178]. Currently there are approximately 1.05 million participants in MMA in the US [179].

Fights normally consist of three 5 minute rounds with championship fights consisting of five 5 minute rounds. The fighters do not wear head protection but wear 110g to 170g gloves. The fight may end prematurely due to knock-out (KO), submission (one fighter concedes victory to the other by tapping the mat or his opponent with his hand), or stoppage by the referee, the fight doctor, or a competitor's corner-man. As MMA involves a more diverse physical interaction between the athletes than boxing, it may result in higher injury rates yet less significant head trauma [180][181]. Boxers are limited to hitting their opponent in the head and body whereas MMA fighters can use a multitude of fighting techniques with the inclusion of wrestling and Brazilian jiu-jitsu.

2.7.2 Injuries in mixed martial arts

In a ten-year review by Buse et al. in 2006 they found that head trauma was the single biggest reason for match stoppages (28.3% of match stoppages) [182]. Another study of 844 MMA fights found that 12.7% of matches were stopped because of knock outs and that it took the referee an average of 3.5 seconds after the knock out to stop the match; during this time the fighter suffered an additional 2.6 strikes to the head [176]. They also found that 19.1% of matches were stopped due to a technical knockout (TKO) (partial loss of responsiveness), in the 30 seconds preceding the stoppage the fighter suffered an average of 17.1 strikes to the head. A third of MMA fighters have reported suffering a TKO and 15% have suffered from a KO, having participated in MMA for an average of 5.8 years [183]. A one year study of 13 MMA fighters found cortical thinning and reduced memory and processing speed when compared to controls (n=14) [184].

2.7.3 Mixed martial arts in Ireland

Safe MMA was setup in 2012 in the United Kingdom and was extended in 2013 to include Ireland. Safe MMA was founded by UK promoters and medical experts to regulate and improve the medical standards in the sport. Fighters need clearance from Safe MMA to be allowed to compete. Safe MMA require a yearly medical, six-monthly blood tests, and pre- and post-fight medical checks.

2.8 References

[1] P. McCrory, W. Meeuwisse, J. Dvorak, M. Aubry, J. Bailes, S. Broglio, *et al.*, “Consensus statement on concussion in sport: the 5 th international conference on concussion in sport held in Berlin, October 2016,” *Br. J. Sports Med.*, p. bjsports-2017-097699, 2017.

[2] J. A. Langlois, W. Rutland-Brown, M. M. Wald, and T. E, “The epidemiology and impact of traumatic brain injury: a brief overview.,” *J. Head Trauma Rehabil.*, vol. 21, no. 5, pp. 375–8, 2006.

[3] M. R. Elliott, S. S. Margulies, M. R. Maltese, and K. B. Arbogast, “Accounting for sampling variability , injury under-reporting , and sensor error in concussion injury risk curves,” *J. Biomech.*, vol. 48, no. 12, pp. 3059–3065, 2015.

[4] S. Rowson and S. M. Duma, “Brain Injury Prediction: Assessing the Combined Probability of Concussion Using Linear and Rotational Head Acceleration,” *Ann. Biomed. Eng.*, vol. 41, no. 5, pp. 873–882, 2013.

[5] A. King, K. Yang, and L. Zhang, “Is head injury caused by linear or angular acceleration,” *IRCOBI Conf.*, no. September, pp. 1–12, 2003.

[6] H. Zetterberg, D. Wilson, U. Andreasson, L. Minthon, K. Blennow, J. Randall, *et al.*, “Plasma tau levels in Alzheimer’s disease,” *Alzheimer’s Research and Therapy*, vol. 5, no. 2. BioMed Central, p. 9, 28-Mar-2013.

[7] T. A. Gennarelli and E. Wodzin, “AIS 2005: A contemporary injury scale,” *Injury*, vol. 37, no. 12, pp. 1083–1091, 2006.

[8] M. Putukian, “The Acute Symptoms of Sport-Related Concussion: Diagnosis and On-field Management,” *Clin. Sports Med.*, vol. 30, no. 1, pp. 49–61, 2011.

[9] J. Michael Tyszka, D. P. Kennedy, R. Adolphs, and L. K. Paul, “Intact bilateral resting-state networks in the absence of the corpus callosum,” *J. Neurosci.*, vol. 31, no. 42, pp. 15154–15162, Oct. 2011.

[10] C. J. Charvet, R. B. Darlington, and B. L. Finlay, “Variation in human brains may facilitate evolutionary change toward a limited range of phenotypes,” *Brain Behav Evol.*, vol. 2013, no. 2, pp. 74–85, 2014.

[11] L. Heimer, *The human brain and spinal cord: functional neuroanatomy and dissection guide.* 1995.

[12] L. Fei, H. Ning, L. Yuanyuan, and C. Lizhou, “MRI shows disrupted connections in the brains of young people with ADHD,” *Radiological Society of North America*, 2014. .

[13] F. Martini and J. Nath, *Fundamentals of Anatomy and Physiology*, vol. 7th, no. 1.

2009.

[14] D. F. Meaney and D. H. Smith, “Biomechanics of Concussion,” *Clin. Sports Med.*, vol. 30, no. 1, pp. 19–31, 2011.

[15] J. J. Pritchard, J. H. Scott, and F. G. Girgis, “The structure and development of cranial and facial sutures,” *J. Anat.*, vol. 90, no. Pt 1, pp. 73-86.3, 1956.

[16] R. Bailer, “Meninges: Function and Layers,” *ThoughCo*, 2019. [Online]. Available: https://teachmeanatomy.info/neuroanatomy/structures/meninges/.

[17] T. P. Naidich, H. M. Duvernoy, B. N. Delman, A. G. Sorensen, S. S. Kollias, and E. M. Haacke, *Duvernoy’s Atlas of the Human Brain Stem and Cerebellum: High-Field MRI, Surface Anatomy, Internal Structure, Vascularization and 3 D Sectional Anatomy*. 2009.

[18] A. Josephson, “Atlas: Corpus Callosum. Central Nervous System - Visual Perspectives,” *Karolinska Institutet*, 2018. .

[19] M. Ghajari, P. J. Hellyer, and D. J. Sharp, “Computational modelling of traumatic brain injury predicts the location of chronic traumatic encephalopathy pathology,” *Brain*, vol. 140, no. 2, pp. 333–343, 2017.

[20] A. Jones, “The Functions of the Four Lobes of the Brain – Virtual Museum of Psychology,” *University of Wisconsin - Green Bay*, 2016. .

[21] V. C. Nieuwenhuys R, Voogd J, *The human central nervous system: a synopsis and atlas.* Springer Science & Business Media, 2008.

[22] G. Dr. Guyatt, “Cerebrospinal fluid: Physiology and utility of an examination in disease states - UpToDate,” *McMaster University*. [Online]. Available: https://www.uptodate.com/contents/cerebrospinal-fluid-physiology-and-utility-of-an-examination-in-disease-states. [Accessed: 09-Apr-2020].

[23] S. E. Paul LK, Brown WS, Adolphs R, Tyszka JM, Richards LJ, Mukherjee P, “Agenesis of the corpus callosum: genetic, developmental and functional aspects of connectivity.,” *Nat. Rev. Neurosci.*, vol. 8, no. (4), pp. 287–99.

[24] A. Post, T. Blaine Hoshizaki, M. D. Gilchrist, and M. D. Cusimano, “Peak linear and rotational acceleration magnitude and duration effects on maximum principal strain in the corpus callosum for sport impacts,” *J. Biomech.*, vol. 61, pp. 183–192, 2017.

[25] A. N. Voineskos, T. K. Rajji, N. J. Lobaugh, D. Miranda, M. E. Shenton, J. L. Kennedy, *et al.*, “Age-related decline in white matter tract integrity and cognitive performance: A DTI tractography and structural equation modeling study,” *Neurobiol. Aging*, vol. 33, no. 1, pp. 21–34, 2012.

[26] E. Luders, P. M. Thompson, K. L. Narr, A. Zamanyan, Y. Y. Chou, B. Gutman, *et al.*, “The link between callosal thickness and intelligence in healthy children and adolescents,” *Neuroimage*, vol. 54, no. 3, pp. 1823–1830, 2011.

[27] R. Lindenberg and E. Freytag, “The mechanism of cerebral contusions. A pathologic-anatomic study.,” *Arch. Pathol.*, vol. 69, pp. 440–69, Apr. 1960.

[28] D. Denny-Brown and W. R. Russell, “Experimental cerebral concussion,” *J. Physiol.*, vol. 99, no. 1, pp. 153–153, Dec. 1940.

[29] A. M. Nahum, R. Smith, and C. C. Ward, “Intracranial Pressure Dynamics During Head Impact,” *21st Stapp Car Crash Conf.*, 1977.

[30] A. S. Pomeroy, "Basic Anatomy of the Brain, Injuries and Pathologies," *Netter Collection of Medical Illustrations*, 2013. [Online]. Available: http://www.compelvisuals.com/compel_blog/basic-anatomy-of-the-brain-injuries-and-pathologies-an-illustrated-review/. [Accessed: 19-Feb-2019].

[31] A. C. Bain, D. F. Meaney, and H. Hall, "Tissue-Level Thresholds for Axonal Damage in an Nervous System White Matter Injury," vol. 122, no. December, 2000.

[32] L. E. Thibault, T. A. Gennarelli, S. S. Margulies, J. Marcus, and R. Eppinger, "The Strain Dependent Patbopbysiological Consequences of lnertial Loading on Central Nervous System Tissue," *IRCOBI Conf.*, pp. 191–202, 1990.

[33] A. I. A. King, K. K. H. Yang, L. Zhang, and W. Hardy, "Is head injury caused by linear or angular acceleration?," *IRCOBI Conf.*, no. September, pp. 1–12, 2003.

[34] A. H. S. Holbourn, "Mechanics of Head Injuries," *Lancet*, vol. 242, no. 6267, pp. 438–441, 1943.

[35] T. A. Gennarelli, J. H. Adams, and D. I. Graham, "Acceleration induced head injury in the monkey.I. The model, its mechanical and physiological correlates.," *Acta Neuropathol. Suppl.*, vol. 7, pp. 23–25, 1981.

[36] T. Gennarellie, "Head injury in man and experimental animals: neuropathology.," *Acta Neurochir. Suppl.*, vol. 32, pp. 15–30, 1983.

[37] F. Hernandez and L. Lopez, Jaime R, Camarillo, David, Wu, "Six Degree of Freedom Measurements of Human Mild Traumatic Brain Injury," vol. 43, no. March, 2016.

[38] D. A. Patton, A. S. McIntosh, S. Kleiven, and T. E, "The Biomechanical Determinants of Concussion : Finite Element Simulations to Investigate Brain Tissue Deformations During Sporting Impacts to the Unprotected Head," *J. Appl. Biomech.*, vol. 29, pp. 721–730, 2013.

[39] T. McAllister, J. Ford, B. Jonathan, L. A. Flashman, K. Paulsen, and R. M. Greenwald, "Maximum Principal Strain and Strain Rate Associated with Concussion Diagnosis Correlates with changes in Corpus Callosum White Matter Indices," *Ann Biomed Eng.*, vol. 40, no. 1, pp. 127–140, 2012.

[40] R. Yount, K. A. Raschke, M. Biru, D. F. Tate, M. J. Miller, T. Abildskov, *et al.*, "Traumatic brain injury and atrophy of the cingulate gyrus," *J. Neuropsychiatry Clin. Neurosci.*, vol. 14, no. 4, pp. 416–423, 2002.

[41] G. E. Strangman, T. M. O'Neil-Pirozzi, C. Supelana, R. Goldstein, D. I. Katz, and M. B. Glenn, "Fractional anisotropy helps predicts memory rehabilitation outcome after traumatic brain injury," *NeuroRehabilitation*, vol. 31, no. 3, pp. 295–310, 2012.

[42] F. Hernandez, C. Giordano, M. Goubran, S. Parivash, G. Grant, M. Zeineh, *et al.*, "Lateral impacts correlate with falx cerebri displacement and corpus callosum trauma in sports-related concussions," *Biomech. Model. Mechanobiol.*, no. 0123456789, 2019.

[43] D. King, C. Gissane, M. Brughelli, P. a. Hume, and J. Harawira, "Sport-related concussions in New Zealand: A review of 10 years of Accident Compensation Corporation moderate to severe claims and costs," *J Sci Med Sport*, vol. 17, no. 3, pp. 250–255, 2013.

[44] F. P. Rivara and R. Graham, *Sports-Related Concussions in Youth*, vol. 311, no. 3. The National Academies Press, 2014.

[45] D. Warden, B. J, C. K, and J. Ecklund, "Persistent prolongation of simple reaction time in sports concussion," *AAN Enterp. Inc*, pp. 2000–2002, 2001.

[46] R. C. Cantu and F. O. Mueller, "Brain Injury-related Fatalities in American Football, 1945–1999," *Neurosurgery*, vol. 52, no. 4, pp. 846–853, Apr. 2003.

[47] M. Mccrea, S. W. Marshall, R. C. Cantu, C. Randolph, W. Barr, J. a Onate, *et al.*, "The NCAA Concussion Study," *J. Am. Med. Assoc.*, vol. 290, no. 19, pp. 2549–2555, 2003.

[48] G. L. Iverson, M. Gaetz, M. R. Lovell, and M. W. Collins, "Cumulative effects of concussion in amateur athletes," *Brain Inj.*, vol. 18, no. 5, pp. 433–443, 2004.

[49] S. P. Broglio, B. Schnebel, and J. Sosnoff, "The Biomechanical Properties of Concussions in High School Football," *Med. Sci. Sports Exerc.*, vol. 42, no. 11, pp. 2064–2071, 2010.

[50] T. W. Mcallister, A. Maerlender, J. G. Beckwith, and J. J. Crisco, "Cognitive effects of one season of head impacts in a cohort of collegiate contact sport athletes," *Neurology*, vol. 79, no. 4, pp. 393–393, 2012.

[51] E. M. Davenport, C. T. Whitlow, J. E. Urban, M. A. Espeland, Y. Jung, D. A. Rosenbaum, *et al.*, "Abnormal White Matter Integrity Related to Head Impact Exposure in a Season of High School Varsity Football," *J. Neurotrauma*, vol. 31, no. 19, pp. 1617–1624, 2014.

[52] H. S. Martland, "Punch drunk," *J. Am. Med. Assoc.*, vol. 91, no. 15, pp. 1103–1107, Oct. 1928.

[53] C. M. Baugh, J. M. Stamm, D. O. Riley, B. E. Gavett, M. E. Shenton, A. Lin, *et al.*, "Chronic traumatic encephalopathy: Neurodegeneration following repetitive concussive and subconcussive brain trauma," *Brain Imaging Behav.*, vol. 6, no. 2, pp. 244–254, Jun. 2012.

[54] A. Schwarz, "N.F.L. Acknowledges Long-Term Concussion Effects - The New York Times," *New York Times*. [Online]. Available: https://www.nytimes.com/2009/12/21/sports/football/21concussions.html. [Accessed: 20-Apr-2020].

[55] K. Belson, "N.F.L. Agrees to Settle Concussion Suit for $765 Million - The New York Times," *The New York Times*, 2013.

[56] V. G. Khurana and A. H. Kaye, "An overview of concussion in sport," *J. Clin. Neurosci.*, vol. 19, no. 1, pp. 1–11, 2012.

[57] B. M. Asken, M. A. McCrea, J. R. Clugston, A. R. Snyder, Z. M. Houck, and R. M. Bauer, "Playing through it: Delayed reporting and removal from athletic activity after concussion predicts prolonged recovery," *J. Athl. Train.*, vol. 51, no. 4, pp. 329–335, 2016.

[58] F. Tagliaferri, C. Compagnone, M. Korsic, F. Servadei, and J. Kraus, "A systematic review of brain injury epidemiology in Europe," *Acta Neurochir. (Wien).*, vol. 148, no. 3, pp. 255–267, 2006.

[59] M. B. Clay, K. L. Glover, and D. T. Lowe, "Epidemiology of concussion in sport: a literature review," *J. Chiropr. Med.*, vol. 12, no. 4, pp. 230–251, 2013.

[60] J. O. Koh, J. D. Cassidy, and E. J. Watkinson, "Incidence of concussion in contact sports: A systematic review of the evidence," *Brain Inj.*, vol. 17, no. 10, pp. 901–917, Oct. 2003.

[61] S. Kemp, "England Professional Rugby Injury Surveillance Project," *Med. Advis. RPA)*, 2018.

[62] S. W. Marshall and R. J. Spencer, "Concussion in Rugby: The Hidden Epidemic," *J. Athl. Train.*, vol. 36, no. 3, pp. 334–338, 2001.

[63] K. Flik, S. Lyman, and R. G. Marx, "American collegiate men's ice hockey: An analysis of injuries," *Am. J. Sports Med.*, vol. 33, no. 2, pp. 183–187, 2005.

[64] A. E. Lincoln, S. V. Caswell, J. L. Almquist, R. E. Dunn, J. B. Norris, and R. Y. Hinton, "Trends in concussion incidence in high school sports: A prospective 11-year study," *Am. J. Sports Med.*, vol. 39, no. 5, pp. 958–963, 2011.

[65] J. C. Murphy, E. O'Malley, C. Gissane, and C. Blake, "Incidence of Injury in Gaelic Football," *Am. J. Sports Med.*, vol. 40, no. 9, pp. 2113–2120, Sep. 2012.

[66] K. M. Guskiewicz, N. L. Weaver, D. A. Padua, and W. E. Garrett, "Epidemiology of concussion in collegiate and high school football players," *Am. J. Sports Med.*, vol. 28, no. 5, pp. 643–650, 2000.

[67] M. A. Booher, J. Wisniewski, B. W. Smith, and A. Sigurdsson, "Comparison of reporting systems to determine concussion incidence in NCAA Division I collegiate football," *Clin. J. Sport Med.*, vol. 13, no. 2, pp. 93–95, 2003.

[68] G. D. Myer, D. Smith, K. D. B. Foss, C. A. Dicesare, A. W. Kiefer, A. M. Kushner, *et al.*, "Rates of concussion are lower in national football league games played at higher altitudes," *J. Orthop. Sports Phys. Ther.*, vol. 44, no. 3, pp. 164–172, 2014.

[69] A. P. Kontos, R. J. Elbin, V. C. Fazio-Sumrock, S. Burkhart, H. Swindell, J. Maroon, *et al.*, "Incidence of Sports-Related Concussion among Youth Football Players Aged 8-12 Years," *J. Pediatr.*, vol. 163, no. 3, pp. 717–720, 2013.

[70] J. G. Beckwith, R. M. Greenwald, J. J. Chu, J. J. Crisco, J. P. Mihalik, S. Anderson, *et al.*, "Head Impact Exposure Sustained by Football Players on Days of Diagnosed Concussion," *Med Sci Sport. Exerc*, vol. 45, no. 4, pp. 737–746, 2014.

[71] M. R. Fraas, G. F. Coughlan, E. C. Hart, and C. McCarthy, "Concussion history and reporting rates in elite Irish rugby union players," *Phys Ther Sport*, vol. 15, no. 3, pp. 136–142, 2014.

[72] J. F. Baker, B. M. Devitt, J. Green, and C. McCarthy, "Concussion among under 20 rugby union players in Ireland: incidence, attitudes and knowledge," *Ir J Med Sci*, vol. 182, no. 1, pp. 121–125, 2013.

[73] W. T. Tsushima, A. M. Siu, H. J. Ahn, B. L. Chang, and N. M. Murata, "Incidence and Risk of Concussions in Youth Athletes: Comparisons of Age, Sex, Concussion History, Sport, and Football Position," *Arch. Clin. Neuropsychol.*, vol. 34, no. 1, pp. 60–69, 2019.

[74] G. Curran-Sills and T. Abedin, "Risk factors associated with injury and concussion in sanctioned amateur and professional mixed martial arts bouts in Calgary, Alberta," *BMJ Open Sport Exerc. Med.*, vol. 4, no. 1, pp. 1–8, 2018.

[75] J. A. Rechel, E. E. Yard, and R. D. Comstock, "An epidemiologic comparison of

high school sports injuries sustained in practice and competition," *J. Athl. Train.*, vol. 43, no. 2, pp. 197–204, 2008.

[76] A. E. Lincoln, S. V. Caswell, J. L. Almquist, R. E. Dunn, J. B. Norris, and R. Y. Hinton, "Trends in Concussion Incidence in High School Sports: A Prospective 11-Year Study," *Am. J. Sports Med.*, vol. 39, no. 5, pp. 958–963, 2011.

[77] A. Ruhe, A. Gänsslen, and W. Klein, "The incidence of concussion in professional and collegiate ice hockey: Are we making progress? A systematic review of the literature," *Br. J. Sports Med.*, vol. 48, no. 2, pp. 102–106, 2014.

[78] A. Dessy, J. Rasouli, A. Gometz, and T. Choudhri, "A review of modifying factors affecting usage of diagnostic rating scales in concussion management," *Clin. Neurol. Neurosurg.*, vol. 122, pp. 59–63, 2014.

[79] R. W. Dick, "Is there a gender difference in concussion incidence and outcomes?," *Br. J. Sports Med.*, vol. 43, no. SUPPL. 1, pp. 46–50, 2009.

[80] A. S. McIntosh, P. McCrory, C. F. Finch, and R. Wolfe, "Head, face and neck injury in youth rugby: incidence and risk factors," *Br J Sport. Med*, vol. 44, no. 3, pp. 188–193, 2010.

[81] L. D. Nelson, K. M. Guskiewicz, W. B. Barr, T. A. Hammeke, C. Randolph, K. W. Ahn, *et al.*, "Age Differences in Recovery After Sport-Related Concussion: A Comparison of High School and Collegiate Athletes," vol. 51, no. 2, pp. 142–152, 2016.

[82] M. McCrea, T. Hammeke, G. Olsen, P. Leo, and K. Guskiewicz, "Unreported Concussion in High School Football Players: Implications for Prevention," *Clin. J. Sport Med.*, vol. 14, no. 1, pp. 13–17, 2004.

[83] Houses of the Oireachtas, "Report on Concussion in Sport," *Houses Oireachtas Jt. Comm. Heal. Child.*, no. December, pp. 15–16, 2014.

[84] S. M. Duma, S. J. Manoogian, W. R. Bussone, P. G. Brolinson, M. W. Goforth, J. J. Donnenwerth, *et al.*, "Analysis of real-time head accelerations in collegiate football players," *Clin J Sport Med*, vol. 15, no. 1, pp. 3–8, 2005.

[85] J. G. Beckwith, R. M. Greenwald, and J. J. Chu, "Measuring head kinematics in football: Correlation between the head impact telemetry system and hybrid III headform," *Ann. Biomed. Eng.*, vol. 40, no. 1, pp. 237–248, 2012.

[86] K. M. Guskiewicz, J. P. Mihalik, V. Shankar, S. W. Marshall, D. H. Crowell, S. M. Oliaro, *et al.*, "Measurement of Head Impacts in Collegiate Football Players," *Neurosurgery*, vol. 61, no. 6, pp. 1244–1253, Dec. 2007.

[87] S. P. Broglio, J. J. Sosnoff, S. H. Shin, X. He, C. Alcaraz, J. Zimmerman, *et al.*, "Head impacts during high school football: a biomechanical assessment," *J Athl Train*, vol. 44, no. 4, pp. 342–349, 2009.

[88] J. J. Crisco, B. J. Wilcox, J. G. Beckwith, J. J. Chu, A.-C. Duhaime, S. Rowson, *et al.*, "Head impact exposure in collegiate football players," *J. Biomech.*, vol. 44, no. 15, pp. 2673–2678, 2011.

[89] R. Jadischke, D. Viano, N. Dau, A. I. King, and J. McCarthy, "On the accuracy of the head impact telemetry (hit) system used in football helmets," *J. Biomech.*, vol. 46, no. 13, pp. 2310–2315, Sep. 2013.

[90] D. A. Patton, "A Review of Instrumented Equipment to Investigate Head Impacts in Sport," *Appl. Bionics Biomech.*, vol. 2016, pp. 1–16, 2016.

[91] H. T. Hurst, S. Atkins, and B. D. Dickinson, "The magnitude of translational and rotational head accelerations experienced by riders during downhill mountain biking," *J. Sci. Med. Sport*, vol. 21, no. 12, pp. 1256–1261, 2018.

[92] D. Nevins, L. Smith, and J. Kensrud, "Laboratory evaluation of wireless head impact sensor," *Procedia Eng.*, vol. 112, pp. 175–179, 2015.

[93] E. McCuen, D. Svaldi, K. Breedlove, N. Kraz, B. Cummiskey, E. L. Breedlove, *et al.*, "Collegiate women's soccer players suffer greater cumulative head impacts than their high school counterparts," *J. Biomech.*, vol. 48, no. 13, pp. 3720–3723, 2015.

[94] D. King, P. Hume, C. Gissane, and T. Clark, "Head impacts in a junior rugby league team measured with a wireless head impact sensor: an exploratory analysis," pp. 1–11, 2016.

[95] E. E. Swartz, S. P. Broglio, S. B. Cook, R. C. Cantu, M. S. Ferrara, K. M. Guskiewicz, *et al.*, "Early results of a helmetless-tackling intervention to decrease head impacts in football players," *J. Athl. Train.*, vol. 50, no. 12, pp. 1219–1222, 2015.

[96] D. King, P. A. Hume, M. Brughelli, and C. Gissane, "Instrumented mouthguard acceleration analyses for head impacts in amateur rugby union players over a season of matches," *Am. J. Sports Med.*, vol. 43, no. 3, pp. 614–624, 2015.

[97] A. Bartsch and S. Samorezov, "Cleveland Clinic intelligent mouthguard: a new technology to accurately measure head impact in athletes and soldiers," *Proc. SPIE 8723, Sens. Technol. Glob. Heal. Mil. Med. Environ. Monit. III*, vol. 8723, p. 87230N, 2013.

[98] L. Wu, L. Zarnescu, V. Nangia, B. Cam, and D. Camarillo, "A head impact detection system using SVM classification and proximity sensing in an instrumented mouthguard," *IEEE Trans. Biomed. Eng.*, vol. 61, no. 11, pp. 2659–2668, 2014.

[99] D. Garza, D. Camarillo, R. Shultz, J. Mattson, P. B. Shull, J. Mattson, *et al.*, "An instrumented mouthguard for measuring linear and angular head impact kinematics in American football," *Ann. Biomed. Eng.*, vol. 41, no. 9, pp. 1939–1949, 2013.

[100] L. Wu, F. Hernandez, C. Kuo, and M. Kurt, "In Vivo Evaluation of Wearable Head Impact Sensors," *Ann. Biomed. Eng.*, vol. 44, no. 4, pp. 1234–1245, 2016.

[101] S. Kleiven and W. N. Hardy, "Correlation of an FE Model of the Human Head with Local Brain Motion--Consequences for Injury Prediction," *Stapp Car Crash J.*, vol. 46, no. November, pp. 123–144, 2002.

[102] T. Brooks, J. E. Choi, M. Garnich, N. Hammer, J. N. Waddell, W. Duncan, *et al.*, "Finite element models and material data for analysis of infant head impacts," *Heliyon*, vol. 4, no. 12, p. e01010, 2018.

[103] S. Cui, H. Li, X. Li, and J. Ruan, "Effects of the Variation in Brain Tissue Mechanical Properties on the Intracranial Response of a 6-Year-Old Child," *Comput. Math. Methods Med.*, vol. 2015, 2015.

[104] M. Iwamoto, Y. Nakahira, A. Tamura, M. Iwamoto, and I. Toyota Central R&D Labs., "Development of Advanced Human Models in THUMS," *6th Eur. LS-Dyna Users's Conf.*, pp. 47–56, 2007.

[105] L. Talebanpour and L. Smith, "A Comparison between Simulated and Measured Human Brain Response under Mild Acceleration," *IRCOBI Conf.*, p. IRC-17-59, 2017.

[106] H. Mao, L. Zhang, B. Jiang, V. V. Genthikatti, X. Jin, F. Zhu, *et al.*, "Development of a Finite Element Human Head Model Partially Validated With Thirty Five Experimental Cases," *J. Biomech. Eng.*, vol. 135, no. 11, p. 111002, 2013.

[107] D. Baumgartner and R. Willinger, "Numerical modeling of the human head under impact: New injury mechanisms and tolerance limits," *Solid Mech. its Appl.*, vol. 124, pp. 195–203, 2005.

[108] J. M. Clark, A. Post, T. B. Hoshizaki, and M. D. Gilchrist, "Determining the relationship between linear and rotational acceleration and MPS for different magnitudes of classified brain injury risk in ice hockey," *2015 IRCOBI Conf. Proc. - Int. Res. Counc. Biomech. Inj.*, pp. 168–179, 2015.

[109] X. Trosseille, C. Tarriére, F. Lavaste, F. Guillon, and A. Domont, "Development of a F.E.M. of the human head according to a specific test protocol," *SAE Tech. Pap.*, 1992.

[110] A. Al-Bsharat, W. Hardy, K. Yang, T. Khalil, S. Tashman, and A. King, "Brain/skull relative displacement magnitude due to blunt head impact: New experimental data and model," *Stapp Car Crash Conf. Proc.*, vol. P-350, no. 724, pp. 321–332, 1999.

[111] W. N. Hardy, M. J. Mason, C. D. Foster, C. S. Shah, J. M. Kopacz, H. Yang, *et al.*, "A study of the response of the human cadaver head to impact," *Stapp Car Crash J*, vol. 51, pp. 17–80, 2008.

[112] N. Yoganandan, F. A. PINTAR, A. Sances, P. R. Walsh, C. L. Ewing, D. J. Thomas, *et al.*, "Biomechanics of skull fracture.," *J. Neurotrauma*, vol. 12, no. 4, pp. 659–668, 1995.

[113] L. Zhang, A. King, and K. Yang, "Concussion in professional football: Brain responses by finite element analysis: Part 9," *Neurosurgery*, vol. 57, no. 5, pp. 891–915, Nov. 2005.

[114] L. Zhang, K. H. Yang, and A. I. King, "A Proposed Injury Threshold for Mild Traumatic Brain Injury," *J. Biomech. Eng.*, vol. 126, no. 2, pp. 226–236, 2004.

[115] W. Zhao, B. Choate, S. Ji, and P. Street, "Material Properties of the Brain in Injury-Relevant Conditions-Experiments and Computational Modeling Graphical abstract HHS Public Access," *J Mech Behav Biomed Mater*, vol. 80, pp. 222–234, 2018.

[116] H. Mao, L. Zhang, K. H. Yang, and A. I. King, "Application of a Finite Element Model of the Brain to Study Traumatic Brain Injury Mechanisms in the Rat," *SAE Tech. Pap.*, vol. 2006-Novem, no. November, pp. 583–600, 2006.

[117] T. J. Horgan and M. D. Gilchrist, "The creation of three-dimensional finite element models for simulating head impact biomechanics," *Int. J. Crashworthiness*, vol. 8, no. 4, pp. 353–366, 2003.

[118] T. J. Horgan and M. D. Gilchrist, "Influence of Fe model variability in predicting brain motion and intracranial pressure changes in head impact simulations," *Int. J. Crashworthiness*, vol. 9, no. 4, pp. 401–418, 2004.

[119] W. Chen, A. Post, C. Karton, M. D. Gilchrist, M. Robidoux, and T. B. Hoshizaki, "A comparison of frequency and magnitude of head impacts between Pee Wee And Bantam youth ice hockey," *Sport. Biomech.*, vol. 00, no. 00, pp. 1–24, 2020.

[120] J. M. Clark, A. Post, T. B. Hoshizaki, and M. D. Gilchrist, "Protective Capacity of Ice Hockey Helmets against Different Impact Events," *Ann. Biomed. Eng.*, vol. 44, no. 12, pp. 3693–3704, 2016.

[121] J. M. Clark, T. B. Hoshizaki, and M. D. Gilchrist, "Assessing Women's Lacrosse Head Impacts Using Finite Element Modelling," *J. Mech. Behav. Biomed. Mater.*, 2018.

[122] T. A. Connor, J. M. Clark, J. Jayamohan, M. Stewart, A. McGoldrick, C. Williams, *et al.*, "Do equestrian helmets prevent concussion? A retrospective analysis of head injuries and helmet damage from real-world equestrian accidents," *Sport. Med. - Open*, vol. 5, no. 1, 2019.

[123] G. M. Kendall, Marshall, Post, Andrew, "A Comparison of dynamic impact response and brain deformation metrics within the cerebrum of head impact reconstructions representing three mechanisms of head injury in ice hockey.," *Int. Res. Counc. Biomech. Inj.*, 2012.

[124] A. Oeur, B. T. Hoshizaki, and M. D. Gilchrist, "The Influence of Impact Angle on the Dynamic Response of a Hybrid III Headform and Brain Tissue Deformation," *Mech. Concussion Sport.*, pp. 56–69, 2014.

[125] T. B. Hoshizaki, A. Post, M. Kendall, J. Cournoyer, P. Rousseau, M. D. Gilchrist, *et al.*, "The development of a threshold curve for the understanding of concussion in sport," *Trauma (United Kingdom)*, vol. 19, no. 3, pp. 196–206, Jul. 2017.

[126] H.-S. Kang, R. Willinger, B. M. Diaw, and B. Chinn, "Validation of a 3D Anatomic Human Head Model and Replication of Head Impact in Motorcycle Accident by Finite Element Modeling," *Stapp Car Crash Conf.*, 1997.

[127] D. Marjoux, D. Baumgartner, C. Deck, and R. Willinger, "Head injury prediction capability of the HIC, HIP, SIMon and ULP criteria," *Accid. Anal. Prev.*, vol. 40, no. 3, pp. 1135–1148, 2008.

[128] C. Deck, N. Bourdet, F. Meyer, and R. Willinger, "Protection performance of bicycle helmets," *J. Safety Res.*, vol. 71, pp. 67–77, 2019.

[129] N. Bourdet, C. Deck, F. Meyer, R. Willinger, N. Bourdet, C. Deck, *et al.*, "Experimental and numerical considerations of helmet evaluation under oblique impact evaluation under oblique impact," *J. Transp. Saf. Secur.*, vol. 0, no. 0, pp. 1–14, 2019.

[130] D. Sahoo, C. Deck, and R. Willinger, "Brain injury tolerance limit based on computation of axonal strain," *Accid. Anal. Prev.*, vol. 92, pp. 53–70, 2016.

[131] S. Kleiven, "Finite Element Modeling of the Human Head," *Dr. thesis*, no. January 2000, 2002.

[132] S. Kleiven, "Predictors for traumatic brain injuries evaluated through accident reconstructions," *Stapp Car Crash J.*, vol. 51, no. April, pp. 81–114, 2007.

[133] K. Laksari, F. Hernandez, J. R. Lopez, A. R. Hoffman, G. A. Grant, D. Camarillo, *et al.*, "Six Degree-of-Freedom Measurements of Human Mild Traumatic Brain Injury," *Ann. Biomed. Eng.*, vol. 43, no. 8, pp. 1918–1934, 2014.

[134] C. Giordano and S. Kleiven, “Evaluation of Axonal Strain as a Predictor for Mild Traumatic Brain Injuries Using Finite Element Modeling,” *Stapp Car Crash J.*, vol. 58, no. 14, pp. 29–61, 2014.

[135] Z. Y. Cui, N. Famaey, B. Depreitere, J. Ivens, S. Kleiven, and J. Vander Sloten, “On the assessment of bridging vein rupture associated acute subdural hematoma through finite element analysis,” *Comput. Methods Biomech. Biomed. Engin.*, vol. 20, no. 5, pp. 530–539, 2017.

[136] M. Iwamoto, Y. Kisanuki, I. Watanabe, K. Furusu, and K. Miki, “Development of a finite element model of the total human model for Safety and Application to Injury Reconstruction,” *IRCOBI Conf.*, pp. 31–42, 2002.

[137] A. Tamura, Y. Nakahira, M. Iwamoto, I. Watanabe, K. Miki, S. Hayashi, *et al.*, “The influence of the traction force due to inertia of the brain mass on traumatic brain injury during SUV-to-pedestrian impact,” *Int. Res. Counc. Biomech. Impact - 2006 Int. IRCOBI Conf. Biomech. Impact, Proc.*, no. September, pp. 361–364, 2006.

[138] S. J, P. Ghadyani, J. Bolander, J. Beckwith, and T. Ford, “Parametric Comparisons of Intracranial Mechanical Responses from Three Validated Finite Element Models of the Human Head,” *Ann Biomed Eng*, vol. 30, no. 3, pp. 371–378, 2015.

[139] E. Gurdjian and V. Roberts, “Tolerance Curves of Acceleration and Intracranial Pressure and Protective Index in Experimental Head Injury,” *J. Trauma*, vol. 6, no. 5, 1966.

[140] E. Pellman, D. Viano, A. M. Tucker, I. Casson, and J. F. Waeckerle, “Concussion in Professional Football: Reconstruction of Game Impacts and Injuries,” *Neurosurgery*, vol. 53, no. 4, p. 796, Oct. 2003.

[141] B. J. Wilcox, J. G. Beckwith, R. M. Greenwald, N. P. Raukar, J. J. Chu, T. W. McAllister, *et al.*, “Biomechanics of head impacts associated with diagnosed concussion in female collegiate ice hockey players,” *J. Biomech.*, vol. 48, no. 10, pp. 2201–2204, 2015.

[142] A. S. McIntosh, D. a Patton, B. Fréchède, P.-A. Pierré, E. Ferry, and T. Barthels, “The biomechanics of concussion in unhelmeted football players in Australia: a case-control study.,” *BMJ Open*, vol. 4, no. 5, p. e005078, 2014.

[143] S. Rowson, S. M. Duma, J. G. Beckwith, J. J. Chu, R. M. Greenwald, J. J. Crisco, *et al.*, “Rotational Head Kinematics in Football Impacts: An Injury Risk Function for Concussion,” *Ann. Biomed. Eng.*, vol. 40, no. 1, pp. 1–13, 2012.

[144] N. Reed, T. Taha, M. Keightley, C. Duggan, J. McAuliffe, J. Cubos, *et al.*, “Measurement of head impacts in youth ice hockey players,” *Int. J. Sports Med.*, vol. 31, no. 11, pp. 826–833, 2010.

[145] S. Stojsih, M. Boitano, M. Wilhelm, and C. Bir, “A prospective study of punch biomechanics and cognitive function for amateur boxers,” *Br. J. Sports Med.*, vol. 44, no. 10, pp. 725–730, 2010.

[146] Viano, I. Casson, and E. Pellman, “Concussion in professional football: Brain responses by finite element analysis: Part 9,” *Neurosurgery*, vol. 57, no. 5, pp. 891–915, 2005.

[147] J. Newman, C. Barr, M. Beusenberg, E. Fournier, N. Shewchenko, E. Welbourne, *et al.*, “A new biomechanical assessment of mild traumatic brain injury, part 2:

results and conclusions,” *Proc. 2000 Int. Conf. Biomech. Impact*, pp. 223–233, 2000.

[148] R. M. Greenwald, J. T. Gwin, J. J. Chu, and J. J. Crisco, “Head Impact Severity Measures for Evaluating Mild Traumatic Brain Injury Risk Exposure,” *Neurosurgery*, vol. 62, no. 4, pp. 789–798, Apr. 2009.

[149] E. G. Takhounts, M. J. Craig, K. Moorhouse, J. McFadden, and V. Hasija, “Development of brain injury criteria (BrIC).,” *Stapp Car Crash J.*, vol. 57, no. November, pp. 243–66, 2013.

[150] F. Hernandez and D. Camarillo, “Voluntary Head Rotational Velocity and Implications for Brain Injury Risk Metrics,” *J. Neurotrauma*, vol. 36, no. 7, pp. 1125–1135, 2019.

[151] J. A. Newman and N. Shewchenko, “A Proposed New Biomechanical Head Injury Assessment Function - The Maximum Power Index,” *SAE Tech. Pap.*, vol. 2000-Novem, no. November, 2000.

[152] A. S. McIntosh, P. McCrory, and J. Comerford, “The dynamics of concussive head impacts in rugby and Australian rules football,” *Med Sci Sport. Exerc*, vol. 32, no. 12, pp. 1980–1984, 2000.

[153] J. Scott Delaney, V. Puni, and F. Rouah, “Mechanisms of injury for concussions in university football, ice hockey, and soccer: a pilot study.,” *Clin. J. Sport Med.*, vol. 16, no. 2, pp. 162–165, 2006.

[154] N. Yoganandan, J. Li, J. Zhang, F. Pintar, and T. Gennarelli, “Influence of angular acceleration-deceleration pulse shapes on regional brain strains,” *J. Biomech.*, vol. 41, no. 10, pp. 2253–2262, 2008.

[155] S. Tiernan and G. Byrne, “The effect of impact location on brain strain,” *Brain Inj.*, vol. 33, no. 01, pp. 1–8, 2019.

[156] W. Zhao and S. Ji, “Brain strain uncertainty due to shape variation in and simplification of head angular velocity profiles,” *Biomech. Model. Mechanobiol.*, vol. 16, no. 2, pp. 449–461, 2017.

[157] S. Kleiven, “Influence of direction and duration of impacts to the human head evaluated using the finite element method,” *Proc. IRCOBI Conf. Prague, Czech Repub.*, no. September, pp. 41–57, 2005.

[158] F. Hernandez, L. Wu, M. C. Yip, K. Laksari, A. R. Hoffman, J. R. Lopez, *et al.*, “Six Degree of Freedom Measurements of Human Mild Traumatic Brain Injury,” *Ann. Biomed. Eng.*, vol. 43, no. 8, pp. 1918–1934, 2015.

[159] C. Deck and R. Willinger, “Improved head injury criteria based on head FE model,” *Int. J. Crashworthiness*, vol. 13, no. 6, pp. 667–678, 2008.

[160] E. Pellman, D. Viano, A. M. Tucker, I. Casson, A. B. Valadka, J. C. Maroon, *et al.*, “Concussion in Professional Football: Location and Direction of Helmet Impacts - Part 2,” *Neurosurgery*, vol. 53, no. 6, pp. 1328–1341, 2003.

[161] S. Kleiven, “Predictors for Traumatic Brain Injuries Evaluated through Accident Reconstructions,” *SAE Tech. Pap.*, vol. 2007-Octob, no. October, pp. 81–114, 2007.

[162] D. Baumgartner and R. Willinger, “Numerical Modeling of the Human Head Under Impact: New Injury Mechanisms and Tolerance Limits,” *IUTAM Proc. Impact Biomech. From Fundam. Insights to Appl.*, pp. 195–203, 2005.

[163] R. W. G. Anderson, “A Study on the Biomechanics of Axonal Injury,” University of Adelaide, 2000.

[164] L. Zhang, K. Yang, and A. King, “A proposed injury threshold for mild traumatic brain injury,” *J Biomech Eng*, vol. 126, no. 2, pp. 226–236, 2004.

[165] L. Zhang, K. Yang, A. King, and D. Viano, “A New Biomechanical Predictor for Traumatic Brain Injury – A Preliminary Finding,” *Proc. 2003 Summer Bioeng. Conf.*, no. 1, pp. 1–2, 2003.

[166] D. Shreiber, A. Bain, D. Meaney, and T. E, “In vivo thresholds for mechanical injury to the blood-brain barrier,” *Stapp Car Crash Conf. Proc.*, no. P-315, pp. 277–291, 1997.

[167] A. Bain and D. Meaney, “Tissue-Level Thresholds for Axonal Damage in an Experimental Model of Central Nervous System White Matter Injury,” *J. Biomech. Eng.*, vol. 122, no. 6, p. 615, 2000.

[168] D. Viano, I. Casson, E. Pellman, C. Bir, L. Zhang, D. Sherman, *et al.*, “Concussion in professional football: Comparison with boxing head impacts - Part 10,” *Neurosurgery*, vol. 57, no. 6, pp. 1154–1170, 2005.

[169] H. Kimpara and M. Iwamoto, “Mild Traumatic Brain Injury Predictors Based on Angular Accelerations During Impacts,” *Ann. Biomed. Eng.*, vol. 40, no. 1, pp. 114–126, Jan. 2012.

[170] A. Post, T. Blaine Hoshizaki, S. Brien, M. D. Cusimano, D. Koncan, S. Marshall, *et al.*, “Characterization of persistent concussive syndrome using injury reconstruction and finite element modelling,” *J. Mech. Behav. Biomed. Mater.*, vol. 41, pp. 325–335, 2014.

[171] E. J. Sanchez, L. F. Gabler, A. B. Good, J. R. Funk, J. R. Crandall, and M. B. Panzer, “A reanalysis of football impact reconstructions for head kinematics and finite element modeling,” *Clin. Biomech.*, vol. 64, no. February, pp. 82–89, 2019.

[172] J. Newman, M. C. Beusenberg, N. Shewchenko, C. Withnall, and E. Fournier, “Verification of biomechanical methods employed in a comprehensive study of mild traumatic brain injury and the effectiveness of American football helmets,” *J. Biomech.*, vol. 38, no. 7, pp. 1469–1481, 2005.

[173] M. Gaetz, “The neurophysiology of brain injury,” *Clinical Neurophysiology*, vol. 115, no. 1. Elsevier Ireland Ltd, pp. 4–18, 01-Jan-2004.

[174] J. T. Povlishock, “Pathobiology of traumatically induced axonal injury in animals and man,” *Ann. Emerg. Med.*, vol. 22, no. 6, pp. 980–986, Jun. 1993.

[175] R. J. H. Cloots, J. A. W. Van Dommelen, S. Kleiven, and M. G. D. Geers, “Multi-scale mechanics of traumatic brain injury: Predicting axonal strains from head loads,” *Biomech. Model. Mechanobiol.*, vol. 12, no. 1, pp. 137–150, 2013.

[176] M. G. Hutchison, D. W. Lawrence, M. D. Cusimano, and T. A. Schweizer, “Head trauma in mixed martial arts,” *Am. J. Sports Med.*, vol. 42, no. 6, pp. 1352–1358, 2014.

[177] K. T. Seungmo Christopher Greenwell Damon PS Andrew and J. F. Lee Daniel Mahony, “An Analysis of Spectator Motives in an Individual Combat Sport: A Study of Mixed Martial Arts Fans,” 2008.

[178] “Cam Newton, LL Cool J, The Weeknd And Others Make Major Investment In UFC.” [Online]. Available: https://www.hotnewhiphop.com/cam-newton-ll-cool-

j-the-weeknd-and-others-make-major-investment-in-ufc-news.24474.html? [Accessed: 13-Feb-2019].

[179] "Mixed Martial Arts News, Video, Rankings, Results, and History," *ESPN Enterprises Inc.*, 2020. [Online]. Available: http://www.espn.com/mma/. [Accessed: 13-Feb-2019].

[180] G. H. Bledsoe, E. B. Hsu, G. Grabowski, J. D. Brill, and G. Li, "Incidence of Injury in Professional Mixed Martial Arts Competitions," ©*Journal Sport. Sci. Med.*, pp. 136–142, 2006.

[181] R. E. Thomas and B. C. Thomas, "Systematic review of injuries in mixed martial arts," *Phys. Sportsmed.*, vol. 46, no. 2, pp. 155–167, 2018.

[182] G. J. Buse, "No holds barred sport fighting: A 10 year review of mixed martial arts competition," *Br. J. Sports Med.*, vol. 40, no. 2, pp. 169–172, 2006.

[183] P. Taylor, C. J. Heath, and J. L. Callahan, "Self-Reported Concussion Symptoms and Training Routines in Mixed Martial Arts Athletes," *Res. Sport. Med.*, no. October 2014, pp. 37–41, 2013.

[184] A. R. Mayer, J. Ling, A. B. Dodd, and Gas, "A Longitudinal Assessment of Structural and Chemical Alterations in MMA Fighters," *J. Neurotrauma*, no. C, pp. 1–46, 2012.

Chapter 3

Evaluation of skin mounted sensor for head impact measurement

Abstract

Background: The requirement to measure the number and severity of head impacts in sports has led to the development of wearable sensors.

Aim: The objective of this study was to determine the reliability and accuracy of a wearable head impact sensor: xPatch, X2 Biosystems Inc.

Methods: The skin mounted sensor, xPatch, was fixed onto a Hybrid III headform, and dropped using an impact test rig. Four hundred impacts were performed, ranging from 20 to 200g linear acceleration, with impact velocities of 1.2m/s to 3.9m/s. During each impact, the peak linear acceleration, angular velocity and angular acceleration, were recorded and compared to reference calibrated data. Impacts were also recorded using a high-speed video camera.

Results: The linear acceleration recorded by the xPatch during frontal and side impacts had errors of up to 24% when compared to the referenced data. The angular velocity and angular acceleration had substantially larger errors of up to 47.5% and 57% respectively. The location of the impact had a significant effect on the results: if the impact was to the side of the head, the device on that side may have an error of up to 71%, thus highlighting the importance of device location. All impacts were recorded using two separate xPatches and, in certain cases, the difference in angular velocity between the devices was 43%.

Conclusion: The xPatch can be useful for identifying impacts and recording linear accelerations during front and side impacts, but the angular velocity and acceleration data needs to be interpreted with caution.

Published: S. Tiernan, G. Byrne, and D. M. O'Sullivan, "Evaluation of skin-mounted sensor for head impact measurement," Proc. Inst. Mech. Eng. Part H J. Eng. Med., vol. 233, no. 7, pp. 735–744, 2019.
DOI: 10.1177/0954411919850961.

This chapter is a reproduction of the published paper except for some minor alterations and the addition of the angular acceleration versus time plot in Figure 3-3.

3.1 Introduction

Concussion in sport is very prevalent, with between 1.6 and 3.8 million sports-related concussions in the United States each year [1]. The diagnosis of concussion is particularly difficult with many studies reporting that approximately 50% of concussions go unreported [2][3]. The 5th international conference on concussion in sport defined concussion as a complex pathophysiological process affecting the brain, induced by biomechanical forces [4]. These biomechanical forces may be induced from a combination of direct and indirect head impacts, causing both linear and angular motion [5]. Abel et al. conducted research in 1978, using monkeys, to investigate the effects of head and brain motion during impacts; they concluded that angular acceleration in particular was linked to concussive injuries [6]. Furthermore, they stated that following an impact, rotational motion is the primary cause of strain in brain tissue. Research has since validated this theory in terms of human injuries [7][8][9]. In addition, the magnitude of strain which the brain undergoes during an impact, has been determined to be dependent on both the magnitude of the impact and the impact location [10][11][12][13].

In 2003, the first wireless impact sensor was developed to measure the severity of impacts in American football [14]. The Head Impact Telemetry System (HITS) sensor is an array of six or nine accelerometers embedded in a football helmet. Its accuracy has been investigated by various groups and determined to be dependent on the fit of the helmet to the head [15][16]. It has been used in numerous American football studies [17][18] and also in boxing [19]. Due to the fact that not all contact sports utilise a helmet for protection, other wireless sensors have been developed, such as instrumented mouth-guards (X2Biosystems Inc.), headbands (Sim-G, Triax Technologies Inc) [20], and skin patches (xPatch, X2Biosystems Inc.). These have been used in studies of head impacts in unhelmeted sports such as soccer [21][22][27] and rugby [23].

To date, the majority of studies on the accuracy of head impact sensors have used a Hybrid III headform [24][25] fitted with a reference a tri-axial linear accelerometer and a tri-axial gyroscope positioned at the centre of gravity. The headform has a viscoelastic skin whose response is strain-independent up to strains of 20% [26]. In a recently published study, helmet-mounted and head-mounted acceleration sensors were tested [25]. The study used a Hybrid III headform fitted with a Riddell helmet, and data was collected from a number of sensors, including the HITS and the xPatch. The results found that the xPatch peak linear acceleration (PLA) errors ranged from 7.7% to 57.9%, while peak angular acceleration errors ranged from 9.5% to 245.6%. This study utilised an impulse hammer and impacted the head in seven locations. The majority of the impacts were below 80g (PLA). A study by Schussler et al. in 2017 on the accuracy of the xPatch, found PLA errors of up to 31% and peak angular acceleration (PAA) errors up to 23.4% [28]. This study impacted a Hybrid III head fitted with a lacrosse helmet.

Despite these errors and unlike other studies, they concluded that the xPatch device measurements were highly correlated with their reference device.

Rowson et al. used the xPatch to record 8,999 head impacts in women's collegiate soccer. However only 1,703 of these impacts could be confirmed by video analysis, thus resulting in a positive prediction rate of only 16.3% [27]. One of the few studies on the accuracy of the xPatch using an unhelmeted headform, was undertaken by Nevin et al. in 2015. Their study was limited in that they only impacted the head in two frontal locations using three types of soft balls; they found that the xPatch had errors of approximately 25% for PLA and under predicted PAA by 25 to 35% [29].

Unhelmeted impacts are quite different to helmeted impacts as the acceleration pulses are of a short duration and contain higher frequency components. This study addresses a number of issues not addressed in the other studies: how does the xPatch sensor perform in unhelmeted impacts above 80g; how does it perform during impacts to the side and rear of the headform; how does the device's output compare when fitted to the left-hand side and right-hand side of the head. Unlike other investigations, this study investigated the accuracy of the device over its full range (20g to 200g) following impacts in four directions to an unhelmeted head.

3.2 Methods

The xPatch sensor is a six degree of freedom measurement device, consisting of three single axis accelerometers and three angular rate sensors. The device measures 37mm by 14mm and is designed to attach to the skin over the mastoid process (behind the ear) of the athlete. During an impact, linear acceleration in x, y and z is recorded, as well as angular velocity about the 3 axes. Data is recorded by the device for 100ms with a sample rate of 1000Hz and 800Hz for linear acceleration and angular velocity respectively. The acceleration data is transformed to calculate linear acceleration at the centre of gravity of the head. Angular acceleration is calculated from angular velocity. Both the transformation and differentiation were carried out using software supplied by X2Biosystems. The transformation is based on Equation 3-2.

$$a_{CG} = a_P + (\alpha \times r_{p-CG}) + \omega \ \times (\omega \times \ r_{p-CG})$$

a_{CG}: linear acceleration at the centre of gravity of the head, a_P: linear acceleration recorded by the device,

ω and α are the angular velocity and acceleration of the head respectively,

$r_{p\text{-}CG}$: geometric relationship between the device and the centre of gravity of the head.

Equation 3-1: Transformation of linear accleration to centre of gravity of the head [28]

Two xPatches were fixed according to the manufacturer's instructions, to a 50th percentile Hybrid III dummy headform. The xPatches were attached using the manufacturer's adhesive patches, to the left and right side of the head, in the area of the mastoid part of the temporal bone as recommended by X2Biosystems Inc: 72 mm from the head's centre of gravity to the inside edge of the xPatch, Figure 3-1.

Reference devices consisting of a triaxial linear accelerometer (Kistler 8688A) and three angular rate sensors (DTS ARS12K), were mounted at the centre of gravity of the headform on a block supplied by the manufacturer (Humanetics Inc. USA). The reference data was sampled at 10,000Hz, and 200ms of data was recorded per impact. Linear acceleration was filtered at 1000Hz and angular velocity was filtered at 300Hz. Fast Fourier transformation within LabVIEW (National Instruments, USA) was used to calculate the amplitude spectrum and verify these as suitable frequencies: i.e. no loss of data [30]. A forward finite difference method was computed to determine angular acceleration (Equation 3-2). All reference data was recorded using a customized LabVIEW 2015 program.

$$f'(x) = \frac{f(x+h) - f(x)}{h}$$

f(x): data point *h:* increment between data point

Equation 3-2: Forward finite difference method

Impacts were created by allowing the headform to drop in a purpose-built drop-test rig and impact a steel hemispherical anvil 0.12m diameter, Figure 3-1. As skull fracture is not being investigated, the diameter of this impactor is not considered significant. This is evident in other studies which have used a wide variety of impactors [25][27][28][29].

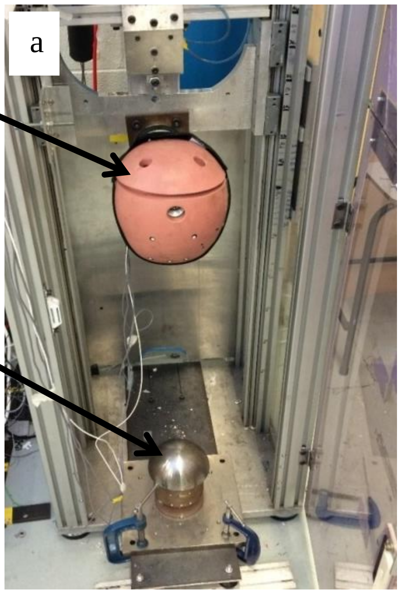

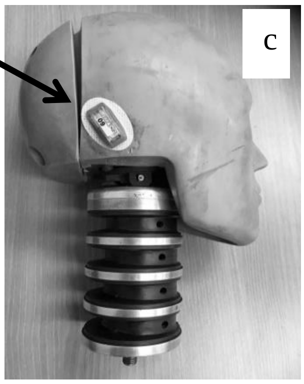

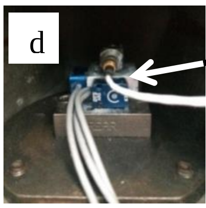

Figure 3-1: (a) Drop test rig (view 1) (b) Drop test rig (view 2). (c)Drop hybrid III head with xPatch attached. (d) Reference sensors.

The Hybrid III head was rigidly attached to the cross bar of the apparatus, this cross bar was constrained to allow only vertical movement. This constraint ensured consistency in the repeatability of the tests. Following an impact, the rotation of the head is a function of the stiffness of the neck, as the base of the neck is rigidly constrained in the vertical direction.

The test conditions were designed to cover the sensors full linear acceleration range of 20g to 200g; this corresponded to drop heights of 160mm to 610mm. The testing procedure consisted of a total of 10 drop heights, and each test was repeated 10 times. Impacts were to four locations: left side, right side, front and rear of the head (Figure 3-2). Thus a total of 400 tests were conducted. A sample of the linear acceleration results from a drop of 360mm is shown in Figure 3-3. The duration of the impact in this case is 12.5ms.

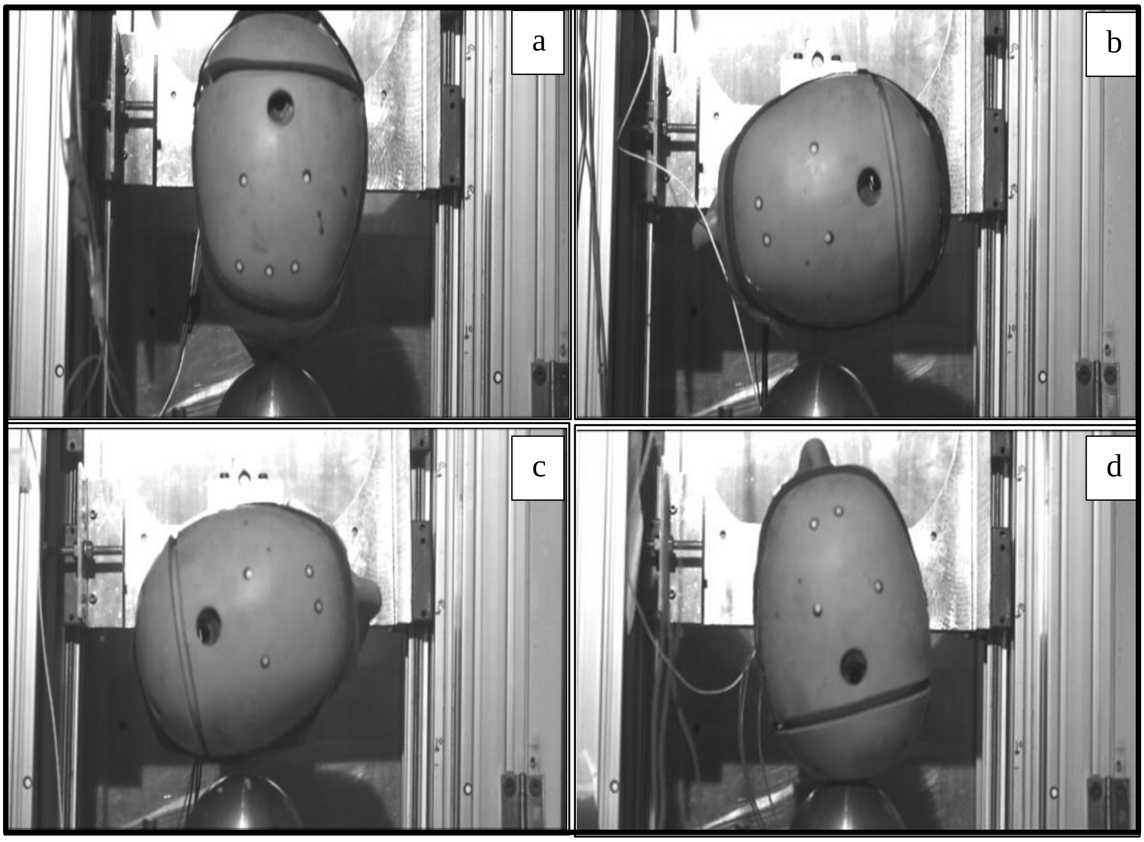

Figure 3-2: Impact locations (a) Front (b)Left, (c) Right, (d) Rear

This study was exempt from IRB approval as it did not involve human participants as outlined by the code of federal regulations (45 CFR 46.102(f)).

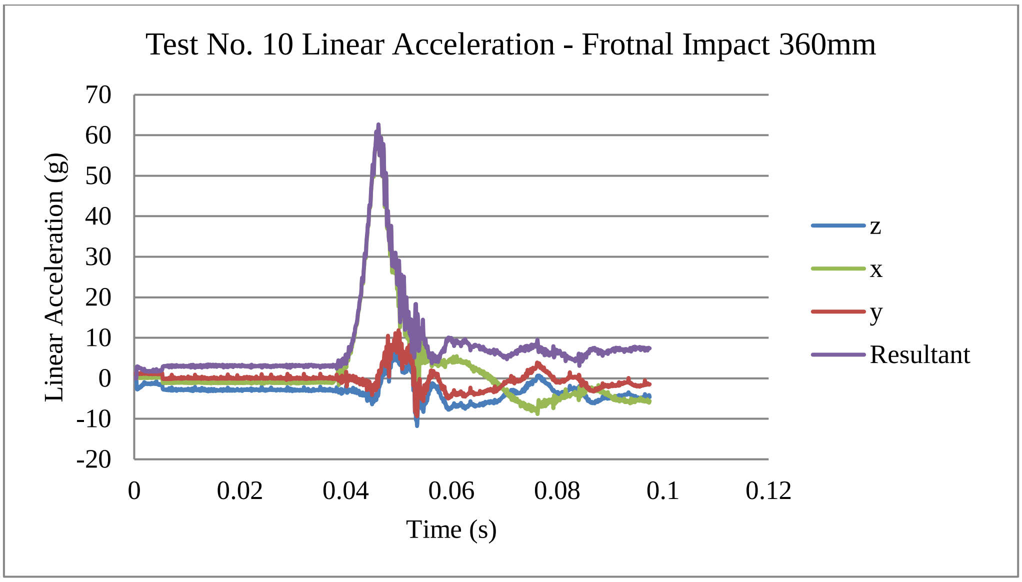

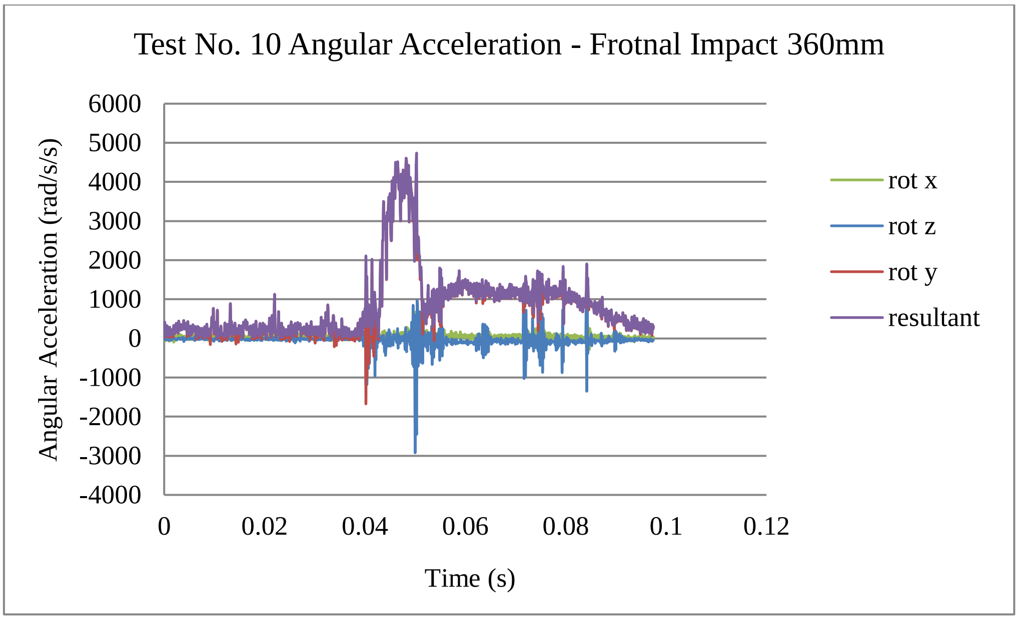

Figure 3-3: Linear and angular acceleration from reference accelerometers following a frontal impact at a drop height of 360mm (Test number 10)

Table 3-1 is a sample of the results from a front drop height of 360mm, the PLA average was 62.83g (standard deviation (SD) 1.80), angular velocity 20.07rad/s (SD 1.62) and the average calculated angular acceleration was 5135.82rad/s^2 (SD 1062).

Table 3-1 : Sample results from a 360mm frontal drop

		Kistler			Biosystems X2 LHS			Biosystems X2 RHS		
No	Test Time	Linear Accel. g	Angular Velocity rad/s	Angular Accel. rad/s/s	Linear Accel. g	Angular Velocity rad/s	Angular Accel. rad/s/s	Linear Accel. g	Angular Velocity rad/s	Angular Accel. rad/s/s
1	14:30	65.58	19.42	4866.10	79.45	23.64	4395.02	79.33	17.33	4007.99
2	14:33	63.74	22.08	4028.00	77.00	23.80	4356.85	77.44	17.69	4151.51
3	14:36	61.70	19.80	3668.20	79.88	24.14	4629.65	85.00	27.41	4242.71
4	14:39	61.23	21.46	5653.60	75.00	23.85	4435.59	77.95	21.45	4059.96
5	14:42	67.03	21.20	6106.20	77.04	23.49	4445.72	82.03	18.29	3943.82
6	14:45	60.37	19.08	4724.10	77.43	24.35	4608.95	84.48	28.54	4330.37
7	14:48	60.71	20.16	7026.20	78.62	24.57	4667.86	82.38	26.30	4319.63
8	14:51	62.44	19.37	6496.60	80.71	24.36	4601.41	83.49	25.22	4256.37
9	14:54	62.84	16.28	4366.20	77.70	23.26	4243.00	85.23	26.27	3879.19
10	14:59	62.70	21.84	4423.00	78.02	24.52	4636.05	82.72	24.20	4369.30
	Average	62.83	20.07	5135.82	78.08	24.00	4502.01	82.01	23.27	4156.09

3.3 Results

3.3.1 Linear acceleration

An analysis of the data found that all the impacts were recorded by the xPatch, i.e. no missing impacts. Table 3-2 gives a sample of the accelerations recorded during frontal impacts, 10 impacts were conducted at each height and the average is reported in the table. The correlation coefficient R^2 and predicted residual error sum of squares (PRESS) statistics were calculated to provide a measure of fit of the data to a linear model and investigate the reliability of the data.

Table 3-2: Summary of linear acceleration results for frontal impacts

	Kistler			LHS X-Patch				RHS X-Patch			
Drop Height (mm)	**Mean (g)**	**Std. Dev.**	**Standard error of mean**	**Mean (g)**	**Std. Dev.**	**Standard error of mean**	**% Error**	**Mean (g)**	**Std. Dev.**	**Standard error of mean**	**% Error**
610	127.6	11.84	3.95	129.7	5.86	1.75	1.69	133.7	0.41	1.25	4.83
560	108.8	4.23	1.83	115.3	3.55	0.40	6.00	125.3	0.32	0.90	15.19
510	97.7	2.57	0.86	108.4	1.64	1.00	10.99	115.0	0.28	0.71	17.78
460	85.2	3.96	1.32	96.1	4.27	0.44	12.89	102.5	0.26	0.64	20.37
410	75.4	2.56	0.85	87.7	2.98	0.54	16.31	93.5	0.48	0.37	23.98
360	62.8	1.80	0.60	78.1	2.48	0.50	24.27	82.0	3.51	0.85	30.51
310	53.4	1.15	0.47	67.4	2.07	0.39	26.21	70.0	0.26	0.37	31.03
260	42.9	0.41	0.17	57.0	1.68	0.40	33.06	58.2	0.36	0.42	35.91
210	36.4	3.08	0.00	46.9	7.14	0.45	28.70	50.9	0.23	0.58	39.64
160	30.9	3.64	1.50	33.5	11.11	1.14	8.59	36.2	0.28	1.29	17.22

The correct location (Left, Right, Front and Rear) of the impact was recorded by both xPatches. When impacted in the front, the linear acceleration of the xPatch device correlated well with the reference accelerometer: R^2 = 0.9527; PRESS statistic = 5403 for the left-hand side (LHS) and R^2 =0.9471; PRESS statistic = 5403 for the right-hand side (RHS), (see Figure 3-4).

The xPatch overestimated the linear acceleration during a frontal impact. This over estimation was on average 16.9% for the LHS xPatch and 23.7% for the RHS xPatch. The linear acceleration for the right and left side impacts, had a poorer correlation than the frontal impacts. The xPatch device on the side that was being impacted overestimated impacts over 110g by 9%, and underestimated impacts under 90g by 16%. The device on the opposite side to the impact overestimated impacts over 110g by 14.5%, and underestimated impacts under 90g by 13%.

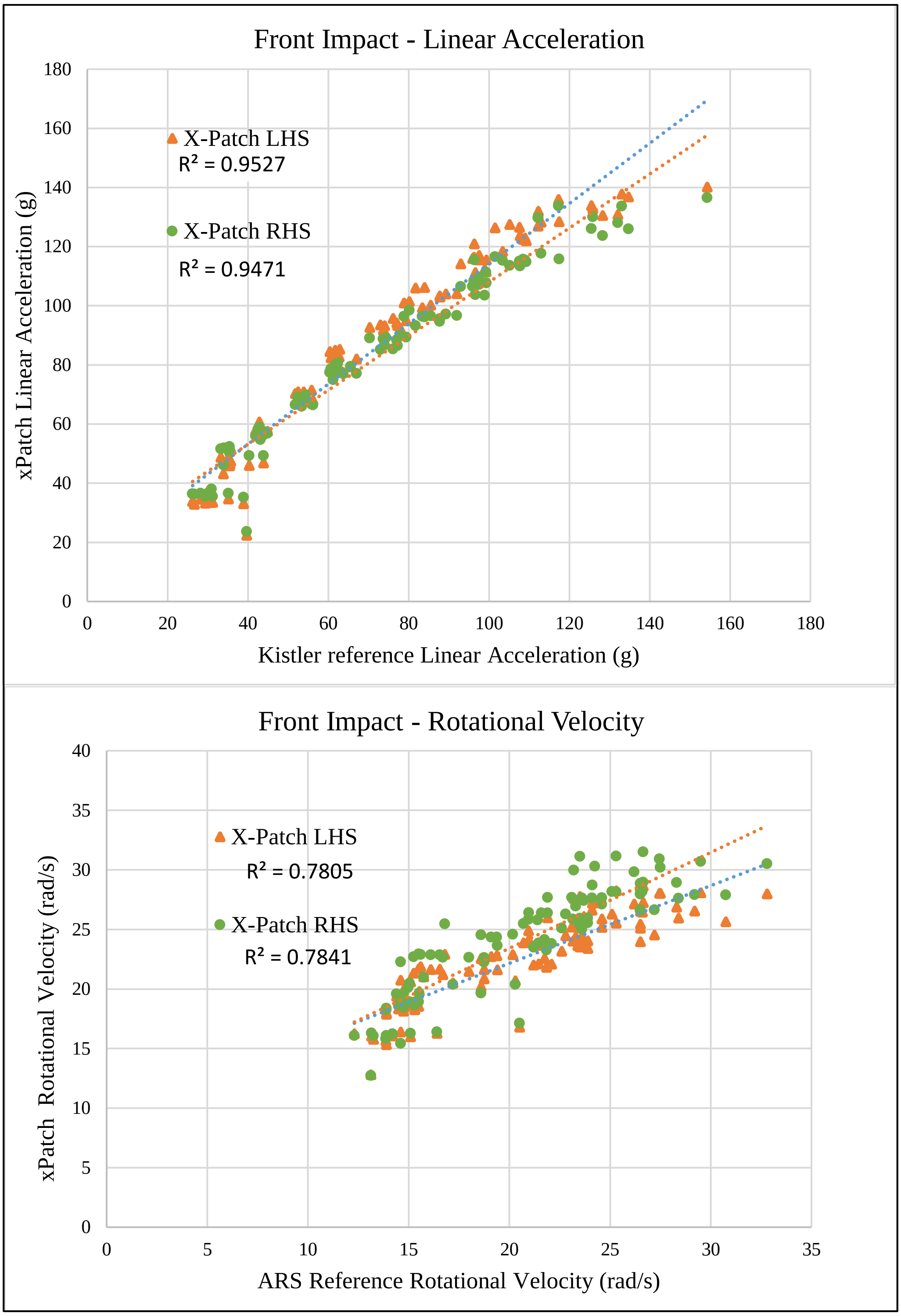

Figure 3-4: Linear acceleration and angular velocity regression analysis for frontal impacts

Figure 3-5, 3-6 and 3-7 show box plots of the median and interquartile range of the linear acceleration recorded by Kistler reference accelerometer and the xPatch devices on the LHS and RHS of the head.

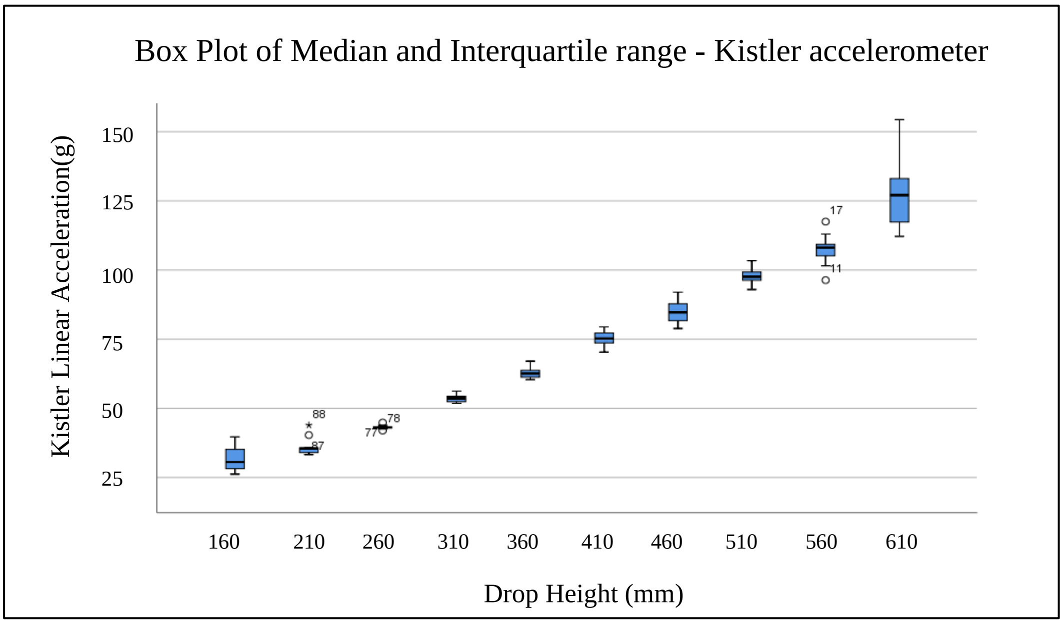

Figure 3-5: Box plot showing median and interquartile range for the linear acceleration recorded by the Kistler accelerometer for each drop height during frontal impact

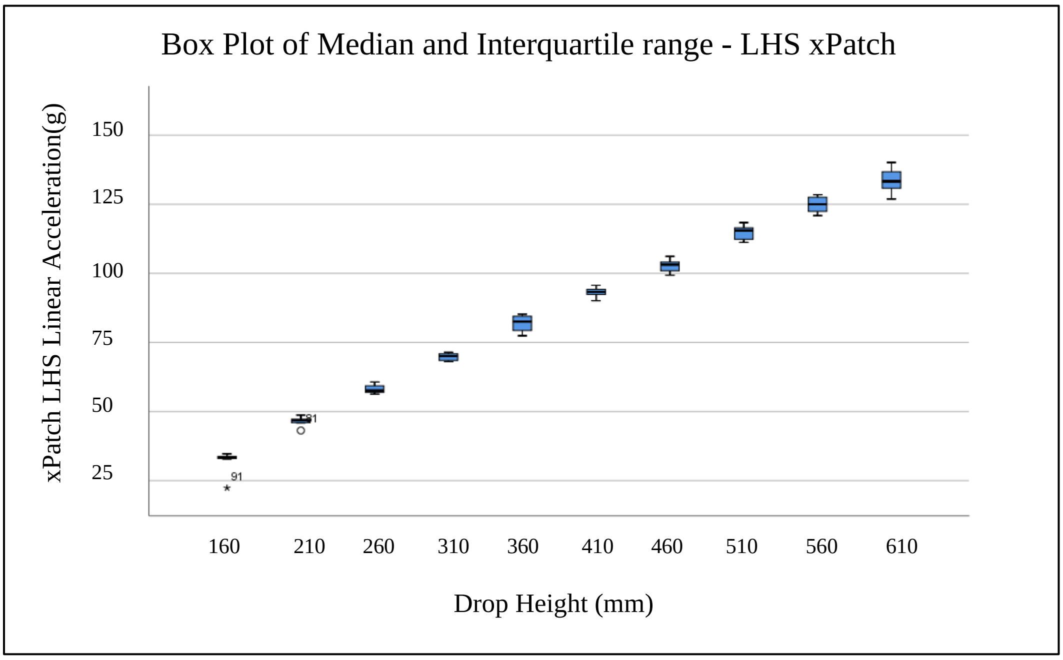

Figure 3-6: Box plot showing median and interquartile range for the linear acceleration recorded by the xPatch on the left side accelerometer for each drop height during frontal impact

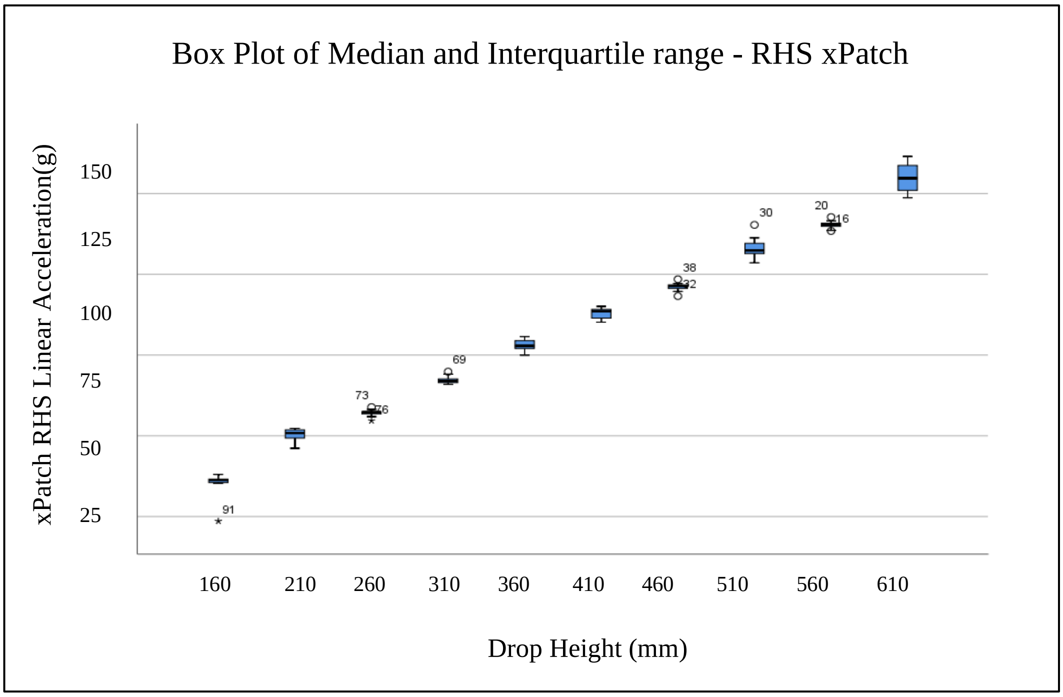

Figure 3-7: Box plot showing median and interquartile range for the linear acceleration recorded by the right hand xPatch on the accelerometer for each drop height during frontal impact

There was a poor correlation of the results from the rear impact tests to the reference data (R^2 for LHS = 0.7311, R^2 for RHS= 0.7021). Similar to the side impacts, the xPatch overestimated the more severe impacts. The xPatch applied to the LHS of the headform, underestimated impacts over 130g on average by 5%, and overestimated impacts under 120g by 30%, on average. The xPatch applied to the RHS, overestimated impacts over 100g by 20% on average, and underestimated impacts under 90g by an average of 30%. A comparison of the xPatch linear and angular acceleration results for a frontal impact are shown in Figure 3-8.

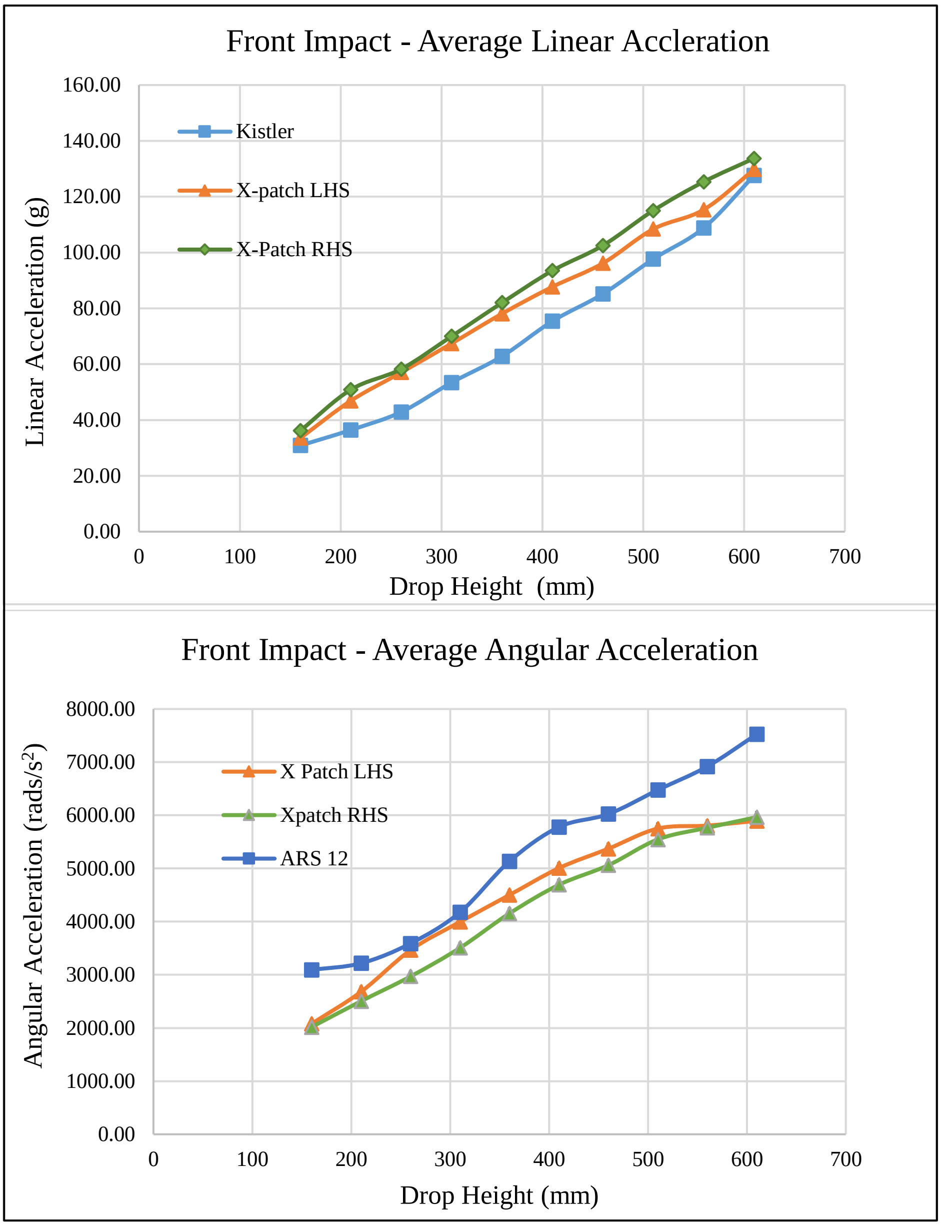

Figure 3-8: Linear and angular acceleration following a frontal impact, LHS and RHS xPatch and reference data shown

3.3.2 Angular velocity

It was found that the angular velocity correlation with the reference device was not as good as that for linear accelerations (R^2 for LHS = 0.7841; PRESS statistic = 566.5, R^2 for RHS = 0.7805; PRESS statistic = 549.3). The xPatch overestimated the angular velocity on average by 17.4% for the sensor on the LHS of the headform, and 13.9% for the RHS of the headform, see Table 3-3. The side impact results revealed a significant difference between the xPatches on the RHS and LHS of the headform, with the device on the opposite side to the impact performing better than the device on the impact side. The device on the side of the impact overestimated the velocity by an average of 47.5% while the device on the opposite side to the impact overestimated the velocity by 23%. The xPatch results from the rear impacts also found that the devices overestimated the angular velocity on average by 20% for the device on the left of the headform and 33% for the device on the right. Rear impacts provided the best angular velocity correlation with the referenced data (R^2 = 0.8896; PRESS statistic = 68 x 10^6 for LHS & R^2 = 0.7919 for RHS; PRESS statistic = 72 x 10^6).

Table 3-3: Summary of angular velocity for frontal impacts

DTS ARS 12K				LHS X-Patch				RHS X-Patch			
Drop Height (mm)	**Average (rad/s)**	**Std. Dev.**	**Standard error of mean**	**Average (rad/s)**	**Std. Dev.**	**Standard error of mean**	**% Error**	**Average (rad/s)**	**Std. Dev.**	**Standard error of mean**	**% Error**
610	25.49	3.59	1.20	30.62	0.52	0.17	20.14	27.90	0.41	0.14	9.45
560	25.01	2.22	0.71	28.45	0.41	0.15	13.76	26.74	0.32	0.10	6.92
510	23.93	2.31	0.77	27.67	0.28	0.14	15.66	25.62	0.28	0.10	7.06
460	23.37	1.88	0.68	26.56	0.45	0.16	13.68	24.15	0.26	0.10	3.36
410	21.81	2.00	0.67	25.58	0.27	0.10	17.29	23.76	0.48	0.17	8.93
360	20.07	1.62	0.54	19.50	2.94	0.14	2.84	23.27	3.51	0.14	15.95
310	16.96	1.49	0.55	22.70	0.19	0.08	33.82	21.43	0.26	0.12	26.32
260	16.25	1.81	0.63	20.13	0.44	0.17	23.87	20.40	0.36	0.15	25.50
210	15.35	1.22	0.65	18.30	0.25	0.17	19.25	18.63	0.23	0.17	21.43
160	14.07	1.07	0.37	15.97	0.32	0.37	13.46	16.04	0.28	0.34	13.96

3.3.3 Angular acceleration

The angular acceleration results had a poor-to-medium correlation (R^2=0.28 to 0.88) with the reference data. The error in the results from the xPatch varied depending on head orientation, xPatch location and impact magnitude. The xPatch underestimated the angular acceleration during frontal impacts with an average error of 14.3% for the LHS device and 19.6% for the RHS device; the errors were substantially higher for impacts to the side and rear of the headform, see Table 3-4. Impacts to the side of the head had an over estimation error of 46.5% for the device on the impact side, and an average underestimation error of 52% for the device on the opposite side to the impact.

Table 3-4: Summary of angular acceleration for frontal impacts

	DTS ARS 12K			LHS X-Patch				RHS X-Patch			
Drop Height (mm)	**Average (rad/s^2)**	**Std. Dev.**	**Standard error of mean**	**Average (rad/s^2)**	**Std. Dev.**	**Standard error of mean**	**% Error**	**Average (rad/s^2)**	**Std. Dev.**	**Standard error of mean**	**% Error**
610	7526.5	1150	517.12	5896.5	290.8	96.94	21.66	5966.0	252.5	84.16	20.73
560	6919.7	724.8	597.20	5806.6	161.0	62.00	16.09	5766.0	127.1	49.66	16.67
510	6477.4	809.5	288.84	5751.6	95.8	33.90	11.21	5547.5	42.5	18.82	14.36
460	6024.7	1311.05	796.59	5372.6	134.2	46.10	10.82	5062.1	132.4	44.61	15.98
410	5780.6	1625	541.70	5007.4	47.4	21.17	13.38	4693.3	121.4	40.59	18.81
360	5135.8	1062.02	355.25	4502.0	6.9	45.97	12.34	4156.1	0.4	55.08	19.08
310	4176.9	798.1	565.17	3996.2	91.5	42.09	4.32	3507.5	71.9	29.28	16.03
260	3590.1	262.3	150.96	3465.2	61.9	28.34	3.48	2970.1	38.9	13.08	17.27
210	3218.1	619.8	221.30	2682.7	32.0	16.84	16.64	2504.9	33.8	17.31	22.16
160	3093.1	613.6	431.70	2079.9	30.5	62.80	32.76	2018.0	26.5	60.01	34.76

Rear impacts had an error of -57% for the LHS xPatch and 12% for the RHS xPatch. The angular acceleration from the xPatch had very poor accuracy and consistency when the headform was impacted on the side and rear. The largest error was a 71% underestimation compared to the reference sensor; this was recorded during impacts to the right side of the headform. The errors for all impacts are summarised in Table 3-5.

Table 3-5: Summary of errors (xPatch relative to reference device)

	Frontal Impact		Side Impact		Rear Impact	
	LHS xPatch	RHS xPatch	xPatch on side of impact	xPatch on opposite side	LHS xPatch	RHS xPatch
Peak Linear Acceleration	+16.9%	+23.7%	+9% >110g -16% < 90g	+14.5% >110g -13% < 90g %	+5% >110g -30% < 90g	+20% >110g -30% < 90g
Angular Velocity	+17.4%	+13.9%	+47.5%	+23%	+20%	+33%
Peak Angular Acceleration	-14.3%	-19.6%	+46.5%	+52%	-57%	+12%

3.4 Discussion

This study assessed the performance of the xPatch sensor in laboratory conditions by comparing the recorded measurements with calibrated reference devices. The results illustrate that the xPatch provides a reasonable indication of linear acceleration during frontal impacts, but with a possible overestimation of up to 18%. This overestimation error was in keeping with Wu et al.'s [31] study of low speed impacts (over-estimation of 15g) and Schussler et al.'s [28] study of helmeted impacts (PLA error 22%). The rear impacts had errors of up to 30% and perhaps of greatest concern is the underestimation of severe (>110g) impacts; this underestimation has not been reported in other studies. Angular velocity errors were large (up to 47.5%) and hence the angular acceleration errors were also large (57%), as this is derived from the angular velocity. This study found that angular acceleration was underestimated by the xPatch; this was similar to Nevin et al.'s [29] findings from their study of frontal impacts. Unlike Nevin et al.'s study, this investigation also tested severe frontal, side and rear impacts; these were found to produce substantially higher errors (up to 71%). A study by Seigmund et al., using the xPatch with a helmeted cadaver, reported much larger errors of PLA 64±41% and PAA 370±456%; this was not broken down by impact location [32]. The large discrepancy between the xPatch and the reference sensor data in Seigmund et al.'s study, may be partly as a result of the degree of coupling between the head and the xPatch: when attached to human skin the device may move up to 4mm relative to the skull, even during low impacts [31].

During the data processing, it was found that the sample rate of both the reference data and the xPatch data was critical in acquiring accurate results. The xPatch is reported to sample linear acceleration at 1000Hz and angular motion at 800Hz. The low sampling frequency may be a possible cause for the under-prediction of results. Unhelmeted impacts require a higher frequency and bandwidth than helmeted sports, due to the shorter duration of the impact. This requirement will have a greater influence on the accuracy of the angular motion data as it has been found that for dummy helmeted impacts, gyroscopes require a bandwidth of 500Hz and 740Hz if numerical differentiation is used to calculate angular acceleration [33]. The bandwidth of the xPatch is considerably less than 500Hz [33]. In this study both the reference and the xPatch angular acceleration data was computed using a numerical differentiation method. This method amplifies the noise on the signal, this was particularly apparent on severe impacts where large errors in the angular acceleration data occurred. In future work it would be interesting to use a 6 or 9 accelerometer array to eliminate the requirement for numerical differentiation [34].

This study demonstrates the usefulness of the xPatch for identifying and recording impacts, as all of the impacts tested were recorded: i.e. no false positives or negatives. However, it must be noted that our study had a controlled setup and is unlike in-field testing; the study by Press and Rowson which resulted in a positive head impact prediction rate of 16.3% questions the reliability of the sensor on the field and highlights the need for video confirmation of all impacts [29]. Recording all head impacts accurately, without either over- or under-prediction, is important in studies of player welfare [35][36]. To date the xPatch sensor has been used to collect cumulative data in helmeted [31] and unhelmeted sports [23]. King et al. utilised the xPatch to measure the magnitude, frequency and location of head impacts sustained by under 9's Rugby Union players over the course of four consecutive matches [23]. A study indicating the usefulness of such sensors in regard to player's welfare was undertaken by Swartz et al. [37]. They conducted a study over the course of an American Football season and used the xPatch with two separate cohorts of players. The objective of the study was to analyse the head impacts of a group who practised unhelmeted drills against those who practised with helmets. It was determined that there was a 28% reduction in head impact frequency recorded by the group that did not use helmets during practices.

Accurately recording the occurrence, magnitude and direction of all impacts is critical in any investigation of head impacts. This study has highlighted that the results from the xPatch device must be treated with caution: frontal impacts are recorded with reasonable accuracy (up to 24%) but angular velocity and acceleration results from side and rear impacts may have large errors.

3.5 Conclusions

This study has shown the xPatch performs reasonably well in terms of linear acceleration but has highlighted that the angular velocity and acceleration measurements recorded by the xPatch have high levels of error and therefore need to be used with caution. This study also found that there is an issue using differentiation to calculate angular acceleration unless the sample frequency and bandwidth are suitable. To improve the angular acceleration measurements either a higher sample rate must be used, or an array of accelerometers that allows the angular acceleration to be calculated without differentiation.

Limitations

This study did not include oblique impacts which may induce high angular accelerations and relatively low linear accelerations [21][22][23].

3.6 References

[1] J. Langlois, W. Rutland-Brown, and M. Wald, “The Epidemiology and Impact of Traumatic Brain Injury A Brief Overview”, *J Head Trauma Rehabil*. 2006;21(5):375–8.

[2] M. Elliott, S. Margulies, M. Maltese, and K. Arbogast, “Accounting for sampling variability , injury under-reporting , and sensor error in concussion injury risk curves”, *J Biomech* [Internet]. 2015;48(12):3059–65. Available from: http://dx.doi.org/10.1016/j.jbiomech.2015.07.026

[3] G. Sye, S. Sullivan, P. McCrory, and C. Milne, “High school rugby players’ understanding of concussion and return to play guidelines”, Commentary. *Br J Sports Med* [Internet]. 2006;40(12):1003–5. Available from: http://bjsm.bmj.com/cgi/doi/10.1136/bjsm.2005.020511

[4] P. McCrory, W. Meeuwisse, J. Dvorak, M. Aubry, J. Bailes, S. Broglio et al., “Consensus statement on concussion in sport—the 5th international conference on concussion in sport held in Berlin”, *Br J Sports* Med Published Online First: 26 April. doi: 10.1136/bjsports-2017-097699, 2017.

[5] S. Broglio, B. Schnebel, J. Sosnoff , S. Shin, X. Feng, X. He, et al., “The biomechanical properties of concussions in high school football”, *Med Sci Sport Exer* 42.11: 2064, 2010.

[6] J. Abel, T. Gennarelli, and H. Segawa, “Incidence and severity of cerebral concussion in the rhesus monkey following sagittal plane angular acceleration”, (No. 780886). SAE Technical Paper. 1978.

[7] P. Bayly, T. Cohen, E. Leister, D. Ajo, E. Leuthardt, and G. Genin, “Deformation of the human brain induced by mild acceleration”, J *Neurotrauma* 22(8): 845-856.

[8] W. Hardy, M. Mason, C. Foster, C. Shah, J. Kopacz, K. Yang, et al. “A study of the response of the human cadaver head to impact”, *Stapp car crash journal* 51: 17, 2007.

[9] A. Post, and T. Hoshizaki, “Rotational acceleration, brain tissue strain, and the relationship to concussion”, *J Biomed Eng* 137(3): 030801, 2015.

[10] A. King, K. Yang, L. Zhang, W. Hardy, and D. Viano, “Is head injury caused by linear or angular acceleration”, *IRCOBI conference* 1-12, 2003.

[11] E. Takhounts, M. Craig, K. Moorhouse, J. McFadden, and V. Hasija, “Development of brain injury criteria (BrIC)”, *Stapp car crash journal* 57:243, 2013.

[12] L. Zhang, K. Yang, and A. King, “Comparison of brain responses between frontal and lateral impacts by finite element modelling”, *J Neurotrauma* 18(1): 21-30, 2001.

[13] L. Zhang, K. Yang, and A. King, “A proposed injury threshold for mild traumatic brain injury”, Transactions-American Society of Mechanical Engineers *Journal of Biomechanical Engineering* 126(2): 226-236, 2004.

[14] R. Greenwald, J. Chu, J. Crisco, and J. Finkelstein, Head Impact “Telemetry System (HITS) for measurement of head acceleration in the field”, *Proceedings*

of the American Society of Biomechanics Annual Meeting, 2003.

[15] E. Hanlon, and C. Bir, “Validation of a wireless head acceleration measurement system for use in soccer play”, *J Appl Biomech* 26(4), 424-431, 2010.

[16] R. Jadischke, D. Viano, N. Dau, A. King, and J. McCarthy, “On the accuracy of the Head Impact Telemetry (HIT) System used in football helmets”, *J Biomech* 46(13), 2310-2315, 2013.

[17] S. Duma, S. Manoogian, W. Bussone, P. Brolinson, M. Goforth, J. Donnenwerth et al., “Analysis of real-time head accelerations in collegiate football players”, *Clin J Sport Med* 15(1), 3-8, 2005.

[18] S. Rowson, S. Duma, J. Beckwith, J. Chu, R. Greenwald, J. Crisco, et al., “Rotational head kinematics in football impacts: an injury risk function for concussion”, *Ann Biomed Eng* 40(1), 1-13, 2012.

[19] J. Beckwith, J. Chu, and R. Greenwald, “Validation of a non-invasive system for measuring head acceleration for use during boxing competition”, *J App Biomech* 23(3): 238-244, 2007.

[20] J. Caccese, L. Lamond, T. Buckley, and T. Kaminski, “Reducing purposeful headers from goal kicks and punts may reduce cumulative exposure to head acceleration”, *Res Sport Med* 24(4): 407-415, 2016.

[21] E. Hanlon, and C. Bir, “Real-time head acceleration measurement in girls' youth soccer”, *Med Sci Sports Exer* 44(6): 1102-1108, 2012.

[22] R. Naunheim, J. Standeven, C. Richter, and L. Lewis, “Comparison of impact data in hockey, football, and soccer”, *J Trauma Acute Care* 48(5): 938-941, 2000.

[23] D. King, P. Hume, C. Gissane, and T. Clark, “Head impacts in a junior rugby league team measured with a wireless head impact sensor: an exploratory analysis”, *J Neurosurg- Pediatr* 19(1): 13-23, 2017.

[24] M. Higgins, P. Halstead, L. Snyder-Mackler, and D. Barlow, “Measurement of impact acceleration: mouthpiece accelerometer versus helmet accelerometer”, *J Ath Training* 42(1): 5, 2007.

[25] B. Cummiskey, D. Schiffmiller, T. Talavage, L. Leverenz, J. Meyer, D. Adams, et al., “Reliability and accuracy of helmet-mounted and head-mounted devices used to measure head accelerations”, *Proceedings of the Institution of Mechanical Engineers, Part P: Journal of Sports Engineering and Technology* 231(2): 144-153, 2017.

[26] G. Wood, M. Panzer, C. Bass, and B. Myers, “Viscoelastic properties of hybrid III head skin”, SAE *International Journal of Materials and Manufacturing* 3(2010-01-0383): 186-193, 2010.

[27] S. Rowson, and J. Press. “Quantifying Head Impact Exposure in Collegiate Women’s Soccer”, *Clin. J. Sport Medicine* Mar 27(2) 104-110, 2017.

[28] E. Schussler, D. Stark, J. Bolte, Y. Kang, and J. Onate. “Comparison of a head mounted impact measurement device to the Hybrid III anthropomorphic testing device in a controlled laboratory setting”, *International Journal of Sports Physical Therapy*.12(4):592-600, 2017.

[29] D. Nevins, L. Smith, and J. Kensrud, “Laboratory evaluation of wireless head

impact sensor", *Procedia Engineering* 112: 175-179, 2015.

[30] National Instruments, LabVIEW "Using Fast Fourier Transforms and Power Spectra in LabVIEW", http://www.ni.com/white-paper/4541/en/ , 2017.

[31] L. Wu, K. Laksari, C. Kuo, L. Luck, S. Kleiven, R. Cameron, et al., "Bandwidth and sample rate requirements for wearable head impact sensors", *J. Biomechanics*, 49(13), 2016.

[32] G. Siegmund, K. Guskiewicz, S. Marshall, A. DeMarco, and S. Bonin, "Laboratory validation of two wearable sensor systems for measuring head impact severity in football players", *Ann Biomed Eng* 44(4): 1257-1274, 2016.

[33] L. Wu, K. Laksari, C. Kuo, L. Luck, S. Kleiven, R. Cameron, et al., "Bandwidth and sample rate requirements for wearable head impact sensors", *J Biomech* 49(13): 2918-2924, 2016.

[34] E. Davenport, C. Whitlow, J. Urban, M. Espeland, Y. Jung, D. Rosenbaum, et al. "Abnormal white matter integrity related to head impact exposure in a season of high school varsity football", *J Neurotrauma*, 31(19), 1617-1624, 2014.

[35] K. Guskiewicz, M. McCrea, S. Marshall, R. Cantu, C. Randolph, W. Barr, et al., "Cumulative effects associated with recurrent concussion in collegiate football players: the NCAA Concussion Study", *Jama*, 290(19): 2549-2555, 2003.

[36] E. McCuen, D. Svaldi, K. Breedlove, N. Kraz, B. Cummiskey, E. Breedlove, et al., "Collegiate women's soccer players suffer greater cumulative head impacts than their high school counterparts", *J Biomech* 48(13): 3720-3723, 2015.

[37] E. Swartz, S. Broglio, S. Cook, R. Cantu, M. Ferrara, K. Guskiewicz, et al., "Early results of a helmetless-tackling intervention to decrease head impacts in football players", *J Ath Training* 50(12): 1219-1222, 2015.

Chapter 4

The accuracy and repeatability of a wireless headband sensor

Abstract

Objective: The objective of this study was to examine the accuracy and repeatability of a headband sensor by comparing it to reference accelerometers and angular rate sensors placed at the centre of gravity of a Hybrid III headform.

Methods: A SIM-G headband sensor was attached to a Hybrid III headform and neck which was equipped with a triaxial accelerometer and 3 angular rate sensors. Reference linear acceleration and angular rate sensors were sampled at 10,000Hz while the SIM-G sensors linear and angular velocity were sampled at 1000Hz and 800Hz, respectively. A drop test was developed to impact the head with linear accelerations from 20 to 140g. Testing consisted of a total of 100 impacts per location to four locations: left occipital, right occipital, front and rear. Multiple tests were performed at the same height to investigate the repeatability of the device.

Results: The SIM-G sensor was found to be highly repeatable as measured by Cronbach's alpha coefficient (α = 0.97 to 0.99). However, the correlation between the SIM-G sensor and the reference sensors demonstrated a weak to very strong relationship using Pearson's Correlation coefficient (r = 0.2 to 0.9).

Conclusion: The weak to strong correlation of the SIM-G to the reference sensors indicates that its accuracy must be carefully considered by clinicians or researchers when using this sensor.

Published: *S. Tiernan, D. O'Sullivan, and G. Byrne, "Repeatability and Reliability evaluation of a Wireless Head-band Sensor," Asian J. Kinesiol., 20(4), pp. 70–75, 2018.*
DOI: doi.*org/10.15758/ajk.2018.20.4.70*

This chapter is a reproduction of the published paper except for some minor alterations and the alteration of Figure 4-2.

4.1 Introduction

Research investigating the biomechanics of head injury has been carried out in many sports including: American football [1][2], soccer [3], boxing [4] and taekwondo [5]. Various head impact monitors have been developed for helmeted and non-helmeted sports [6][7][8]. The Head Impact Telemetry (HIT) system incorporates a nine-accelerometer array and has been used in US football [1][2][7] and ice-hockey [9], but has also been modified for use in soccer [3] and boxing [10].

As not all impact sports have helmets or protective headgear, instrumented mouthpieces [11] have been developed for the dual purpose of orofacial protection and head impact data collection [12]. Three of the organisations that have developed instrumented mouthguards are: X2 Biosystems Inc., Seattle, USA, Protecht, Cleveland Clinic, USA, and CAMLab, Stanford University, USA [13,14]. Other impact sensors include instrumented skin patches (xPatch, X2 Biosystems Inc., USA), and instrumented skullcaps and headbands, Checklight (Reebok; Canton, USA), Shockbox HD (Impakt Protective Inc., Kanak, Canada), and SIM-G (Triax, USA).

To date, there is an absence of peer reviewed articles which have tested the repeatability and accuracy of the SIM-G headband sensor (Figure 2-10). Karton et al. used a pendulum test system to impact an instrumented Hodgson headform fitted with the SIM-G sensor [15,16]. Karton et al.'s study only tested a limited range of the sensor. A postgraduate research project in Purdue University, USA tested the SIM-G using an impulse hammer to impact an American football helmet worn by a Hybrid III headform [17]. Peak linear acceleration recorded by the SIM-G sensor was compared to the headform reference data and root mean square errors of 17.91 to 74.68%, and mean absolute errors of 10.3 to 50.36%, were reported for seven impact locations. The accuracy of the angular velocity or acceleration was not reported [17].

4.2 Methods

4.2.1 Measurement device

The SIM-G headband sensor (Triax Technologies, USA) is a six degree of freedom measurement device consisting of a high-g triaxial accelerometer (up to 1000g), low-g triaxial accelerometer (up to 100g) and a triaxial gyroscope [15]. The linear accelerometers were sampled at a frequency of 1000Hz and the gyroscope was sampled at a frequency of 800Hz [15]. Each impact above a 16g threshold (manufacture selected) was recorded for 10ms pre-impact and 52ms post-impact [15].

4.2.2 Data processing

Reference devices consisting of a triaxial linear accelerometer (Kistler 8688A) and three angular rate sensors (DTS ARS12K) were mounted at the centre of gravity of the headform on a manufacturer provided block (Humanetics Inc. USA). The reference data was sampled at 10,000Hz and 200ms of data was recorded for each impact. Linear acceleration was filtered at 1000Hz and angular velocity was filtered at 300Hz. These filter frequencies were verified as suitable using a Fourier transformation to calculate the amplitude spectrum and ensuring that there was no loss of data. A finite difference method was computed in Matlab (Mathworks Inc.) to calculate angular acceleration. All reference data was recorded using a customised Labview 2015 program (Texas Instruments, USA).

4.2.3 Testing procedure

The testing procedure consisted of a total of 400 impacts to four locations: left occipital, right occipital, front and rear impacts. The test conditions were designed to test the sensors full linear acceleration range from 20g to 140g. To create these conditions, the headform was fixed in the drop test rig in various orientations and released from heights ranging from 0.09m to 0.61m. The headform impacted a steel hemisphere of 0.12m diameter as shown in Figure 4-1. Ten tests were completed at each of the drop heights to investigate the repeatability of the devices. The position of the sensors did not change during testing. All impact tests were recorded using a high-speed video camera.

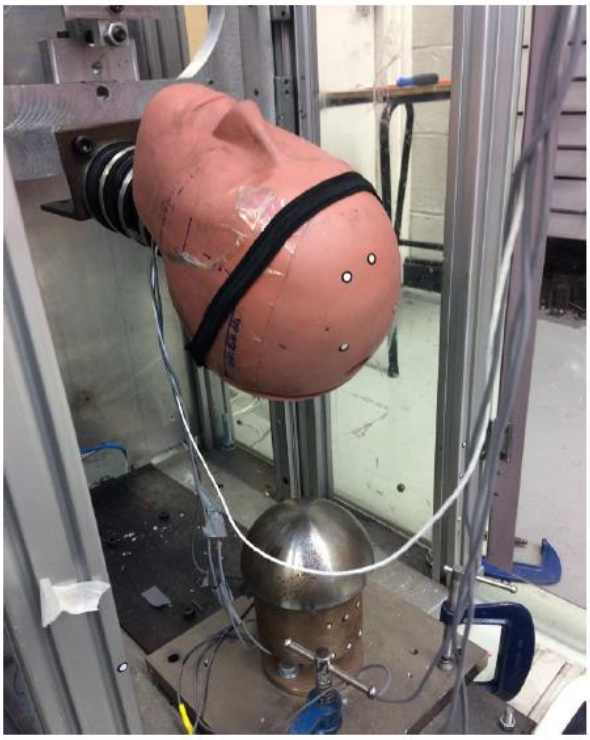

Figure 4-1: Hybrid 3 headform with SIM-G sensor (standard triaxial linear accelerometers and gyroscopes are placed at the head's centre of gravity and sim-g as placed on the back).

4.2.4 Statistical analysis

The impact data was analysed using SPSS (version 23.0). Pearson's Correlation coefficient (Table 4-1) and Cronbach's Alpha coefficient (Table 4-2) were calculated.

4.3 Results

The relationship between the two devices was investigated by calculating Pearson's Correlation coefficient. The correlation of the SIM-G linear and angular sensors with the reference sensors is shown in Table 4-1. The reliability and repeatability of the SIM-G device was investigated by calculating the Cronbach's Alpha score and is shown in Table 4-2.

Table 4-1: Pearson's Correlation coefficients for data from the SIM-G and the reference sensors

	Pearson's Correlation coefficient (r)		
Impact Location	**Resultant linear acceleration**	**Resultant angular velocity**	**Resultant angular acceleration**
Rear	0.74	0.90	0.59
Right	0.21	0.46	0.37
Left	0.27	0.79	0.75
Front	0.88	0.56	0.62

Table 4-2: Cronbach's Alpha coefficient (α) for the repeatability of the SIM-G sensor

	Cronbach's Alpha coefficient (α)		
Impact location	**Resulting linear acceleration**	**Resultant angular velocity**	**Resultant angular acceleration**
Rear	0.978	0.979	0.984
Right	0.993	0.998	0.998
Left	0.957	0.991	0.970
Front	0.999	0.998	0.998

Figure 4-2 shows the linear acceleration for both the triaxial and SIM-G sensors for frontal impacts. There was a similar trend in the data for the impacts to other locations, i.e. left, right, and rear.

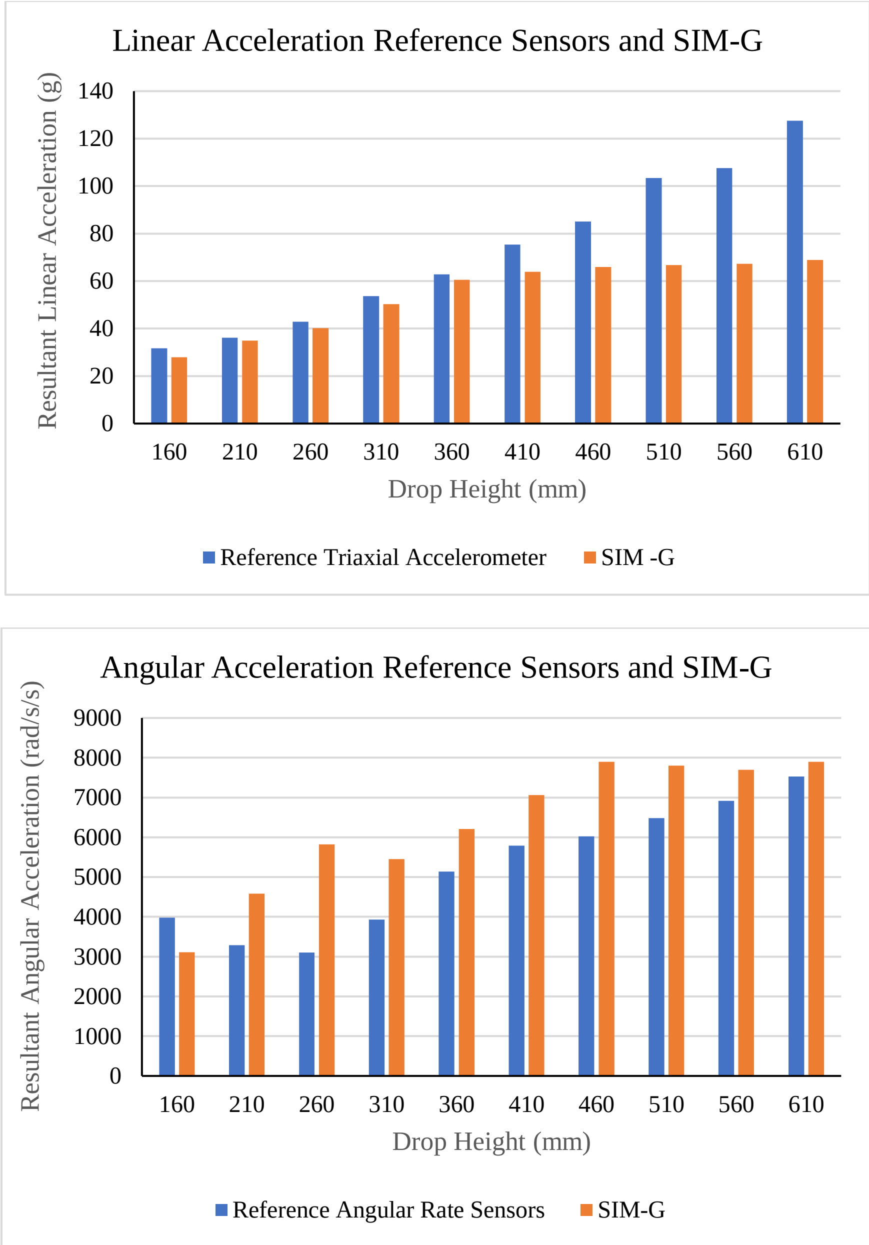

Figure 4-2: Comparison of SIM-G linear and angular acceleration with reference sensors

4.4 Discussion

The main objective of this study was to investigate the accuracy and repeatability of the SIM-G sensor by comparing it with a gold standard triaxial accelerometer and 3 angular rate sensors. The repeatability of the 10 trials at the 10 different heights is very strong (above $\alpha < 0.9$). However, the Pearson's correlation coefficient (r), which measures the accuracy had a large range from 0.2 to 0.9, which corresponds to a weak to very strong correlation and is dependent on the impact location and the magnitude of the acceleration [18].

It was noted that as the impact severity exceeded approximately 80g, the resultant linear acceleration of the SIM-G was non-linear, unlike the resultant linear acceleration of the reference triaxial accelerometer. Hence the results were divided into two categories: from 25 to 80g and above 80g. The Pearson's correlation coefficient for the peak linear acceleration of the two categories was $r = 0.97$, $r = 0.82$, respectively. This partially agrees with Karton et al. who reported that the SIM-G is highly correlated with a reference sensor for impacts with a linear acceleration up to 80g ($r = 0.91$ peak linear acceleration) [15]. The test data demonstrates that over 80g the SIM-G underestimates both the linear and angular acceleration. Thus, researchers or clinicians must be careful in interpreting the data from the SIM-G for accelerations over 80g, which are typical of impacts that may result in a head injury [19][20].

This investigation found that the accuracy of both the linear and angular accelerations recorded by the SIM-G varies largely depending on the location of the impact. A critical source of error is the movement of the headband and sensor relative to the head when the headform was impacted. This movement was observed using the high-speed recording of the tests, it has also been reported previously [14]. Errors may also be due to the SIM-G's sensors having an insufficient sampling frequency and narrow bandwidth [13][14]. The methodology could be improved by measuring the displacement of the sensor during an impact to determine the contribution of this movement to the overall error. In addition oblique impacts could be added to better replicate the types of impacts that occur in the real world.

4.5 Conclusions

This study demonstrated that the SIM-G headband must be used with caution as the sensor underestimates both linear and angular acceleration data for impacts with a linear acceleration above 80g. Clinicians and researchers must be wary of using the system for recording head impact data as it underestimates potentially injurious impacts.

Limitations

This study did not include oblique impacts which may induce high angular accelerations and relatively low linear accelerations [21][22][23]. Also, the study did not investigate the accuracy of the impact location reported by the SIM-G sensor.

4.6 References

[1] J. Schmidt, K. Guskiewicz, J. Mihalik, J. Blackburn, G. Siegmund and S. Marshall, "Head impact magnitude in American high school football", *Pediatrics*. Jul 18:e20154231, 2016.

[2] E. Wasserman, J. Mihalik, K. Campbell, P. Combs, M. Fraser, E. Grand, et al. "Innovative behaviour modification strategies to reduce concussion risk in high school American football athletes", *Br J Sports Med*. Jun 1;51(11):A67-A67, 2017.

[3] R. Lynall, M. Clark, E. Grand, J. Stucker, A. Littleton, A. Aguilar, et al., "Head Impact Biomechanics in Women's College Soccer", *Med Sci Sport Exer*. Sep;48(9):1772-8, 2016.

[4] I. Loturco, F. Nakamura, G. Artioli, R. Kobal, K. Kitakura, C. Adad, et al., "Strength and power qualities are highly associated with punching impact in elite amateur boxers", *J Strength Cond Res*. 2016 Jan 1;30(1):109-16, 2016.

[5] D. O'Sullivan, and P. Gabriel, "Biomechanical head impact characteristics during sparring practice sessions in high school taekwondo athletes", *Pediatrics* 19.6 (2017): 662-667, 2017.

[6] G. Siegmund, K. Guskiewicz, S. Marshall, A. DeMarco, and S. Bonin, "Laboratory validation of two wearable sensor systems for measuring head impact severity in football players", *Ann Biomed Eng* 2016 Apr 1;44(4):1257-74, 2016.

[7] K. O'Connor, S. Rowson, S. Duma, and S. Broglio, "Head-impact measurement Devices: A systemic review", 52(3): *J. Athletic Training*, 206-227, 2017.

[8] K. Campbell, M. Warnica, I. Levine, J. Brooks, A. Laing, T. Burkhart, et al., “Laboratory evaluation of the gForce Tracker™, a head impact kinematic measuring device for use in football helmets”, *Ann Biomed Eng*. Apr 1;44(4):1246-56, 2016.

[9] B. Wilcox, J. Beckwith, R. Greenwald, J. Chu, T. McAllister, L. Flashman et al., “Head impact exposure in male and female collegiate ice hockey players”, *J Biomech*. 47(1):109-14, 2014.

[10] S. Stojsih, M. Boitano, M. Wilhelm, and C. Bir, “A prospective study of punch biomechanics and cognitive function for amateur boxers”, *Br J Sports Med*. Aug 1;44(10):725-30, 2010.

[11] D. King, P. Hume, C. Gissane, and M. Brughelli, “The influence of head impact threshold for reporting data in contact and collision sports: systematic review and original data analysis”, *Sports med.* Feb 1;46(2):151-69, 2016.

[12] Y. Tanaka, T. Tsugawa, and Y. Maeda, “Effect of mouthguards on impact to the craniomandibular complex”, *Dent Traumatol*. Feb 1;33(1):51-6, 2017.

[13] L. Wu, K. Laksari, C. Kuo, J. Luck, S. Kleiven, C. Bass, et al., “Bandwidth and sample rate requirements for wearable head impact sensors”, *J Biomech*. Sep 6;49(13):2918-24, 2016.

[14] L. Wu, V. Nangia, K. Bui, B. Hammoor, M. Kurt, F. Hernandez, et al., “In vivo evaluation of wearable head impact sensors”, *Ann Biomed Eng.* 2016 Apr 1;44(4):1234-45.

[15] C. Karton, R. Oeur, and T. Hoshizaki, “Measurement accuracy of head impact monitoring sensor in sport”, *ISBS-Conference Proceedings Archive* 2016 Nov 6 (Vol. 34, No. 1), 2016.

[16] R. Oeur, C. Karton, and T. Hoshizaki, “Impact frequency validation of head impact sensor technology for use in sport”, *ISBS-Conference Proceedings Archive* Nov 6 (Vol. 34, No. 1), 2016.

[17] B. Cummiskey, “Characterization and evaluation of head impact sensors and varsity football helmets” [M.S. thesis], Purdue University, West Lafayette, Ind, USA, 2015.

[18] D. Hinkle, W. Wiersma, and S. Jurs, Applied Statistics for the Behavioural Sciences 5th ed. Boston: Houghton Mifflin 2003.

[19] S. Rowson, S. Duma, B. Stemper, A. Shah, J. Mihalik, J. Harezlak, et al., “Correlation of concussion symptom profile with head impact biomechanics: a case for individual-specific injury tolerance”, *J Neurotrauma* Nov 13, 2017.

[20] S. Broglio, A. Lapointe, K. O'Connor, and M. McCrea, “Head Impact Density: A model to explain the elusive concussion threshold”, *J Neurotrauma* May 24(ja), 2017.

[21] M. Aare, S. Kleiven, and P. Halldin, “Injury tolerances for oblique impact helmet testing”, *Int J Crashworthiness*. 2004 Jan 1;9(1):15-23.

[22] A. McIntosh, A. Lai, and E. Schilter, “Bicycle helmets: head impact dynamics in helmeted and unhelmeted oblique impact tests”, *Traffic Inj Prev*. Jul 4;14(5):501-8, 2013.

[23] N. Mills, and A. Gilchrist, “Oblique impact testing of bicycle helmets”, *Int J Impact Eng.* Sep 1;35(9):1075-86, 2008.

Chapter 5

Measurement of 6-Dimensional Kinematics in Mixed Martial Arts

Abstract

Background: Concern about the consequences of head impacts in US football motivated researchers to investigate and develop instrumentation to measure the severity of these impacts. However, the severity of head impacts in unhelmeted sports is largely unknown as miniaturised sensor technology has only recently made it possible to measure these impacts in vivo.

Aim: The objective of this study was to measure the linear and angular head accelerations in impacts in mixed martial arts (MMA), and correlate these with concussive injuries.

Methods: Thirteen MMA fighters were fitted with the Stanford instrumented mouthguard (MiG2.0). The mouthguard records linear acceleration and angular velocity in 6 degrees of freedom. Angular acceleration was calculated by differentiation. All events were video recorded, time stamped and reported impacts confirmed.

Results: 451 verified head impacts above 10g were recorded during 19 sparring events (n=298) and 11 competitive events (n=153). The average resultant linear acceleration was 38.0g ± 24.3g while the average resultant angular acceleration was 2567 ± 1739rad/s^2. The competitive bouts resulted in five concussions being diagnosed by a medical doctor. The average resultant acceleration (of the impact with the highest angular acceleration) in these bouts was 86.7 ± 18.7g and 7561 ± 3438rads/s^2. The average maximum Head Impact Power (HIP) was 20.6kW in the case of concussion and 7.15kW for the uninjured athletes.

Conclusion: The study recorded novel data for sub-concussive and concussive impacts. Events that resulted in a concussion had an average maximum angular acceleration that was 24.7% higher and an average maximum HIP that was 189% higher than events where there was no injury. The findings are significant in understanding the human tolerance to short-duration, high linear and angular accelerations.

Published: S. Tiernan, A. Meagher, D. O'Sullivan. Concussion and the Severity of Head Impacts in Mixed Martial Arts. Part H: Journal of Engineering in Medicine. Aug 2020
DOI: 10.1177/0954411920947850

This chapter is a reproduction of the published paper with the following exceptions:

- The introduction has been shortened to remove the duplication of material that is already in the literature review in Chapter 2.
- Details on the background and injuries in MMA have been removed as these are in Chapter 2 Section 2.4.1, 2.4.2 and 2.4.3.
- The results section 5.3.1 has been added which details the kinematic data for the concussion cases.
- Labels have been added to Figure 5-7.

5.1 Introduction

Generally, concussion can be classified as an injury to the brain resulting from blunt trauma or acceleration/deceleration of the head and neck, with one or more of the following symptoms attributable to the head injury during the post-traumatic surveillance period: transient confusion, dysfunction of memory, headache, dizziness, irritability, fatigue, or poor concentration [1]. Typically contusions are associated with linear accelerations while diffuse axonal injuries are associated with angular accelerations [2]. The role of predisposing factors in determining an individual's susceptibility to concussion such as age, sex, concussion history and genetic characteristics are still unknown [3][4].

Historically efforts have focused on using linear acceleration to indicate head injury. This has changed in the last decade to include angular velocity and angular acceleration. A validation study of the HITS sensor system using a medium sized US football helmet on a Hybrid III anthropomorphic dummy head, found that HITS, overestimated peak linear acceleration (PLA) by 0.9% and underestimated peak angular acceleration (PAA) by 6.1% [5]. However, Jadischke et al. determined that a large helmet should be used with a Hybrid III head-form and this increased the angular acceleration error. In Jadischke's study 85.7% of impacts with the large helmet had an angular acceleration error greater than 15% [6]. A study of the HITS data by Rowson et al. found that concussive impacts had an average PLA of 104 ± 30g and PAA of 4726 ± 1931rad/s^2; the data included 300,977 impacts and 57 concussions [7]. Despite the possible errors in HITS it provides the only large head impact acceleration dataset. Head accelerations that have resulted in a concussion have been investigated by many authors using different techniques. Most of the studies in Table 5-1 agree on an approximate threshold for concussion of 100g for linear acceleration but the reported angular acceleration threshold varies from 4300 to 7229rad/s^2 - this may in part be due to the techniques used to determine angular acceleration.

The alternative to measuring head accelerations *in vivo* is to recreate the impact using video data in a laboratory or using dynamic modelling software. Several video angles are required for this to be successful and it is a difficult, time consuming and error prone task [8]. A study by McIntosh et al. of unhelmeted impacts in Australian football used video data to reconstruct 40 head impacts (13 uninjured and 27 concussion cases) [9]. The mean peak linear and angular acceleration for concussive injuries was 103.4g and 7951rad/s^2 and for no injury was 59g and 4300rad/s^2. McIntosh's study also found that

60% of concussive cases had a greater proportion of impacts to the temporal area of the head than non-concussive. The study concluded that there was a 75% probability of a concussion from a PAA of 2296rad/s^2 in the coronal plane, and a 75% probability of concussion from a resultant PLA in excess of 88.5g. However in a brain simulation study Zhang et al. used brain tissue criteria to determine that 66g and 4600rad/s^2, 82g and 5900rad/s^2 and 106g and 7900rad/s^2 corresponded to a 25%, 50% and 80% probability of concussion [10].

Table 5-1: Published linear and angular accelerations thresholds for concussion

Author	**Linear Acceleration**		**Angular Acceleration**		**No. Cases**	**Impact**	**Sport**	**Method**	**Year**
	No Injury	Concussion	No Injury (rad/s^2)	Concussion (rad/s^2)	No Injury	Concussion			
Wilcox [11]		43g (11.5g)		4029.5 (1243)	58	4	Ice Hockey	HITS	2015
McIntosh [9]		103.45g	4300 (3657)	7951 (3562)	40	13	Australian Football	Kinematic simulation	2014
Rowson [12]	26g (19g)	104g (30g)	1072 (850)	4726 (1931)	62974	37	US Football	HITS	2013
Rowson [7]			1230 (915)	5022 (1791)	300977	57	US Football	HITS	2011
Reed [13]	22.1g		1557.4		1821	0	Ice Hockey	HITS	2010
Stojsih [14]	191g (PLA)		17156 (PAA)		60	0	Boxing	Modified HITS	2010
Guskiewicz [15]		114.6g (54.1g)		5312	88	13	US Football	HITS	2007
Pellman[16] [17]	60g (24g)	98g (28g)	4029 (1438)	6432 (1813)	182	31	US Football	Lab re-construction	2007
Duma [18]	32g (25g)	81g	2022 (2042)	5595	3311	1	US Football	HITS	2005
Newman [19]	54.3g	97.9g	4159	6664	33	25	US Football	Lab re-construction	2000
Broglio [20]	25.1g	105g	1626	7229.5	54247	13	US Football	HITS	2010

Note: Standard Deviation shown in brackets.

The relationship between impact severity and duration has been investigated since John Strapp's work in the 1940s. In 1964 Gurdjian et al. published the Wayne State

Tolerance Curve (WSTC) shown in Figure 5-1[21]. This curve was developed from a variety of experiments on animals, cadavers and human volunteers. In 1975 the US National Highway Safety Administration adopted the Head Injury Criteria (HIC), which is a formula to fit the WSTC. HIC values in excess of 1000 are used to predict moderate or serious injury with probable concussion with or without skull fracture [22].

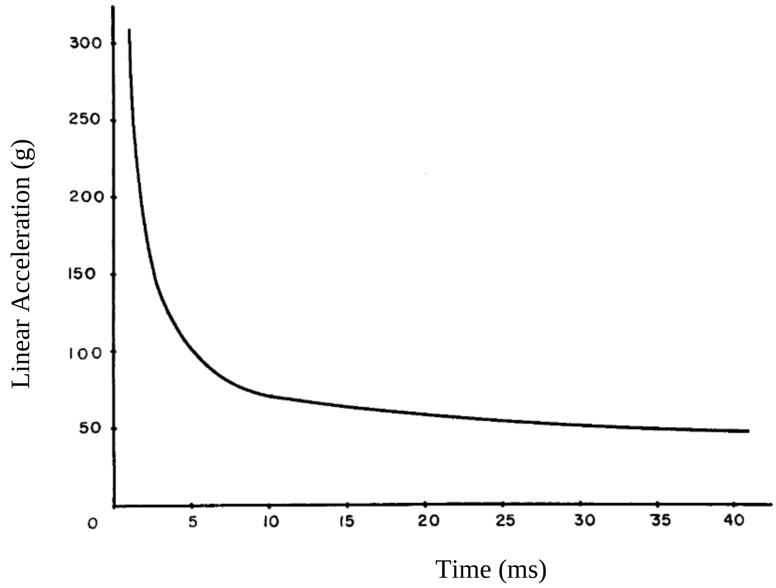

Figure 5-1: Wayne State Tolerance Curve [21]

The HIC and WSTC incorporate linear acceleration and duration but do not include angular acceleration. In 2000 Newman et al. proposed a new kinematic criterion termed the Head Impact Power (HIP), shown in Equation 5-1 [23]. This criterion has the advantage of incorporating linear and angular acceleration and duration.

$$HIP = \Big[ma_x \int a_x dt + ma_y \int a_y dt + ma_z \int a_z dt + I_{xx} \propto_x \int \propto_x dt + I_{yy} \propto_y \int \propto_y dt + I_{zz} \propto_z \int \propto_z dt\Big]$$

m =mass of the head, I_{xx}, I_{yy} and I_{zz} = moments of inertia of the head around the X, Y and Z axes

a_x, a_y and a_z =linear accelerations of the head in the X, Y and Z directions

α_x, α_y and α_z =angular accelerations of the head around the X, Y and Z axes

Equation 5-1: Head Impact Power [23]

Newman et al.’s study recreated 12 US football impacts, which included 24 players and 9 concussions. They determined that there was a 5%, 50% and 95% probability of concussion from HIP values of 4.7, 12.79 and 20.88kW, respectively [23].

Following experimental work with animals Gennarelli et al. proposed that concussion is primarily due to angular accelerations [24]. This has been corroborated by statistical studies of the HITS database [25][7]. A simulation study by Post et al. found that linear acceleration primarily affected the brain’s strain response for short duration events (<15ms) but as the duration increases, angular acceleration becomes the dominant contributor to brain strain [26]. It is difficult to determine a threshold for PAA as it depends on impact location, direction and duration [8][27]. A kinematic study by Hoshizaki et al. found that the risk of head injury was a function of both the magnitude and duration of an impact; the study determined that a PAA of 5krad/s^2 over 25ms had a similar risk of injury as a PAA of 50krad/s^2 impact over 2ms [28].

5.1.1 Head impact sensors

Few studies have measured the severity of head impacts *in vivo* in unhelmeted sports due to the lack of suitable instrumentation. Types of impact sensors including the xPatch and the SIM-G sensors are discussed in Chapter 2 Section 2.5.2 and 2.5.3.

Instrumented mouthguards have been in development for approximately 50 years. Most of the early devices were large, protruded from the mouth and were hard wired back to a fixed station. The instrumented mouthguard has been shown to be the most accurate method of measuring head accelerations *in vivo* [29]. This is primarily due to the degree of coupling between the head and the mouthguard. X2 Biosystems developed an instrumented mouthguard that was used by King et al. in 2013 to measure head impacts in junior rugby but no concussions were recorded in this study [30]. Bartsch et al. at Cleveland Clinic (US) have also developed an instrumented mouthguard with reported errors of 3% PLA and 17% PAA [31][32]. There have not yet been any known published studies which have used this device to record concussive injuries. An instrumented mouthguard has also been developed by CAMLab at Stanford University [33] - this mouthguard is used in the study reported in this paper. The accuracy of this mouthguard was investigated by the CAMLab group by fitting it to an anthropomorphic test head fitted with a US football helmet [33]. The helmet was impacted with a spring-loaded horizontal impactor and 128 impacts were carried out. The peak linear acceleration correlated very well (R^2 = 0.96) with the reference sensors and the linear regression slope (m = 1.01) indicated an accurate prediction of the linear acceleration. The peak angular accelerations also correlated with the reference sensors (R^2 = 0.89) while the linear regression slope was 0.9, indicating an under prediction of the angular acceleration by the mouthguard. The normalised root mean error was determined to be 9.9±4.4% for linear acceleration and 9.7±7.0% for angular acceleration. The CAMLab study did not include any direct impacts to the mouthguard hence the current study does not include any such impacts as the mouthguard has not been validated for these. The coupling of the mouthguard to the skull was compared to a skin patch sensor and a head band sensor by Wu et al. [29]. Sensor coupling was quantified by measuring the displacement of the sensor relative to an ear-canal reference sensor while heading a soccer ball. The mouthguard error was <1mm while the skin patch and head band sensors displaced by up to 4 and 13mm with reference to the ear canal sensor. The group at Stanford have used the mouthguard to measure head impacts in US football; this is the only known *in vivo* measurement of head accelerations that resulted in a concussive event by a device other than the HITS system [34]. Two concussions were reported, one case involved a loss of consciousness and the other was self-reported. The loss of consciousness injury had a PLA of 106g and a PAA of 12,900rad/s^2, the duration of the linear resultant acceleration was approximately 35ms.

5.1.2 Mixed martial arts (MMA)

MMA is a competitive, full-contact sport that involves an amalgamation of elements drawn from boxing, wrestling, karate, taekwondo, jujitsu, muay thai, judo, and kickboxing [35]. Details on the background and injuries in MMA is discussed in Chapter 2 Section 2.4.1, 2.4.2 and 2.4.3.

5.2 Method

Thirteen adult MMA fighters took part in this study, 12 professional or semi-professional and 1 amateur. Fighters took part in both sparring and competitive events, as shown in Table 5-2. None of the events included 2 of the participants competing against each other. The fighters were fitted with the Stanford instrumented mouthguard (MiG2.0) and ethical approval was granted by the Institute of Technology Tallaght Ethics committee REC-STF1-201819. To ensure that the mouthguard was a tight fit a dental impression was taken and two mouthguards were manufactured for each fighter: one fitted with sensors and a ‘dummy’ one which had the look and feel of the instrumented one. The mouthguards were manufactured by OPRO, England a leading gum shield manufacturer. The fit of the mouthguards was checked and each fighter was given the ‘dummy’ mouthguard for training, this ensured that the fighters were familiar with the mouthguard and that the instrumented mouthguard would not become worn or damaged (Figure5-2).

Figure 5-2: CAMLab Instrumented mouthguard

The mouthguard has a triaxial accelerometer to measure linear acceleration and a triaxial gyroscope to measure angular rate. The sensors, processor and battery are completely sealed in three layers of ethylene vinyl acetate in a dental moulded mouthguard. Data is downloaded from the device post event via Bluetooth [36].

In this study impacts were recorded when linear accelerations exceeded the 10g threshold established in previously published studies [37][38]. The acquisition window was 50ms pre-trigger and 150ms post-trigger. Linear acceleration and angular velocity were sampled at 1000Hz and all data was filtered using a 4th order Butterworth low-pass filter with a cut-off frequency of 300Hz [39].

Table 5-2: Study Participants

	No. of Events					
	Sparring	**Competition**	**Weight Class**	**Max Weight**	**Gender**	**Level**
Fighter 1		1	Lightweight	70.3kg	Male	Pro
Fighter 2	2	1	Lightweight	70.3kg	Male	Pro
Fighter 3	3	2	Middleweight	83.9kg	Male	Pro
Fighter 4	1	2	Lightweight	70.3kg	Male	Pro
Fighter 5	4	1	Lightweight	70.3kg	Male	Pro
Fighter 6	1	1	Flyweight	56.7kg	Female	Pro
Fighter 7	1		Strawweight	52.2kg	Female	Pro
Fighter 8	1		Bantamweight	61.2kg	Male	Amateur
Fighter 9	3	1	Featherweight	65.9kg	Male	Pro
Fighter 10	1	1	Bantamweight	61.2kg	Male	Semi - Pro
Fighter 11	1		Lightweight	70.3kg	Male	Semi-Pro
Fighter 12		1	Strawweight	52.2kg	Female	Pro
Fighter 13	1		Welterweight	77kg	Male	Semi - Pro

Angular acceleration was estimated using a 5-point stencil derivative of the measured angular velocity [40]. The accelerations were transformed to the centre of gravity using Equation 5-2 and the offsets for a 50th percentile human head (-0.07764m, 0, 0.07207m) [41].

$$\overrightarrow{a_{CG}} = \overrightarrow{a_s} + \overrightarrow{\propto} (\overrightarrow{r_s}) + \vec{\omega}(\vec{\omega}\, x\, \overrightarrow{r_s})$$

Where a_{CG} is the head linear acceleration at the centre of gravity a_s is the linear acceleration at the mouthguard sensor, α is the head angular acceleration, ω is the head angular velocity and r_s is the vector position of the mouthguard sensor to the centre of gravity of the head.

Equation 5-2: Transformation of linear acceleration to centre of gravity of head [29]

5.2.1 Data capture and analysis

Each event was recorded by two cameras placed at different angles around the arena and the video was recorded at 60 frames per second. In addition, TV coverage was available for the competitive events. The time on the mouthguard data was aligned with the video time-line and the video was examined frame by frame by two researchers using Kinovea video analysis software. The video data was used to confirm that a head impact had occurred and that the direction of the impact conformed to the direction indicated by the mouthguard. To define the impact direction the head was divided into 8 equal transverse sectors as shown in Figure 5-3.

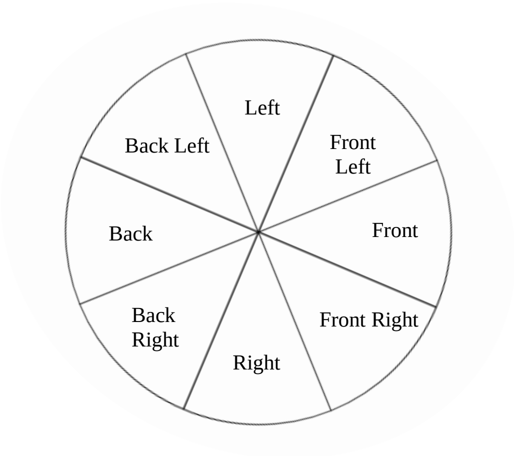

Figure 5-3: Impact direction sectors

If an impact could not be confirmed it was removed from the analysis. In addition, if it was found from the video that an impact was directly to the mouthguard and thus sensors, it was removed as it may produce a sharp spike in the acceleration data. This method was used to remove forty-seven impacts which were suspected to have been direct impacts to the mouthguard.

Reported linear and angular accelerations are calculated peak resultants. The duration reported for the impacts is the time interval over which the acceleration first exceeded a predetermined threshold, an example of how this calculation was performed is shown in Figure 5-4. A threshold of 10g, as established in other studies [37][38], was utilised for linear acceleration. A threshold for the calculation of angular acceleration duration is not specified by other researchers, hence 500rad/s^2 was used as this was greater than any spurious data. This approach allowed for a consistent and repeatable method to carry out a comparative analysis of the impact durations.

The MMA athletes were medically examined before the study commenced, immediately after competitive bouts and again approximately 48 hours after the competitive events. The medical examinations were conducted by an emergency medicine doctor. Prior to the events the examination included a physical examination and the recording of the participant's medical history. After the events, the athletes had a physical examination and were checked for any concussion symptoms such as persistent headaches, visual disturbance and imbalance. If a concussion was suspected the athlete was examined using the version 5 of the Sports Concussion Assessment Tool (SCAT5). It should be noted that the concussed fighters received between 4 and 26 head impacts during their bouts. It is not possible to identify which impact caused their injury. To determine the severity of the impacts the Head Impact Power (HIP) was computed using the method developed by Newman et al. as shown in Equation 5-1 [29]. The HIP is calculated over the 200ms capture time of each impact and the maximum value is reported.

To investigate the relationship between peak resultant linear and peak resultant angular acceleration a linear regression analysis was performed, using Minitab LLC, for each impact site. Pearson's Correlation coefficient and adjusted R^2 values were calculated to determine if a linear relationship existed and if so the strength of that relationship.

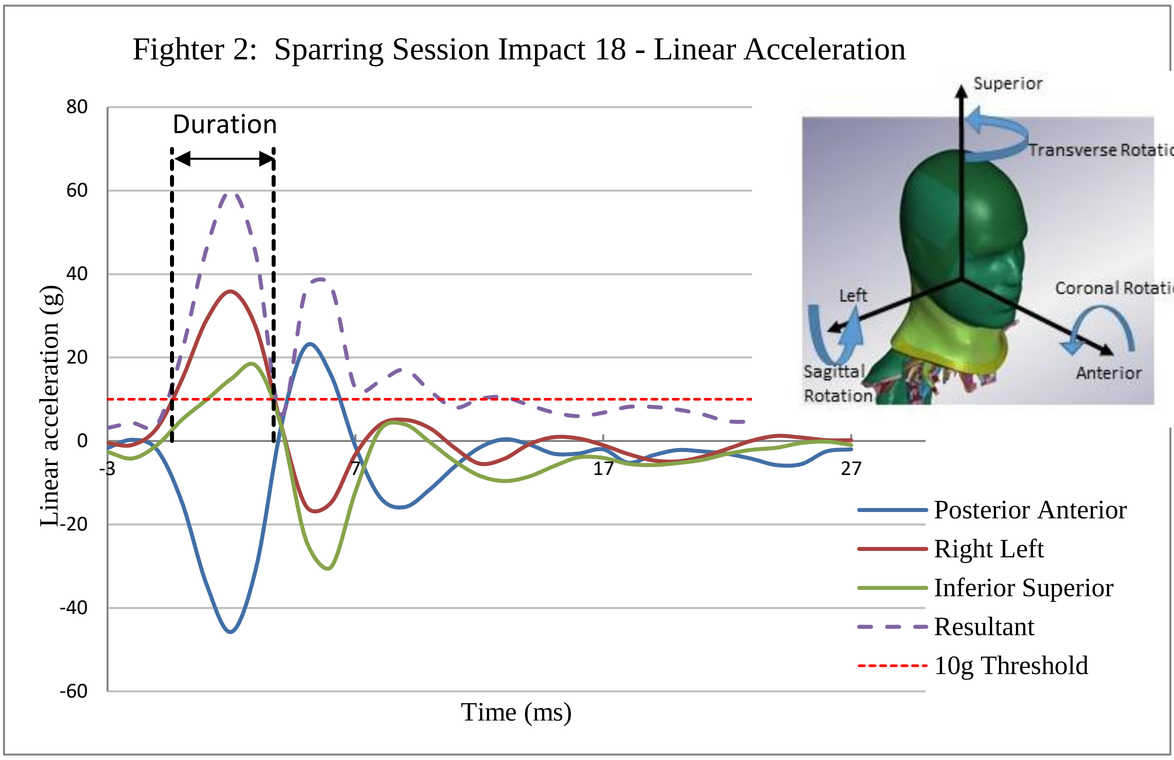

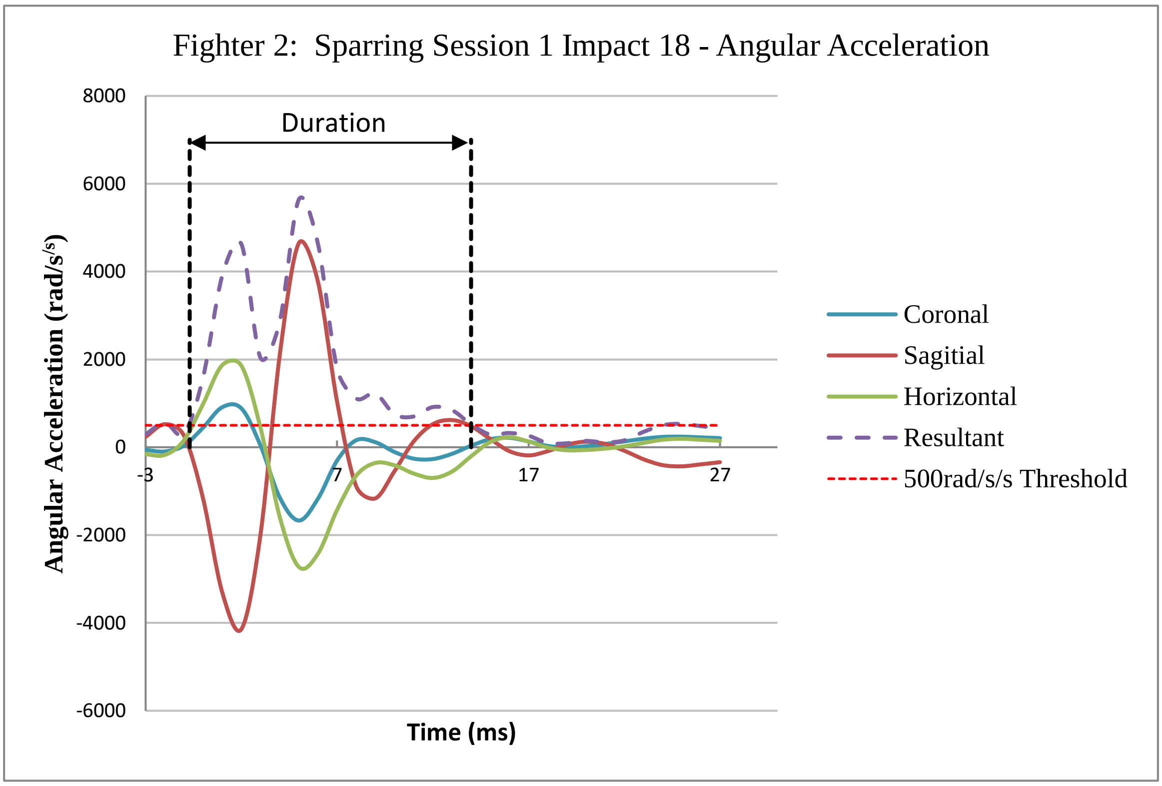

Figure 5-4: Sample data from sparring session
Note: 3ms pre trigger and 27ms post trigger is displayed)

5.3 Results

During this study data was recorded during sparring sessions and competitive events. All fighters participated in sparring sessions and 9 in competitive events. Above 10g, 298 confirmed head impacts were recorded during 19 sparring sessions, resulting in an average of 15.74 head impacts per sparring session. The average PLA for all impacts sustained during the sparring sessions was 32.0g ± 17.2g while the PAA was 2149 ± 14285rad/s^2. The median accelerations for the sparring sessions had a PLA of 28.4g and a PAA of 1701rad/s^2. No injuries were occurred during the sparring sessions. Figure 5-4 shows an example of the mouthguard data recorded during a typical sparring head impact.

Eleven competitive events were studied at which 153 confirmed head impacts above 10g were recorded, resulting in an average of 13.9 head impacts per event. The median PLA for the competitive events was 36.8g and the PAA was 2956rad/s^2. The average PLA for all impacts sustained during competitive events was 46.5 ± 29.9g and the average PAA was 3355 ± 1912rad/s^2. Five of the competitive events resulted in the fighter sustaining a concussion.

Histograms of the linear and angular accelerations of the impacts from both sparring and competitive events are shown in Figure 5-5. As expected, these are skewed to the left demonstrating that the majority of impacts are below 50g (77.5%) and 4000rad/s^2 (74.4%).

The impacts with the highest PAA from each competitive bout were selected from each competitive event (Table 5-3). These impacts were selected as angular acceleration has been correlated with concussion [25][7][24]. HIP values were calculated for all impacts. The average of the maximum values from each event that resulted in a concussion was 20.6kW. The maximum HIP value for both sparring and competitive events at which there was no head injury was averaged and found to be 7.15kW.

Table 5-3: Head Impacts from each competitive event with the highest resultant angular acceleration

Fighter Number	Event No.	Impact No.	Linear Accel. (g)	Duration (>10g) (ms)	Angular Accel. (rad/s^2)	Duration (>500rad/s^2) (ms)	HIP (kW)	Direction	Diagnosis
Fighter 1	Bout 1	71	50.5	13	4458	20	7.33	FL	Concussion
Fighter 2	Bout 1	9	93.1	25	6527	20	11.46	R	Concussion
Fighter 3	Bout 1	56	94.2	11	4090	15	9.29	FL	Concussion
Fighter 3	Bout 2	8	105.7	12	8722	17	4.8	F	Uninjured
Fighter 4	Bout 1	53	90.8	27	9439	26	8.43	F	Concussion
Fighter 4	Bout 2	5	54.5	8	5407	22	6.44	R	Uninjured
Fighter 5	Bout 1	21	104.9	11	13290	25	18.91	F	Concussion
Fighter 6	Bout 1	47	57.5	9	5870	7	3.02	FL	Uninjured
Fighter 9	Bout 1	4	60.4	8	8524	14	7.22	L	Uninjured
Fighter 10	Bout 1	50	75.7	5	7543	12	2.83	FR	Uninjured
Fighter 12	Bout 1	8	45.5	9	6351	20	2.72	FL	Uninjured

Averages and standard deviations were calculated for impacts with the highest PAA recorded at each competitive bout and sparring session, these are presented in Table 5-4. The competitive events were divided into injury and non-injury categories, with no injuries occurring at sparring sessions.

In competitive events the average PLA was 30.3% higher, and the PAA was 6.9% higher in the cases of concussion. In concussive cases in competitive events the average PLA was 69% higher and the PAA was 49.6% higher than the sparring sessions. The impact with the highest PAA in each competitive and sparring event was analysed and the duration of the linear acceleration versus the duration of the angular acceleration of that event is plotted in Figure 5-6.

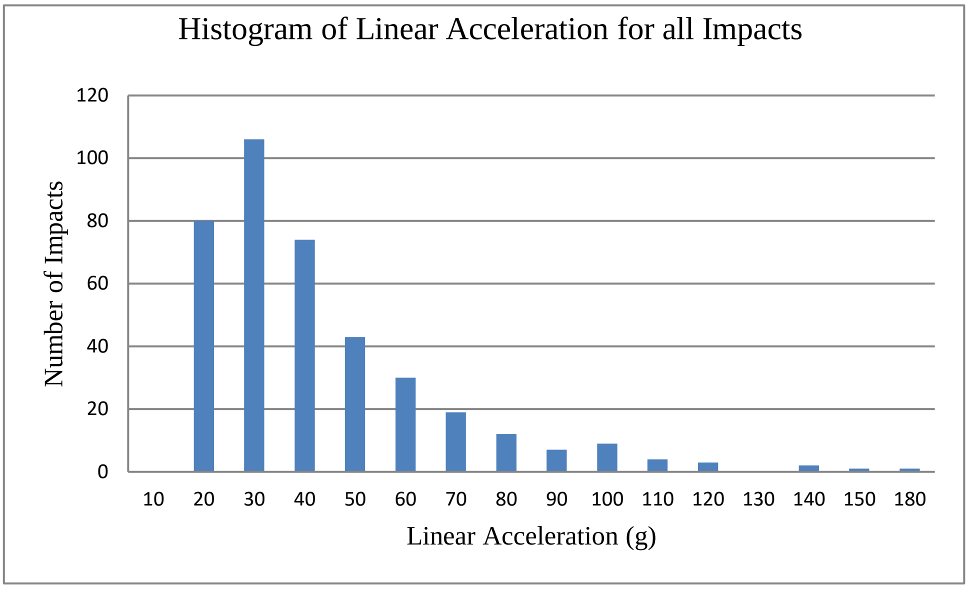

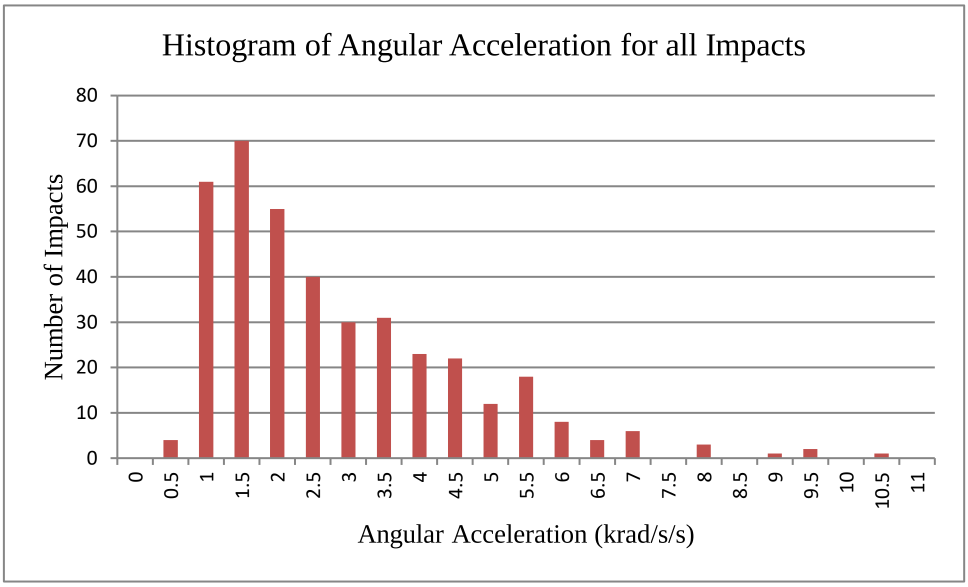

Figure 5-5: Number and severity of linear and angular accelerations during competitive events

Table 5-4: Averages and standard deviations of the impacts with the highest angular acceleration at competitive events and sparring sessions

Event	Injury	Parameter	Linear Acceleration	Duration (10g)	Angular Acceleration	Duration (500rad/s/s)	HIP
			(g)	(ms)	(rad/s/s)	(ms)	(kW)
Competition	Concussion	Average	86.7	19.0	7560.8	20.0	11.1
		Std Dev	(18.7)	(6.5)	(3437)	(4.3)	(4.1)
Competition	No Injury	Average	66.6	9.2	7069.5	12.3	4.5
		Std Dev	(19.7)	(2.1)	(1277)	(4.9)	(1.8)
Sparring	No injury	Average	51.3	10.1	5055.7	12.5	5.0
		Std Dev	(18.3)	(2.6)	(1374)	(4.20	(3.1)

Note: standard deviation shown in brackets

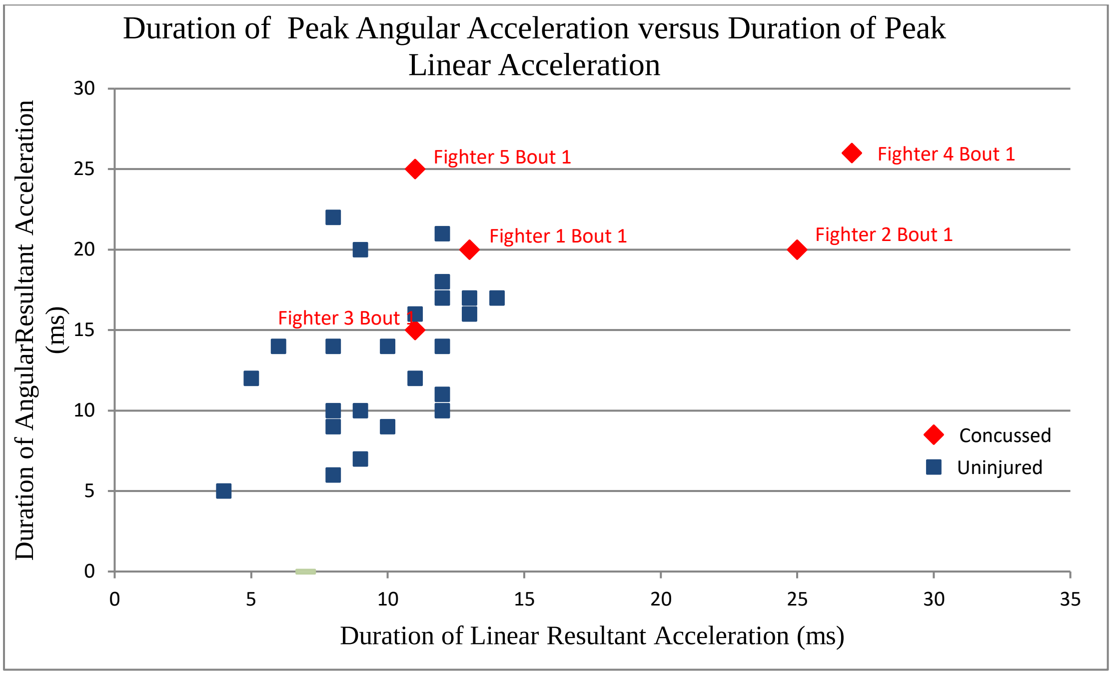

Figure 5-6: Duration of linear and angular resultant accelerations of the most severe impact (highest angular acceleration) recorded at each competitive event and sparring session

These high angular acceleration impacts were from impacts with the gloved fist as opposed to body impacts. From Figure 5-6 it is evident that the majority of impacts that resulted in a concussion had longer durations than the those that did not result in an injury. Four impacts that resulted in a concussion had an angular acceleration duration ≥ 20ms. Figure 5-7 shows a plot of the angular acceleration versus the linear acceleration. The concussed and uninjured fighters are indicated by red diamonds and blue squares, respectively.

The impact direction shown in Figure 5-8 was determined from the azimuthal and polar angles of the resultant linear acceleration vector and verified by video analysis. It was found that 57.5% of the impacts in sparring and competitive events were to the front of the head (including front, front left and front right 135^0) with 33.9% of these being to the front left of the head (45^0 quadrant).

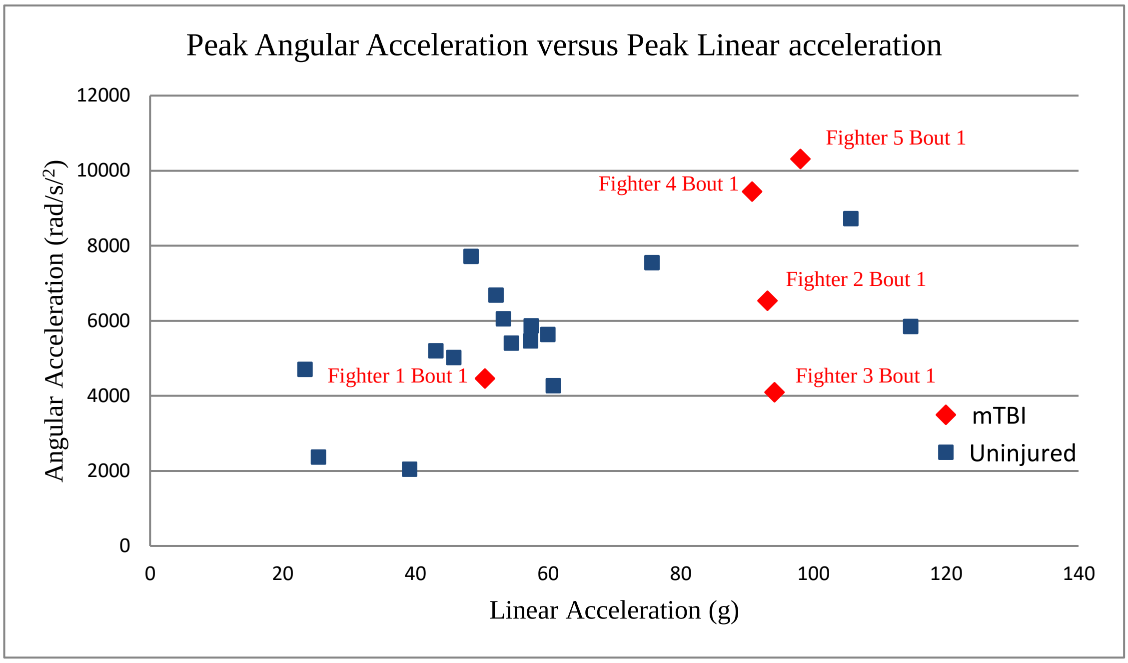

Figure 5-7: Angular acceleration versus linear acceleration of the most severe impact (highest angular acceleration) recorded at each competitive event and sparring session

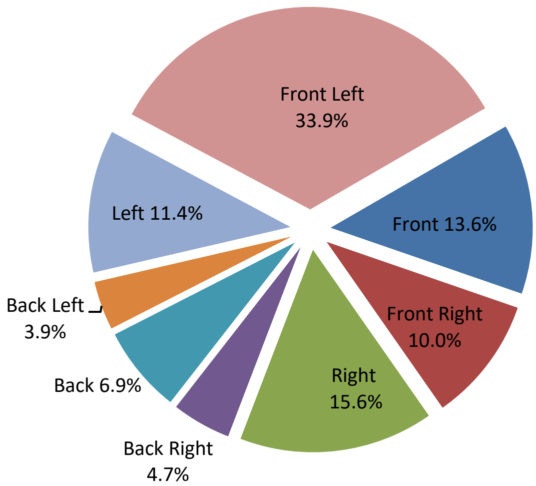

Figure 5-8: Percentages of impacts in different directions from both sparring sessions and competition

The relationship between linear and angular acceleration was also investigated as shown in

Table 5-5. Using a statistical regression model the best fit line was found to be from impacts to the back right of the head (n = 21), where R^2 adjusted was 0.70. This was followed by impacts to the front left of the head (n=156) where R^2 adjusted was 0.61.

No relationship was evident between the linear and angular accelerations for impacts from other directions as R^2 adjusted was less than 0.6.

Table 5-5: Correlation between linear and angular acceleration for each impact direction

Direction	Number of Impacts	R^2 adjusted	Pearson Correlation
Front	63	38.5%	0.623
Front Right	46	8.0%	0.302
Front Left	156	61.4%	0.784
Left	53	17.6%	0.444
Right	72	51.9%	0.726
Back Right	21	69.7%	0.846
Back Left	18	23.3%	0.541
Back	32	59.4%	0.651

5.3.1 Results for the concussed fighters

This section describes the 5 events that resulted in concussions being sustained by the fighters. This was not included in the published paper. The AIS level of all the injuries in this study was level 1, indicating a mild concussion. Table 5-6 gives the directional linear and angular accelerations of the impact with the highest angular acceleration from each event. Figures 5-9 to 5-13 illustrates these impacts with graphs of the 6-D kinematics and photographs of the moment before and during the impact.

Case 1: Fighter 1 Bout 1

Event Duration: Full 3 rounds (each round 5 minutes). 22 confirmed impacts. Impact rate = 1.47 impacts/minute.

Diagnosis: Fighter only displayed concussive symptoms during the post-event medical examination, approximately 48 hours after the event. Symptoms included headaches and visual aura which lasted for approximately 5 days. AIS 1.

Fighter History: 4 previous concussions.

Comment: This fighter appears to have been vulnerable to concussion either due to previous history or is pathologically prone to concussion.

Case 2: Fighter 2 Bout 1

Event Duration: The fight was stopped in the final minute of round 3 as the referee deemed the fighter in the study to be unresponsive (technical knockout). The fighter was on the ground and took repeated blows to the head in the final 30 seconds of the event. 36 confirmed impacts. Impact rate = 2.48 impacts/minute.

Diagnosis: Fighter diagnosed with concussion post event. Symptoms included vertigo and dizziness and symptoms lasted for 4 weeks post-event. AIS 1.

Fighter History: No previous concussions

Comment: This fighter suffered a series of severe impacts. He was punched repeatedly in the head in the final 30 seconds of the fight including one with a linear acceleration of 147g and angular acceleration of 3400rad/s^2. It is likely that the concussion was a result of repeated blows rather than a singular impact.

Case 3: Fighter 3 Bout 1

Event Duration: The fight was stopped after 1 minute and 45 seconds as the referee deemed the fighter to be unresponsive and unable to defend themselves (technical knockout). 4 confirmed impacts. Impact rate = 2.67 impacts/min.

Diagnosis: Transient loss of consciousness (< 1second). No other symptoms. AIS 1.

Fighter History: 1 concussion more than one year previously.

Comment: The reason for the transient loss of consciousness is unknown.

Case 4: Fighter 4 Bout 1

Event: The fight continued for the full 3 rounds. 27 confirmed impacts. Impact rate = 5.4 impacts/minute.

Diagnosis: Diagnosed with concussion post event, symptoms lasted 24 hours. AIS 1.

Fighter History: 1 concussion more than 2 years previously.

Comment: Impact to the side of the head side resulted in very high sagittal rotation (9378rad/s^2).

Case 5 : Fighter 5 Bout 1

Event: Fight lasted for 3 minutes of round one. The event was stopped as the referee deemed fighter to be unable to defend themselves (technical knockout). 29 confirmed impacts. Impact rate = 9.67 impacts/minute.

Diagnosis: Diagnosed with concussion post event, symptoms lasted 1 hour. AIS 1.

Fighter History: 3 concussions, the most recent was approximately one year before the study commenced.

Comment: Impact to left hand side of the head resulted in very high coronal rotation (11862rad/s^2). The second peak on the acceleration curves may be due the impact of the lower jaw onto the mouthguard.

Table 5-6: Details of the impact with the highest angular acceleration for each event that ended with a concussion

Fighter No. Bout No. Impact No.	Linear acceleration X	Linear acceleration Y	Linear acceleration Z	Result Linear Acceleration	Angular accel about X	Angular accel about Y	Angular accel about Z	Resultant Angular Acceleration	Head Impact Power
	g	g	g	g	rad/s/s	rad/s/s	rad/s/s	rad/s/s	kW
F1 B1 H71	28.6	43.8	30.5	50.5	3596	3650	921	4458	7.33
F2 B1 H9	32	89.9	31.3	93.1	2491	1638	781	6527.4	11.46
F3 B1 H56	50.3	63.2	55.7	94.2	3800	733	1691	4090	9.29
F4 B1 H53	41.4	31.7	40	90.8	2150	8740	391	9438.5	8.43
F5 B1 H21	48.3	84.2	49.2	104.9	8655	5848	3531	13289.7	18.91

Fighter 1 Bout 1 Impact 71 (Instrumented Fighter on LHS)

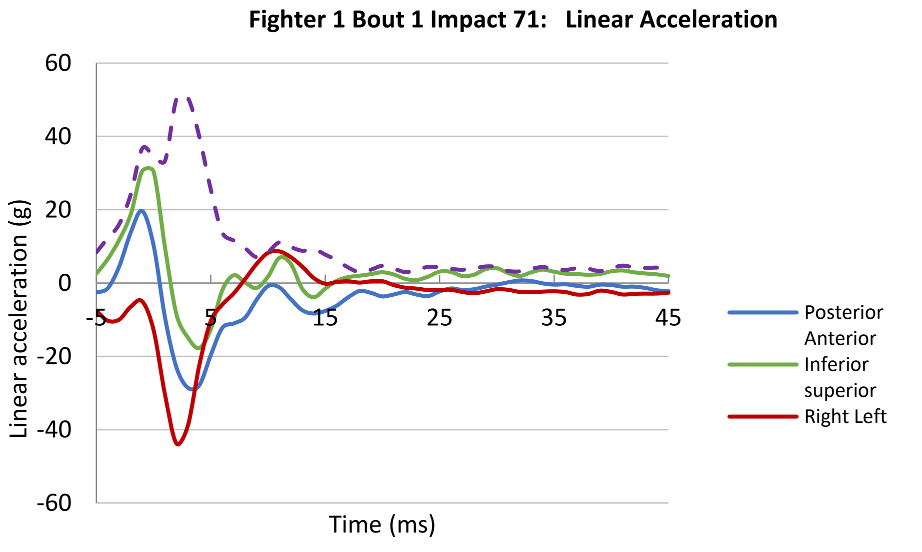

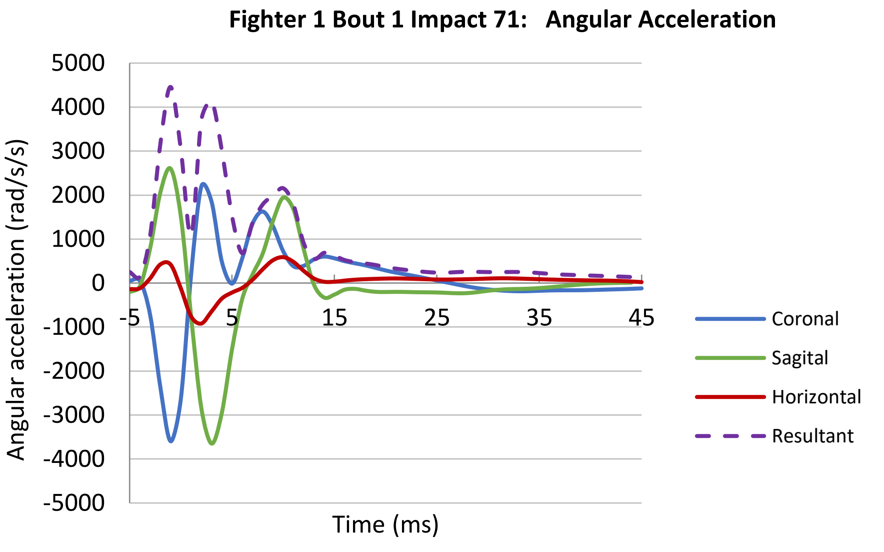

Figure 5-9: Concussion Case 1

Fighter 2 Bout 1 Impact 9 (Instrumented Fighter on RHS)

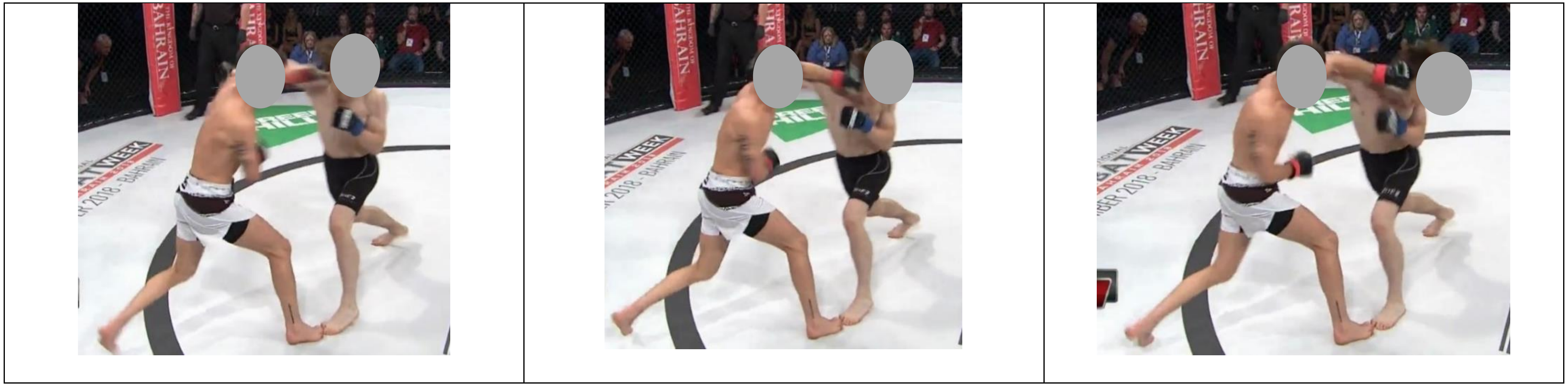

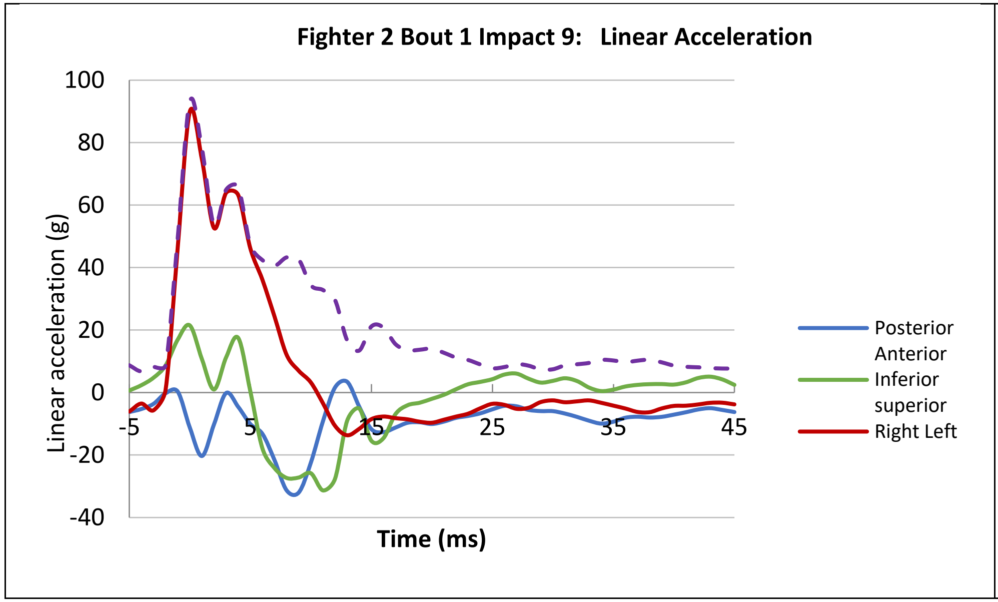

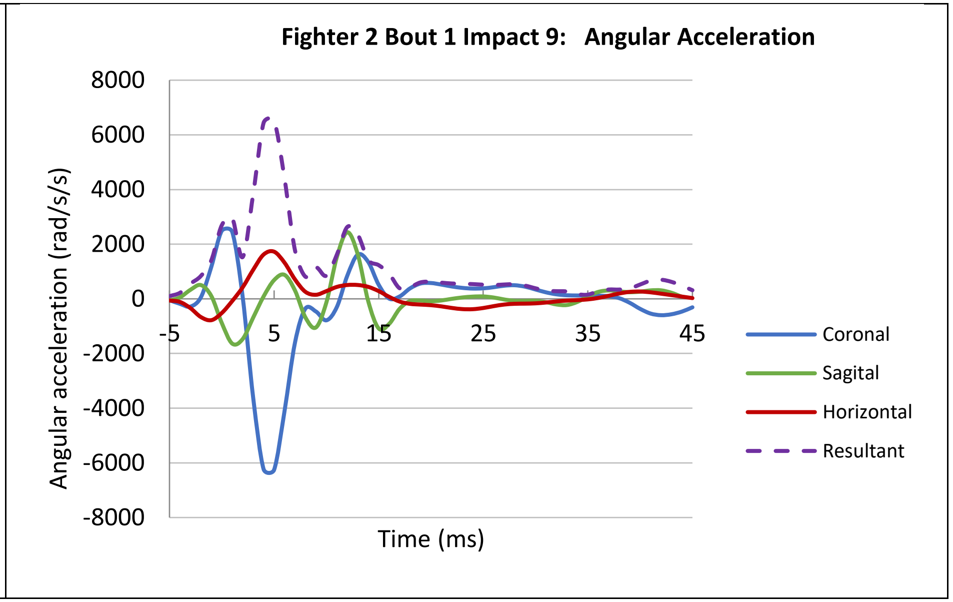

Figure 5-10: Concussion Case 2

Fighter 3 Bout 1 Impact 56 (Instrumented Fighter on RHS, in foreground)

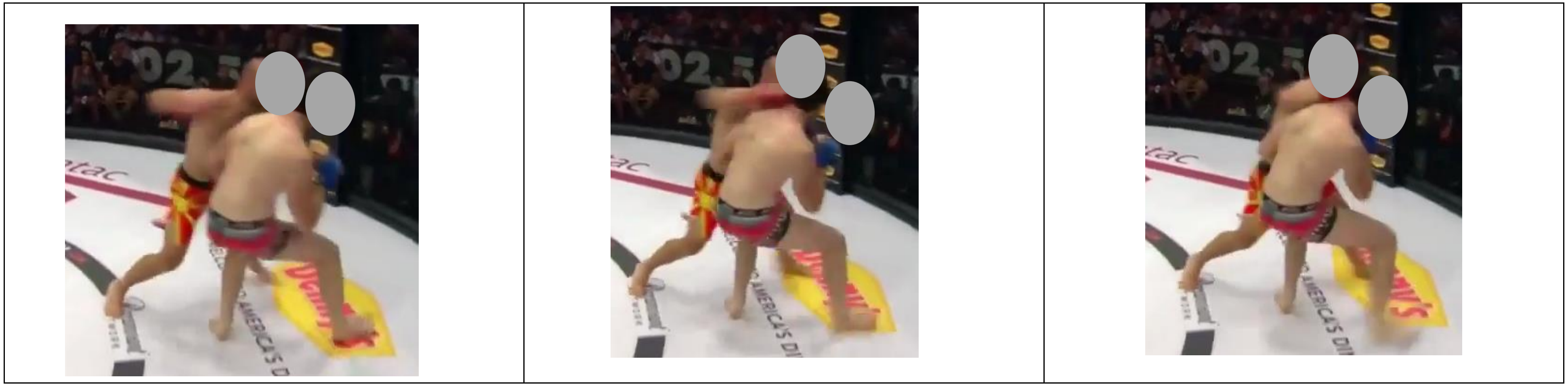

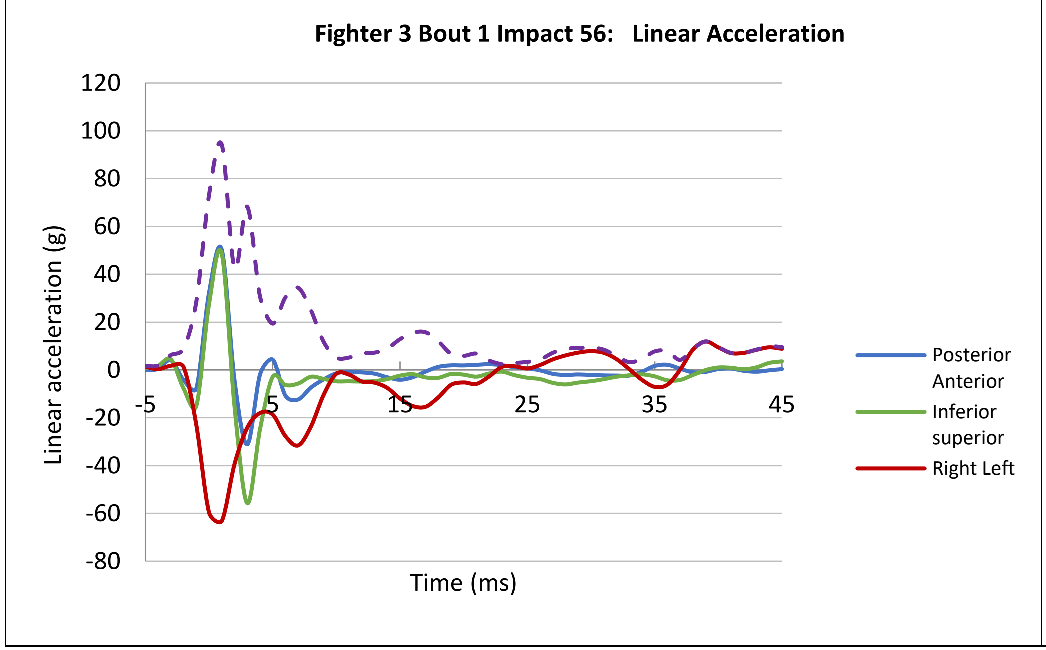

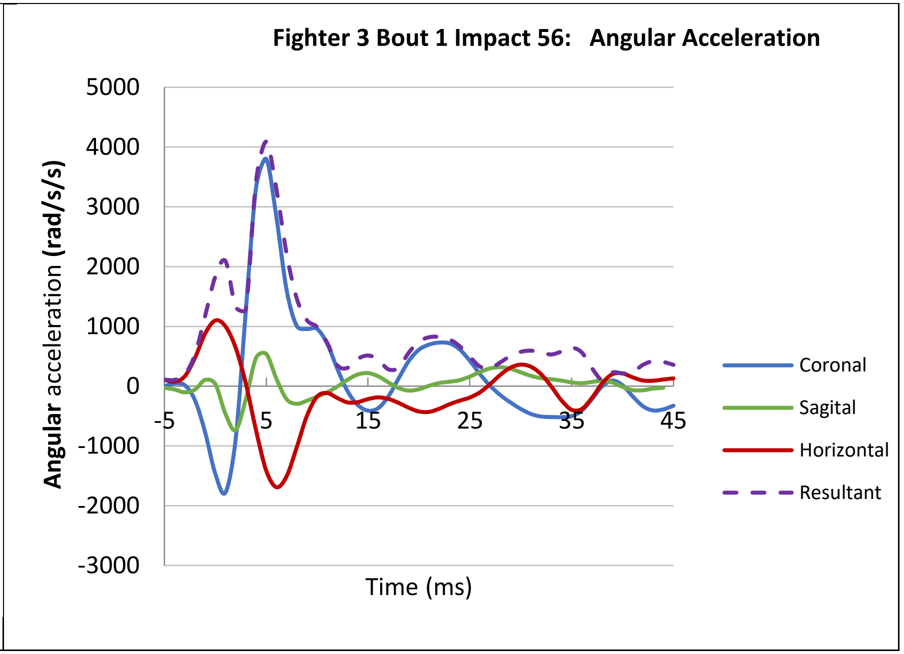

Figure 5-11: Concussion Case 3

Fighter 4 Bout 1 Impact 53 (Instrumented Fighter in background)

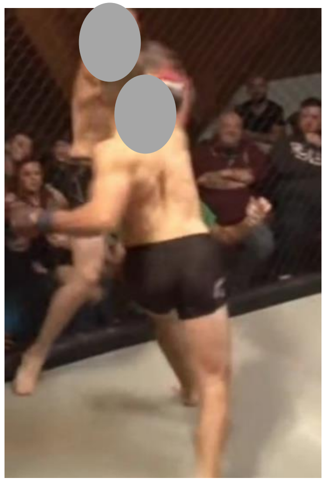

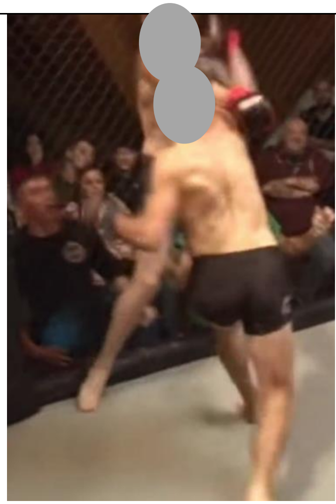

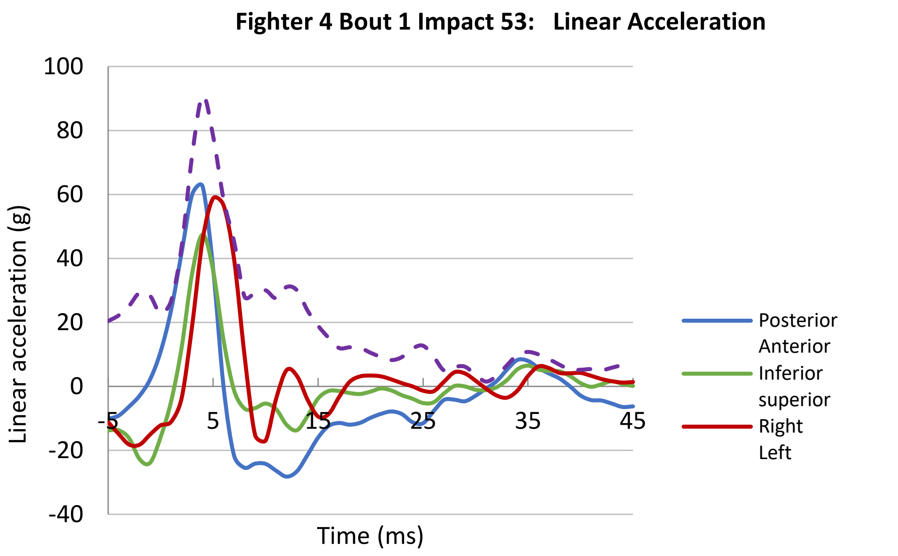

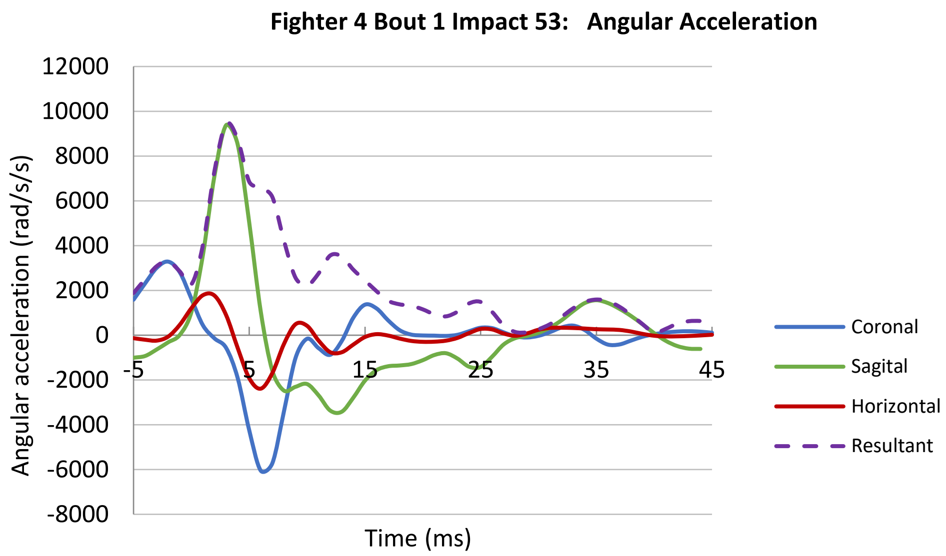

Figure 5-12: Concussion Case 4

Fighter 5 Bout 1 Impact 21 (Instrumented Fighter on RHS)

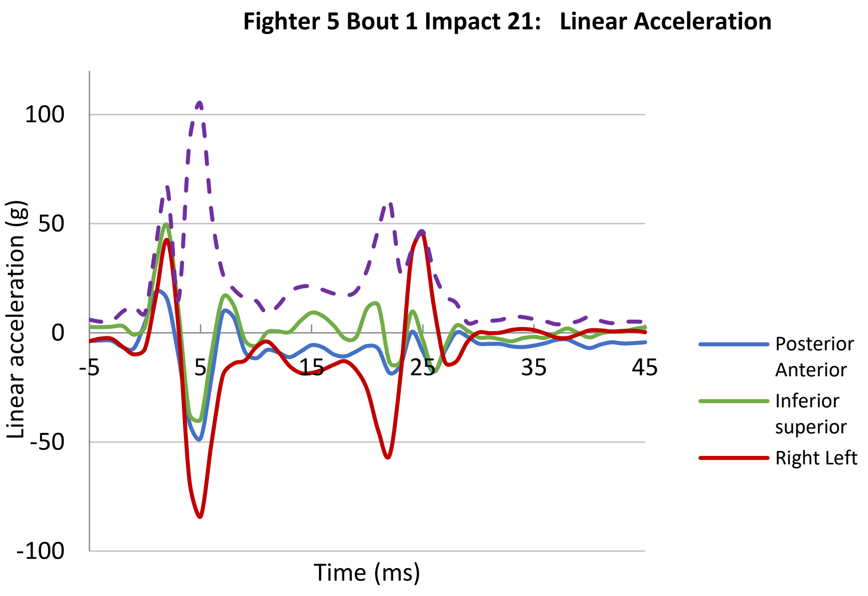

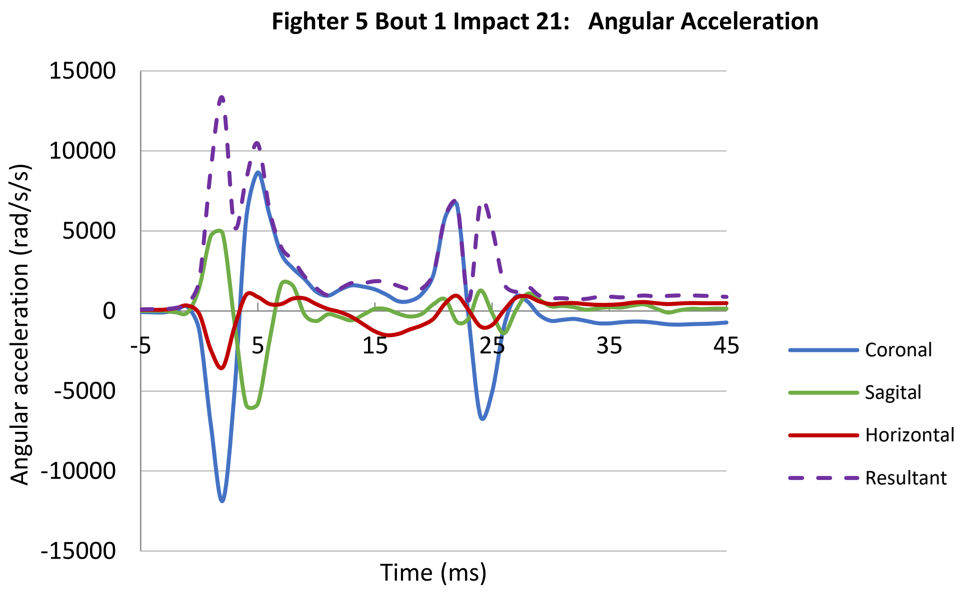

Figure 5-13: Concussion Case 5

5.4 Discussion

This study measured head impacts *in vivo* during 19 sparring MMA sessions and 11 competitive MMA bouts. Five of the fighters were diagnosed with a concussion following their competitive bouts. Four of the concussions were diagnosed immediately after the event whilst the other one was diagnosed during the 48 hour follow-up medical examination. There are few studies where *in vivo* head accelerations have been measured in unhelmeted sports and the studies that do exist are of non-injurious impacts [41][30][42]. The majority of published head acceleration data has been acquired through laboratory tests, kinematic reconstructions or in-helmet sensors as shown in Table 5-1.

The impacts experienced by the fighters were complex three dimensional waves (Figure 5-4). The average PLA of the concussive events was 86.7g which was lower than Australian rugby at 103.4g [9] and US football at 105g [12][20]. The average PAA of the concussive events was 7561rad/s^2 which was similar to Australian football at 7951rad/s^2 [9] and higher than the range published for US football, 4726rad/s^2 [7] to 7230rad/s^2 [20]. In a study by Viano et al. where boxers punched a Hybrid III head (including neck and upper torso) the PAA ranged from 3181 to 9306 rad/s^2 depending on the type of punch [43]. Punches in this study had a lower PLA than US football but higher PAA due to the higher moment applied to the head, this is in agreement with other studies that analysed punches to the head [43]. Although concussion has been associated with angular acceleration the graph in Figure 5-7 would indicate that linear acceleration may be a better predictor of injury. This finding is similar to that of Rowson et al. who found that the prediction of concussion using their combined probability criteria was not significantly different to using linear acceleration alone [12]. The prediction of concussion based on acceleration alone is not reliable [12] as impact duration is also an important factor [26][44]. Punches in MMA (using light gloves and no head protection) result in large angular accelerations of short duration. The risk of brain injury is dependent on both the magnitude of the accelerations and their duration, as demonstrated by the Wayne State tolerance curve [21]. This study found that the impact durations were considerably longer in the cases of concussion. PLA and PAA duration was on average 87.0% and 72.1% longer in the cases of concussion when compared to the uninjured fighters. Deck et al. reported the duration of linear acceleration in pedestrian head impacts to be 9 to 14.5ms, these impacts were unhelmeted and the duration is comparable to the average of 13.4ms found in this study [44]. This contrasts with longer linear acceleration durations in US football due to the level of padding in the helmets and the body armour worn by the players [45]. The duration of an impact is dependent on a number of factors including the compliance of the impact surface, the impact direction and the energy absorption of any head protection, if worn. In a concussive impact recorded by the Stanford mouthguard in US football the duration was approximately 35ms [40], which is considerably longer than the 17.4ms average duration of the concussive impacts in this study, demonstrating that the dynamics of unhelmeted and helmeted impacts are different.

Four of the mTBI's reported in this study were to fighters who sustained impacts with a linear acceleration duration ≥ 11ms and an angular acceleration duration ≥ 20ms (Table 5-2 and Figure 5-6). This study suggests that repeated impacts within a short time are also a factor in concussion: Fighter 3 in Bout 1 was concussed and sustained 4 short duration impacts within 3 seconds, the most severe of which had a PLA of 94.2g and PAA of 4100rad/s^2. This is different to the normal second impact syndrome reported in sport in which repeated impacts may be over days or weeks [46]. The present study recorded some interesting data on sub-concussive impacts. There were 8 non-injurious impacts recorded in competitive and sparring events whose PAA exceeded 6000rad/s^2.

It is hypothesised that these were non-injurious as duration of the angular acceleration was less than 20ms.

Some researchers have proposed that linear and angular acceleration are correlated [7][17], but this was not apparent in this study. Impacts to the front and back right had the highest R^2 adjusted value (0.46 and 0.70) and Pearson Correlation Coefficient (0.69 and 0.85 respectively). It is thought that the relationship between PLA and PAA depends on the style of fighting of both opponents.

The impact with the highest HIP value did not correspond to the impact with the maximum angular acceleration in three of the five cases of concussion. The average HIP value for the concussed cases was 20.6 and that for the uninjured fighters was 7.15. Newman et al. determined that a HIP of 12.79 and 20.88 corresponded to a probability of concussion of 50% and 95% respectively. Thus the average HIP value of concussed athletes in this study compares with the 95% probability determined by Newman [19]. Marjoux et al. determined a much higher HIP value of 24kW for a 50% risk of injury but their study included severe neurological injuries and head fractures [47].

The direction of the impact was investigated and found that 54.9% of sparring impacts and 36.4% of impacts in competition were sustained to the front left section of the head. This is consistent with the majority of fighters being right handed and hook style or jaw punches. Four of the five impacts that resulted in concussion were to the front or front left of the head. Impact location is significant as impacts in the temporal region have been shown to be more likely to result in a concussion [48][8].

5. 5 Conclusion

This study measured head linear and angular accelerations *in vivo* in MMA during both sparring sessions and competitive bouts. It is one of very few studies to record *in vivo* concussive and sub-concussive impacts in an unhelmeted sport. No injuries resulted from the sparring sessions despite 3 impacts which had PAAs in excess of 6000rad/s^2. The eleven competitive bouts studied resulted in five concussions being diagnosed either immediately after the event or in a 48 hour check-up. The average PAA differed by 24.7%, between concussed and uninjured fighters, but the duration of the linear and angular acceleration was considerably longer in the cases of concussion; 87% for linear acceleration and 52.5% for angular acceleration.

The impacts in MMA are of a shorter duration than those experienced in US football due to the light gloves worn by the fighters and the lack of head protection gear. The human tolerance to repeated relatively short severe impacts is unknown, but the data in this study is important to help understand the magnitude and variation of impacts that can cause an injury.

Limitations

The number of fighters and events in this study was limited; a greater number of impacts are required to improve the robustness of these findings, as well as further validation of the mouthguard in MMA style impacts such as direct strikes. The duration was calculated based on 10g and 500rad/s^2 thresholds; this is not directly comparable to other studies as they have not specified their methods of calculation. Impacts that could not be video verified and also impacts that appeared to be direct hits to the mouthguard were removed; this may have resulted in some valid data not being included. The concussed fighters received multiple impacts during their bouts therefore it is not possible to identify which impact caused the injury.

5.6 References

[1] P. McCrory, W. Meeuwisse, J. Dvorak, M. Aubry, J. Bailes, S. Broglio, *et al.*, "Consensus statement on concussion in sport: the 5 th international conference on concussion in sport held in Berlin, October 2016," *Br. J. Sports Med.*, p. bjsports-2017-097699, 2017.

[2] B. Hoshizaki, P. Andrew, K. Marshall, K. Clara, and B. Susan, "The Relationship between Head Impact Characteristics and Brain Trauma," *J. Neurol. Neurophysiol.*, vol. 05, no. 01, pp. 1–8, 2014.

[3] C. C. Giza, J. S. Kutcher, S. Ashwal, J. Barth, T. S. D. Getchius, G. a Gioia, *et al.*, "Summary of evidence-based guideline update: evaluation and management of concussion in sports: report of the Guideline Development Subcommittee of the American Academy of Neurology.," *Neurology*, vol. 80, no. 24, pp. 2250–7, 2013.

[4] C. A. Mcgrew, "Sports-related Concussion V Genetic Factors," *Am. Coll. Sport. Med.*, vol. 18, no. 1, pp. 20–22, 2019.

[5] J. G. Beckwith, R. M. Greenwald, and J. J. Chu, "Measuring head kinematics in football: Correlation between the head impact telemetry system and hybrid III headform," *Ann. Biomed. Eng.*, vol. 40, no. 1, pp. 237–248, 2012.

[6] R. Jadischke, D. Viano, N. Dau, A. I. King, and J. McCarthy, "On the accuracy of the head impact telemetry (hit) system used in football helmets," *J. Biomech.*, vol. 46, no. 13, pp. 2310–2315, Sep. 2013.

[7] S. Rowson, S. M. Duma, J. G. Beckwith, J. J. Chu, R. M. Greenwald, J. J. Crisco, *et al.*, "Rotational Head Kinematics in Football Impacts: An Injury Risk Function for Concussion," *Ann. Biomed. Eng.*, vol. 40, no. 1, pp. 1–13, 2012.

[8] E. Pellman, D. Viano, A. M. Tucker, I. Casson, A. B. Valadka, J. C. Maroon, *et al.*, "Concussion in Professional Football: Location and Direction of Helmet Impacts - Part 2," *Neurosurgery*, vol. 53, no. 6, pp. 1328–1341, 2003.

[9] A. S. McIntosh, D. a Patton, B. Fréchède, P.-A. Pierré, E. Ferry, and T. Barthels, "The biomechanics of concussion in unhelmeted football players in Australia: a case-control study.," *BMJ Open*, vol. 4, no. 5, p. e005078, 2014.

[10] L. Zhang, K. Yang, and A. King, "A proposed injury threshold for mild traumatic brain injury," *J Biomech Eng*, vol. 126, no. 2, pp. 226–236, 2004.

[11] B. J. Wilcox, J. G. Beckwith, R. M. Greenwald, N. P. Raukar, J. J. Chu, T. W. McAllister, *et al.*, "Biomechanics of head impacts associated with diagnosed concussion in female collegiate ice hockey players," *J. Biomech.*, vol. 48, no. 10, pp. 2201–2204, 2015.

[12] S. Rowson and S. M. Duma, "Brain Injury Prediction: Assessing the Combined Probability of Concussion Using Linear and Rotational Head Acceleration," *Ann. Biomed. Eng.*, vol. 41, no. 5, pp. 873–882, 2013.

[13] N. Reed, T. Taha, M. Keightley, C. Duggan, J. McAuliffe, J. Cubos, *et al.*, "Measurement of head impacts in youth ice hockey players," *Int. J. Sports Med.*, vol. 31, no. 11, pp. 826–833, 2010.

[14] S. Stojsih, M. Boitano, M. Wilhelm, and C. Bir, "A prospective study of punch biomechanics and cognitive function for amateur boxers," *Br. J. Sports Med.*,

vol. 44, no. 10, pp. 725–730, 2010.

[15] K. M. Guskiewicz, J. P. Mihalik, V. Shankar, S. W. Marshall, D. H. Crowell, S. M. Oliaro, *et al.*, "Measurement of Head Impacts in Collegiate Football Players," *Neurosurgery*, vol. 61, no. 6, pp. 1244–1253, Dec. 2007.

[16] Viano, I. Casson, and E. Pellman, "Concussion in professional football: Brain responses by finite element analysis: Part 9," *Neurosurgery*, vol. 57, no. 5, pp. 891–915, 2005.

[17] E. Pellman, D. Viano, A. M. Tucker, I. Casson, and J. F. Waeckerle, "Concussion in Professional Football: Reconstruction of Game Impacts and Injuries," *Neurosurgery*, vol. 53, no. 4, p. 796, Oct. 2003.

[18] S. M. Duma, S. J. Manoogian, W. R. Bussone, P. G. Brolinson, M. W. Goforth, J. J. Donnenwerth, *et al.*, "Analysis of real-time head accelerations in collegiate football players," *Clin J Sport Med*, vol. 15, no. 1, pp. 3–8, 2005.

[19] J. Newman, C. Barr, M. Beusenberg, E. Fournier, N. Shewchenko, E. Welbourne, *et al.*, "A new biomechanical assessment of mild traumatic brain injury, part 2: results and conclusions," *Proc. 2000 Int. Conf. Biomech. Impact*, pp. 223–233, 2000.

[20] S. P. Broglio, B. Schnebel, and J. Sosnoff, "The Biomechanical Properties of Concussions in High School Football," *Med. Sci. Sports Exerc.*, vol. 42, no. 11, pp. 2064–2071, 2010.

[21] E. Gurdjian and V. Roberts, "Tolerance Curves of Acceleration and Intracranial Pressure and Protective Index in Experimental Head Injury," *J. Trauma*, vol. 6, no. 5, 1966.

[22] M. Shojaati, "Correlation between injury risk and impact severity index ASI," *Swiss Transp. Res. Conf.*, pp. 1–10, 2003.

[23] J. A. Newman and N. Shewchenko, "A Proposed New Biomechanical Head Injury Assessment Function - The Maximum Power Index," *SAE Tech. Pap.*, vol. 2000-Novem, no. November, 2000.

[24] T. Gennarellie, "Head injury in man and experimental animals: neuropathology.," *Acta Neurochir. Suppl.*, vol. 32, pp. 15–30, 1983.

[25] M. R. Elliott, S. S. Margulies, M. R. Maltese, and K. B. Arbogast, "Accounting for sampling variability , injury under-reporting , and sensor error in concussion injury risk curves," *J. Biomech.*, vol. 48, no. 12, pp. 3059–3065, 2015.

[26] A. Post, T. Blaine Hoshizaki, M. D. Gilchrist, and M. D. Cusimano, "Peak linear and rotational acceleration magnitude and duration effects on maximum principal strain in the corpus callosum for sport impacts," *J. Biomech.*, vol. 61, pp. 183–192, 2017.

[27] S. Kleiven, "Influence of Impact Direction on the Human Head in Prediction of Subdural Hematoma," *J. Neurotrauma*, vol. 20, no. 4, pp. 365–379, 2003.

[28] T. B. Hoshizaki, A. Post, M. Kendall, J. Cournoyer, P. Rousseau, M. D. Gilchrist, *et al.*, "The development of a threshold curve for the understanding of concussion in sport," *Trauma (United Kingdom)*, vol. 19, no. 3, pp. 196–206, Jul. 2017.

[29] L. C. Wu, V. Nangia, K. Bui, B. Hammoor, M. Kurt, F. Hernandez, *et al.*, "In Vivo Evaluation of Wearable Head Impact Sensors," *Ann. Biomed. Eng.*, vol. 44, no. 4, pp. 1234–1245, 2016.

[30] D. King, P. Hume, C. Gissane, and T. Clark, “Head Impacts in a Junior Rugby League Team Measured with Wireless sensor X patch,” *JNS Pediatr.*, vol. 19, no. January, pp. 13–23, 2017.

[31] A. Bartsch, S. Samorezov, and E. Benzel, “Validation of an" intelligent mouthguard" single event head impact dosimeter,” *Stapp car crash*, vol. 58, no. November, 2014.

[32] A. Bartsch and S. Samorezov, “Cleveland Clinic intelligent mouthguard: a new technology to accurately measure head impact in athletes and soldiers,” *Proc. SPIE 8723, Sens. Technol. Glob. Heal. Mil. Med. Environ. Monit. III*, vol. 8723, p. 87230N, 2013.

[33] D. Garza, D. Camarillo, R. Shultz, J. Mattson, P. B. Shull, J. Mattson, *et al.*, “An instrumented mouthguard for measuring linear and angular head impact kinematics in American football,” *Ann. Biomed. Eng.*, vol. 41, no. 9, pp. 1939–1949, 2013.

[34] F. Hernandez, L. Wu, M. C. Yip, K. Laksari, A. R. Hoffman, J. R. Lopez, *et al.*, “Six Degree of Freedom Measurements of Human Mild Traumatic Brain Injury,” *Ann. Biomed. Eng.*, vol. 43, no. 8, pp. 1918–1934, 2015.

[35] M. G. Hutchison, D. W. Lawrence, M. D. Cusimano, and T. A. Schweizer, “Head trauma in mixed martial arts,” *Am. J. Sports Med.*, vol. 42, no. 6, pp. 1352–1358, 2014.

[36] C. Kuo, L. Wu, B. T. Hammoor, J. F. Luck, H. C. Cutcliffe, R. C. Lynall, *et al.*, “Effect of the mandible on mouthguard measurements of head kinematics,” *J. Biomech.*, vol. 49, no. 9, pp. 1845–1853, 2016.

[37] D. King, P. Hume, C. Gissane, M. Brughelli, and T. Clark, “The Influence of Head Impact Threshold for Reporting Data in Contact and Collision Sports: Systematic Review and Original Data Analysis,” *Sport. Med.*, 2015.

[38] D. King, P. a Hume, M. Brughelli, and C. Gissane, “Instrumented Mouthguard Acceleration Analyses for Head Impacts in Amateur Rugby Union Players Over a Season of Matches,” *Am J Sport. Med*, vol. ePub, no. ePub, p. ePub-ePub, 2014.

[39] L. Wu, K. Laksari, C. Kuo, J. Luck, S. Kleiven, C. Bass, *et al.*, “Bandwidth and sample rate requirements for wearable head impact sensors,” *J. Biomech.*, vol. 49, no. 13, pp. 2918–2924, 2016.

[40] K. Laksari, F. Hernandez, J. R. Lopez, A. R. Hoffman, G. A. Grant, D. Camarillo, *et al.*, “Six Degree-of-Freedom Measurements of Human Mild Traumatic Brain Injury,” *Ann. Biomed. Eng.*, vol. 43, no. 8, pp. 1918–1934, 2014.

[41] L. Wu, F. Hernandez, C. Kuo, and M. Kurt, “In Vivo Evaluation of Wearable Head Impact Sensors,” *Ann. Biomed. Eng.*, vol. 44, no. 4, pp. 1234–1245, 2016.

[42] B. J. Paris AJ, Antonini KR, “Accelerations of the Head During Soccer Ball Heading,” *Accel. head Dur. soccer ball Head. InProceedings ASME Summer Bioeng. Conf.*, p. (pp. 815-816), 2010.

[43] D. Viano, I. Casson, E. Pellman, C. Bir, L. Zhang, D. Sherman, *et al.*, “Concussion in professional football: Comparison with boxing head impacts - Part 10,” *Neurosurgery*, vol. 57, no. 6, pp. 1154–1170, 2005.

[44] C. Deck and R. Willinger, “Improved head injury criteria based on head FE model,” *Int. J. Crashworthiness*, vol. 13, no. 6, pp. 667–678, 2008.

[45] W. Zhao and S. Ji, “Brain strain uncertainty due to shape variation in and simplification of head angular velocity profiles,” *Biomech. Model. Mechanobiol.*, vol. 16, no. 2, pp. 449–461, 2017.

[46] L. A. McLendon, S. F. Kralik, P. A. Grayson, and M. R. Golomb, “The Controversial Second Impact Syndrome: A Review of the Literature,” *Pediatr. Neurol.*, vol. 62, pp. 9–17, 2016.

[47] D. Marjoux, D. Baumgartner, C. Deck, and R. Willinger, “Head injury prediction capability of the HIC, HIP, SIMon and ULP criteria,” *Accid. Anal. Prev.*, vol. 40, no. 3, pp. 1135–1148, 2008.

[48] A. Oeur, B. T. Hoshizaki, and M. D. Gilchrist, “The Influence of Impact Angle on the Dynamic Response of a Hybrid III Headform and Brain Tissue Deformation,” *Mech. Concussion Sport.*, pp. 56–69, 2014.

Chapter 6

Setup and Sensitivity Analysis of the GHBMC Head and Neck Model

6.1 Introduction

Simulation studies play a unique role in head impact investigations as they enable the estimation of brain tissue stress and strain resulting from trauma. As discussed in Section 2.6 there are a number of finite element head models that have been used to investigate concussion. This chapter will discuss the head and neck portions of the GHBMC model as this was used in all simulations performed in this project.

6.1.1 GHBMC head model

The Global Human Body Model Consortium (GHBMC) is a multi-institutional organization created in 2006 that includes 6 universities and 8 automotive manufacturers. The organization aims to produce the world's most bio-fidelic simulation body models. A family of models have been created to represent the large male, average male, average female and a child. The model heads were developed by Wayne State University, the necks by the University of Waterloo, and the thorax and pelvises by the University of Virginia. These models are available to researchers under license from Elemance Ltd., USA. There are also vehicle occupant and pedestrian models. This project will only use head and neck portion of the average 50th percentile US male model M50-O version 4.5. The head portion of the GHBMC model is one of the most detailed head models available and is capable of simulating impacts up to 200g and 12krad/s^2 [1][2][22][23]. The model includes the scalp, skull, brain, meninges, cerebral spinal fluid, dura, pia, tentorium, falx, sinus, white and grey matter and the ventricles. The head and neck portion of the GHBMC consists of 532,608 elements and 426 parts (Figure 6-1) of which 246,831 elements and

71 parts make up the head (Figure 6-2). In 2013 Mao et al. updated the material properties of the model and published a validation of version 4.5 of this model by comparing the model results with 35 experimental cases [2]. Intracranial pressure was compared to cadaver experiments by Nahum et al. and Trosseille et al. [3][4]. Brain motion was validated using data from Hardy et al.'s experiments which tracked embedded neutral density targets in cadaver heads [5][6]. Version 4.5 was further validated in 2017 by comparing the model's brain motion with the brain motion in human volunteers [7]. The human experiments were carried out in an MRI scanner.

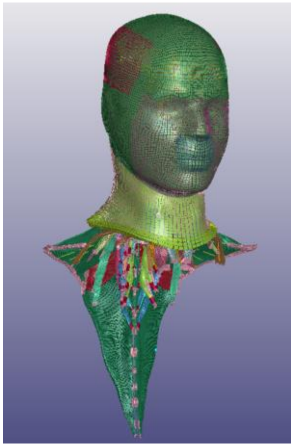

Figure 6-1: The GHBMC head and neck model

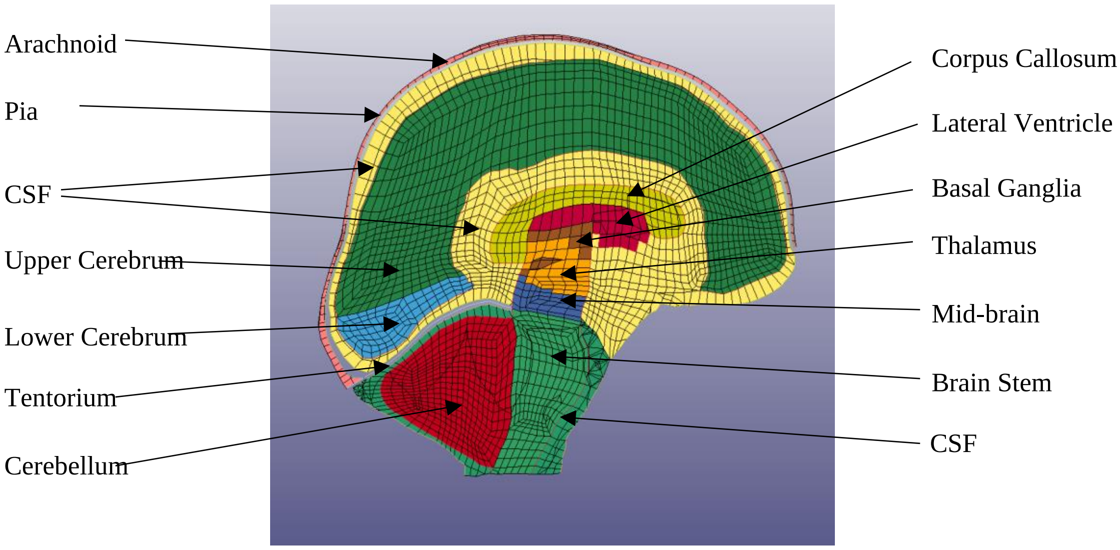

Figure 6-2: Brain parts in the GHBMC model

The brain tissue including the cerebrum, cerebellum, corpus callosum, thalamus and brain stem is modelled as linear viscoelastic materials using a Maxwell model [8]. A summary of the viscoelastic material properties is presented in Table 6-1. More details are available in Appendix 4.

Table 6-1: Material properties of principal brain parts of version 4.5 GHBMC

Description	Number of Elements	Volume	Density	Bulk Modulus	Shear Modulus Short term	Shear Modulus Long term	Decay Constant
		mm^3	ρ (kg/m^3)	K (MPa)	G_O (kPa)	G_I (kPa)	s^{-1}
Grey matter: Cerebrum	22700	463186	1060	2190	6.0	1.2	125
White matter: Cerebrum	23440	428965	1060	2190	7.5	1.5	125
Cerebellum	14280	115665	1060	2190	6.0	1.2	125
Corpus Callosum	980	19691	1060	2190	7.5	1.5	125
Thalamus	260	11261	1060	2190	6.0	1.2	125
Brain stem	2280	9134	1060	2190	12.0	2.4	125
Mid-brain	504	20881	1060	2190	12.0	2.4	125
Sagittal-Sinus	880	4429	1060	2190	0.5	0.1	125
Cerebrospinal Fluid	14477	291214	1040	2190	0.5	0.1	125

6.2 Co-ordinate systems

The GHBMC model uses the normal anatomical planes as shown in Figure 6-3.

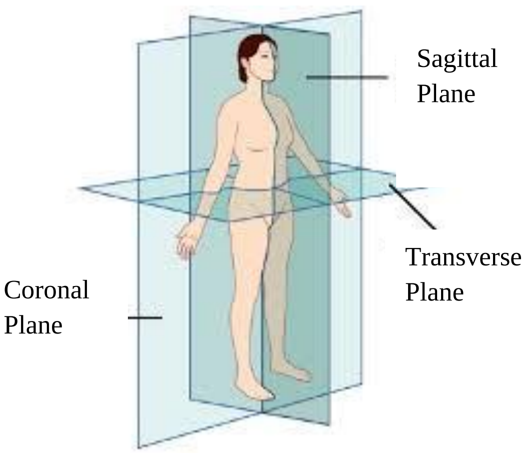

Figure 6-3: Anatomical Planes

Mouthguard co-ordinates

The Stanford instrumented mouthguard uses the normal anatomical directions: X posterior to anterior, Y right to left, and Z inferior to superior.

Rotations are defined as:

- Rotation around X axis – also referred to as rotation in the coronal plane.
- Rotation around Y axis – also referred to as rotation in the sagittal plane.
- Rotation around Z axis – also referred to as rotation in the transverse plane.

Simulation model co-ordinates

The co-ordinate system of the GHBMC simulation model differs from the norm as it is rotated about the X axis by 180 degrees, as shown in Figure 6-4.

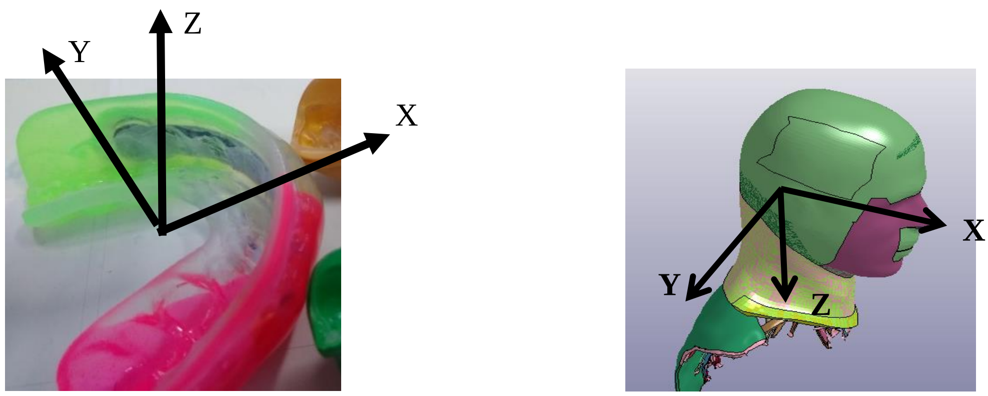

Figure 6-4: Co-ordinate system of the Stanford mouthguard and GHBMC head model

Position of the mouthguard

The centre of gravity of the head is 77.64mm posterior, 0mm in the y direction and 72.07mm superior to the position of the mouthguard.

Units

The mouthguard outputs linear acceleration in multiples of the acceleration due to gravity (g's) and angular velocity in rad/s. The units used in the GHBMC model are: length in millimetres, time in milliseconds, and density in kg/mm^3. To maintain consistency of units stress results are output from the model in kN/mm^2.

6.2.1 Preparation of acceleration data for simulation

Matlab, Mathworks, scripts (Appendix 3) were used to prepare the acceleration data for application to the head model in the following ways:

- Angular velocity is down-sampled from 8000Hz to 1000Hz to match the number of linear acceleration data points.
- Data is filtered using a 4th order Butterworth filter with a cut off frequency of 300Hz.
- Angular acceleration is calculated by differentiating angular velocity.
- Data is transformed to the centre of gravity of the head.
- Data from a 50ms interval is selected (5ms pre-trigger and 45ms post-trigger).
- The co-ordinate system is rotated through 180 degrees.
- Units are converted to mm, ms and radians.
- A file for each linear and angular axis is output as an individual comma separated variable (csv) file.

6.2.2 Application of acceleration data to the simulation model

Ls-PrePost, Livermore Software Technology Corp. (version 4.6) was used to prepare the model for simulation. The preparation included:

- Setting the material of the hyoid inferior skull plate to rigid.
- Specifying that loads would be applied in the local co-ordinate system to the node (1990002) at the centre of gravity of the head.
- Defining load curves for each of the six degrees of freedom by importing the CSV acceleration data for each axis.
- Applying the load curves to the model using boundary prescribed motion.
- Setting the frequency for outputting data using Database binary d3plot.
- Setting the termination time for the simulation.

6.2.3 Solving and post-processing

When the model files were ready for solving instances were started on Amazon cloud computing services. The instances were setup to use the Linux operating system with 72 cores and 144Gbytes of memory. Simulations of 50ms required a run-time of approximately 2.5 hours. 50ms has been identified as a suitable simulation time to capture the complete strain event [9]. Upload of model files and download of results files required an additional 2 hours per simulation.

LS Prepost was used for all post-processing tasks. Green Lagrange strain was used to determine strain as the constitutive properties of the material were assumed to change due to large deformations during the solution. The first principal Green Lagrange strain was determined by locating the maximum within a region and averaging the strain around the adjacent elements, thus avoiding unrealistic singularities.

6.3 Investigation of model sensitivity

Some preliminary simulation work was carried out to analyse the head model's strain response to changes in angular acceleration and changes in material parameters. Three separate investigations were undertaken:

1. Angular accelerations of varying magnitudes and directions were applied to the head model.
2. Angular accelerations with varying durations were applied to the model.
3. Three different material models were applied to the GHBMC head model.

6.3.1 Method 1: Strain versus angular acceleration - magnitude and direction

Angular accelerations of 2.5krad/s^2, 5krad/s^2, 7.5krad/s^2 and 10krad/s^2 about the X, Y and Z axes were applied to the head model to investigate the relationship between angular acceleration and strain in the corpus callosum The accelerations were applied as half sine waves as shown in Figure 6-5.

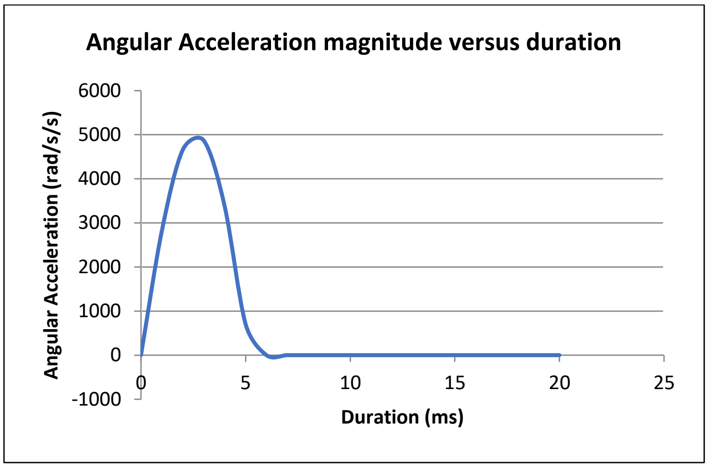

Figure 6-5: Sample angular acceleration curve: 5krad/s/s and 6ms duration

6.3.2 Method 2: Strain versus impact duration

The duration of impacts in helmeted sports are longer than those in unhelmeted sports due to the energy absorbing effect of the protective equipment. Impact durations of 3, 6, 11, 16 and 21ms were applied to the model to investigate the effect of duration on brain strain. The impacts were applied about the X and Z axes as half sine waves with a magnitude of 5krad/s^2.

6.3.3 Method 3: Strain versus brain tissue stiffness

The viscoelastic material models of finite element head models have evolved over the years. There can be substantial differences in the material properties used by different researchers even when using the same head model. Three different material models (Table 6-2) were compared to investigate the influence of viscoelastic stiffness on strain in the corpus callosum. In 2005 the head model of the GHBMC had relatively stiff brain tissue which had been determined from experimental tissue tests, in particular those performed by Thibault and Margulies [10][11]. This was revised in 2013 (GHBMC v4.5) by Mao et al. who proposed that the stiffness of the brain tissue should be reduced by between 40% and 47% (Table 6-2) [2][7]. In the latest version of the model GHBMC v5.0 (2020) the stiffness has been reduced by a further 50% compared to version 4.5. A comparison of the material stiffness of the 3 versions of the model is shown in Figure 6-6. In general, all versions of the material model have assumed that the brain stem is approximately twice as stiff as the grey matter. In the 2005 version and version 4.5 the white mater including the corpus callosum was assumed to be 25% stiffer than the grey matter. This has changed in version 5 and the corpus callosum is assumed to be less stiff than the grey matter. This change was made to reflect the brain tissue testing and modelling work of Professor Budday [12]. A validation study of version 5 of the model has not yet been published.

Table 6-2: Development of the material properties of the GHBMC

Description	Head Model version	Brain Region	Shear Modulus short term kPa	Shear Modulus long term kPa	Decay Const s
Material Model 1	GHBMC v5.0 (2020)	White Matter – Cerebrum & Corpus Callosum	3.75	0.75	200
		Thalamus, Basal Ganglia & Cerebellum	3.00	0.60	200
		Mid-brain, Brain Stem	6.00	1.2	200
Material Model 2	GHBMC v4.5 Validation Mao 2013 [2]	White matter & Corpus Callosum	7.5	1.5	125
		Grey Matter, cerebrum & cerebellum	6	1.2	125
		Brain stem & Mid-Brain	12	2.4	125
Material Model 3	Wayne State Uni. Head Injury Model 2005 [10]	White Matter & Cerebellum & Corpus Callosum	12.5	2.5	80
		Grey Matter	10	2	80
		Brain stem	22.5	4.5	80

Three versions of the head model were created, each with a different material model (Table 6-2). An angular acceleration of 5krad/s^2 around the X axis was applied to each of the models with a duration of 3ms, 6ms and 11ms.

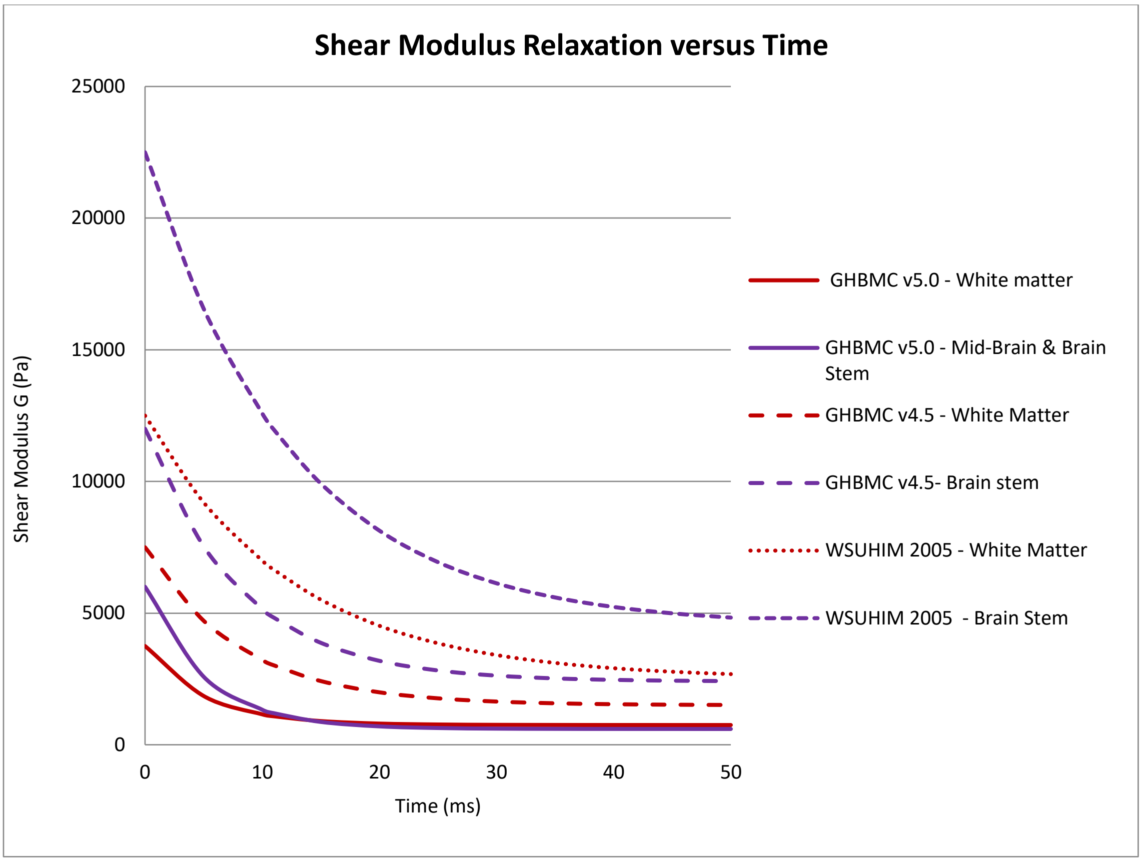

Figure 6-6: Shear modulus of the GHBMC viscoelastic brain material

6.4 Results

6.4.1 Results 1: Acceleration magnitude and direction

It was found, as shown in Figure 6-7, that strain was proportional to angular acceleration and that angular accelerations about X and Z (that is rotations in the coronal and transverse planes) resulted in approximately double the strain compared to rotations about the Y axis (rotation in the sagittal plane). Figure 6-8 shows sagittal and transverse strain results for impacts of 5krad/s^2 with a duration of 6ms. The bottom row of Figure 6-8 focuses on the core brain regions which include the corpus callosum, thalamus, mid-brain and brain stem.

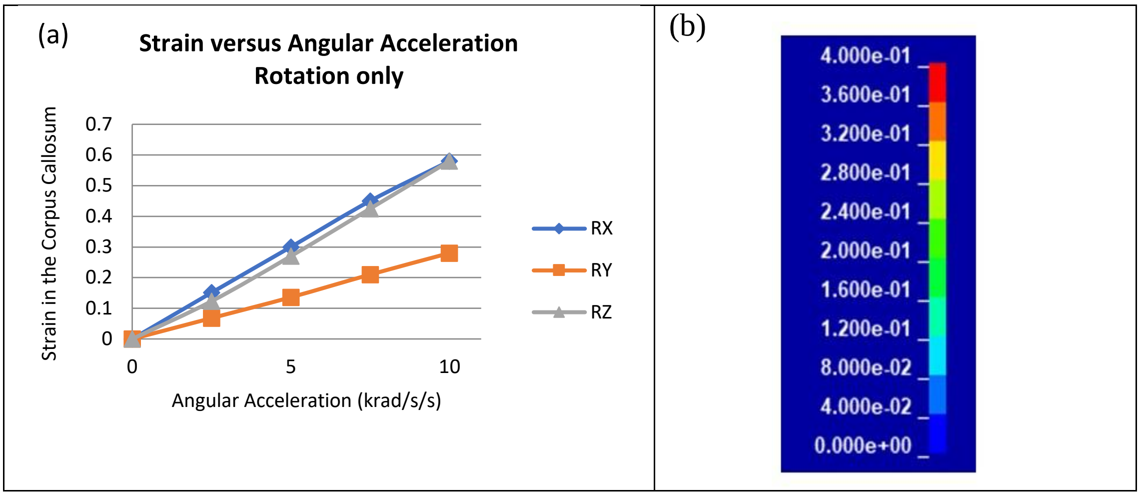

Figure 6-7: (a) Strain in the corpus callosum from angular accelerations about a single axis. (b) Green Lagrange Strain Scale (used in plots in Figure 6-8)

Angular Acceleration – X axis	Angular Acceleration – Y axis	Angular Acceleration – Z axis
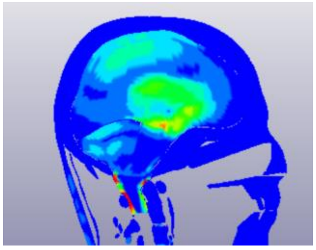	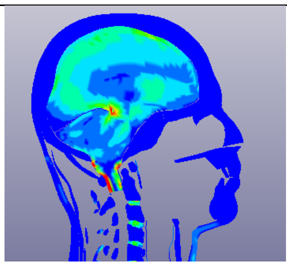	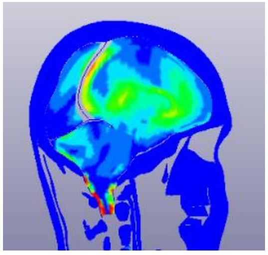
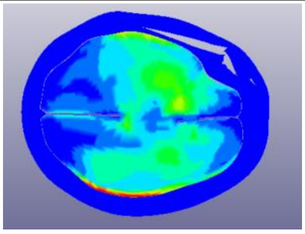	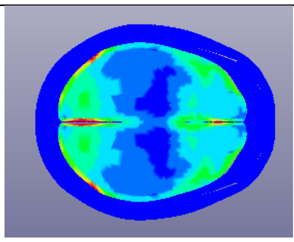	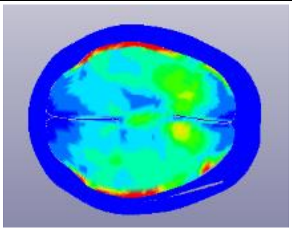
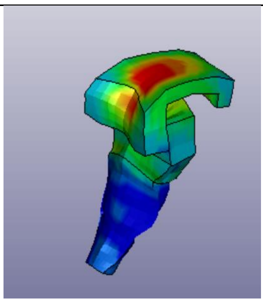	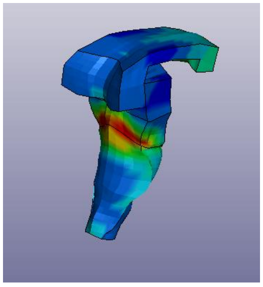	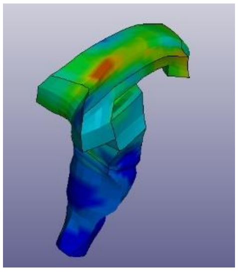

Figure 6-8: Strain plots for Angular Acceleration only around X, Y, and Z axis magnitude 5krad/s/s and duration 6ms
(Top row: Sagittal section, Middle row: transverse section, Bottom row: Corpus callosum, thalamus, mid-brain and brain stem). Strain scale sown in Figure 6-7

6.4.2 Results 2: Duration

The strain in the corpus callosum following an angular acceleration of 5krad/s^2 was approximately linear up to a duration of 15ms when it began to level off (Figure 6-9). Figure 6-10 shows strain in the corpus callosum, thalamus, mid-brain and brain stem for varying impact durations.

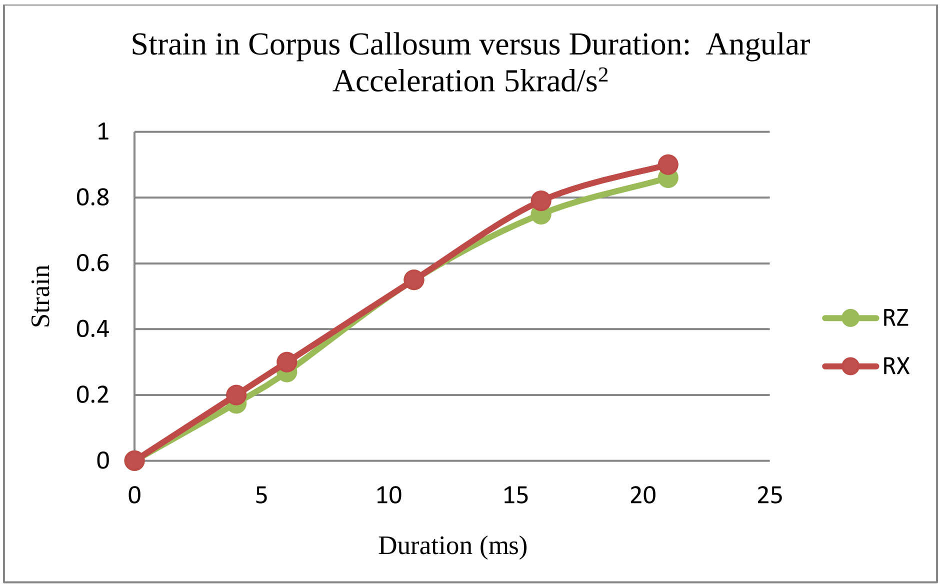

Figure 6-9: Strain versus duration for angular accelerations about X and Z axis

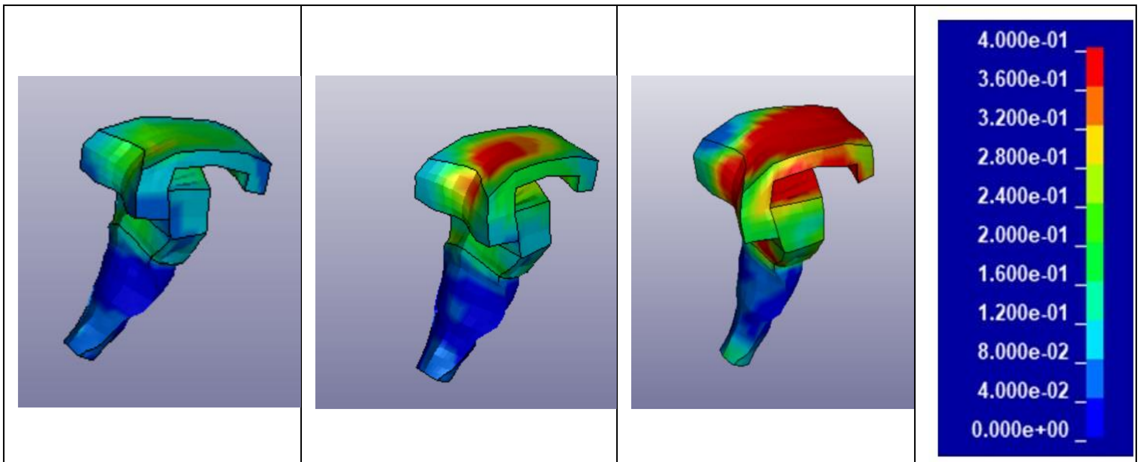

Duration 3ms	Duration 6ms	Duration 11ms	Strain Scale

Figure 6-10: Strain plots - 5krad/s/s angular acceleration about X axis.

6.4.3 Results 3: Material Properties

A comparison of the results from each of the 3 material models described in 6.2.3 and Table 6-2 is shown in Figure 6-9. It is evident from Figure 6-11 that the shear modulus has a large effect on the strain results. Strain in the corpus callosum of material model 2 (GHBMC v4.5) increased by 6% for short duration impacts (4ms) and 22% for longer impacts (11ms) when compared to material model 3 (WSUHIM 2005). This change in strain is due to a reduction in stiffness of the white matter of 40%. The strain is higher again in the simulations using material model 1 again due to the reduction in stiffness of the materials compared to material models 2 and 3.

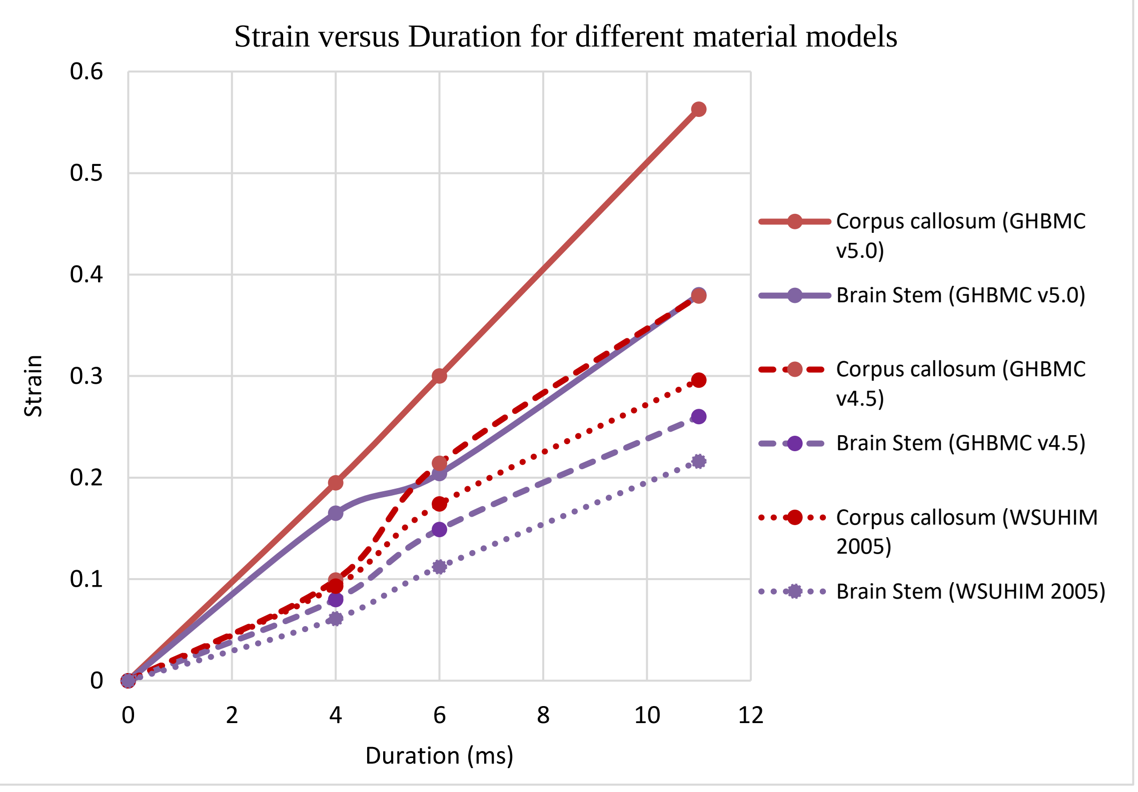

Figure 6-11: Stain for different materials models

6.5 Discussion

Angular Acceleration - magnitude and direction

This investigation found that angular accelerations about the X axis (rotations in the coronal plane) created high strains in the superior portion of the corpus callosum (Figure 6-5). While angular accelerations about the Z axis created high strains in the inferior part of the corpus callosum. This finding is similar Kleiven et al's. who found that lateral angular accelerations (in the coronal plane) gave rise to higher strains than impacts from other directions [13]. High strains in the corpus callosum may be due to the movement of the relatively stiff corpus callosum in the more compliant grey matter of the cerebrum [14]. A contributing factor may also be the distortion of the falx and tentorium which connect the corpus callosum to the superior and inferior sinus [15]. Strains decrease in regions inferior to the mid brain as movement is prevented due to the restraining effect of the spinal cord [14].

Interestingly angular accelerations around the Y axis, which typically occur following impacts to the front, or rear of the head cause high strains lower down in the mid-brain (Figure 6-6). These strains are approximately half the magnitude of the strains from similar angular accelerations around the X and Z axes, corroborating the US football findings that concussions are unlikely to occur from impacts to the front of the head (Section 2.1.5) [16].

Angular acceleration duration

Durations of 3 to 5ms have been reported for unhelmeted impacts to hard surfaces [17] whereas durations in US football are typically longer than 15ms [18]. Short duration impacts cause stretching of the vasculature and 'bumping' of the brain against the skull [19] whereas longer durations can lead to more diverse nerve damage such as DAI [20]. Angular accelerations of 5krad/s^2 about the X axis with a duration greater than 6ms were found to cause very high strains (>0.3) in the corpus callosum. This demonstrates that magnitude alone is not the only consideration when evaluating strain.

The duration was less significant for impacts greater than 6krad/s^2. A relationship between impact duration and magnitude has previously been reported by Post et al. who found a steady increase in brain strain with duration for rotational only accelerations. They reported that the strain response from an impact of 2500rad/s^2 with a duration of 10ms was similar to an impact of 5000rad/s^2 with a duration of 2.5ms [21]. This study found that for a particular strain level the magnitude of the angular acceleration was inversely proportional to the duration up to 6krad/s^2 but that the constant of proportionality was approximately 50% of that found by Post et al. It is hypothesised that this difference may be due to the higher magnitudes of angular acceleration used by Post el al. and the different material properties used in the head models [21].

Care must be taken in interpreting the duration of impacts reported in research publications as the method by which they have been calculated is rarely reported.

Material Properties

The simulation studies reported in this thesis have used material properties from the 2013 version (v4.5) of the GHBMC model (material model 2). The original material model (material model 3) developed by Wayne State University and incorporated into the GHBMC model in 2005 had white matter that was 33.3% stiffer than the version used in this study (v4.5). Simulations run using this older material model resulted in strains in the corpus callosum which were 22% lower than the strains reported in this study.

The stiffness of the white matter in the latest (2020 v5.0) version of the GHBMC head is 50% lower than that in the 2013 (v4.5) version used in this study. This reduction in stiffness results in a 40% to 49% increase in strain in the corpus callosum. The validation of this new (2020) material model (material model 3) has not been published yet.

From this investigation it is apparent that the stiffness of the brain tissue is paramount in determining brain strains. It is therefore necessary to careful consider the validation studies of any simulation model used to study head impacts. The rationale for using version 4.5 of the GHBMC head model throughout this project is that it has been well documented and validated by Mao et al. in 2013 [2] and Talebanpout et al. in 2017 [7].

6.6 References

[1] Zhang, K. Yang, and A. King, “Recent advances in brain injury research: a new human head model development and validation,” *Stapp Car Crash J*, 2001. .

[2] H. Mao, L. Zhang, B. Jiang, V. V. Genthikatti, X. Jin, F. Zhu, *et al.*, “Development of a Finite Element Human Head Model Partially Validated With Thirty Five Experimental Cases,” *J. Biomech. Eng.*, vol. 135, no. 11, p. 111002, 2013.

[3] G. Belingardi, G. Chiandussi, and I. Gaviglio, “Development and validation of a New Finite Element Model of Human Head,” *Proc. 19th Int. Tech. Conf. Enhanc. Saf. Veh.*, pp. 1–9, 2005.

[4] X. Trosseille, C. Tarriére, F. Lavaste, F. Guillon, and A. Domont, “Development of a F.E.M. of the human head according to a specific test protocol,” *SAE Tech. Pap.*, 1992.

[5] S. Kleiven and W. N. Hardy, “Correlation of an FE Model of the Human Head with Local Brain Motion--Consequences for Injury Prediction,” *Stapp Car Crash J.*, vol. 46, no. November, pp. 123–144, 2002.

[6] W. N. Hardy, M. J. Mason, C. D. Foster, C. S. Shah, J. M. Kopacz, H. Yang, *et al.*, “A study of the response of the human cadaver head to impact,” *Stapp Car Crash J*, vol. 51, pp. 17–80, 2008.

[7] L. Talebanpour and L. Smith, “A Comparison between Simulated and Measured Human Brain Response under Mild Acceleration,” *IRCOBI Conf.*, p. IRC-17-59, 2017.

[8] V. Effinger and P. A. Du Bois, “Modelling of viscoelastic materials with LS-Dyna,” *LS-Dyna Theory Man.*, pp. 1–22, 2012.

[9] E. J. Sanchez, L. F. Gabler, A. B. Good, J. R. Funk, J. R. Crandall, and M. B. Panzer, “A reanalysis of football impact reconstructions for head kinematics and finite element modeling,” *Clin. Biomech.*, vol. 64, no. February, pp. 82–89, 2019.

[10] L. Zhang, A. King, and K. Yang, “Concussion in professional football: Brain responses by finite element analysis: Part 9,” *Neurosurgery*, vol. 57, no. 5, pp. 891–915, Nov. 2005.

[11] S. S. Margulies, L. E. Thibault, and T. A. Gennarelli, “Physical model simulations of brain injury in the primate.,” *J. Biomech.*, vol. 23, no. 8, pp. 823–36, 1990.

[12] S. Budday, T. C. Ovaert, G. A. Holzapfel, P. Steinmann, and E. Kuhl, *Fifty Shades of Brain: A Review on the Mechanical Testing and Modeling of Brain Tissue*, vol.

27, no. 4. Springer Netherlands, 2019.

[13] S. Kleiven, "Influence of direction and duration of impacts to the human head evaluated using the finite element method," *Proc. IRCOBI Conf. Prague, Czech Repub.*, no. September, pp. 41–57, 2005.

[14] A. A. Sabet, E. Christoforou, B. Zatlin, G. M. Genin, P. V. Bayly, V. Philip, *et al.*, "Deformation of the human brain induced by mild angular head acceleration," *Computer (Long. Beach. Calif).*, vol. 41, no. 2, pp. 307–315, 2008.

[15] K. Laksari, F. Hernandez, J. R. Lopez, A. R. Hoffman, G. A. Grant, D. Camarillo, *et al.*, "Six Degree-of-Freedom Measurements of Human Mild Traumatic Brain Injury," *Ann. Biomed. Eng.*, vol. 43, no. 8, pp. 1918–1934, 2014.

[16] S. Rowson, G. Brolinson, M. Goforth, D. Dietter, and S. Duma, "Linear and Angular Head Acceleration Measurements in Collegiate Football," *J. Biomech. Eng.*, vol. 131, no. 6, p. 061016, 2009.

[17] M. C. Doorly and M. D. Gilchrist, "The use of accident reconstruction for the analysis of traumatic brain injury due to head impacts arising from falls," *Comput. Methods Biomech. Biomed. Engin.*, vol. 9, no. 6, pp. 371–377, 2006.

[18] E. Pellman, D. Viano, A. Tucker, I. Casson, and J. Waeckerle, "Concussion in Professional Football: Reconstruction of Game Impacts and Injuries," *Neurosurgery*, vol. 53, no. 4, p. 796, 2003.

[19] R. Willinger, R. Ryan, A. McLean, and C. Kopp, "Mechanisms of Brain Injury Related to Mathematical Modelling and Epidemiological Data," *Accid. Anal. and Prev.*, vol. 26, no. 6, pp. 767–779, 1994.

[20] S. S. Margulies and L. E. Thibault, "A proposed tolerance criterion for diffuse axonal injury in man," *J. Biomech.*, vol. 25, no. 8, pp. 917–923, 1992.

[21] A. Post, T. Blaine Hoshizaki, M. D. Gilchrist, and M. D. Cusimano, "Peak linear and rotational acceleration magnitude and duration effects on maximum principal strain in the corpus callosum for sport impacts," *J. Biomech.*, vol. 61, pp. 183–192, 2017.

Chapter 7

The effect of impact location on brain strain

Abstract

Objective: To determine the effect of impact direction on strains within the brain.

Methods: A hybrid III head-form instrumented with accelerometers and gyroscopes was dropped from 10 different heights in four orientations: front, rear, left and right-hand side. Twelve impacts with constant impact energy were chosen to simulate to determine the effect of impact location on brain strain. A finite element head model with 6 degrees of freedom was used to simulate these impacts. Following this a further set of simulations were performed, where the same acceleration profiles were applied to different head locations.

Results: The angular accelerations recorded were up to 30% higher in lateral and rear impacts when compared to frontal impacts. High strains in the mid-brain (0.36) were recorded from severe frontal impacts (130g and 6000rad/s^2) whereas high strain in the corpus callosum (0.44) resulted from lateral impacts with the same energy.

Conclusion: Impact direction is very significant in determining the subsequent strains developed in the brain. Lateral impacts result in high strains in the corpus callosum and frontal impacts result in high strains in the mid-brain.

Published: S. Tiernan and G. Byrne, "The effect of impact location on brain strain," Brain Inj., vol. 33, no. 01, pp. 1–8, 2019.

DOI: 10.1080/02699052.2019.1566834

This chapter is a reproduction of the published paper except for some minor alterations.

7.1 Introduction

The introduction to this chapter has been edited from the original version published in the paper to reduce the duplication of information.

Head accelerations have been measured in US football using the HIT system. Also kinematic data from head impacts has been acquired from laboratory and kinematic simulation studies [1][2]. Data from these studies has been used in finite element models to determine strain within the brain Patton et al. determined that maximum principal strain was significantly associated with concussion [2]. Gilchrist et al. investigated the relationship between linear and angular acceleration and the durations of these accelerations [1]. They found that as the duration increased the angular acceleration becomes dominant and an angular acceleration as low as 2500rad/s^2, over 10 to 15ms, can result in a brain injury. A number of other studies have investigated the magnitude, shape [3] and duration [1] of the acceleration pulses but there has been little analysis, to date, on how the location and direction of the impact effects different regions of the brain.

Large principal strains have been proposed as one of the causes of diffuse axonal injury [4], and high strains in the corpus callosum have been associated with concussion [5]. Margulies et al. used a porcine model to investigate diffuse axonal injury [6]. They applied a sudden rotation in the coronal plane without an impact. From this they determined that an angular acceleration above 9000rad/s^2 may lead to a moderate to severe DAI, but they state that there is a continuum of axonal injury, and that concussion might be associated with much lower levels of angular acceleration. In one of the few studies of the movement of the living human brain, subjected to small impacts, it was determined that DAI may also be caused by linear acceleration [7]. They hypothesised that the motion of the brain is constrained by structures in the front and base of the skull and that the tangential components of linear forces cause the brain to rotate about its centre of mass [7].

Camarillo et al. found that criteria that included six degrees of freedom kinematics were better at indicating an injury compared to criteria such as peak linear acceleration and head impact criteria (HIC), but they also found that the most accurate predictor of injury was strain in the corpus callosum [5]. McAllister et al. reported that peak principal strains in the corpus callosum of 0.28 ± 0.089 resulted in concussion [8]. McAllister's study recreated impacts in the laboratory and applied the recorded head accelerations to the Dartmouth head model. A similar study by Zhang et al., using the Wayne State University head injury model, found that shear stress in the brain stem provided the strongest correlation with the occurrence of concussion [9]. Patton et al. studied 27 concussive cases in helmeted and unhelmeted sports; the average linear acceleration for the injury cases was 103.8g and the average angular acceleration was 7141rad/s^2. Using the KTH model Patton et al. concluded that the best predictor of injury was strain in the corpus callosum, thalamus and white matter [2]. A comparison of brain strain injury criteria is shown in Table 7-1. This study investigated the relationship between impact location, magnitude and direction and the subsequent strain in the central region of the brain. In particular the strain in the corpus callosum, thalamus, mid-brain and brain stem were investigated as these regions have been identified as '*hot spots*' related to concussive injuries [10].

Table 7-1: Finite element strain injury criteria

Region	Corpus Callosum		Mid-brain		Thalamus		Model
	No Injury	Concussive injury	No Injury	Concussive injury	No Injury	Concussive injury	
McAllister [8]		0.28					Dartmouth
Patton [11]	0.12	0.31	0.13	0.25	0.1	0.26	KTH FEHM
Viano [12]			0.23	0.34	0.21	0.38	WSUHIM

7.2 Method

7.2.1 Drop tests

An anthropomorphic head was dropped in a purpose built tower from a range of heights in a number of orientations to represent impacts to the front, rear and side of the head. The head was fitted with reference accelerometers and gyroscopes and data was gathered as described in Chapter 3 Section 3.2.

The tests consisted of 400 impacts in four locations, left occipital, right occipital, front and rear impacts to the head. The head form was dropped from 10 different heights from 160mm to 610mm and impacted a 120mm diameter steel hemisphere. Ten tests were completed at each height to investigate the repeatability of the devices, the results at each drop height were then averaged, see Table 7-2. Impacts at each height were also recorded using a high-speed camera at 2000 frames per second. Impact velocities were calculated from the video using motion tracking software.

Table 7-2: Average resultant peak accelerations measured for frontal impacts

Frontal Impacts				
Drop Height mm	Impact Energy Joules	Linear Acceleration g	Angular Velocity rad/s	Angular Acceleration rad/s/s
610	26.93	127.6	25.5	7426.5
560	24.72	108.8	25.2	7857.4
510	22.51	97.7	23.9	6570.7
460	20.31	85.2	23.1	7494.3
410	18.10	75.4	21.9	5786.9
360	15.89	62.8	20.1	5135.8
310	13.68	53.4	16.8	3930.6
260	11.48	42.9	16.1	3102.3
210	9.27	36.4	15.6	3289.9
160	7.06	30.9	14.0	3981.2

7.2.2 Simulation

The drop tests were simulated using the head portion of the GHBMC (Figure 7-1) as described in Chapter 6 Section 6.2.

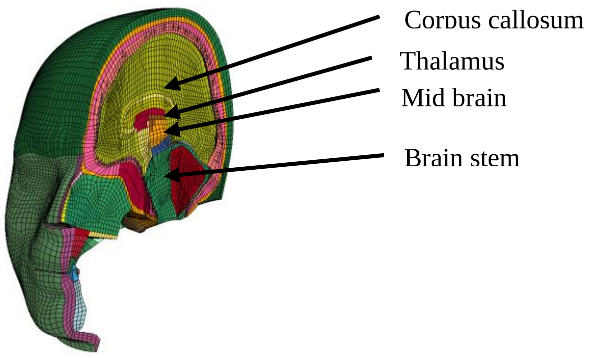

Figure 7-1: Head portion of the GHBMC model

Two sets of simulations were performed. The first set of simulations kept the energy of the impact constant (i.e. the same drop height) and the front, side and rear of the head were impacted. Six degree of freedom accelerations as recorded from the drop tests were applied to the centre of gravity of the model. Table 7-3 gives a summary of the resultant accelerations and the pressure and strain results from the simulations.

The second set of simulations kept the peak linear and angular accelerations the same, for impacts again, to the front, side and rear of the head-form. Accelerations in these cases were applied in two degrees of freedom as sinusoidal waveforms in the direction of the impact and about the principal plane of rotation (Table 7-4). The accelerations ranged from 30g and 2000rads/s^2 to 130g and 6000rads/s^2. This acceleration range was based on the accelerations reported to cause concussion in rugby and US football [13][14]. The profiles were determined by averaging the results of the head accelerations and time durations, acquired from the drop tests. Simulations were run for 30ms, thus ensuring that there was sufficient time to examine the brain's response to the impact.

Table 7-3: Acceleration and strain data from tests in which the impact energy was constant

Frontal Impact								
	Impact Energy	Linear Acceleration	Angular Acceleration	Corpus Callosum	Mid-brain	Brain Stem	Thalamus	Maximum Intracranial Pressure
	J	g	rad/s^2	Strain				kPa
Severe	26.9	128	7427	0.36	0.41	0.32	0.26	277
Serious	22.5	98	6571	0.21	0.34	0.29	0.23	194
Moderate	13.7	53	3931	0.16	0.26	0.16	0.14	107
Mild	7.1	31	3981	0.12	0.20	0.17	0.10	41
Lateral Impact								
Severe	26.9	150	7171	0.44	0.20	0.19	0.24	239
Serious	22.5	105	5020	0.31	0.15	0.16	0.17	199
Moderate	13.7	78	4267	0.24	0.12	0.14	0.15	152
Mild	7.1	31	2346	0.13	0.07	0.09	0.08	30
Rear Impact								
Severe	26.9	169	6292	0.22	0.29	0.26	0.23	214
Serious	22.5	124	5097	0.19	0.24	0.19	0.17	151
Moderate	13.7	87	3568	0.12	0.20	0.15	0.15	109
Mild	7.1	25	1819	0.05	0.09	0.07	0.08	52

Table 7-4: Acceleration data, for simulations where the same acceleration was applied in different directions

Acceleration Data					
Classification	**Impact number**	**Linear Acceleration**	**Duration of linear accel**	**Angular Acceleration**	**Duration of angular accel**
		g	ms	rad/s^2	ms
Severe	1	130	8	6000	6
	2	100	9	5300	7
	3	80	11	4500	8
	4	57	13	3500	9
	5	46	12	2670	10
Mild	6	30	15	2000	12

7. 3 Results

7.3.1 Constant Impact energy

The first set of results, where the impact energy remained constant, found that the peak linear impact accelerations were generally higher (up to 12%) during rear and lateral impacts of the head form compared to frontal impacts, the most severe lateral impact differed to this, see Table 7-3. The angular accelerations were also generally higher (up to 30%) in lateral and rear impacts when compared to frontal impacts. Following the most severe lateral impact (150g, 7171rad/s^2) the strain in the corpus callosum was 0.44, this reduced to 0.19 in the brain stem (Table 7-3). Strain in the mid-brain increased linearly as the impact energy increased. The mid-brain also experienced higher strains during frontal impacts, and the least strain during lateral impacts.

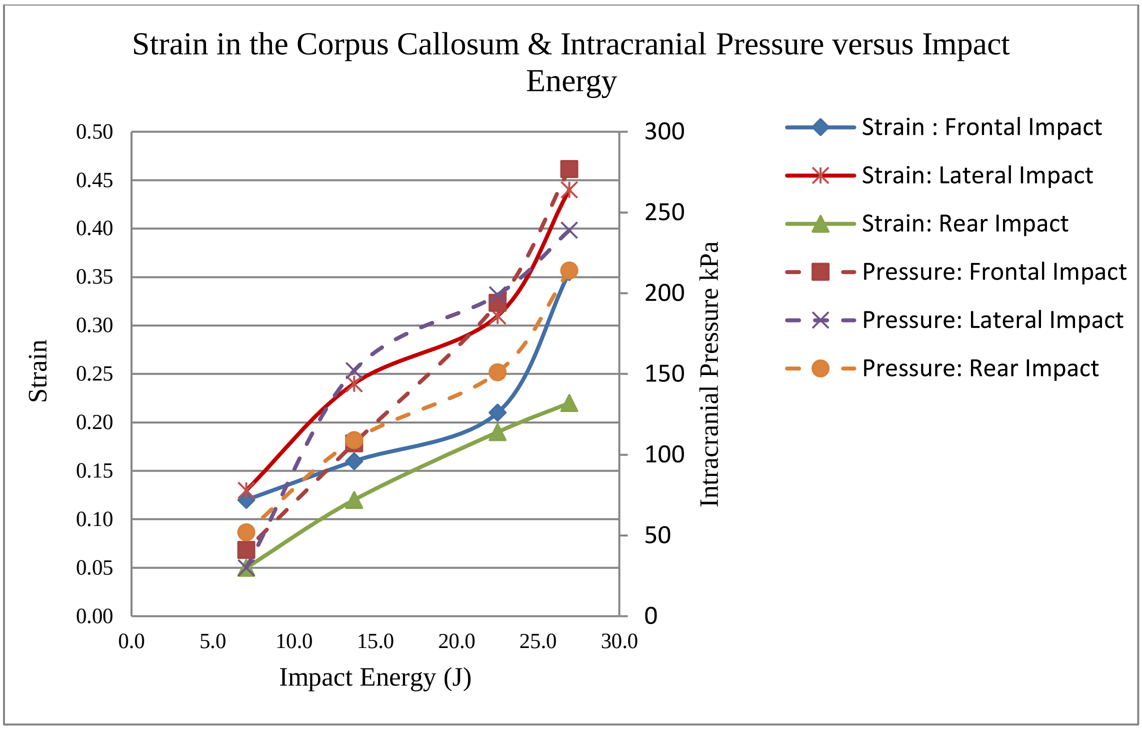

Figure 7-2: Strain and pressure in the corpus callosum

Intracranial pressure was also examined using these simulations (Figure 7-3). It was found to increase as impact energy increased and the maximum difference between pressure following impacts to different locations was 22%. Only the severest impact exceeded the limit of 235kPa for concussion, suggested by Ward et al.[15].

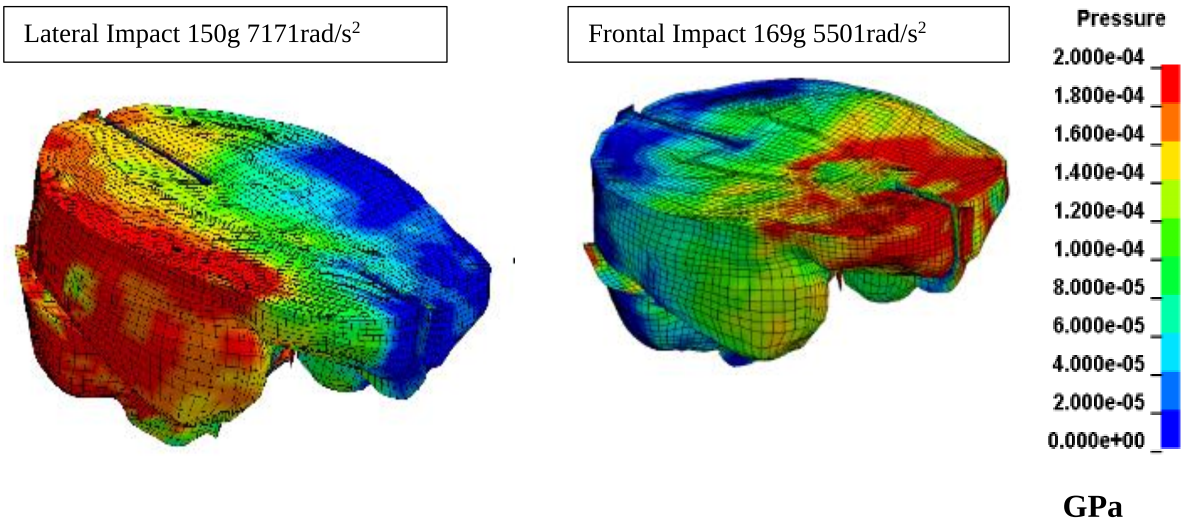

Figure 7-3: Pressure response following severe impact

7.3.2 Same acceleration profiles applied to different locations

The second set of results relate to simulations where the same acceleration profiles were applied to represent impacts to the front, rear and side of the head. Again, the strains in the corpus callosum and mid-brain were larger than in the thalamus or brain stem, see Figure 7-4. Frontal impacts resulted in higher strains (up to 0.35) in the mid-brain, than impacts from the other directions. Lateral impacts resulted in strains higher in the corpus callosum than in other brain regions. A maximum strain of 0.45 was recorded in the corpus callosum following a lateral impact of 130g and 6000rad/s^2, while a 0.24 strain was recorded following a frontal impact of the same magnitude, a difference in strain of 48%. On average, lateral impacts resulted in a strain increase of 43% in the corpus callosum compared to frontal impacts. The strain injury thresholds determined by Patton et al. [2] are shown in Figure 7-4. Following all severe and serious impacts these thresholds were met or exceeded in at least one of the brain regions investigated. The moderate impact indicated the possibility of an injury in the mid-brain during a frontal impact. Ward et al.'s pressure criterion was only exceeded in the most severe frontal impact: this would indicate that strain provides a lower threshold than pressure to indicate injury [15].

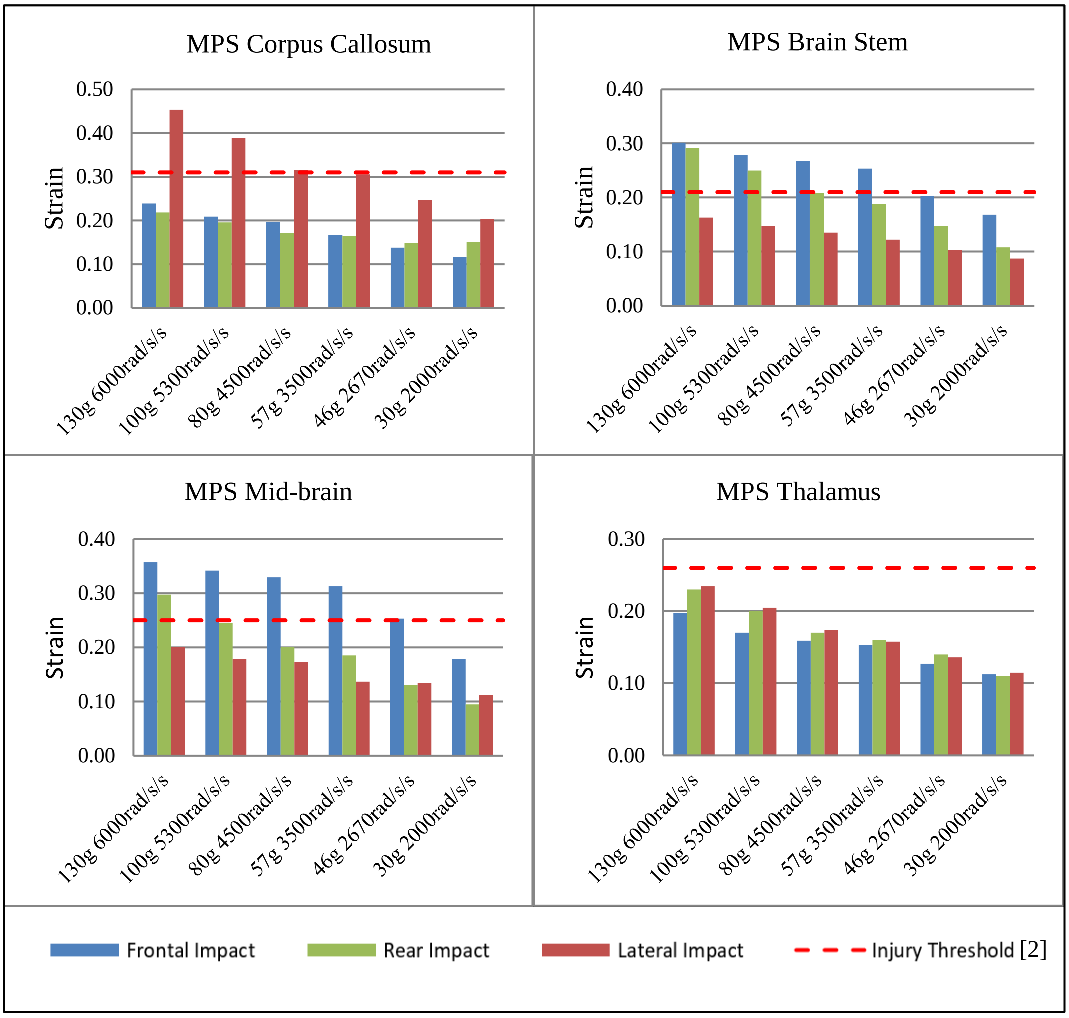

Figure 7-4: Maximum principal strain in different brain regions. Injury threshold from Patton et al. [2]

7.4 Discussion

The mechanism of concussion is not fully understood, since it is not possible to measure the response of a living brain following a severe impact to the head. Several studies have used animal models and scaled the effect to represent a human brain [6][16][17], while others have conducted cadaver studies [18][15]. Finite element (FE) simulations are an important tool to help understand the mechanical response of the brain. Using FE analysis it has been shown that increases in intracranial pressure are associated with linear accelerations, while shear strain and diffuse axonal injury (DAI) are associated with angular acceleration [6][9].

The simulation results, from the impact tests in which the impact energy was kept constant, indicate that only lateral impacts exceeded Patton et al's strain based criterion for injury within the corpus callosum [2]. The strain following a lateral impact was widely dispersed within the corpus callosum as shown in Figure 7-5.

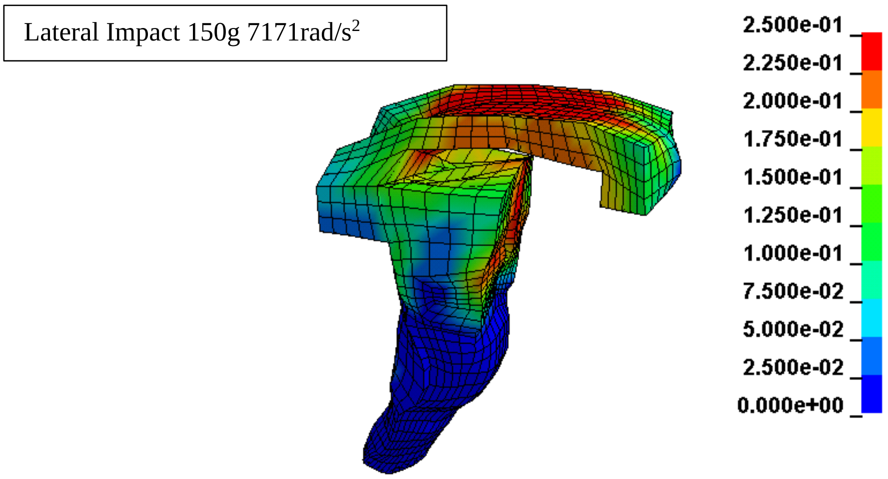

Figure 7-5: Maximum principal strain following a severe lateral impact

Elkin et al. also reported a significant increase in strain from lateral impacts in their study of head impacts in helmeted sports [19]. Angular acceleration in the coronal plane has also been shown to have a strong correlation with concussive injuries in un-helmeted sport, this is possibly due to an injury in the corpus callosum [11]. The corpus callosum plays a vital role in the brain's function as it is the communication hub between the left and right hemispheres and has been linked with traumatic brain injury [8]. The high strains in the corpus callosum may be partially explained by the movement of the corpus callosum, as it follows the motion of the skull more closely than the more compliant grey matter that surrounds it [7]. Previous studies which have examined the relationship between the falx and the corpus callosum have identified this region as mechanically vulnerable due to the connection between the longitudinal falx and corpus callosum [20]. It was found that the areas of high strain following lateral impacts are concentrated in the superior sections of the brain core. Strain was lower in brain regions located anatomically lower due to the tethering effect of the vascular, neural and dural elements that bind the brain to the base of the skull [7]. This study provides evidence that the regions anatomically closer to the centre of the brain (corpus callosum and thalamus) are more vulnerable during lateral impacts.

In contrast, front and rear impacts had a higher strain response than lateral impacts within the lower part of the brain structure (mid-brain and brain stem). This may be due to the stretching of the lower structures during the coup, contra coup response following a frontal or occipital impact [7]. An impact to the front of the head produced, on average, 47% and 37% more strain in the mid-brain than a lateral or rear impact, respectively. An analysis of the brain stem following a rear impact found that there was a noticeable strain response in the lower section of the brain stem during the initial phase of the impact. It was found that the strain response in the brain stem was due to the angular acceleration (the linear acceleration was removed and the simulation re-run). Strain based injuries such as diffuse axonal injury have been linked to angular acceleration [6][16][21], while linear acceleration is thought to be related to an increase in intracranial pressure and more focal injuries [22].

There is considerable variation in the linear and angular accelerations reported to cause concussion, this study found that accelerations of 57g and 3500rad/s^2 resulted in a 50% likelihood of concussion. The magnitude of the angular acceleration is similar to that found by Zhang et al. in their reconstruction of 24 cases of concussion in American football [9]. It must be borne in mind that the duration of impacts in US football is longer than those in this study and in unhelmeted sports. Duration of the acceleration pulse has been shown to influence the strain response [23]. Patton et al.'s study of head impacts in rugby found that impacts with angular accelerations as low as 1747rad/s^2 in the coronal plane may cause concussion [11]. This contrasts with Margulies et al.'s study which used porcine models to determine that angular accelerations above approximately 9,000rad/s^2 would cause a moderate to severe DAI, but they do acknowledge that accelerations much lower than this may cause a concussion [6].

This study has shown that the mid-brain and the superior area of the brain stem are 'hot spots' for strain during frontal and rear impacts (Figure 7-6), this is similar to a finite element study which recreated 25 cases of concussion US football impacts [12]. This is significant as studies which have analysed head impacts in American Football determined that the highest numbers of impacts are sustained to the front of the head [24]. Blurred vision and motor control have been reported to be common symptoms of concussive injuries within American football [25]; these symptoms may relate to the role the mid-brain plays in the central nervous system. This study also found that moderate (Table 7-3) lateral impacts causing rotation in the coronal plane are likely to cause injury, these are of particular importance in unhelmeted sports as 50% of concussions are reported to occur following this type of impact [26].

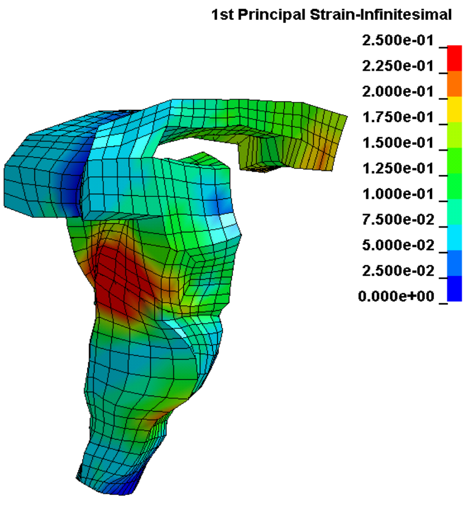

Figure 7-6: Maximum principal strain following a severe frontal impact

These simulations indicate that the impact location is significant in determining the brain region affected and extent of any injury that may be sustained.

7.5 Conclusion

This study analysed the effect of impact location on the resulting strain response within the central region of the brain. The study simulated six degree of freedom drop tests in which impact energy was kept constant, but impact location was varied. This investigation found that impact location was significant. To investigate this further impacts to three locations were simulated, the same accelerations in two directions being applied to each location.

The study found that the superior regions of the brain (corpus callosum and thalamus) produced a higher strain response during lateral impacts while the inferior regions (mid-brain and brain stem) produced a higher strain response following frontal and rear impacts. The study highlights the need to consider the location of the impact as a parameter when analysing brain injuries due to a head impact.

Limitations

The head model only represents the 50th percentile male, it is also only partially validated using human cadaver tests. Published injury thresholds vary widely and a precise injury threshold has not yet been determined.

7.6 References

[1] A. Post, T. Blaine Hoshizaki, M. D. Gilchrist, and M. D. Cusimano, "Peak linear and rotational acceleration magnitude and duration effects on maximum principal strain in the corpus callosum for sport impacts," *J. Biomech.*, vol. 61, pp. 183–192, 2017.

[2] D. A. Patton, A. S. McIntosh, S. Kleiven, and T. E, "The Biomechanical Determinants of Concussion : Finite Element Simulations to Investigate Brain Tissue Deformations During Sporting Impacts to the Unprotected Head," *J. Appl. Biomech.*, vol. 29, pp. 721–730, 2013.

[3] N. Yoganandan, J. Li, J. Zhang, F. A. Pintar, and T. A. Gennarelli, "Influence of angular acceleration – deceleration pulse shapes on regional brain strains," *J. Biomech.*, vol. 41, pp. 2253–2262, 2008.

[4] A. Bain and D. Meaney, "Tissue-Level Thresholds for Axonal Damage in an

Experimental Model of Central Nervous System White Matter Injury," *J. Biomech. Eng.*, vol. 122, no. 6, p. 615, 2000.

[5] K. Laksari, F. Hernandez, J. R. Lopez, A. R. Hoffman, G. A. Grant, D. Camarillo, *et al.*, "Six Degree-of-Freedom Measurements of Human Mild Traumatic Brain Injury," *Ann. Biomed. Eng.*, vol. 43, no. 8, pp. 1918–1934, 2014.

[6] S. S. Margulies and L. E. Thibault, "A proposed tolerance criterion for diffuse axonal injury in man," *J. Biomech.*, vol. 25, no. 8, pp. 917–923, 1992.

[7] A. A. Sabet, E. Christoforou, B. Zatlin, G. M. Genin, P. V. Bayly, V. Philip, *et al.*, "Deformation of the human brain induced by mild angular head acceleration," *Computer (Long. Beach. Calif).*, vol. 41, no. 2, pp. 307–315, 2008.

[8] T. McAllister, J. Ford, B. Jonathan, L. A. Flashman, K. Paulsen, and R. M. Greenwald, "Maximum Principal Strain and Strain Rate Associated with Concussion Diagnosis Correlates with changes in Corpus Callosum White Matter Indices," *Ann Biomed Eng.*, vol. 40, no. 1, pp. 127–140, 2012.

[9] L. Zhang, K. Yang, and A. King, "A proposed injury threshold for mild traumatic brain injury," *J Biomech Eng*, vol. 126, no. 2, pp. 226–236, 2004.

[10] Viano, I. Casson, and E. Pellman, "Concussion in professional football: Brain responses by finite element analysis: Part 9," *Neurosurgery*, vol. 57, no. 5, pp. 891–915, 2005.

[11] A. S. McIntosh, D. a Patton, B. Fréchède, P.-A. Pierré, E. Ferry, and T. Barthels, "The biomechanics of concussion in unhelmeted football players in Australia: a case-control study.," *BMJ Open*, vol. 4, no. 5, p. e005078, 2014.

[12] D. C. Viano, I. R. Casson, E. J. Pellman, L. Zhang, A. I. King, and K. H. Yang, "Concussion in professional football: Brain responses by finite element analysis: Part 9," *Neurosurgery*, vol. 57, no. 5, pp. 891–915, 2005.

[13] B. B. Reynolds, J. Patrie, E. J. Henry, H. P. Goodkin, D. K. Broshek, M. Wintermark, *et al.*, "Quantifying Head Impacts in Collegiate Lacrosse," *Am. J. Sports Med.*, vol. 44, no. 11, pp. 2947–2956, 2016.

[14] B. B. Reynolds, J. Patrie, E. J. Henry, H. P. Goodkin, D. K. Broshek, M. Wintermark, *et al.*, "Practice type effects on head impact in collegiate football.," *J. Neurosurg.*, vol. 124, no. 2, pp. 501–10, 2015.

[15] A. M. Nahum, R. Smith, and C. C. Ward, "Intracranial Pressure Dynamics During Head Impact," *21st Stapp Car Crash Conf.*, 1977.

[16] A. C. Bain, D. F. Meaney, and H. Hall, "Tissue-Level Thresholds for Axonal Damage in an Nervous System White Matter Injury," vol. 122, no. December, 2000.

[17] D. F. Meaney, D. H. Smith, D. I. Shreiber, C. Allison, R. T. Miller, D. T. Ross, *et al.*, "Experimental Injury," *J. Comput. Assist. Tomogr.*, vol. 12, no. 4, 1995.

[18] W. N. Hardy, M. J. Mason, C. D. Foster, C. S. Shah, J. M. Kopacz, H. Yang, *et al.*, "A study of the response of the human cadaver head to impact," *Stapp Car Crash J*, vol. 51, pp. 17–80, 2008.

[19] B. S. Elkin, L. F. Gabler, M. B. Panzer, and G. P. Siegmund, "Brain tissue strains vary with head impact location: A possible explanation for increased concussion risk in struck versus striking football players," *Clin. Biomech.*, no. 2017, 2018.

[20] F. Hernandez, C. Giordano, M. Goubran, S. Parivash, G. Grant, M. Zeineh, *et al.*, "Lateral impacts correlate with falx cerebri displacement and corpus callosum trauma in sports-related concussions," *Biomech. Model. Mechanobiol.*, no. 0123456789, 2019.

[21] A. Post and T. Blaine Hoshizaki, "Rotational Acceleration, Brain Tissue Strain, and the Relationship to Concussion," *J. Biomech. Eng.*, vol. 137, no. 3, p. 030801, 2015.

[22] A. King, K. Yang, and L. Zhang, "Is head injury caused by linear or angular acceleration," *IRCOBI Conf.*, no. September, pp. 1–12, 2003.

[23] G. M. Kendall, Marshall, Post, Andrew, "A Comparison of dynamic impact response and brain deformation metrics within the cerebrum of head impact reconstructions representing three mechanisms of head injury in ice hockey.," *Int. Res. Counc. Biomech. Inj.*, 2012.

[24] C. A. Taylor, J. M. Bell, M. J. Breiding, and L. Xu, "Traumatic Brain Injury–Related Emergency Department Visits, Hospitalizations, and Deaths — United States, 2007 and 2013," *MMWR. Surveill. Summ.*, vol. 66, no. 9, pp. 1–16, 2017.

[25] E. Pellman, D. Viano, A. M. Tucker, I. Casson, A. B. Valadka, J. C. Maroon, *et al.*, "Concussion in Professional Football: Location and Direction of Helmet Impacts - Part 2," *Neurosurgery*, vol. 53, no. 6, pp. 1328–1341, 2003.

[26] A. S. McIntosh, P. McCrory, and J. Comerford, "The dynamics of concussive head impacts in rugby and Australian rules football," *Med Sci Sport. Exerc*, vol. 32, no. 12, pp. 1980–1984, 2000.

Chapter 8

Finite Element Simulation of Head Impacts in Mixed Martial Arts

Abstract

Thirteen MMA athletes were fitted with the MiG2.0 Stanford instrumented mouthguard. 451 video confirmed impacts were recorded during sparring sessions and competitive events. The competitive events resulted in five concussions. The impact with the highest angular acceleration from each event was simulated using the GHBMC head model. Average strain in the corpus callosum of concussed athletes was 0.27, which was 87.9% higher than uninjured fighters and was the best strain indicator of concussion. The best overall predictor of concussion found in this study was shear stress in the corpus callosum which differed by 111.4% between concussed and uninjured athletes.

Published: *S. Tiernan, D. O'Sullivan, A. Meagher, E. Kelly, "Finite Element Simulation of Head Impacts in Mixed Martial Arts," Comput Methods Biomech Biomed Engin. Methods. Sept. 2020.*
DOI: 10.1080/10255842.2020.1826457

This chapter is a reproduction of the published paper with the following exceptions:

- The introduction and methods sections of this chapter have been to reduce the duplication of information. The background information is covered in the literature review in Chapter 2 and the method used to capture acceleration data using instrumented mouthguards is described in Chapter 5.
- The description of the FE model and the method used to apply boundary conditions and post process results is described in Chapter 6.

- Section 8.3.1 has been added which gives simulation results of the concussion cases.

8.1 Introduction

Generally, kinematic data is used to define the boundary conditions for simulation models. To determine the kinematics of head impacts in US football Newman et al. recreated 27 impacts in a laboratory [1]. It has been reported that there is a significant correlation between strain and concussive symptoms [2]. Several researchers have used this data with simulation models to find the average strain in various brain regions of concussed athletes or the strain that related to a 50% probability of concussion. In US football a 50% probability of concussion has been reported for strains in the corpus callosum from 0.13 [3] to 0.21 [4]. The average strain in the corpus callosum of concussed Australian rules football and rugby players was found to be 0.31 [5][6]. High strains in the corpus callosum are thought to be due to lateral distortions of the falx, caused by high coronal angular accelerations [7].

Strain rate has also been found to be associated with the risk of concussion. Strain rates of $48.5s^{-1}$ [4] and $60s^{-1}$ [8] have been related to a 50% probability of concussion.

8.2 Method

Head impact acceleration data was collected during MMA sparring sessions and competitive events using the Stanford instrumented mouthguard MiG2.0 as described in Chapter 5. Figure 8-1 shows the linear and angular accelerations of a typical head impact. Simulations were performed by applying linear and angular accelerations about the 3 axes of the local co-ordinate system at the centre of gravity of the GHBMC head model as described in Chapter 6.

Simulation results were divided into the two categories: concussed and uninjured. The acceleration, strain and shear stress results in each category were then averaged.

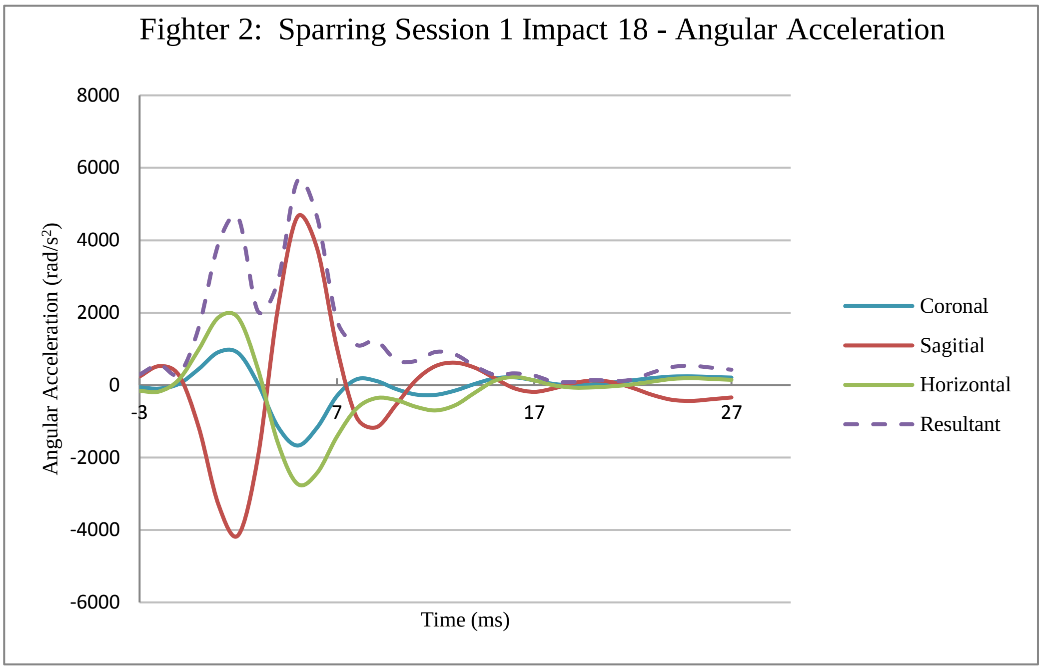

Figure 8-1: Typical head acceleration data collected by instrumented mouthguard

8.2.1 Statistical Analysis

Descriptive statistics including means, standard deviations and t-tests were processed using MiniTab (Version 19.2020). A two sample independent t-test was used to compare concussive and uninjured data. The dependant variable was concussion/uninjured while the continuous variables were resultant linear acceleration, resultant angular velocity, resultant angular acceleration, strain in the corpus callosum, thalamus, mid-brain and brain stem, Tresca shear stress in the corpus callosum, and strain rate in the corpus callosum. A statistical significance of $p < .05$ was used to reject the null hypothesis. Cohen's effect sizes were calculated to quantify the magnitude of the differences between the concussion injury data and the uninjured data. Cohen's number (d) defines the effect sizes as $d < 0.01$ very small, $d < 0.2$ small, $d < 0.5$ medium, $d < 0.8$, large, $d < 1.2$ very large, and $d > 2.0$ huge [9].

8.3 Results

Data was recorded during 19 sparring sessions and 11 competitive events. Above 10g, 298 confirmed head impacts were recorded during the sparring sessions and 153 impacts at the competitive events. The average number of impacts above 10g in the sparring sessions was 15.7. No injuries occurred during the sparring sessions. Five of the competitive events resulted in the fighter sustaining a concussion, all five fighters were professional or semi-professional and were in weight categories above 70kg. The concussions were diagnosed by a medical doctor either immediately after the event or at a 48 hour check-up. Symptoms reported included: a very short loss of consciousness (< 1 second), persistent headaches in the days following the event, visual disturbance and imbalance. The number of impacts in the events that ended with a concussion ranged from 4 to 26. The number of impacts in fights that ended with a concussion ranged from 4 to 26 with an average of 16.0 impacts, while the average number of impacts in competitive events that had no injury was 12.2.

A simulation was performed of the impact with the highest resultant angular acceleration from each of the 30 events. Maximum strain in the corpus callosum, thalamus, mid-brain, brain stem and overall (any brain region) were recorded from the simulations. Also recorded were the shear stress (Tresca), Von Mises distortion stress and strain rate within the corpus callosum. Maximum principal strain and stress results were averaged and are plotted in Figure 8-2 and 8-3.

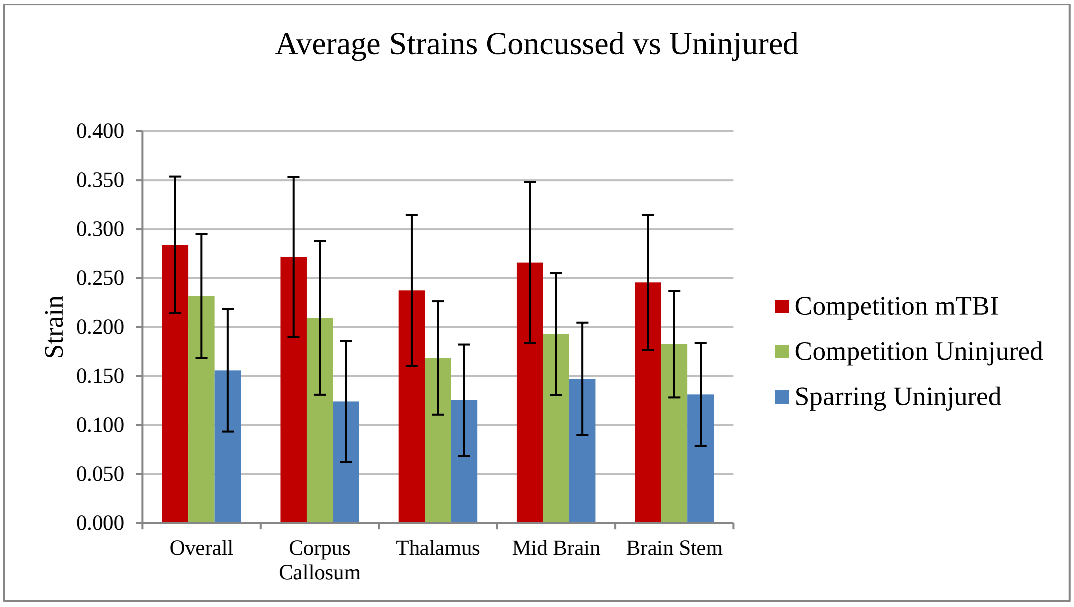

Figure 8-2: Average strains with standard deviation in various brain regions

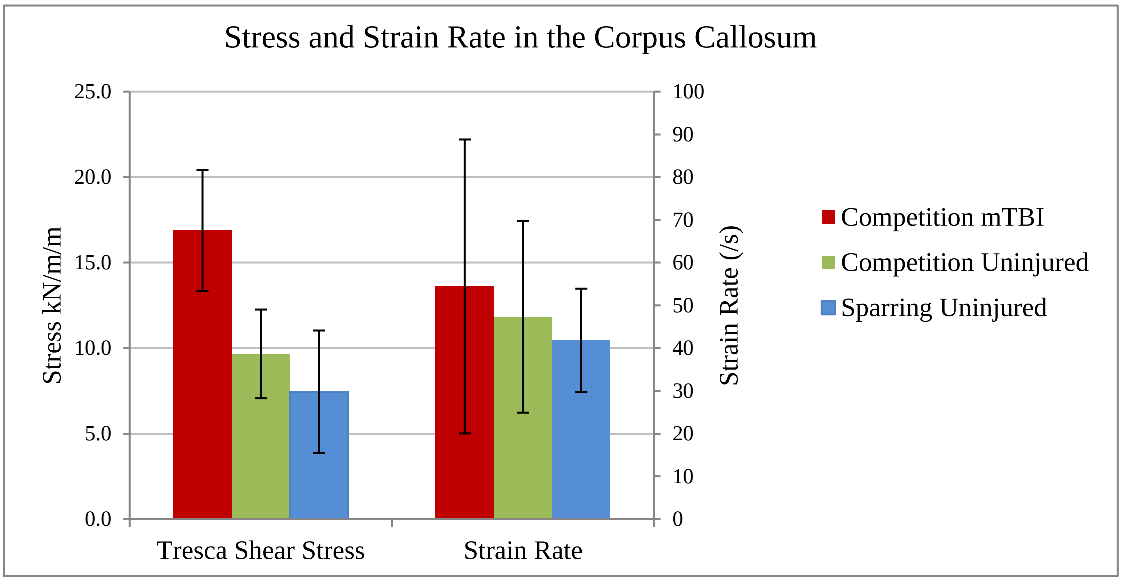

Figure 8-3: Stress and strain rate with standard deviation in the corpus callosum

The statistical differences between the concussed and uninjured athletes was investigated using independent sample t-tests (shown in Table 8-1). T-tests showed significant differences in the resultant linear acceleration, $t(4) = 2.9$, $p < .05$, $d = 1.4$ (very large effect size), strain in the corpus callosum $t(4) = 2.9$, $p < .05$, $d = 1.51$ (very large effect size), strain in the brain stem $t(4) = 2.8$, $p < .05$, $d = 1.49$ (very large effect size), and the shear stress in the corpus callosum t(5) = 4.7, $p < .05$, d = 2.36 (huge effect size). The effect size is quoted as per Sawilowsky et al.'s recommendation [9]. There was no other significant difference between concussed and uninjured athletes in the resultant angular velocity, resultant angular acceleration, strain in the thalamus and mid brain, and the strain rate in the corpus callosum.

Table 8-1: Results of statistical t-tests between concussed and uninjured athletes

	Resultant Linear Acceleration	**Resultant Angular Velocity**	**Resultant Angular Acceleration**	**Corpus Callosum**	**Thalamus**	**Mid-Brain**	**Brain Stem**	**Tresca Shear Stress in Corpus Callosum**	**Strain Rate in Corpus Callosum**
	(g)	(rad/s)	(rad/s^2)	Strain				kPa	s^{-1}
Competition concussed	**86.7**	24.0	7561	**0.27**	0.24	0.27	**0.25**	**16.87**	54.40
Standard Deviation concussed	**21.0**	4.7	1825	**0.08**	0.06	0.06	**0.06**	**3.57**	13.70
Average Uninjured	**56.8**	13.6	5169	**0.14**	0.14	0.16	**0.14**	**7.98**	45.05
Standard Deviation uninjured	**21.6**	10.7	3843	**0.09**	0.09	0.09	**0.08**	**3.94**	38.40
Difference in Averages	**52.7%**	76.7%	46.3%	**87.9%**	75.0%	68.1%	**71.2%**	**111.4%**	20.8%
t value	**2.9**	2.1	1.4	**2.9**	2.5	2.5	**2.8**	**4.7**	0.5
p value	**0.034**	0.1	0.245	**0.033**	0.066	0.067	**0.049**	**0.005**	0.619
Effect size (d)	**1.40**	1.26	0.80	**1.51**	1.36	1.37	**1.49**	**2.36**	0.32

NB: Significant differences ($p < .05$) are in bold

Figure 8-4 shows sample transverse and sagittal cross sections of the simulated brain strain of Fighter 5, Bout 1, impact 21 who was concussed. High strains are evident in the corpus callosum and thalamus. The high strains on the periphery of the brain are in the cerebrospinal fluid (CSF), hence they are not actual strains in the brain tissue. The strains in the CSF are due to the fluid being modelled with solid elements with the bulk modulus of water. Figure 8-5 shows cross sections of an uninjured athlete (Fighter 10, Bout 1 impact 50).

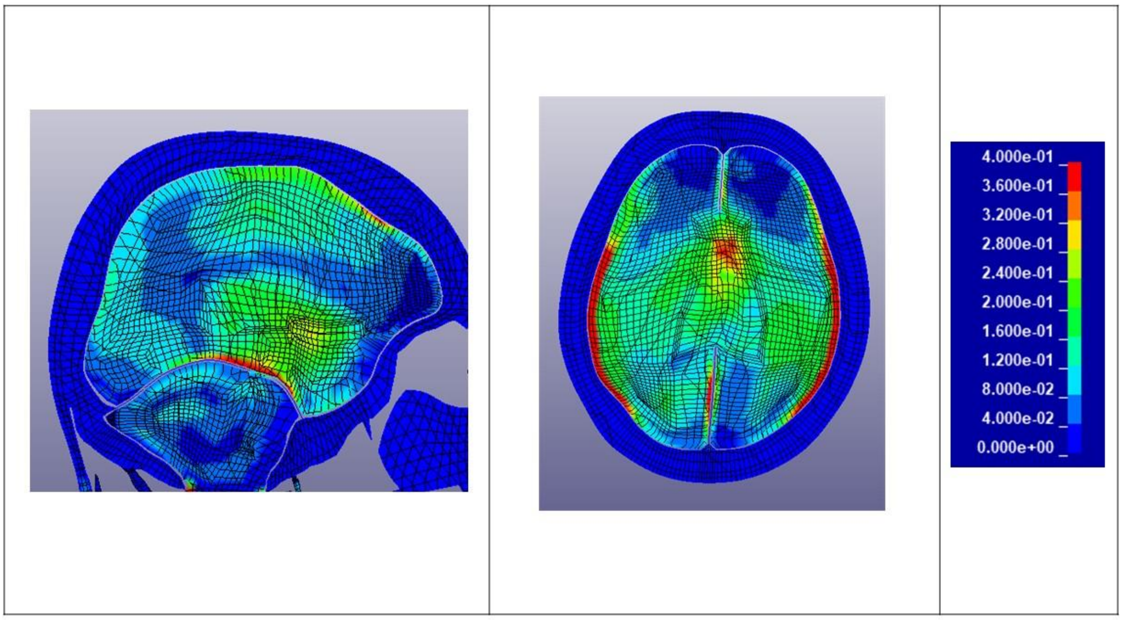

Figure 8-4: Transverse and Sagittal cross sections: Strain plots – Fighter 5 Bout 1 Impact 21 – Concussed

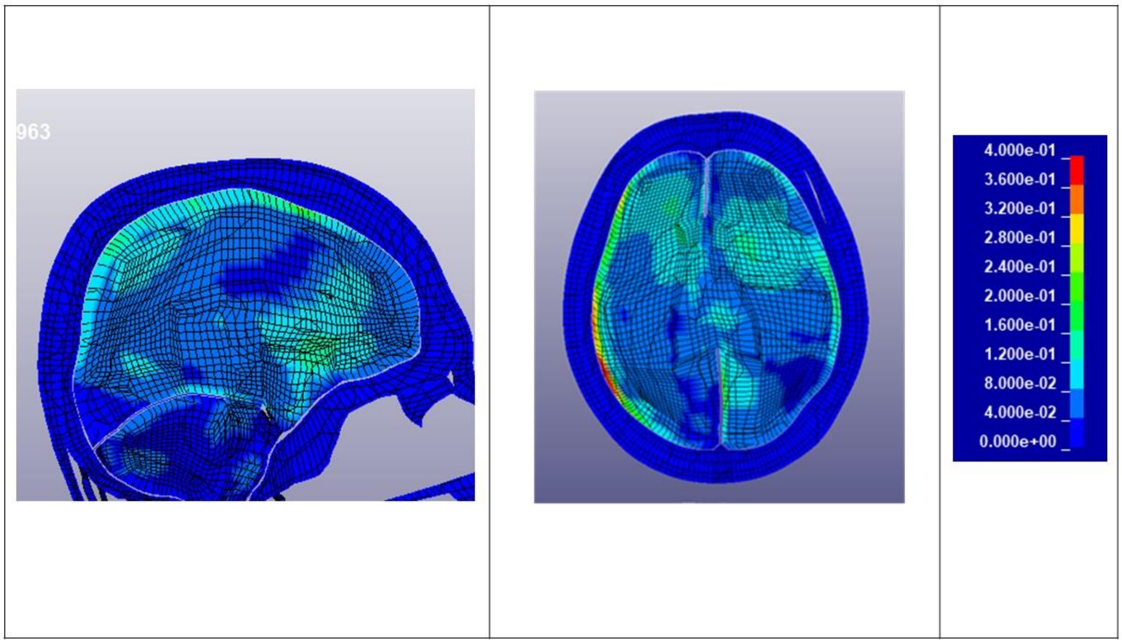

Figure 8-5: Transverse and Sagittal cross sections: Strain – Fighter 10 Bout 1 Impact 50 – Uninjured

8.3.1 Simulation of the concussion cases

The following are the results from the simulations of the impact with the highest angular acceleration from each vent that ended in concussion. The kinematics of each of these events is in Chapter 5 Table 5-6. Table 8-2 gives the stress and strain results for each case.

Table 8-2: Results of statistical t-tests between concussed and uninjured athletes

	Overall Maximum Strain	Strain Corpus Callosum	Thalmus	Mid Brain	Brain Stem	Tresca Shear kN/m/m	Von Mises kN/m/m	Strain Rate in CC /s	Strain rate x strain CC /s
F1 B1 H71	0.17	0.128	0.122	0.15	0.158	11.66	12.7	38	4.864
F2 B1 H9	0.31	0.35	0.26	0.29	0.30	18.50	32.11	89.00	31.15
F3 B1 H56	0.24	0.24	0.175	0.19	0.18	13.68	21.97	52	12.48
F4 B1 H53	0.35	0.29	0.32	0.35	0.25	21.11	36.60	93.00	26.97
F5 B1 H21	0.35	0.34	0.31	0.35	0.34	19.4	34.6	147	49.98

Figure 8-6 to Figure 8-10 show images of the strain from each of the concussive events and also the blood brain barrier (BBB) disruption from each fighter pre and post event is shown. The analysis of the BBB was carried out by the project collaborators at St James's Hospital and Trinnity College Dublin. Note that the scale used for BBB disruption is a normalised value for the permeability of the tissue. This was obtained by determining a normal permeability from non-contact sports athletes. Brain voxels with values higher than this normal are coloured in increasing intensities of red. Details of the BBB investigation have been published by O'Keeffe et al. [10].

In Case 1 and Case 4 there is considerable BBB disruption pre-event this may be the result of previous concussions. Case 1 had 4 previous concussions whereas Case 4 has had one. This prior history of concussion may have been the reason for the injury in Case 1 as the strain would not have indicated an injury. The magnitude of the maximum principal strain was found to correlated (R^2 = 0.84) with the volume fraction of BBB disruption but the location of the maximum strain did not correspond to the location of BBB disruption.

Case 1: Fighter 1 Bout 1 Impact 71

Strain		
Transverse Section	**Sagittal Section**	**Strain Scale**
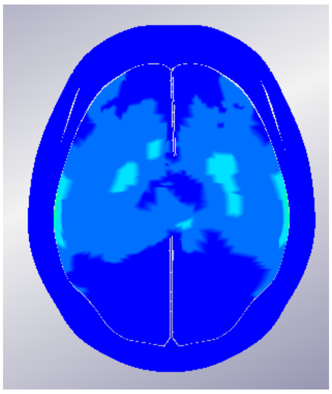	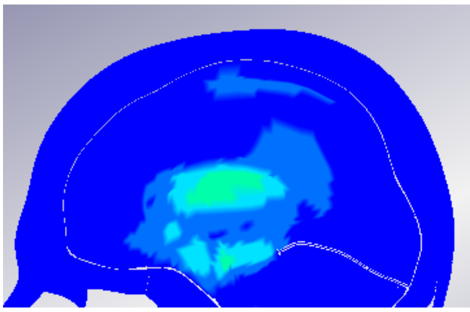	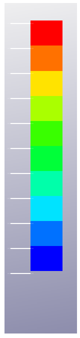
Contrast MRI*		
Baseline	**48 hours Post Injury**	**BBB Disruption Scale**
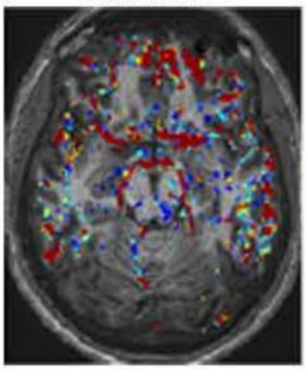	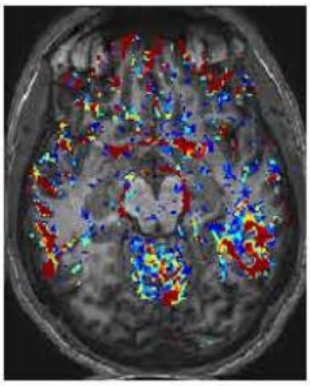	

Figure 8-6: Strain and blood brain barrier disruption for Case 1

Case 2: Fighter 2 Bout 1 Impact 9

<table>
<tr><th colspan="3">Strain</th></tr>
<tr><th>Transverse Section</th><th>Sagittal Section</th><th>Strain Scale</th></tr>
<tr><td>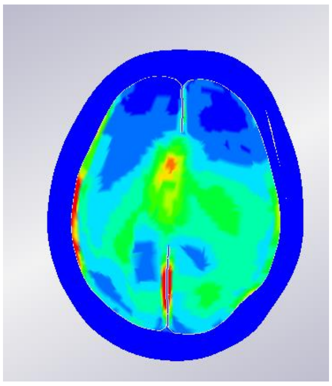</td><td>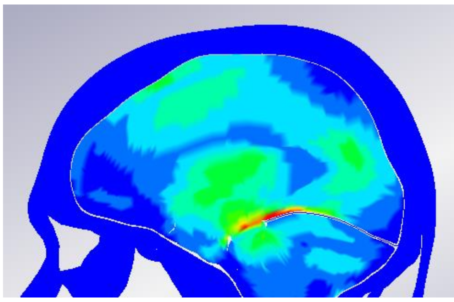</td><td>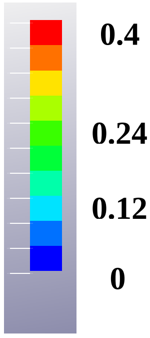</td></tr>
<tr><th colspan="3">Contrast MRI*</th></tr>
<tr><th>Baseline</th><th>48 hours Post Injury</th><th>BBB Disruption Scale</th></tr>
<tr><td>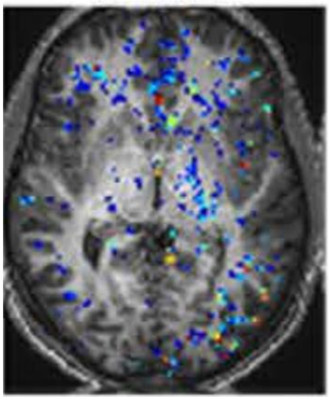</td><td>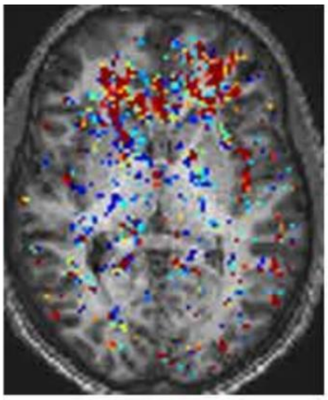</td><td>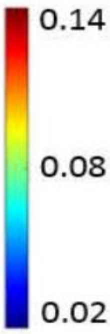</td></tr>
</table>

Figure 8-7: Strain and blood brain barrier disruption for Case 2

Case 3: Fighter 3 Bout 1 Impact 56

Strain		
Transverse Section	**Sagittal Section**	**Strain Scale**
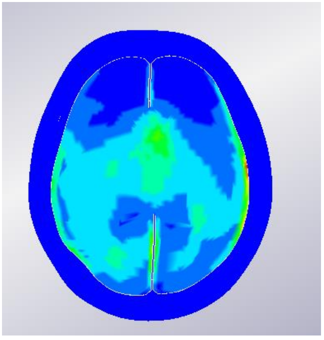	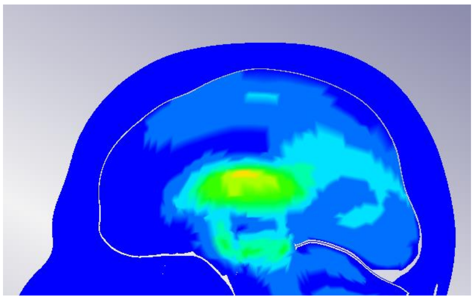	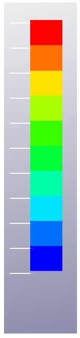 0.4 0.24 0.12 0
Contrast MRI*		
Baseline	**120 hours Post Injury**	**BBB Disruption Scale**
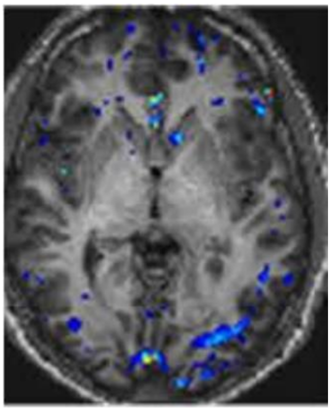	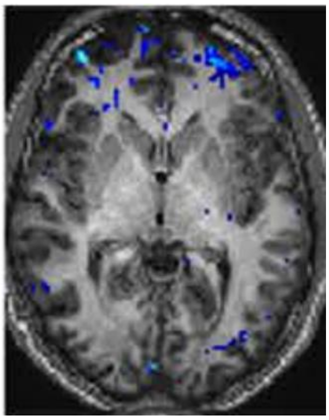	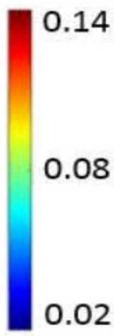

Figure 8-8: Strain and blood brain barrier disruption for Case 3

Case 4: Fighter 4 Bout 1 Impact 53

Strain		
Strain – Transverse Section	**Strain – Sagittal Section**	**Strain Scale**
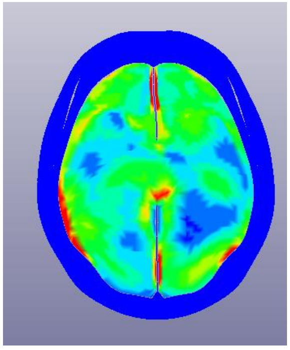	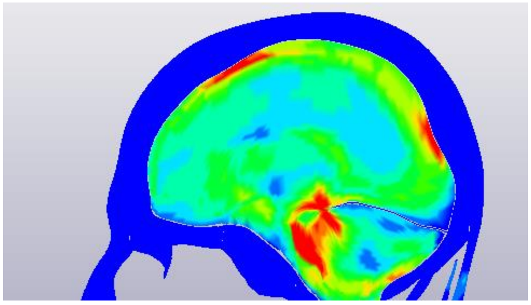	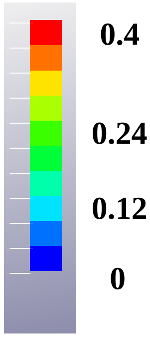
Contrast MRI*		
Baseline	**18 hours Post Injury**	**BBB Disruption Scale**
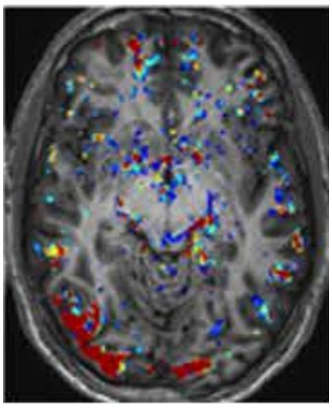	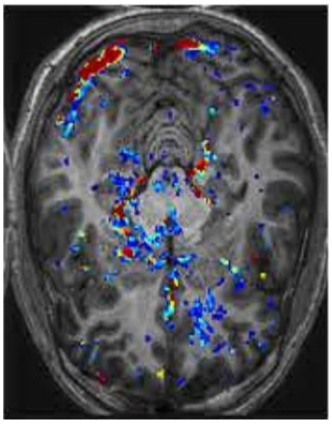	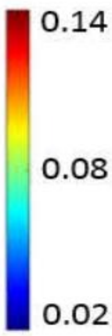

Figure 8-9: Strain and blood brain barrier disruption for Case 4

Case 5: Fighter 5 Bout 1 Impact 21

Strain		
Transverse Section	**Sagittal Section**	**Strain Scale**
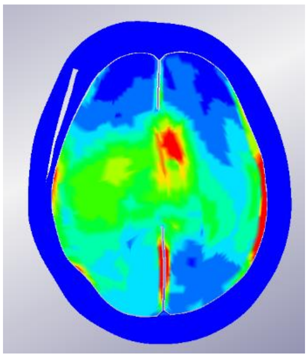	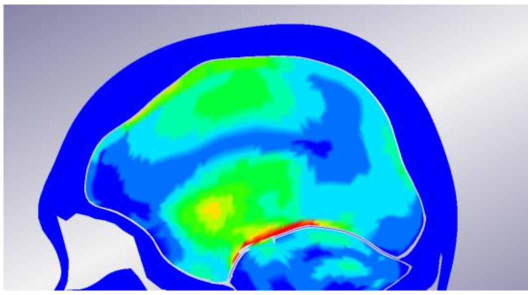	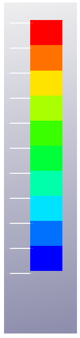 0.4 0.24 0.12 0
Contrast MRI*		
Baseline	**18 hours Post Injury**	**BBB Disruption Scale**
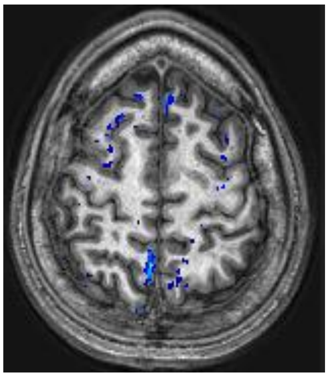	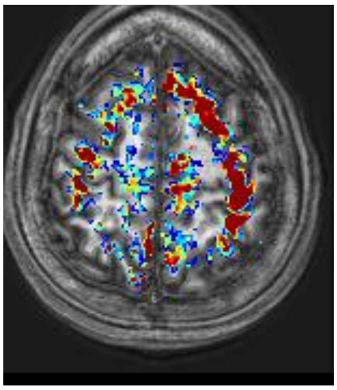	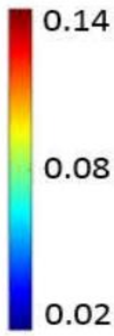

Figure 8-10: Strain and blood brain barrier disruption for Case 5

* Contrast MRI and BBB disruption analysis was carried out by St James's Hospital and the Genetics Department at Trinity college Dublin and is published by O'Keeffe et al. [10].

8.4 Discussion

Head acceleration data was recorded from 451 video confirmed impacts in MMA at 30 events. This is the only known study to measure head accelerations *in vivo* that have resulted in a concussive injury in an unhelmeted sport. The impact with the highest resultant angular acceleration from each event was simulated using the GHBMC head model. Linear accelerations to the side of the head (Y direction) were 62.2% higher in impacts that resulted in a concussive injury. Punches to the jaw create high lateral accelerations and due to the offset from the head's centre of gravity this leads to high angular accelerations about the X axis (coronal plane). Viano et al. studied boxers punching a Hybrid III head and found that 'hook' type punches lead to high moments about the X axis and very high angular accelerations [11]. Impacts to the side of the head have been found to correlate with concussive injuries [12][6][13].

In this study, linear acceleration, strain in the corpus callosum and brain stem and shear stress in the corpus callosum were significantly different ($p < .05$) between concussed and uninjured athletes. In this study, the strain in the corpus callosum differed by 87.9% ($p < .05$) between concussed and uninjured athletes. This difference in strain in the corpus callosum was greater than any other brain region indicating that it may be the best strain indicator for concussion. The average strain in the corpus callosum of the concussed athletes was 0.27; this compares well with the strain of 0.3 found by Hernandez et al. in US football, although it should be noted that Hernandez's study only included 2 cases of concussion [14]. Newman et al. reconstructed 58 impacts in US football and determined that the average linear and angular accelerations of concussed players was 97.8g and 6432rad/s^2 [15][1]. Kleiven simulated Newman's impacts and determined that the average strain in the corpus callosum of the concussed players was approximately 0.23 and predicted a 50% probability of concussion for a strain of 0.21 [4]. Kleiven reported an average strain in the corpus callosum which was 28.6% lower than that found in this study but also reported an average angular acceleration which was 17.6% lower. Sanchez et al. found that there was an error in some of the accelerometer data in Newman et al.'s study which may have resulted in an average error in the maximum principal strain of 23% [16].

In a simulation study of concussion in an unhelmeted sport, kinematic data from computer reconstructions was used to simulate impacts in Australian rugby and football [5]. Patton et al. found that the average angular acceleration in concussive impacts was 7951rad/s^2 [5] which is similar to the average angular acceleration of 7561rad/s^2 found in this study. Although the angular acceleration was similar, Patton's average strain of 0.31 ± 0.16 in the corpus callosum was 14.8% higher than in this study. Patton et al's study had a wider spread of data than this study as indicated by his standard deviation of 0.16. The greater spread of data in Patton's study may be due to the variation in magnitude and direction of impacts inherent in football as opposed to MMA and the methods employed in the re-creation of the impacts.

Shear stress in the corpus callosum differed between concussed and uninjured athletes by 111.4% with a huge effect size (2.36) [9]. This indicates that shear stress, in this study, was the best parameter to predict a concussive injury, followed by the strain in the corpus callosum. Shear stress has been reported in very few studies of concussion. A US football study [17] reported that the shear stress in the mid-brain was the best predictor of concussion. They found that shear stress in the thalamus differed by 58.5% between concussed and uninjured athletes, but they did not report on the magnitude of the shear stress in the corpus callosum.

The best injury predictor was found to be strain in the corpus callosum as a threshold value of 0.24 would have resulted in 1 false negative and 2 false positives. This was the least number of false positives and negatives that could be obtained from any parameter investigated using the data in this study. For example, a shear stress threshold value of 12.5kPa would have resulted in 1 false negative and 3 false positives whereas a Von Mises stress threshold value of 20kPa would have resulted in 1 false negative and 4 false positives.

The comparison of the strain result and the BBB investigation found that the magnitude of the maximum principal strain correlated (R^2 = 0.84) with the volume fraction of BBB disruption but the location of the maximum strain did not correspond to the location of BBB disruption [10].

8.5 Conclusion

This is the first known study to measure head accelerations *in vivo* in an unhelmeted sport, which included five concussions. The study found significant differences ($p < .05$) in the strain in the corpus callosum, and brain stem of concussed athletes compared to uninjured. The magnitude of the strain in the corpus callosum was higher than in concussed athletes in a US football study due to a higher average angular acceleration. The single best predictor of concussion in this study was shear stress in the corpus callosum ($t(5) = 4.7$, $p < .05$, $d = 2.36$). The high strains and shear stresses in the core brain regions were primarily due to lateral impacts which resulted in high angular accelerations in the coronal plane.

Limitations

The number of fighters and events in this study was limited - a greater number of impacts are required to improve the robustness of these findings. The mouthguard has been validated for indirect impacts but further validation is required for impacts directly to the sensors. Impacts that could not be video verified and impacts that appeared to be direct hits to the mouthguard were removed; this may have resulted in some valid data not being included. The GHBMC head model has limitations inherent in finite element models and the material properties are approximations for brain tissue and assume homogeneous and isotropic behaviour. One of the criteria used to validate the GHBMC head model is relative brain-skull motion [18]. Zhou et al. have suggested that this may not be sufficient for models intended for strain prediction [19]. The cerebrospinal fluid in the brain was modelled with solid elements with the bulk modulus of water. The concussed fighters received multiple impacts during their bouts therefore it is not possible to identify which impact caused the injury.

8.6 References

[1] J. Newman, C. Barr, M. Beusenberg, E. Fournier, N. Shewchenko, E. Welbourne, *et al.*, "A new biomechanical assessment of mild traumatic brain injury, part 2: results and conclusions," *Proc. 2000 Int. Conf. Biomech. Impact*, pp. 223–233, 2000.

[2] Viano, I. Casson, and E. Pellman, "Concussion in professional football: Brain responses by finite element analysis: Part 9," *Neurosurgery*, vol. 57, no. 5, pp. 891–915, 2005.

[3] C. Giordano and S. Kleiven, "Evaluation of Axonal Strain as a Predictor for Mild Traumatic Brain Injuries Using Finite Element Modeling," *Stapp Car Crash J.*, vol. 58, no. 14, pp. 29–61, 2014.

[4] S. Kleiven, "Predictors for Traumatic Brain Injuries Evaluated through Accident Reconstructions," *SAE Tech. Pap.*, vol. 2007-Octob, no. October, pp. 81–114, 2007.

[5] D. A. Patton, A. S. McIntosh, S. Kleiven, and T. E, "The Biomechanical Determinants of Concussion : Finite Element Simulations to Investigate Brain Tissue Deformations During Sporting Impacts to the Unprotected Head," *J. Appl. Biomech.*, vol. 29, pp. 721–730, 2013.

[6] A. S. McIntosh, D. a Patton, B. Fréchède, P.-A. Pierré, E. Ferry, and T. Barthels, "The biomechanics of concussion in unhelmeted football players in Australia: a case-control study.," *BMJ Open*, vol. 4, no. 5, p. e005078, 2014.

[7] J. Ho, Z. Zhou, X. Li, and S. Kleiven, "The peculiar properties of the falx and tentorium in brain injury biomechanics," *J. Biomech.*, vol. 60, no. June, pp. 243–247, 2017.

[8] L. Zhang, K. Yang, A. King, and D. Viano, "A New Biomechanical Predictor for Traumatic Brain Injury – A Preliminary Finding," *Proc. 2003 Summer Bioeng. Conf.*, no. 1, pp. 1–2, 2003.

[9] S. S. Sawilowsky, "New Effect Size Rules of Thumb," *J. Mod. Appl. Stat.*

Methods, vol. 8, no. 2, pp. 597–599, 2009.

[10] E. O'Keeffe, E. Kelly, Y. Liu, C. Giordano, E. Wallace, M. Hynes, *et al.*, "Dynamic blood brain barrier regulation in mild head trauma," *J. Neurotrauma*, pp. 1–27, 2019.

[11] D. Viano, I. Casson, E. Pellman, C. Bir, L. Zhang, D. Sherman, *et al.*, "Concussion in professional football: Comparison with boxing head impacts - Part 10," *Neurosurgery*, vol. 57, no. 6, pp. 1154–1170, 2005.

[12] Zhang, K. Yang, and A. King, "Recent advances in brain injury research: a new human head model development and validation," *Stapp Car Crash J*, 2001. .

[13] F. Hernandez, C. Giordano, M. Goubran, S. Parivash, G. Grant, M. Zeineh, *et al.*, "Lateral impacts correlate with falx cerebri displacement and corpus callosum trauma in sports-related concussions," *Biomech. Model. Mechanobiol.*, no. 0123456789, 2019.

[14] F. Hernandez, L. Wu, M. C. Yip, K. Laksari, A. R. Hoffman, J. R. Lopez, *et al.*, "Six Degree of Freedom Measurements of Human Mild Traumatic Brain Injury," *Ann. Biomed. Eng.*, vol. 43, no. 8, pp. 1918–1934, 2015.

[15] J. Newman, M. C. Beusenberg, N. Shewchenko, C. Withnall, and E. Fournier, "Verification of biomechanical methods employed in a comprehensive study of mild traumatic brain injury and the effectiveness of American football helmets," *J. Biomech.*, vol. 38, no. 7, pp. 1469–1481, 2005.

[16] E. J. Sanchez, L. F. Gabler, A. B. Good, J. R. Funk, J. R. Crandall, and M. B. Panzer, "A reanalysis of football impact reconstructions for head kinematics and finite element modeling," *Clin. Biomech.*, vol. 64, no. February, pp. 82–89, 2019.

[17] L. Zhang, K. H. Yang, and A. I. King, "A Proposed Injury Threshold for Mild Traumatic Brain Injury," *J. Biomech. Eng.*, vol. 126, no. 2, pp. 226–236, 2004.

[18] H. Mao, L. Zhang, B. Jiang, V. V. Genthikatti, X. Jin, F. Zhu, *et al.*, "Development of a Finite Element Human Head Model Partially Validated With Thirty Five Experimental Cases," *J. Biomech. Eng.*, vol. 135, no. 11, p. 111002, 2013.

[19] Z. Zhou, X. Li, S. Kleiven, C. S. Shah, and W. N. Hardy, "A Reanalysis of Experimental Brain Strain Data: Implication for Finite Element Head Model Validation," *SAE Tech. Pap.*, vol. 2019-Novem, no. November, 2018.

Chapter 9

Conclusion

9.1 Summary of the original contributions of this research

This project measured and simulated head impacts in MMA. It is unique in that it is the only known study that has recorded *in vivo* the kinematics of head impacts that have resulted in concussive injuries in an unhelmeted sport. It is also unique in the broad scope and multi-disciplinary nature of the project which was made possible by the collaborations undertaken. The principal unique findings of this project are:

Kinematics

- The average resultant linear acceleration of the concussive events was 86.7g which was 21% lower than studies of US football [1]. While the average resultant angular acceleration was 7561rad/s^2 which was 37.5% higher than US football [1]. It is hypothesised that these differences are due to the 'hook' style punches in MMA rather than the high energy frontal impacts in US football.
- The most severe impact in four of the five events that resulted in a concussion had a linear acceleration greater than 90g and an angular acceleration greater than 4krad/s^2 with a duration in excess of 15ms. All 5 concussions were sustained following impacts to the side of the head (3 to the left side of the head and 2 to the right). The impacts were within ± 40^0 of the Y axis, thus corroborating the US football finding that lateral impacts are more likely to cause concussion [1].
- The average peak HIP value in the events that resulted in concussion was 20.6kW and 11.9kW in the events at which there was no head injury. It may be expected that HIP would be the best kinematic indicator of an injury as it incorporates both

linear and angular acceleration and impact duration. Newman et al. proposed that a HIP threshold of 20.88kW related to a 95% probability of concussion [3]. This threshold would have indicated 3 false positives and 2 false negatives in this study thus it was not found to be a reliable indicator of concussion.

- The kinematics of the impacts that resulted in a concussive injury in this project are below both the Wayne State tolerance curve, and the Brain Injury Leuven curve [4]. It is thought that this is due to more severe brain injuries being included in the development of these thresholds.
- Eight impacts with angular accelerations in excess of 6krad/s^2 occurred without any injury to the fighters. This is important as it indicates the human tolerance to short duration severe impacts.
- In conjunction with CAMLab at Stanford University, MMA impacts were compared to US football impacts. It was found that:
    - Brain injury criteria such as HIP, HIC, and BrIC are only accurate if used on the same type of head impacts as used in their development [5][6].
    - The spectral densities of the MMA impacts were in a higher frequency range (100 to 200Hz) compared to US football and automotive head impacts (0 to 50Hz) [7]. This is due to the lack of energy absorbing and damping materials in MMA impacts.

Strain

- In this study strain in the corpus callosum was found to be the best indicator of concussion. The average strain in the corpus callosum of the concussed athletes was 0.27 which was 88% higher than that of uninjured fighters [8]. This average strain was 28.6% lower than that reported in US football [9]. This may be due to the small number of concussive cases in this study and the range of severity of the concussions in the US football studies.

- The study found that frontal impacts resulted in large strains in the mid-brain whereas lateral impacts of the same magnitude resulted in 100% more strain in the corpus callosum. This may help to explain why lateral impacts are more likely to result in concussion. This also helps to explain why unconsciousness is more easily induced in animals from rotations in the coronal plane than rotations in any other plane [10].
- In the cases of concussion, the strain in the corpus callosum correlated with the magnitude of the linear acceleration in the Y direction (side impacts) and angular velocity about the Z axis ($R^2 > 0.80$). Strain in the lower brain regions of the thalamus and mid-brain correlated with the magnitude of the resultant angular velocity ($R^2 > 0.9$).

Sensors

- Skin patch and head-band sensors were found to be unsuitable for the measurement of the severity of head impacts due to their high angular acceleration errors (57% xPatch and 73% SIM-G) [11][12]. These large errors are in part due to the movement of the sensor relative to the skull [13].

Blood Brain Disruption

- In conjunction with TCD the BBB disruption was investigated. It was found that the maximum principal strain of the concussed fighters correlated ($R^2 = 0.84$) with the volume fraction of BBB disruption [14]. The changes in BBB may serve as a biomarker for concussion.

A combination of strain and kinematic data would have predicted 4 of the 5 concussions in this study. In this study there were 15 impacts with a linear acceleration greater than 90g and an angular acceleration greater than 4000rad/s^2. When these 15 impacts were simulated only the 4 concussed fighters had a strain in the corpus callosum greater than 0.24. The fighter who suffered from the other case of concussion did not receive any impacts over 90g and 4000rad/s^2. In this case the reason for the injury is thought to be due to a vulnerability as the fighter had 4 previous concussions. In summary, kinematic data will indicate which cases should be simulated and strain data can further refine the cases for suspected cases of injury. In order to complete an injury risk analysis, the medical history of the athlete needs to be considered.

This information can help inform clinicians about the possible severity and location of an injury but will not replace an experienced medical examination and diagnosis [15][16].

9.2 Recommendations and future work

The findings from this project highlight the need to gather more quantitative data on unhelmeted impacts as the knowledge and understanding of helmeted head impacts cannot simply be transferred to unhelmeted head impacts. Using this data, the risk of head injury in unhelmeted contact sports such as rugby and boxing may be understood. This information can be used by sporting organisations to develop rules and techniques to mitigate some of this risk.

Research in the following areas will improve our understanding of concussion:

- Instrumented mouthguards will soon be available for purchase by the general public. This may make it possible to collect very large head impact data sets. Accurate interpretation, validation and classification of this data will be necessary if it is to be of use to sporting organisations and clinicians.
- Automatic classification of head impacts from kinematic data is required to avoid the necessity of manual video confirmation of each impact. Such a system would use impact severity, direction and the frequency range of the data to determine the type and validity of an impact.

- The impacts reported in this study could yield more accurate results if subject specific head models were used. These are currently being developed at a number of research centres (see section 9.2.1).
- The development of more representative brain tissue material models is ongoing. Currently most head models use linear viscoelastic material models and assume that the brain tissue is isotropic and homogeneous within regions. New material models will be more representative as they will include anisotropic non-linear material properties.
- Further validation of head models is required. To date the validation of all head models is based on 4 sets of cadaver studies (Nahum [17], Hardy [18][19], Trosellie [20]). Using current technology, it is possible to carry out more accurate and detailed cadaver experiments. It is expected that current FE head models will be revised to reflect this data when it becomes available.
- Neural networks, artificial intelligent systems or reduced order models are required to quickly compute brain strains to allow pitch-side indication of athletes who require a medical assessment following a head impact.
- Currently there is no method that can determine injury risk based on the accumulation of head impacts over time. As more head impact data becomes available this may become possible.

9.2.1 Potential collaborations for future work

CADFEM Ireland & United Kingdom – Mr. Derek Sweeney

Simulating the impacts is a time-consuming process, it requires approximately one day to prepare, run, and post-process the data from a single impact. A project is currently underway with CADFEM Irl & UK to develop a reduced order model in OptiSlang (ANSYS Corp). This model will be similar to a neural network in that it will 'learn' from existing data to create a model to predict brain strain. This could enable side-line data analysis and the identification of athletes that require a medical examination.

Trinity College Dublin & St James Hospital & Stanford University - Dr. Mathew Campbell, Dr. Colin Doherty and Dr. David Camarillo

The project reported in this thesis will continue when contact sports resume (following the global pandemic). The focus of the group will be to investigate novel metrics to aid in the understanding, prediction and diagnosis of concussion.

Pusan University – Dr. David O'Sullivan.

I have collaborated with David for approximately 6 years. David's research group in South Korea are also investigating head impacts in martial arts, particularly Taekwondo.

University of Arizona – Dr. Kaveh Laksari

This group have developed a brain model based on a 3 degree of freedom lumped parameter brain model. The model has been developed from data gathered using the Stanford mouthguard in US football, the MMA data gathered in this project and voluntary head movements. This work was published in Journal of Neurotrauma in April 2020 [21].

Duke University – Dr. Dale Cameron.

Duke University are interested in comparing MMA and their US football data. The objective is to improve the risk function metrics for assessing concussion.

University of Leeds – Dr. Greg Tierney

Dr. Tierney is working with Dr. Matt Panzer of the University of Virginia to develop subject specific finite element head models. They now require 'real world' data to apply to their models, they will compare their results with my finite element results.

University of Washington – Dr. Per Reinhall

This research group have developed a new US football helmet and wish to test it in a laboratory by applying our 'real world' impact data to it.

University of Michigan – Dr. Jingwen Hu

Dr. Jingwen and his group have developed a large number of subject specific brain models by morphing the elements in the GHBMC model. Dr. Jingwen would like us to share our MRI data for the MMA fighters to create subject specific head models and then investigate how the strain differs from the 50th percentile model used in this study. We are currently discussing how we can make this collaboration work.

The strength of concussion research in the future will depend on the incorporation of many disciplines including: sports science, medicine, radiology, physiology, psychology, engineering and computing.

9.3 References

[1] S. Rowson and S. M. Duma, "Brain Injury Prediction: Assessing the Combined Probability of Concussion Using Linear and Rotational Head Acceleration," *Ann. Biomed. Eng.*, vol. 41, no. 5, pp. 873–882, 2013.

[2] S. P. Broglio, B. Schnebel, and J. Sosnoff, "The Biomechanical Properties of Concussions in High School Football," *Med. Sci. Sports Exerc.*, vol. 42, no. 11, pp. 2064–2071, 2010.

[3] J. A. Newman and N. Shewchenko, "A Proposed New Biomechanical Head Injury Assessment Function - The Maximum Power Index," *SAE Tech. Pap.*, vol. 2000-Novem, no. November, 2000.

[4] T. B. Hoshizaki, A. Post, M. Kendall, J. Cournoyer, P. Rousseau, M. D. Gilchrist, *et al.*, "The development of a threshold curve for the understanding of concussion in sport," *Trauma (United Kingdom)*, vol. 19, no. 3, pp. 196–206, Jul. 2017.

[5] X. Zhan, Y. Li, Y. Liu, A. Domel, and S. Tiernan, "Prediction of brain strain across head impact subtypes using 18 brain injury criteria," *J. R. Soc. Interface*, 2020.

[6] X. Zhan, Y. Li, Y. Liu, A. G. Domel, H. V. Alizadeh, Z. Zhou, *et al.*, "Predictive Factors of Kinematics in Traumatic Brain Injury from Head Impacts Based on Statistical Interpretation," 2021.

[7] X. Zhan, Y. Li, Y. Liu, N. Cecchi, S. Raymond, Z. Zhou, *et al.*, "Classification of head impacts based on the spectral density of measurable kinematics," *J. Biomech.*, 2021.

[8] S. Tiernan, A. Meagher, D. O. Sullivan, E. O. Kelly, S. Tiernan, A. Meagher, *et al.*, "Finite element simulation of head impacts in mixed martial arts," *Comput. Methods Biomech. Biomed. Engin.*, vol. 0, no. 0, pp. 1–11, 2020.

[9] S. Kleiven, "Predictors for Traumatic Brain Injuries Evaluated through Accident Reconstructions," *SAE Tech. Pap.*, vol. 2007-Octob, no. October, pp. 81–114, 2007.

[10] B. D. Stemper and F. A. Pintar, "Biomechanics of concussion," *Prog. Neurol. Surg.*, vol. 28, no. 1, pp. 14–27, 2014.

[11] S. Tiernan, G. Byrne, and D. M. O'Sullivan, "Evaluation of skin-mounted sensor for head impact measurement," *Proc. Inst. Mech. Eng. Part H J. Eng. Med.*, vol. 233, no. 7, pp. 735–744, 2019.

[12] S. Tiernan, D. O'Sullivan, G. Byrne, D. O'Sullivan, and G. Byrne, "Repeatability and reliability evaluation of a wireless head-band sensor," *Asian J. Kinesiol.*, vol. 20, no. 4, pp. 1–18, 2018.

[13] L. Wu, F. Hernandez, C. Kuo, and M. Kurt, "In Vivo Evaluation of Wearable Head Impact Sensors," *Ann. Biomed. Eng.*, vol. 44, no. 4, pp. 1234–1245, 2016.

[14] E. O'Keeffe, E. Kelly, Y. Liu, C. Giordano, E. Wallace, M. Hynes, *et al.*, "Dynamic blood brain barrier regulation in mild head trauma," *J. Neurotrauma*, pp. 1–27, 2019.

[15] F. Hernandez, L. Wu, M. C. Yip, K. Laksari, A. R. Hoffman, J. R. Lopez, *et al.*, "Six Degree of Freedom Measurements of Human Mild Traumatic Brain Injury," *Ann. Biomed. Eng.*, vol. 43, no. 8, pp. 1918–1934, 2015.

[16] S. Kleiven, "Evaluation of head injury criteria using a finite element model validated against experiments on localized brain motion, intracerebral acceleration, and intracranial pressure," *Int. J. Crashworthiness*, vol. 11, no. 1, pp. 65–79, 2006.

[17] A. M. Nahum, R. Smith, and C. C. Ward, "Intracranial Pressure Dynamics During Head Impact," *21st Stapp Car Crash Conf.*, 1977.

[18] A. Al-Bsharat, W. Hardy, K. Yang, T. Khalil, S. Tashman, and A. King, "Brain/skull relative displacement magnitude due to blunt head impact: New experimental data and model," *Stapp Car Crash Conf. Proc.*, vol. P-350, no. 724, pp. 321–332, 1999.

[19] W. N. Hardy, M. J. Mason, C. D. Foster, C. S. Shah, J. M. Kopacz, H. Yang, *et al.*, "A study of the response of the human cadaver head to impact," *Stapp Car Crash J*, vol. 51, pp. 17–80, 2008.

[20] X. Trosseille, C. Tarriére, F. Lavaste, F. Guillon, and A. Domont, "Development of a F.E.M. of the human head according to a specific test protocol," *SAE Tech. Pap.*, 1992.

[21] K. Laksari, M. Fanton, L. Wu, T. Nguyen, M. Kurt, C. Giordano, *et al.*, "Multi-directional dynamic model for traumatic brain injury detection," *J. Neurotrauma*, vol. 37, no. 7, pp. 1–48, 2019.

Appendix 1: Author Contributions for each paper

Paper 1: Evaluation of Skin Mounted Sensor for Head Impact Measurement

Published: S. Tiernan, G. Byrne, and D. M. O'Sullivan, "Evaluation of skin-mounted sensor for head impact measurement," *Proc. Inst. Mech. Eng. Part H J. Eng. Med.*, vol. 233, no. 7, pp. 735–744, 2019. DOI: 10.1177/0954411919850961

Author contributions:

S. Tiernan: Conceived, designed and performed experiments, analysed data and wrote the paper.
G. Byrne: Data collection and analysis.
D.O'Sullivan: Data collection and analysis.

I acknowledge the accuracy of the contributions as stated above.

Mr. G. Byrne ____________ Dr. D.O'Sullivan ____________

Paper 2: Repeatability and reliability evaluation of a wireless head-band sensor.

Published: S. Tiernan, D. O'Sullivan, and G. Byrne, "Repeatability and Reliability Evaluation of a Wireless Head-band Sensor," *Asian J. Kinesiol.*, *20(4)*, pp. 70–75, 2018. DOI: 10.15758/ajk.2018.20.4.70

Author contributions:

S. Tiernan: Conceived, designed and performed experiments, analysed data and wrote the paper.
G. Byrne: Data collection and analysis.
D.O'Sullivan: Data collection and analysis.

I acknowledge the accuracy of the contributions as stated above.

Mr. G. Byrne ____________ Dr. D.O'Sullivan ____________

Paper 3: Concussion and the Severity of Head Impacts in Mixed Martial Arts

Published: S. Tiernan, A. Meagher, D. O'Sullivan, E. O'Keefe, E. Kelly, E. Wallace, C. Doherty, M. Cambell, Y. Liu, A. G. Domel, *"Concussion and the Severity of Head Impacts in Mixed Martial Arts.* Part H: Journal of Engineering in Medicine. Aug 2020. DOI: 10.1177/0954411920947850.

Author contributions:

S. Tiernan: Conceived, designed and performed experiments, analysed data and wrote the paper.

A. Meagher & D. O'Sullivan: Acceleration data collection and analysis

E. Kelly: Medical Examination and reporting

M. Campbell (Principal Investigator), C. Doherty, E. Wallace & E.O'Keefe: Data collection and analysis

Y. Liu & A. Domel: Mouthguard validation, software and firmware

I acknowledge the accuracy of the contributions as stated above:

Mr. A Meagher ______________ Dr. D.O'Sullivan ______________

Dr. E. Kelly ______________ Dr. A. G. Domel ______________

Dr. Y. Liu yuzhe liu ______________ Dr. M. Campbell ______________

Paper 4: The effect of impact location on brain strain

Published: S. Tiernan and G. Byrne, "The effect of impact location on brain strain," *Brain Inj.*, vol. 33, no. 01, pp. 1–8, 2019. DOI: 10.1080/02699052.2019.1566834.

Author contributions:

S. Tiernan: Conceived, designed and performed experiments, analysed data and wrote the paper.

G. Byrne: Analysis of data.

I acknowledge the accuracy of the contributions as stated above.

Mr. G. Byrne ______________

Paper 5: Finite Element Simulation of Head Impacts in Mixed Martial Arts

Published: S. Tiernan, A. Meagher, D. O'Sullivan, E. Kelly, "Finite Element Simulation of Head Impacts in Mixed Martial Arts,*"Comput Methods Biomech Biomed Engin. Methods.* Accepted Sept. 2020. DOI: 10.1080/10255842.2020.1826457

Author contributions:

S. Tiernan:	Conceived, designed and performed all simulations, analysed data and wrote the paper.
A. Meagher:	Data collection.
D.O'Sullivan:	Data collection.
E. Kelly:	Medical Examination and reporting.

I acknowledge the accuracy of the contributions as stated above.

Mr. A. Meagher ________________ Dr. D.O'Sullivan ________________

Dr. E. Kelly: ________________

Appendix 2: Sample Matlab Programs

Program 1 – Calculates max resultants, HIP, impact direction and elevation. Plots graphs and outputs data to Excel

```
%reads file created by matlab srcipt from mouthguard data
clc %clear command window
clearvars %clear variables
clear %clears workspace
%Selects path, file to open and output file
selpath = uigetdir(path);%selects folder for opening and saving
cd(selpath);%changes to the selected path
file = uigetfile; %opens user dialogue to select file (*.mat)
load(file); %loads data from that file
Prompt='Enter name of output file (this creates a txt file that can be imported into excel)= ';
output_file=input(Prompt,'s'); %sets the output filename;
Prompt2='Enter IR sensor threshold ';
threshold=input(Prompt2); %sets the IR threshold;
Prompt3='Enter hit number to start ';
start=input(Prompt3); %sets the number of hit to start analysis;
Prompt4='Enter hit nummber to end, enter 0 if all hits required   ';
N=input(Prompt4); %sets the hit number to end;
Prompt5='Graph individual hits? 1 for yes, any number for no'; %do you want jpg of hits
graph=input(Prompt5);
Prompt6='Graph start time -0.05 (50ms pre post) or 0 (for 100 prepost)'; %do you want jpg of hits
st_time=input(Prompt6);

%st_time=-0.05;  % -0.05 sets the x axis start time
end_time=st_time+.2; % 0.1 sets the x axis end time
if N==0;%if 0 inlude all hits
   N=length(mg_data); %puts N = number of events
   else;
end;
events=(N-start);
fprintf('Number of Events = %2d,\n',events+1)  %prints to screen
set(0,'DefaultFigureVisible','off');%figures disapear
r=0; %row number for significant events

for i=start:N
   %creating matrices
   IR(i)=0;% remove IRcheck [mg_data(i).Info.IR]; %finds IR values
   if IR(i)>=threshold;
     if mg_data(i).lin_acc_CG_mag<400; %if linear accel is greater than 400g
       r=r+1; %creates row number for events that are above threshold and below accel limt
       IRN(r)=[mg_data(i).Info.IR]; %only IR valuefor events counted
       eventdate={mg_data(1).Info.Day,mg_data(1).Info.Month,mg_data(1).Info.Year};
       eventhour(r)={mg_data(i).Info.Hour};%captures time info
       ehour(r)=str2double(eventhour(r));
       eventmin(r)={mg_data(i).Info.Minute};
       emin(r)=str2double(eventmin(r));
       eventsec(r)={mg_data(i).Info.Second};
       esec(r)=str2double(eventsec(r));
       ang_vel_length=length(mg_data(i).ang_vel); %is this short
       T=mg_data(i).t;%creates vector of time

       L=mg_data(i).lin_acc_CG;%creates 3 column matrix of linear acc X,Y,Z
       AV=mg_data(i).ang_vel; %creates 3 column matrix of rot velocities X,Y,Z
       AA=mg_data(i).ang_acc; %creates 3 column matrix of rot accel X,Y,Z
       L_mag=mg_data(i).lin_acc_CG_mag; %creates 1 column of resultant linear accel
```

```
        AA_mag=mg_data(i).ang_acc_mag; %creates 1 column of resultant ang accel
        AV_mag=mg_data(i).ang_vel_mag; %creates 1 column of resultant ang vel
        T=T(1:ang_vel_length,1:1); %shortens to min ang vel length
        L=L(1:ang_vel_length,1:3);
        L_mag=L_mag(1:ang_vel_length,1:1);
        ALL=[T,L,AA,AV,L_mag,AA_mag,AV_mag];
        A_resultant=[T,L_mag,AA_mag,AV_mag];
       %Calculating HIP criteria
        L_SI=L*9.81; %convert L into m/s/s CHECK TIME UNITS
        Int_L=cumtrapz(L_SI); %intergates linear terms
        P1_HIP=L_SI.*Int_L; % multiplies linear value by integral
        Int_AA=cumtrapz(AA); %intergates linear terms
        P2_HIP=AA.*Int_AA; % multiplies linear value by integral
           for row=1:length(L)

HIP(row)=4.5*(P1_HIP(row,1)+P1_HIP(row,2)+P1_HIP(row,3))+P2_HIP(row,1)*0.016+P2_HIP(row,2)*0.02
4+P2_HIP(row,3)*0.022;%adds terms together
           end
        HIP_max(r)=max(HIP)/1e6; %finds max value in kW plus divides by 1000 as time step is .001

        %finding max linear and rotational accels
        I(r)=i; %row = significant hit number
        M = max(A_resultant);
        Max_linear(r)=M(1,2);%max linear resultant
        Max_rotational_accel(r)=M(1,3);
        Max_rotational_vel(r)=M(1,4);
        if (Max_linear(r)>150); impact='Very Severe';else
        if (Max_linear(r)>120 && Max_linear(r)<150); impact='Severe';else
        if (Max_linear(r)>90 && Max_linear(r)<120); impact='Very Serious';else
        if (Max_linear(r)>60) && (Max_linear(r)<90); impact='Serious';else
        if (Max_linear(r)>30) && (Max_linear(r)<60); impact='Moderate';else
        if (Max_linear(r)>10) && (Max_linear(r)<30); impact='Low';else
        if (Max_linear(r)<10); impact='NaN';else
         end;end;end;end;end;end;end
        Impact(r)= cellstr(impact);
       % find impact direction
      vi=find(mg_data(i).lin_acc_CG_mag(:,1)==Max_linear(r));%finds index of row with max resultant linear
      Max_L_row=mg_data(i).lin_acc_CG(vi,:); % finds max linear row
      [azz,ell,mag]=cart2sph(Max_L_row(1,1),Max_L_row(1,2),Max_L_row(1,3));%az rotation angle, el
elevation angle
       az(r)=azz*180/pi+180; %converts to degress and sets front as zero
       el(r)=ell*180/pi;
       direction='undefined';
       %fprintf('Rotation angle from front= %4.2f degrees\n',az)  %prints to screenfprintf('Rotation Angle from
front,r')%prints to screen
        %fprintf('Elevation angle from horiz= %4.2f degrees\n',el)  %prints to screen
           if (az(r)> 337.5) && (az(r)< 361);direction='F';   else;
           if (az(r)> 0) && (az(r)< 22.5);direction='F';   else;
           if (az(r)> 22.5) && (az(r)< 67.5); direction='FL';  else;
           if (az(r)> 67.5) && (az(r)< 112.5); direction='L'; else;
           if (az(r)> 112.5) && (az(r)< 157.5); direction='BL'; else;
           if (az(r)> 157.5) && (az(r)< 202.5); direction='B';   else;
           if (az(r)> 202.5) && (az(r)< 247.5); direction='BR';  else;
           if (az(r)> 247.5) && (az(r)< 292.5); direction='R';  else;
           if (az(r)> 292.5) && (az(r)< 337.5); direction='FR';  else;
          end;end;end;end;end;end;end;end;end;
Direction(r)= cellstr(direction);
elevation='undef';
        if (el(r)> 45);elevation='Top';   else;
        if (el(r)>= 0) && (el(r)<= 45);elevation='Upper';   else;
        if (el(r)>= -45) && (el(r)< 0); elevation='Lower';  else;
        if (el(r)< -45);elevation='Neck';else
```

```
        end;end;end;end;
Elevation(r) = cellstr(elevation);
          hit_number=num2str(i);%creats string of hit number for plotting

        if graph==1;
        %plotting
        clf reset %clears figure window
        %co-ord of lower left, width,height
        figure(i);
        %set(gcf,'position',(0,0,1000,1000));%set size and position of fig
        subplot(2,3,1);%plot linear accel X Y Z
        plot(T,L);
        axis([st_time end_time -inf inf]);
        title('C of G Linear Acc');
        grid on;
        grid minor;
        xlabel('Time(s)');
        ylabel('Linear acc (g)');

        subplot(2,3,4); % plot linear resultant
        plot(T,L_mag);
        axis([st_time end_time -inf inf]);
        title('C of G Linear Accel Resultant');
        grid on;
        grid minor;
        xlabel('Time(s)');
        ylabel('C of G Linear Resultant (g)');
        text(.025,8,'Hit Number:','color','red');
        text(.08,8,hit_number,'color','red');

        subplot(2,3,2);% plot rotation accel
        plot(T,AA);%plots
        axis([st_time end_time -inf inf]);
        title('C of G Rotational Acc');
        grid on;
        grid minor;
        legend('x','y','z');
        xlabel('Time(s)');
        ylabel('Rotational Acc (rad/s/s)');

        subplot(2,3,5);% plot rotation accel resultant
        plot(T,AA_mag);%plots
        axis([st_time end_time -inf inf]);
        title('Rotational Acc Resultant');
        grid on;
        grid minor;
        xlabel('Time(s)');
        ylabel('Rotational Acc (rad/s/s)');
        %saving figures to files
        figs=figure(i);
        print(figs,hit_number,'-djpeg'); %save a jpg file of the plot
%angular velocity
        subplot(2,3,3);% plot rotation velocity
        plot(T,AV);%plots
        axis([st_time end_time -inf inf]);
        title('C of G Rotational Velocity');
        grid on;
        grid minor;
        legend('x','y','z');
        xlabel('Time(s)');
        ylabel('Rotational Vel (rad/s)');
```

```
        subplot(2,3,6);% plot rotation vel resultant
        plot(T,AV_mag);%plots
        axis([st_time end_time -inf inf]);
        title('Rotational Vel Resultant');
        grid on;
        grid minor;
        xlabel('Time(s)');
        ylabel('Rotational Vel (rad/s)');
        %saving figures to files
        figs=figure(i);
        print(figs,hit_number,'-djpeg'); %save a jpg file of the plot
  else
  end
        %creates excel file, new sheet for each event
        % REMOVE TO RUN ON MAC
        warning('off', 'MATLAB:xlswrite:AddSheet');
        col_headert={'Hit Number'};
        xlswrite(output_file,col_headert,hit_number,'A1'); %writes excel file 1st worksheet
        xlswrite(output_file,hit_number,hit_number,'A2'); %writes excel file 1st worksheet
        col_header={'Time','Linear Acc X','Lin Acc Y','Lin Acc Z','Rot Acc X','Rot Acc Y','Rot Acc Z','Rot Vel
X','Rot Vel Y','Rot Vel Z','Result Linear Accel','Result Rot Accel','Res Rot Vel'};
        xlswrite(output_file,col_header,hit_number,'A3'); %writes excel file 1st worksheet
        xlswrite(output_file,ALL,hit_number,'A4');% T,L,AA,linear resultant, rot resultant
        else
          fprintf('Event number %d above linear accel limit,\n',i)  %prints to screen
        end
      else
         fprintf('Event number %d below IR threshold,\n',i)  %prints to screen
    end
end
device={mg_data(1).Info.Device};
Maxs=[I;ehour;emin;esec;IRN;Max_linear;Max_rotational_accel;Max_rotational_vel;az;el;HIP_max];%forms
matrix of max values for each hit
Maxs_transpose=Maxs';
Imp_No=I';Hour=ehour';Min=emin';Sec=esec';IR=IRN';Max_linear=Max_linear';Max_rotational_accel=Max_r
otational_accel';Max_rotational_vel=Max_rotational_vel';
az=az';el=el';HIP_max=HIP_max';

DirT=Direction';
ElevT=Elevation';
Imp=Impact';

% adds summary summary sheet REMOVE FOR MAC
warning('off', 'MATLAB:xlswrite:AddSheet');
col_header1={'Day','Month','Year'};
col_header2={'Hit number','Hour','Minute','Sec','IR value','Max Result Linear Accel', 'Max Result Rotational
Accel','Max Result Rot Vel','Rot Angle','Elev Angle','Impact','Sector','Elev','HIP'};
col_header3={'Threshold set to'};
col_header4={'','','','','','g','rad/s/s','rad/s','Degrees','Degrees','','','','kW'};
xlswrite(output_file,device,'summary','A1'); %writes device name to summary worksheet
xlswrite(output_file,col_header1,'summary','A2'); %writes date header
xlswrite(output_file,eventdate,'summary','A3'); %writes date
xlswrite(output_file,col_header3,'summary','A4'); %writes header for threshold
xlswrite(output_file,threshold,'summary','C4'); %writes threshold
xlswrite(output_file,col_header2,'summary','A6'); %writes header for data
xlswrite(output_file,col_header4,'summary','A7'); %writes header for data
xlswrite(output_file,Maxs_transpose,'summary','A8');% T,writes resultants
xlswrite(output_file,Imp,'summary','K8');% T,writes resultants
xlswrite(output_file,DirT,'summary','L8');% T,writes resultants
xlswrite(output_file,ElevT,'summary','M8');% T,writes resultants
xlswrite(output_file,HIP_max,'summary','N8');% T,writes HIP
```

```
%Mac create table this is instead of xlswrite on windows PC
Table2=table(Imp_No,Hour,Min,Sec,IR,Max_linear,Max_rotational_accel,Max_rotational_vel,az,el,DirT,ElevT
,Imp,HIP_max);
writetable(Table2,output_file); %write table to file

    clf reset %clears figure window
    set(0,'DefaultFigureVisible','on')
    figure;
    fig=figure;
    subplot(1,3,1);%plot linear accel X Y Z
    bar(I,Max_linear);
    title('Hits Vs Max Linear Accel');
    grid;
    grid minor;
    xlabel('Hit Number');
    ylabel('Max Linear Accel(g)');

    subplot(1,3,2)%plot rot accel X Y Z
    bar(I,Max_rotational_accel);
    title('Hits Vs Max Rotational Accel');
    grid;
    grid minor;
    xlabel('Hit Number');
    ylabel('Max Rotational Accel (rad/s/s)');
    print(fig,output_file,'-djpeg'); %save a jpg file of the summary
    fprintf('IR sensor threshold set = %2d,\n',threshold)  %prints to screen
    fprintf('Total Number of Events = %2d,\n',N+1)  %prints to screen
    fprintf('Number of Events over IR threshold and below accel limit = %2d,\n',r)  %prints to screen

     subplot(1,3,3)%plot rot vel X Y Z
    bar(I,Max_rotational_vel);
    title('Hits Vs Max Rotational Vel');
    grid;
    grid minor;
    xlabel('Hit Number');
    ylabel('Max Rotational Vel (rad/s)');
    print(fig,output_file,'-djpeg'); %save a jpg file of the summary
    fprintf('IR sensor threshold set = %2d,\n',threshold)  %prints to screen
    fprintf('Total Number of Events = %2d,\n',N+1)  %prints to screen
    fprintf('Number of Events over IR threshold and below accel limit = %2d,\n',r)  %prints to screen
```

Program 2: Transforms data, converts units, separates each axis data

```
%COPY YOUR DATA FILE INTO NEW DIRECTORY FOR THIS EVENT
%BEFORE RUNNING THIS
%IF IT DOESN'T RUN INCREASE TOL TO 20
%reversed y and z axis and rotations about y and z - 14 Feb 2019
%reads file created by matlab srcipt from mouthguard data
clc %clear command window
clearvars %clear variables
clear %clears workspace
%Selects path, file to open and output file
selpath = uigetdir(path);%selects folder for opening and saving
cd(selpath);%changes to the selected path
file = uigetfile; %opens user dialogue to select file (*.mat)
load(file); %loads data from that file
%Prompt2='Enter IR sensor threshold ';
threshold=0; %input(Prompt2); %sets the out IR threshold;
Prompt3='Enter event number ';
i=input(Prompt3); %sets the event number
```

```
Prompt4='Start Time in ms (95 MiG1 and -5 MiG2) '; %start time for output
st_time=input(Prompt4);
Prompt5='Number of ms to output (default 50)';
time_ms=input(Prompt5);
end_time=(st_time+time_ms)/1000; %default 0.015 for Mig2  % default 0.11 for Mig1
st_time=st_time/1000;
n=10;  %linear accel being looked for to measure duration
tol=500; %linear default n + of the value being looked for eg data points between 10 and 10+10
nA=500; %ang accel being looked for to measure duration
tolA=1000; %%ang default 100 + of the value being looked for
min_time=.005; %min time difference acceptable, times can't be that close

set(0,'DefaultFigureVisible','off');%figures disapear
r=0; %row number for significant events

  %creating matrices
  IR(i)=0;%[mg_data(i).Info.IR]; %finds IR values
  if IR(i)>=threshold;
   if mg_data(i).lin_acc_CG_mag<400; %if linear accel is greater than 400g
    r=r+1; %creates row number for events that are above threshold and below accel limt
    IRN(r)=[mg_data(i).Info.IR]; %only IR valuefor events counted
    eventdate={mg_data(1).Info.Day,mg_data(1).Info.Month,mg_data(1).Info.Year};
    eventhour(r)={mg_data(i).Info.Hour};%captures time info
    ehour(r)=str2double(eventhour(r));
    eventmin(r)={mg_data(i).Info.Minute};
    emin(r)=str2double(eventmin(r));
    eventsec(r)={mg_data(i).Info.Second};
    esec(r)=str2double(eventsec(r));
    ang_vel_length=length(mg_data(i).ang_vel); %is this short
    T=mg_data(i).t;%creates vector of time


    L=mg_data(i).lin_acc_CG;%creates 3 column matrix of linear acc X,Y,Z
    AV=mg_data(i).ang_vel; %creates 3 column matrix of rot velocities X,Y,Z
    AA=mg_data(i).ang_acc; %creates 3 column matrix of rot accel X,Y,Z
    L_mag=mg_data(i).lin_acc_CG_mag; %creates 1 column of resultant linear accel
    AA_mag=mg_data(i).ang_acc_mag; %creates 1 column of resultant linear accel
    AV_mag=mg_data(i).ang_vel_mag; %creates 1 column of resultant linear accel
    T=T(1:ang_vel_length,1:1); %shortens to min ang vel length
    L=L(1:ang_vel_length,1:3);
    L_mag=L_mag(1:ang_vel_length,1:1);
    ALL=[T,L,AA,L_mag,AA_mag];
    A_resultant=[T,L_mag,AA_mag];

    %finding max linear and rotational accels
    I(r)=i; %row = significant hit number
    M = max(A_resultant);
    Max_linear(r)=M(1,2);%max linear resultant
    Max_rotational_accel(r)=M(1,3);

    % find duration of peak acceleration linear accel
P= find(L_mag>(n) & L_mag<(n+tol)); %find the values within tolerance
t1=T(P(1)); %timeof the first data value
nni=1;
  t2=T(P(nni+1));  %time of the 2nd datavalue
  tdiff=t2-t1 ; %time difference
  if tdiff<=min_time;  %is the time diff less than min time
    nni=nni+1;   % if so than go to the next time in the Data A
    t2=T(P(nni+1));
    tdiff=t2-t1;  %re calc time diff
  else
    end
```

```
  acc1=L_mag(find(T==t1)); acc2=L_mag(find(T==t2));
    Data_pts=[t1 t2;acc1 acc2]'    %the next data value, with time diff > than min time
  Duration_of_impact_Linear_accel_ms=tdiff*1000
  % find duration of peak acceleration angular accel
  PA= find(AA_mag>(nA) & AA_mag<(nA+tolA)); %find the values within tolerance
tA1=T(PA(1)); %timeof the first data value
nniA=1;
    tA2=T(PA(nni+1));  %time of the 2nd datavalue
    tdiffA=tA2-tA1 ; %time difference
    if tdiffA<=min_time;  %is the time diff less than min time
        nniA=nniA+1;   % if so than go to the next time in the Data A
        tA2=T(PA(nniA+1));
        tdiffA=tA2-tA1;  %re calc time diff
    else
        end
  ang_acc1=AA_mag(find(T==tA1)); ang_acc2=AA_mag(find(T==tA2));
    Data_pts=[tA1 tA2;ang_acc1 ang_acc2]'    %the next data value, with time diff > than min time
  Duration_of_impact_Angular_accel_ms=tdiffA*1000

        % find impact direction
      vi=find(mg_data(i).lin_acc_CG_mag(:,1)==Max_linear(r));%finds index of row with max resultant linear
      Max_L_row=mg_data(i).lin_acc_CG(vi,:); % finds max linear row
      [azz,ell,mag]=cart2sph(Max_L_row(1,1),Max_L_row(1,2),Max_L_row(1,3));%az rotation angle Atan(y/x),
el elevation angle Acos(z/r)
       az=azz*180/pi+180; %converts to degress and sets front as zero
       el=ell*180/pi;

       %changes units and co-ord system to match GHBMC units for lin mm/ms
        % rotation is rad/ms/ms
        T=T*1000; %convert time to ms
       st_time=st_time*1000;
       end_time=end_time*1000;
         X=[T,L(:,1)*9.81/1000]; Y=[T,L(:,2)*-9.81/1000];Z=[T,L(:,3)*-9.81/1000];
         RX=[T,AA(:,1)/1000/1000]; RY=[T,AA(:,2)/-1000/1000];RZ=[T,AA(:,3)/-1000/1000];
       %to output only time of interesst
       st_index=find(T>(st_time-0.0005) & T<(st_time+0.0005));
       end_index=find(T>(end_time-0.0005) & T<(end_time+0.0005));
       X=X(st_index:end_index,:); Y=Y(st_index:end_index,:); Z=Z(st_index:end_index,:);
       RX=RX(st_index:end_index,:);RY=RY(st_index:end_index,:);RZ=RZ(st_index:end_index,:);
        X(:,1)=[0:1:time_ms];Y(:,1)=[0:1:time_ms];Z(:,1)=[0:1:time_ms]; %sets time column to time_ms
      RX(:,1)=[0:1:time_ms];RY(:,1)=[0:1:time_ms];RZ(:,1)=[0:1:time_ms]; %sets time column to time_ms

       %plotting in mouthguard co-ord system
       time_diff=num2str(tdiff*1000);
       hit_number=num2str(i);%creats strings for plotting
       Duration_of_impact_Linear_accel_ms=num2str(Duration_of_impact_Linear_accel_ms);
       Duration_of_impact_Angular_accel_ms=num2str(Duration_of_impact_Angular_accel_ms);
         clf reset %clears figure window
         %co-ord of lower left, width,height
         figure(i);

         %set(gcf,'position',(0,0,1000,1000));%set size and position of fig
         subplot(2,3,1);%plot linear accel X Y Z
         plot(T,L); %linear accel 3 dirs
         title('C of G Linear Acc - Mouthg co-ords');
         grid on;
         grid minor;
         xlabel('Time(ms)');
         ylabel('Linear acc (g)');
         legend({'x Pos Ant','y Rgt lft','z Inf Sup'},'Location','northeast','orientation','horizontal','Fontsize',8);

         subplot(2,3,4); % plot linear output time only
```

```
hold on;
plot(T,L);
plot(T,L_mag);
hold off;
axis([st_time end_time -inf inf])
title('C of G Linear Accel Output time only');
grid on;
grid minor;
xlabel('Time(ms)');
ylabel('Linear acc (g)');
text(st_time,60,'Linear Duration:','color','red');
text(st_time,30,Duration_of_impact_Linear_accel_ms,'color','red');
legend({'x Pos Ant','y Rgt lft','z Inf
Sup','Resultant'},'Location','northeast','orientation','horizontal','Fontsize',8);

subplot(2,3,2);% plot rotation accel
plot(T,AA);%plots 3 aixs rot accel
title('C of G Rotational Acc');
grid on;
grid minor;
xlabel('Time(ms)');
ylabel('Rotational Acc (rad/s/s)');
text(0,2000,'Rotation Angle:','color','red','Fontsize',6);
az
az=num2str(az);
text(0,500,az,'color','red','Fontsize',8);
text(0,-500,'Elevation Angle:','color','red','Fontsize',6);
el=num2str(el);
text(0,-2000,el,'color','red','Fontsize',8);

subplot(2,3,5);% plot rotation accel out put time only
hold on
plot(T,AA);%plots
plot(T,AA_mag);
hold off;
axis([st_time end_time -inf inf])
title('Rotational Acc Output time only');
grid on;
grid minor;
xlabel('Time(ms)');
ylabel('Rotational Acc (rad/s/s)');
text(st_time,5000,'Angular Duration:','color','red');
text(st_time,2500,Duration_of_impact_Angular_accel_ms,'color','red');

 subplot(2,3,3);% plot rotation vel
plot(T,AV);%plots
title('Rotational Vel rad/s');
grid on;
grid minor;
legend({'1 Rot in Cor.','2 Rot in Sag.','3 Rot in
Horiz'},'Location','northeast','orientation','horizontal','Fontsize',8);
xlabel('Time(ms)');
ylabel('Rotational Vel (rad/s)');


subplot(2,3,6);% plot rotation vel output time only
hold on;
plot(T,AV);%plots
plot(T,AV_mag);
hold off;
axis([st_time end_time -inf inf])
title('Rotational Vel Output time only');
```

```
        grid on;
        grid minor;
        xlabel('Time(ms)');
        ylabel('Rotational Vel (rad/s)');
        text(st_time,15,'Hit Number:','color','red');
        text(st_time,5,hit_number,'color','red');
        legend({'1 Rot in Cor.','2 Rot in Sag.','3 Rot in
Horiz','Resultant'},'Location','northeast','orientation','horizontal','Fontsize',8);

        %saving figures to files
        figs=figure(i);
        print(figs,hit_number,'-djpeg'); %save a jpg file of the plot
        device={mg_data(1).Info.Device};
        %creates csv files
        csvwrite('X.csv',X)
        csvwrite('Y.csv',Y)
        csvwrite('Z.csv',Z)
        csvwrite('RX.csv',RX)
        csvwrite('RY.csv',RY)
        csvwrite('RZ.csv',RZ)

  else
          fprintf('Event number %d above linear accel limit,\n',i)  %prints to screen
        end
      else
          fprintf('Event number %d below IR threshold,\n',i)  %prints to screen
    end

device={mg_data(1).Info.Device};

%create table with all components
Lin_R=sqrt((X(:,2).^2)+(Y(:,2).^2)+(Z(:,2).^2));
Ang_R=sqrt((RX(:,2).^2)+(RY(:,2).^2)+(RZ(:,2).^2));
Y1=Y(:,2);Z1=Z(:,2);RY1=RY(:,2);RZ1=RZ(:,2); %renames for header in table
Table4=table(X,Y1,Z1,Lin_R,RX,RY1,RZ1,Ang_R); % creates table with time and then components
writetable(Table4,'all'); %write table to file
```

Program 3: Fast Fourier Transformation of acceleration data to identify high frequency ‘noisy’ signals.

```
%THIS USES FILTERED DATA BUT SHOULD USE UNFILTERED
%studies a single impact
clc %clear command window
clearvars %clear variables
clear %clears workspace
%Selects path, file to open and output file
selpath = uigetdir(path);%selects folder for opening and saving
cd(selpath);%changes to the selected path
file = uigetfile; %opens user dialogue to select file (*.mat)
load(file); %loads data from that file
Prompt1='Enter name of output file = ';
output_file=input(Prompt1,'s'); %sets the output filename;
%Prompt2='Enter event to study = ';
%i=input(Prompt2); %sets impact number
Prompt2='Enter hit number to start ';
start=input(Prompt2); %sets the number of hit to start analysis;
Prompt3='Enter hit nummber to end  ';
N=input(Prompt3); %sets the hit number to end;
```

```
r=0;
for i=start:N
   L_mag=mg_data(i).lin_acc_CG_mag;
   L_mag_max=max(L_mag);
   if L_mag_max>30; %if linear accel is greater than 400g
   r=r+1; %creates row number for events that are above threshold and below accel limt
   %creating matrices
    eventdate={mg_data(1).Info.Day,mg_data(1).Info.Month,mg_data(1).Info.Year};
      ang_vel_length=length(mg_data(i).ang_vel); %is this short
      T=mg_data(i).t;%creates vector of time
      L=mg_data(i).lin_acc_CG;%creates 3 column matrix of linear acc X,Y,Z
      AV=mg_data(i).ang_vel; %creates 3 column matrix of rot velocities X,Y,Z
      AA=mg_data(i).ang_acc; %creates 3 column matrix of rot accel X,Y,Z
      L_mag=mg_data(i).lin_acc_CG_mag; %creates 1 column of resultant linear accel
      AA_mag=mg_data(i).ang_acc_mag; %creates 1 column of resultant linear accel
      AV_mag=mg_data(i).ang_vel_mag; %creates 1 column of resultant linear accel
      T=T(1:ang_vel_length,1:1); %shortens to min ang vel length
      L=L(1:ang_vel_length,1:3);
      L_mag=L_mag(1:ang_vel_length,1:1);
      ALL=[T,L,AA,AV,L_mag,AA_mag,AV_mag];
      A_resultant=[T,L_mag,AA_mag,AV_mag];
     %FFT
      Fs = 1000;            % Sampling frequency
      T_period = 1/Fs;             % Sampling period
      L_signal = 200;             % Length of signal
      t = (0:L_signal-1)*T_period;        % Time vector
      AYFFT = fft(L(:,2));  %FFT of ang accel RY
      PAY2 = abs(AYFFT/L_signal);   %double sided spectrum ??
      PAY1 = PAY2(1:L_signal/2+1); %single sided spectrum
      PAY1(2:end-1) = 2*PAY1(2:end-1);
      f = Fs*(0:(L_signal/2))/L_signal;
       PAY11(:,r+1)=PAY1;

      AXFFT = fft(L(:,1));  %FFT of ang accel RX
      PAX2 = abs(AXFFT/L_signal);   %double sided spectrum ??
      PAX1 = PAX2(1:L_signal/2+1); %single sided spectrum
      PAX1(2:end-1) = 2*PAX1(2:end-1);
       PAX11(:,r+1)=PAX1;

     AZFFT = fft(L(:,3));  %FFT of ang accel RZ
      PAZ2 = abs(AZFFT/L_signal);   %double sided spectrum ??
      PAZ1 = PAZ2(1:L_signal/2+1); %single sided spectrum
      PAZ1(2:end-1) = 2*PAZ1(2:end-1);
       PAZ11(:,r+1)=PAZ1; %forms matrix of Z data
     Hit_No(1,(r+1))=i  ; % forms 1 row of hit numbers

      hit_number=num2str(i);%creats string of hit number for plotting
      %plotting
      clf reset %clears figure window
      figure(i)
      subplot(3,1,1);% plot rotation accel
      plot(f,PAX1);
      title('FFT Linear Acc RX');
      grid on;
      grid minor;
      xlabel('Freq (HZ)');
      ylabel('Amp');
      text(350,300,'Hit Number:','color','red');
      text(450,300,hit_number,'color','red');

     subplot(3,1,2);% plot rotation accelfigure(2)
      plot(f,PAY1);
```

```
        title('FFT of Linear Accel RY');
        grid on;
        grid minor;
        xlabel('Frequency (Hz)');
        ylabel('Amplitude');

        subplot(3,1,3);% plot rotation accelfigure(2)
        plot(f,PAZ1);
        title('FFT of Linear Accel RZ');
        grid on;
        grid minor;
        xlabel('Frequency (Hz)');
        ylabel('Amplitude');

        figs=figure(i);
        print(figs,hit_number,'-djpeg'); %save a jpg file of the plot
          else
        fprintf('Event number %d below 30g accel,\n',i)  %prints to screen
    end


end
device={mg_data(1).Info.Device};
PAX11(:,1)=f;  %adds frequency to the first column
PAY11(:,1)=f;
PAZ11(:,1)=f;
PAX11=[Hit_No;PAX11]; %adds hit numbers to top row
PAY11=[Hit_No;PAY11];
PAZ11=[Hit_No;PAZ11];


% adds summary summary sheet
warning('off', 'MATLAB:xlswrite:AddSheet');
col_header1={'Day','Month','Year'};
col_header2={'Hit number'};
xlswrite(output_file,device,'FFT_RX','A1'); %writes device name to summary worksheet
xlswrite(output_file,col_header1,'FFT_RX','A2'); %writes date header
xlswrite(output_file,eventdate,'FFT_RX','A3'); %writes date
xlswrite(output_file,col_header2,'FFT_RX','A6'); %writes header for data
xlswrite(output_file,PAX11,'FFT_RX','A8');% T,writes resultants
xlswrite(output_file,col_header2,'FFT_RY','A6'); %writes header for data
xlswrite(output_file,PAY11,'FFT_RY','A3');% T,writes resultants
xlswrite(output_file,col_header2,'FFT_RZ','A6'); %writes header for data
xlswrite(output_file,PAZ11,'FFT_RZ','A3');% T,writes resultants
```

Appendix 4: GHBMC version 4.5 Material Properties

Element Type	Part ID	Description		Volume mm³	RO (Density) kg/mm³	kg	E kN/mm²	PR	Yield Stress GPa	Tangent Yield GPa	Bulk Modulus	Shear Modulus Short Time G_0 (GPa)	Long Time G_∞ (GPa)	Delay Constant DC (ms)
Solid	1100000	HE_OR_Cerebellum_3D	ViscoElastic	115665	1.06E-06	0.123					0.2	6.00E-06	1.20E-06	0.125
Solid	1100001	HE_OR_Cerebrum-Gray-Lower_3D	ViscoElastic	136353	1.06E-06	0.145					0.2	6.00E-06	1.20E-06	0.125
Solid	1100002	HE_OR_Cerebrum-Gray-Upper_3D	ViscoElastic	326833	1.06E-06	0.346					0.2	6.00E-06	1.20E-06	0.125
Solid	1100003	HE_OR_CorpusCallosum_3D	ViscoElastic	19691	1.06E-06	0.021					0.2	7.50E-06	1.50E-06	0.125
Solid	1100004	HE_OR_Thalamus_3D	ViscoElastic	11261.6	1.06E-06	0.012					0.2	6.00E-06	1.20E-06	0.125
Solid	1100005	HE_CF_Ventricle-Lateral_3D	ViscoElastic	23661.7	1.04E-06	0.025					0.2	5.00E-07	1.00E-07	0.125
Solid	1100006	HE_OR_Brain-Midstem-Midbrain_3D	ViscoElastic	9133.9	1.06E-06	0.010					0.2	1.20E-05	2.40E-06	0.125
Solid	1100007	HE_OR_Brainstem_3D	ViscoElastic	20881.1	1.06E-06	0.022					0.2	1.20E-05	2.40E-06	0.125
Solid	1100008	HE_CF_CSF-Cerebrum_3D	ViscoElastic	205650	1.04E-06	0.214					0.2	5.00E-07	1.00E-07	0.125
Solid	1100009	HE_OR_BasalGanglia_3D	ViscoElastic	24671.1	1.06E-06	0.026					0.2	6.00E-06	1.20E-06	0.125
Shell (0.5mm)	1100010	HE_MG_Pia_2D	Linear		1.10E-06		0.00125	0.35						
Shell (1mm)	1100011	HE_MG_Tentorium_2D	Linear		1.10E-06		0.0315	0.3						
Solid	1100012	HE_CF_CSF-Cerebellum_3D	ViscoElastic	85563.9	1.04E-06	0.089					0.2	3.00E-06	6.00E-07	0.125
Shell (0.5mm)	1100013	HE_MG_Arachnoid-Cerebrum_2D	Linear		1.10E-06		0.012	0.35						
Shell (0.5mm)	1100014	HE_MG_Arachnoid-Cerebellum_2D	Linear		1.10E-06		0.012	0.35						
Shell (1mm)	1100015	HE_MG_Falx_2D	Linear		1.10E-06		0.0125	0.35						
Solid	1100016	HE_CF_Ventricle-Third_3D	ViscoElastic	1986.57	1.04E-06	0.002					0.2	5.00E-07	1.00E-07	0.125

Element Type	Part ID	Description		Volume mm³	RO (Density) kg/mm³	kg	E kN/mm²	PR	Yield Stress GPa	Tangent Yield GPa	Bulk Modulus	Shear Modulus Short Time G_0 (GPa)	Shear Modulus Long Time G_∞ (GPa)	Delay Constant DC (ms)
Solid	1100017	HE_VS_Sagittal-Sinus_3D	ViscoElastic	4033.3	1.04E-06	0.004					0.2	5.00E-07	1.00E-07	0.125
Solid	1100018	HE_VS_Sagittal-Sinus-Anterior_3D	ViscoElastic	395.8	1.06E-06	0.000					0.2	5.00E-07	1.00E-07	0.125
Shell (1mm)	1100019	HE_VS_Sinus-Dural_2D	Bi-Linear		1.10E-06		0.0315	0.35						
Solid	1100020	HE_OR_Cerebrum-White_3D	ViscoElastic	428965	1.06E-06	0.455					0.2	7.50E-06	1.50E-06	0.125
Beam (2.76mm)	1200001	HE_VE_Bridging_Veins_1D	Bi-Linear		1.13E-06		0.03	0.48	0.00413	0.0122				
Solid	1400003	HE_BT_Skull-Dipole_3D	Bi-Linear	209581	1.00E-06	0.210	0.6	0.3	0.004	0.02				
Solid	1400010	HE_SN_Sphenoidal_3D	Linear	21383.7	1.00E-06	0.021	0.001	0.3						
Solid	1400019	HE_SN_Frontal_3D	Linear	6331.7	1.00E-06	0.006	0.001	0.3						
Solid	1400021	HE_BC_Skull-Outer_3D	Bi-Linear	86672.9	2.10E-06	0.182	10	0.25	0.09	0.5				
Solid	1400022	HE_BC_Skull-Inner_3D	Bi-Linear	173346	2.10E-06	0.364	10	0.25	0.09	0.5				
Shell (1mm)	1400023	HE_MG_Dura_2D	Linear		1.10E-06		0.0315	0.35						
Shell (1mm)	1400024	SK_Head-Skin_2d	Linear		1.10E-06		0.01	0.45						
Solid	1400036	HE_FL_Scalp_3D	Viscoelastic	498462	1.10E-06	0.548					0.02	8.50E-03	3.40E-03	3.00E-05
Solid	1400037	HE_BC_Skull-Outer_3D	Bi-Linear	198631	2.10E-06	0.417	15	0.25	0.09	0.5				
Solid	1400038	HE_BC_Skull-Inner_3D	Bi-Linear	156175	2.10E-06	0.328	15	0.25	0.09	0.5				
Shell (1mm)	1900055	HE_Spinal-Cap_2D	Linear		1.10E-06		0.0315	0.315						
Shell (0.3mm)	2090001	HE-NK_Hyoid-inferior-skull-plate	Linear		1.00E-07		10	0.25						

Publication List

Journal Papers

In review

[1] X. Zhan, Y. Li, Y, Liu, N. Cecchi, S. Raymond, H. Alizadeh, Z. Zhou, **S. Tiernan**, J. Ruan, S. Barbat, O. Gevaert, M. Zeineh, G. Grant, D. Camarillo "Classification of head impacts based on the spectral density of measurable kinematics," Journal of Biomechanics.

[2] X. Zhan, Y. Li, Y. Liu, A. Domel, and **S. Tiernan**, h. Alizadeh, A. Domel, S. Raymond, J. Ruan, S. Barbat, O. Gevaert, M. Zeineh, G. Grant, "Prediction of brain strain across head impact subtypes using 18 brain injury criteria*," J. R. Soc. Interface,* 2020 In review

Published

[3] X. Zhan, Y. Li, Y, Liu, A. Domel, H. Alizadeh, Z. Zhou, N. Cecchi, **S. Tiernan**, J. Ruan, S. Barbat, O. Gevaert, M. Zeineh, G. Grant, D. Camarillo "Predictive Factors of Kinematics in Traumatic Brain Injury from Head Impacts Based on Statistical Interpretation," *Annals of Biomedical Engineering* 2021, DOI: arxiv-2102.05020. Available: http://arxiv.org/abs/2102.05020.

[4] P. Purcell, M. Tyndyk, F. McEvoy, **S. Tiernan,** D. Sweeney, S. Morris "A Multiscale Finite Element Analysis of Balloon Kyphoplasty to Investigate the Risk of Bone-Cement Separation In Vivo" *Int. Journal of Spine Surgery* April 2021, 15 (2) 302-314; DOI: https://doi.org/10.14444/8040.

[5] **S. Tiernan**, D. O'Sullivan, A. Meagher*, E. Kelly "Finite Element Simulation of Head Impacts in Mixed Martial Arts,"*Comput Methods Biomech Biomed Engin. Methods. Sept. 2020. DOI: 10.1080/10255842.2020.1826457.

[6] **S. Tiernan**, A. Meagher and D. O'Sullivan, "Concussion and the severity of head impacts in mixed martial arts." Repeatability and Reliability Evaluation of a Wireless Head-band Sensor," *Part H: Journal of Engineering in Medicine.* Aug. 2020.DOI: 10.1177/0954411920947850.

[7] K. Laksari, M. Fanton, L. Wu, T. Nguyen, M. Kurt, C. Giordano, E. Kelly, E. O'Keeffe, E. Wallace, C. Doherty, M. Campbell, **S. Tiernan**, G. Grant, J. Ruan, S. Barbat and D. Camarillo, "Multi-directional dynamic model for traumatic brain injury detection," *J. Neurotrauma*, pp. 1–48, 2019, doi: 10.1089/neu.2018.6340.

[8] M. Cambell. E O'Keeffe , E Kelly, C Giordano, E Wallace, **S. Tiernan**, A. Meagher, C Greene, S Hughes, T Burke, J Kealy, N Doyle, A Hay, M Farrell, G. Grant, A Friedman, R Veksler, "Dynamic blood brain barrier regulation in mild head trauma," *Neurotrauma*, 2019.

[9] **S. Tiernan** and G. Byrne, "The effect of impact location on brain strain," *Brain Inj.*, vol. 33, no. 01, pp. 1–8, 2019.

[10] **S. Tiernan**, David O'Sullivan, and G. Byrne, "Evaluation of Skin Mounted Sensor for Head Impact Measurement." Proc IMechE Part H, 1-10, 2019
[11] **S. Tiernan**, G. Byrne, D.O'Sullivan, "Repeatability and reliability evaluation of a wireless head-band sensor," *Asian J. Kinesiol.*, pp. 1–18, 2018.
[12] M. Beakey, M. Roe, **S. Tiernan**, B. Keenan, K. Collins, "Cross-Sectional Investigation of Self- Reported Concussions and Reporting Behaviours in 866 Adolescent Rugby Union Players: Implications Educational Strategies," Clin. J. Sport Med., 2018;0:1-7.
[13] M. Beakey, B. Keenan, **S. Tiernan**, and K. Collins, "Is It Time to Give Athletes a Voice in the Dissemination Strategies of Concussion-Related Information? Exploratory Examination of 2444 Adolescent Athletes," Clin. J. Sport Med., p. 1, Aug. 2018.
[14] C. Bright, **S. Tiernan**, F. McEvoy, and P. Kiely, "Fatigue and damage of porcine pars interarticularis during asymmetric loading," *J. Mech. Behav. Biomed. Mater.*, vol. 78, no. November 2017, pp. 505–514, 2018.
[15] C. Bright, **S. Tiernan**, F. McEvoy, and P. Kiely, "Development of a Porcine FE Model for the Investigation of Vertebral Laminae Strains Resulting From Facet Tropism," *J. Biomed. Eng. Biosci.*, vol. 4, pp. 34–42, 2017.
[16] C. Bright, **S. Tiernan**, F. McEvoy, and P. Kiely, "Strain distribution in the porcine lumbar laminae under asymmetric loading," *Proc. Inst. Mech. Eng. Part H J. Eng. Med.*, vol. 231, no. 10, pp. 945–951, Oct. 2017.
[17] M. Beakey, C. Blake, **S. Tiernan**, and K. Collins, "Are Irish Sporting Organisations Review article," Eur. J. Sport. Med., vol. 3, no. 2, pp. 41–54, 2016.
[18] P. Purcell, **S. Tiernan**, F. McEvoy, and S. Morris, "Strong similarities in the creep and damage behaviour of a synthetic bone model compared to human trabecular bone under compressive cyclic loading," *J. Mech. Behav. Biomed. Mater.*, vol. 48, pp. 51–59, 2015.
[19] P. Purcell, **S. Tiernan**, M. Tyndyk, F. Mcevoy, D. Sweeney, and S. Morris, "A Parametric Finite Element Analysis of the bone-cement Interface following Balloon Kyphoplasty," *IMechE J. Eng. Med.*, vol. 228, pp. 89–97, 2014.
[20] P. Purcell, **S. Tiernan**, F. McEvoy, and M. Tyndyk, "Making an Impact on Vertebral Compression Fractures," *Eng. J.*, no. 3, 2013.
[21] P. Purcell, M. Tyndyk, F. McEvoy, **S. Tiernan**, and S. Morris, "Stress distribution at the bone-cement interface changes during Kyphoplasty rehabilitation," in *Proceedings - 29th Southern Biomedical Engineering Conference, SBEC 2013*, 2013.
[22] K. Norris and **S. Tiernan**, "An analysis of the performance of foams used in hurling helmets," *WIT Trans. Built Environ.*, vol. 98, pp. 117–126, 2008.
[23] **S. Tiernan** and M. Fahy, "Dynamic FEA modelling of ISO tank containers," *J. Mater. Process. Technol.*, vol. 124, no. 1–2, pp. 126–132, 2002.
[24] M. Fahy and **S. Tiernan**, "Finite element analysis of ISO tank containers," *J. Mater. Process. Technol.*, vol. 119, no. 1–3, pp. 293–298, 2001.

Conferences (Since 2012)

[1] **S. Tiernan**, A. Meagher, D. O'Sullivan, E. Kelly, M. Cambell, C. Doherty, *Biomechanics of Head Impacts in an Unhelmeted sport*, 2021 GHBMC Users Workshops, April 2021.

[2] **S. Tiernan** *The Measurement and Simulation of Head Impacts in Mixed Martial Arts.* IRCOBI 2019. Florence, September 2019.

[3] A. Meagher, **S. Tiernan,** *Head Impacts in MMA.* Bioengineering in Ireland 2019, January 18-19 Limerick.

[4] A. Kelly, **S. Tiernan**, F. McEvoy, *An Experimental Investigation of Cement Application Methods in Balloon Kyphoplasty*, European Orthopaedic Research Society, Galway Sept 2018.

[5] **S. Tiernan,** *The Investigation of the Relationship between Impact Direction and Principal strain within the Brain.* World BioEngineering Conference, Dublin July 2018. Poster.

[6] **S. Tiernan,** *The Measurement & Simulation of Head Impacts in Mixed Martial Arts.* United Kingdom Ansys Users Conference, May 2018, Coventry UK.

[7] **S. Tiernan,** G. Byrne, *The Measurement & Simulation of Head Impacts in Mixed Martial Arts*. Ansys Irl Users Conference, May 2018, Coventry UK.

[8] **S. Tiernan,** G. Byrne, *The Measurement & Simulation of Head Impacts in Mixed Martial Arts.* Ansys Irl Users Conference, May 2018, Coventry UK.

[9] G. Byrne, **S. Tiernan,** *Simulation and Analysis of Head Impacts*. Bioengineering in Ireland 2018, January 26-27 2018 Johnstown, WestMeath.

[10] G. Byrne, **S. Tiernan,** *An Investigation of the Effect of Impact Location on Strain within the Brain.* IRCOBI, Sept. 2017.

[11] G. Byrne, **S. Tiernan,** *Validation of Skin Mounted Accelerometers and Finite Element Model for the Measurement and Analysis of Head Impacts*. Bioengineering in Ireland, January 20-21 2017 Templepatrick.

[12] Bright C, **Tiernan S,** F. McEvoy, P. Kiely, *Static and Dynamic Response of Porcine Lumbar Vertebrae to Asymmetric Loading*. Proceedings of the 23rd Annual Conference of the Section of Bioengineering of the Royal Academy of Medicine in Ireland, Jan 2017.

[13] A. Kelly, F. McEvoy, **S. Tiernan,** *Optimisation of the Kyphoplasty Cement Augentation Surgical Technique.* Bioengineering in Ireland 2017, January 20-21 2017 Templepatrick.

[14] G. Byrne, **S. Tiernan,** *Validation of Skin Mounted Accelerometers and Finite Element Model for the Measurement and Analysis of Head Impacts.* Bioengineering in Ireland 2017, January 20-21 2017 Templepatrick.

[15] C. Bright, **S. Tiernan,** F. McEvoy, P. Kiely, *Development of a Porcine FE Model for the Investigation of Spondylolytic Vertebral Fractures*. Proceedings of the ICBES, Prague, July 2014, Prague.

[16] B. Lawless, **S. Tiernan, F.** McEvoy, S. Morris, *Anatomical and vertebral body compression failure load comparison of sika and fallow deer vertebrae (T3-T10) to human*. Proceedings of the 20th Annual Conference of the Section of Bioengineering

of the Royal Academy of Medicine in Ireland, Jan 24th-25th 2014, Castletroy Park Hotel.

[17] C. Bright, **S. Tiernan,** F. McEvoy, P. Kiely, *Determination of Magnitude and Direction of Maximum Principal Strain under Static Conditions in the Porcine Pars Interarticularis, a Validated FEA Study*. Proceedings of the 20th Annual Conference of the Section of Bioengineering of the Royal Academy of Medicine in Ireland, Jan 2014.

[18] P. Purcell, F. McEvoy, **S.** T**iernan, S.** Morris, *Experimental quantification of the compacted zone in a synthetic bone model treated using Balloon Kyphoplasty.* Proceedings of the 19th Annual Conference of the Section of Bioengineering of the Royal Academy of Medicine in Ireland, Jan 18th-19th 2013, Johnstown House Hotel.

[19] B. Lawless, **S. Tiernan,** F**.** McEvoy, S. Morris, *Effect of Flexion Angle during Impact on the Replication of Spinal Fractures.* International Conference on Biomedical Engineering and Systems. 2014 Prague, Czech Republic, p. Paper No: 61 2014.

[20] P. Purcell, M. Tyndyk, F. McEvoy, **S**. **Tiernan**, S. Morris, *Stress distribution at the bone-cement interface changes during Kyphoplasty rehabilitation.* Proceedings of the 29th Southern Biomedical Engineering Conference, May 3rd-5th 2013, Miami, USA. Purcell P, Tyndyk M.

[21] C. Bright, **S. Tiernan S,** F**.** McEvoy, S. Morris, *The Optimisation of Posterior Spinal Dynamic Stabilisation Surgery.* Proceedings of the 19th Annual Conference of the Section of Bioengineering of the Royal Academy of Medicine in Ireland, Jan 2013.

[22] P. Purcell, M. Tyndyk, F. McEvoy, **S. Tiernan,** S. Morris, *Kyphoplasty height subsidence increases fracture risk at the treated level.* Proceedings of the 19th Congress of the European Society of Biomechanics, August 25th-28th 2013, Patras, Greece.

[23] P. Purcell, F. McEvoy, **S**. **Tiernan,** S**.** Morris, *Implications of Balloon Kyphoplasty on Load Transfer to Adjacent Vertebrae*. Proceedings of the 18th Annual Conference of the Section of Bioengineering of the Royal Academy of Medicine in Ireland, Jan 28th-29th 2012, Hilton Hotel, Templepatick, Belfast.

Short Papers

[1] P. Purcell, M. Tyndyk, F. McEvoy, **S. Tiernan,** S. Morris. *A novel method for computational modeling of compacted bone following Balloon Kyphoplasty.* Institution of Mechanical Engineers & Engineers Ireland, Young Research Engineer Award 2012.

[2] P. Purcell, M. Tyndyk, F. McEvoy, **S. Tiernan,** S. Morris, *Making an impact on compression fractures of the human spine.* The Engineers Journal, Issue 3, April 18th 2013,